Development of RTgutGC as a Tool for Fish Feed Development

by

Patrick Gilles Pumputis

A thesis
presented to the University of Waterloo
in fulfillment of the
thesis requirement for the degree of
Master of Science
in
Biology

Waterloo, Ontario, Canada, 2017

AUTHOR'S DECLARATION

I hereby declare that I am the sole author of this thesis. This is a true copy of the thesis, including any required final revisions, as accepted by my examiners.

I understand that my thesis may be made electronically available to the public.

ABSTRACT

A rainbow trout intestinal epithelial cell line, RTgutGC, has been used in this thesis to investigate the effects of various stresses in aquaculture on the gastrointestinal (GI) tract and for identifying possible beneficial actions to take to protect gut health. RTgutGC cells were studied in four kinds of media. L15 with a supplement of fetal bovine serum (FBS) was the normal growth medium (L15/FBS). Serum starvation was done in the basal medium alone, L15. Deprivation of serum, amino acids, and vitamins was accomplished in L15/ex, which had only L-15 salts with galactose and pyruvate. Complete starvation of all nutrients was achieved in L15/salts. In these studies, cell viability was assessed with alamar Blue (AB) for metabolic activity and with carboxyfluorescein diacetate acetoxymethyl ester (CFDA-AM) for plasma membrane integrity. Confocal microscopy together with immunocytochemical (ICC) staining was used to evaluate microtubule organization and tight junctions and with fluorescent phalloidin staining to detect F-actin. Western blotting was used to measure specific protein levels, such heat shock protein 70 (HSP70). Intestinal epithelial barrier function was evaluated in a culture system in which RTgutGC monolayers divided a culture chamber into top and bottom wells and trans epithelial electrical resistance (TEER) and Lucifer Yellow (LY) permeability across the cell monolayers were measured. Intestinal epithelial wound healing and/or restitution was examined in a plastic fence assay in which cells formed monolayers on both sides of culture inserts that were then removed to form a gap or wound. Five general lines of investigation were explored on the topics of starvation, phytochemicals, antinutrionals, temperature, and phytochemical/temperature interactions. The results for each are summarized in the following five paragraphs.

Rainbow trout intestinal epithelial cell monolayers survived serum starvation (L15), the deprivation of serum, amino acids, and vitamins (L15/ex), and the complete absence of nutrients (L15/salts) but some cellular activities and structures were altered, depending on the severity of the deprivation. During these three kinds of nutritional deprivation, most cells survived at least seven days as judged by their continued adherence to the plastic growth surface as observed by phase contrast microscopy and by cell viability measurements with AB and CFDA-AM. However, energy metabolism as measured with AB was diminished, especially in L15/salts with approximately an 85% decline. Under all types of nutrient

deprivation, the cytoskeleton of cells remained intact. However, during nutritional deprivation, the actin stress fibers became thicker and many cells acquired circumferential fibers, especially in L15/salts. In L15/ex and L15/salts, the fibers of the α-tubulin network appeared thicker and longer and as well the microtubular organizing centres were larger and more intensely stained. ZO-1 (tight junction protein-1) was detected at the periphery of cells in monolayers, with nutritional deprivation causing only a slight change. However, in L15/salts epithelial barrier functions were impaired. In L15/FBS the TEER was around 30-40 Ω cm^2 and approximately 75 % of the LY was retained in the top chamber. In L15/salts the TEER was approximately 15-20 Ω cm^2 and only about 30 % of the LY was retained in the top chamber. Seven days after the creation of gaps in monolayers, the gaps were filled by RTgutGC cells in L15/FBS. As cells proliferate in L15/FBS as well as migrate, this is considered wound healing. By contrast, RTgutCG in L15 filled the gap much more slowly, and as most fish cells do not proliferate in L15 alone, the gap closing is considered to be due to cell migration alone or restitution. RTgutGC in L15/salts failed to migrate into gaps, but if after seven days L15/FBS was added, the cells did, emphasizing that they were still alive. When after seven days in either L15/FBS or L15/salts monolayers were trypsinized, the diameter and volumes of cells were respectively 17.9 ± 1.6 μm and 3.1 ± 0.8 pL for L15/FBS and 15.0 ± 0.3 μm and 1.8 ± 0.1 pL for L15/salts. Despite this reduction in size, when placed in L15/FBS, these cells could reattach to plastic and grow to form monolayers, emphasizing again that they were viable after seven days in L15/salts. Thus rainbow intestinal epithelial cells survived for at least seven days in the complete absence of nutrients but starvation impaired their barrier functions and ability to repair wounds.

RTgutGC, a rainbow trout intestinal epithelial cell line, was used as an intestinal model to study the effects of naringenin (N), a plant secondary metabolite found in grapefruits with antioxidant, anti-inflammatory, and anti-carcinogenic properties. 30 and 100 μM N generated a flattened cell morphology with more defined cell borders. Most significant reductions in cellular viability were seen when incubated with 100 μM N, where in L15 medium, metabolic activity decreased by 59% and plasma membrane integrity decreased by 31%. However, lower concentrations of N had no effect on cellular viability. With the cytoskeleton still intact, N increased circumferential actin while decreasing the amount of stress fibers in the cells. Increasing concentrations of N caused a dose response increase in TEER. A significant

reduction (39%) in monolayer permeability as measured by LY rejection assay was observed with 100 μM N. No changes in ZO-1 or claudin 3 staining was observed. Significant reductions in migration and restitution were observed with 50 and 75 μM N, but not lower concentrations. N did not cause any changes in HSP70 protein expression. The work, though *in vitro*, demonstrates the potential beneficial effects of N (concentration of 30 μM) as a possible feed additive.

RTgutGC was used to study the effects of antinutritional factors (ANFs) on intestinal epithelial cell restitution. 100 μg/mL of Bowman-Birk inhibitor significantly ($p < 0.05$) reduced restitution where cells reached a total percent migration of 13 ± 3% (control = 23 ± 7%.). 0.75 and 2.25 μg/mL of wheat germ agglutinin (WGA) significantly ($p < 0.01$) reduced restitution at a total percent migration of 13% ± 3% and -11 ± 3% respectively (control = 49 ± 16%). Additionally, WGA caused the loss of actin stress fibers with actin being more peripherally located. 8 mM of butyrate significantly ($p < 0.05$) reduced restitution with cells reaching a total percent migration of 18 ± 6% (control = 39 ± 11%). Increasing vacuole formation was also observed with increasing concentrations of butyrate. Kunitz inhibitor and soybean agglutinin had little to no effect on RTgutGC restitution. For the first time, we have shown negative effects of ANFs on fish intestinal cell restitution and demonstrated preliminary uses of RTgutGC as an *in vitro* method to screen ANFs.

The capacity of rainbow trout epithelial cells in L15/FBS to heal a wound whether through a combination of cell migration and proliferation or just cell migration (restitution) was profoundly influenced by temperature. Relative to the normothermic temperature of 18 °C for RTgutGC, a decrease in temperature to 4 ^{o}C caused a significant reduction in wound healing. Increasing the temperature to 26 ^{o}C slightly but not significantly increased wound healing. However, an increase to 32 ^{o}C (heat stress) during the wound healing assay caused the cell monolayer to shrivel up and die. Additionally, if cells were exposed to a heat stress temperature (32 ^{o}C) for 3 h before the start of wound healing, small numbers of individual migrating cells could be observed, not reaching full gap closure. The induction of a thermotolerant state by heat pre-conditioning (26 ^{o}C for 24 h) before heat stress (32 ^{o}C for 3 h) restored wound healing to a capacity similar to the non-heat stress control, with full gap closure seen within 3 days. The study suggests that cellular wound healing can be highly

dependent on temperature and that preventative measures, such as heat pre-conditioning, can help mitigate the negative effects of heat stress on wound healing.

Possible protective actions of N on the recovery of rainbow trout intestinal epithelial cells from heat stress were investigated but N only modestly improved recovery of cellular morphology. RTgutGC monolayers in either L15/FBS, L15 or L15/salts with or without N were subjected to heat stress of 32 °C for 1.5 or 3 h and returned to 18 °C to recover for 24 h. At one hour after the end of the heat treatments the monolayers were no longer confluent but had holes as a result of cells shrivelling and rounding. When the heat stress had been 1.5 h, the cellular morphology was largely restored 24 h later whether N was present or not. When the heat stress had been 3 h, N improved the adherence and shape of cells 24 h later, especially for recovery in L15/salts. However, with increasing N concentrations of up to 100 μM, no trend of improvement was observed in cell viability as measured with AB or CFDA-AM and 100 μM N did not alter the heat activation of caspase-3. Yet increasing N did alter the organization of F-actin during recovery. Stress fibers were diminished but circumferential actin became more pronounced with increasing N. This was true whether the cells were in L15/FBS or L15/salts but more evident in L15/salts. Thus the reorganization F-actin to the cell periphery might have improved the recovery of cell shape after a heat stress. Naringenin failed to modulate HSP70 levels in cultures at 18 °C whether the cultures were recovering from a heat stress or not. Therefore, HSP70 was unlikely to be mediating the improvement by N in the recovery of cell shape from heat stress.

ACKNOWLEDGEMENTS

First and foremost, I would like to thank both my MSc supervisors Dr. Niels Bols and Dr. Vivian Dayeh. Dr. Bols, your love, excitement, and enthusiasm for science is contagious and I have learned a lot from you over the past two years. I always looked forward to chatting with you in your office, discussing data, and listening to your ideas. Your guidance was unparalleled. I am extremely grateful for the opportunity to have studied and develop as a researcher in your lab. Dr. Dayeh, from the first time I stepped into BIOL 273 during my second year of undergrad and to now being my MSc co-supervisor, your input on my work has always oriented me in the right direction. Your encouragement and assistance help guide me through my MSc studies and I would like to thank you. I could not have asked for better supervisors and mentors.

Secondly, I would like to thank my MSc committee members Dr. Lucy Lee, Dr. Barbara Butler, and Dr. Bernard Duncker for their continued support throughout the two years and for their valuable input and ideas towards my project.

Thirdly, thank you Dr. Nathan Vo and Dr. John Pham for providing me with guidance and wonderful support. Nathan, I owe a lot to you for giving me the opportunity to volunteer under you during my undergrad and introducing me to the Bols lab. You opened my door to research and I am truly grateful. John your friendliness and helpfulness in project related issues was greatly appreciated. Also it was great chatting with you about anime, TV, food, and travel over the shelf separating our desks. The two of you made my time in the Bols lab as great of an experience as possible.

I have to thank all the current and past Bols lab members that I crossed path with. Mark, it was great having you in the lab, cracking jokes, talking sports, playing golf and sharing beer with you. Zhenzhen and Senthuri, thanks for the helping hands and exploring RTgutGC with me. Amreen and John Kim, you two brought so much positive energy to the lab and made any task enjoyable. Annie, Winnie, Sumayyah, Laura, Dustin, and Liz, thank you for being great lab mates and I wish you bunch (and everyone) the best in their future endeavors.

To the friends outside the lab, Steven, what better friend I could ask for. When times got rough you were there for me and always engaged in a conversation. You supported me throughout the two years and shared the same excitement to grapefruit as I did. Jesse and Irene, my life as a grad student would not have been as exciting and fun if it wasn't for you two. Thanks for being great friends and pushing me to strive further. Sarah, I thank you for putting up with me talking about my research, helping me through the tough times of writing, and continuously supporting me.

Lastly, I would like to thank my loving parents Carole and Mark Pumputis, my brother Philip, and my family to whom I am forever grateful.

This research was supported by NSERC strategic grant partnering with Skretting Canada Inc. under Dr. Niels C. Bols and Dr. Lucy E.J. Lee.

DEDICATION

This thesis is dedicated to my family and my late grandmother, Claudette (Mamie).

TABLE OF CONTENTS

LIST OF FIGURES

LIST OF ABBREVIATIONS

AA	Amino acid
AB	Alamar blue
AJ	Adherens junction
ANF	Antinutritional factor
Arp2/3	Actin-related proteins 2/3
BB	Blocking buffer
BBI	Bowman-Birk inhibitor
BCA	Bicinchoninic acid
BCIP	5-bromo-4-chloro-3'-indolyphosphate
Caco-2	Human colon adenocarcinoma cell line
cAMP	Cyclic adenosine monophosphate
CFDA-AM	5'-carboxyfluorescein diacetate, acetoxymethyl ester
CHSE-214	Chinook salmon embryo cell line
DAPI	4′,6-Diamidine-2′-phenylindole dihydrochloride
DHA	Docosahexaenoic acid
DMSO	Dimethyl sulfoxide
DPBS	Dulbecco’s phosphate-buffered saline solution
EGF	Epidermal growth factor
EPA	Eicosapentaenoic acid
ERM	Ezrin, radixin, and moesin protein family
FGF	Fibroblast growth factor
FITC	Fluorescein isothiocyanate
F-actin	Filamentous actin
FBS	Fetal bovine serum
G-actin	Globular actin
GAKS	Goldfish scale cell line
GI	Gastrointestinal
GLA	γ-linolenic acid
GRP78	Glucose-related protein 78

GTP	Guanosine triphosphate
HB-EGF	Heparin-binding EGF-like growth factor
HBP	hexosamine biosynthetic pathway
HEW	Haddock embryo cell line
HGF	Hepatocyte growth factor
HRA	Human ovarian cancer cell line
HS	Heat stress
HSF-1	Heat shock factor 1
HSP	Heat shock protein
HSR	Heat shock response
HT-29	Human colorectal adenocarcinoma cell line
ICC	Immunocytochemistry
IEC	Intestinal epithelium cell
IEC-6	Rat intestinal epithelial cell line 6
IEC-18	Rat intestinal epithelial cell line 18
IL-4	Interleukin 4
ISEMF	Intestinal subepithelial myofibroblast
KI	Kunitz inhibitor
L15	Leibovitz's L15 medium
L15/ex	Simplified Leibovitz's L15 medium with L15 inorganic salts and galactose and pyruvate
L15/FBS	Leibovitz's L15 medium supplemented with fetal bovine serum
L15/salts	Simplified Leibovitz's L15 medium with L15 inorganic salts
LA	Linolenic acid
LPA	Lysophosphatidic acid
LS174T	Human Duke's type B colorectal adenocarcinoma cell line
MDCK	Canine Cocker Spaniel kidney cell line
mitoBK	Mitochondrial big potassium channel
MTOC	Microtubule-organizing center
nc-MTOC	Non-chromosomal microtubule-organizing center

NBT	Nitro blue Tetrazolium Chloride
NO	Nitric oxide
PDGF-BB	Platelet-derived growth factor subunit B (homodimer)
PHL	Pacific herring larvae cell line
PKA	Protein kinase A
PUFA	Polyunsaturated fatty acid
RFU	Relative fluorescent unit
RIPA	Radioimmunoprecipitation assay
RTG-2	Rainbow trout gonadal cell line
RTgutGC	Rainbow trout intestinal epithelial cell line
RTS11	Rainbow trout macrophage cell line
SAV	Serum, amino acids, and vitamins
SBA	Soybean agglutinin
Sp1	Specificity protein 1
T84	Human colon carcinoma cell line
TBS-T	Tris-buffered saline with tween 20
TEER	Transepithelial electrical resistance
TGF	Transforming growth factor
TJ	Tight junction
TT	Thermotolerance
UDP	Uridine diphosphate
VEGF	Vascular endothelial growth factor
WGA	Wheat germ agglutinin
ZO	Zonula occludens

CHAPTER 1

General Introduction

1.1. FISH AQUACULTURE

The aquaculture industry is one of the largest food production sectors showing impressive growth, near doubling since 1993 (FAO, 2016). As a result of population growth, fish consumption also increased in the last couple decades, where the average world per capita apparent fish consumption in 2013 was 19.7 kg compared to 9.9 kg during the 1960s (FAO, 2016). It is predicted that this average worldwide consumption will continue to rise. Popular fresh water fish in the Canadian aquaculture industry are salmonids, such as rainbow trout. Salmonids account for 73% of the total aquaculture production in Canada (FOC, 2012).

Sustaining the success of salmonid aquaculture requires further knowledge on many anatomical and physiological systems and how their functions can be impaired, improved, or protected. An example of such a system is the intestinal mucosa. Potentially the intestinal mucosa can be impaired by some aquaculture practices, such as new feeds, and by heat stress, arising from climate change. On the other hand, the health of the intestinal mucosa can potentially be protected or improved by feed additives.

The intestinal mucosa is the innermost structure of the gastrointestinal (GI) tract, surrounding the lumen of the gut. Intestinal mucosa consists of three histological layers. Intestinal epithelium cells (IEC) form a monolayer of cells that directly face the lumen. On the body side of the intestinal mucosa, the intestinal epithelium sits on the lamina propria. The third and outermost layer of the intestinal mucosa is the lamina muscularis that gently agitates the mucosa to aid interaction between luminal contents and intestinal epithelium. Functionally, the key cells of the intestinal mucosa are the IECs. The IECs have two broad functions. One is to absorb nutrients and water. The second and equally important function is to act as a selective barrier to protect the animal. The epithelial barrier is also essential for the proper absorption of nutrients and water. Thus understanding the fish intestinal epithelial barrier and being able to identifying potential damaging and healing treatments should improve aquaculture.

1.2. THE INTESTINAL EPITHELIAL BARRIER

IECs form the largest barrier between the external and internal environment. This simple columnar epithelium allows for protection and separation of the internal environment from the external by forming a physical and biochemical barrier (Peterson & Artis, 2014). This protection is important because the gut lumen may contain many commensal bacteria but also some pathogenic microorganisms (Peterson & Artis, 2014). Interestingly, IECs are known to increase their barrier function in response to microbial stimuli while also helping coordinate an immune response (Peterson & Artis, 2014). The mammalian intestinal epithelium has a crypt-villus structure forming a larger surface area for greater nutrient absorption (Umar, 2010). However, there is a lack of villi and crypts in teleosts (Wallace et al., 2005). Instead, wide irregular intestinal folds are seen (Fig 1.1). Some teleosts appear to lack a muscularis mucosa and a submucosa (Wallace et al., 2005), although whether this is true for all fish is unclear.

Enterocytes, enteroendocrine cells, goblet cells, transit amplifying cells, and Paneth cells are all considered IECs and arise from intestinal epithelial stem cells located within the intestinal crypt base (Umar, 2010). Other than zebrafish, which appear to lack Paneth cells, the teleost intestinal epithelium contains the same IEC types that all originate from intestinal epithelial stem cells at the base of the folds (Wallace et al., 2005). Enterocytes are the most common IECs and mainly contribute to barrier functions and nutrient absorption, enteroendocrine cells are hormone secreting cells important for nutrient metabolism, goblet cells secret mucus which protects the intestinal epithelium, Paneth cells secret anti-microbial compounds and are also important in maintaining stem cell population in crypts, and transit amplifying cells are partially differentiated cells that will eventually form differentiated IECs (Umar, 2010). These cells contribute to the dynamic properties of the intestinal epithelium (Peterson & Artis, 2014).

Directly below the epithelium is the lamina propria housing intestinal subepithelial myofibroblasts (ISEMF). ISEMFs have paracrine functions, making them extremely important supportive cells in intestinal epithelial homeostasis (Powell et al., 1999). They secrete growth factors that support intestinal epithelial growth and restitution (Powell et al., 1999). ISEMFs also have important roles in the growth and differentiation of intestinal epithelial stem cells. Lei et al. (2014) demonstrated that ISEMFs support the growth and differentiation of intestinal

epithelial stem cells by supplying them with R-spondin1 and R-spondin2. These two growth factors are involved in the Wnt pathway, which is widely recognized for its essential function in stem cell growth and differentiation programs (Lei et al., 2014). Other beneficial roles of ISEMFs include water and electrolyte transport and immune related functions (Powell et al., 1999).

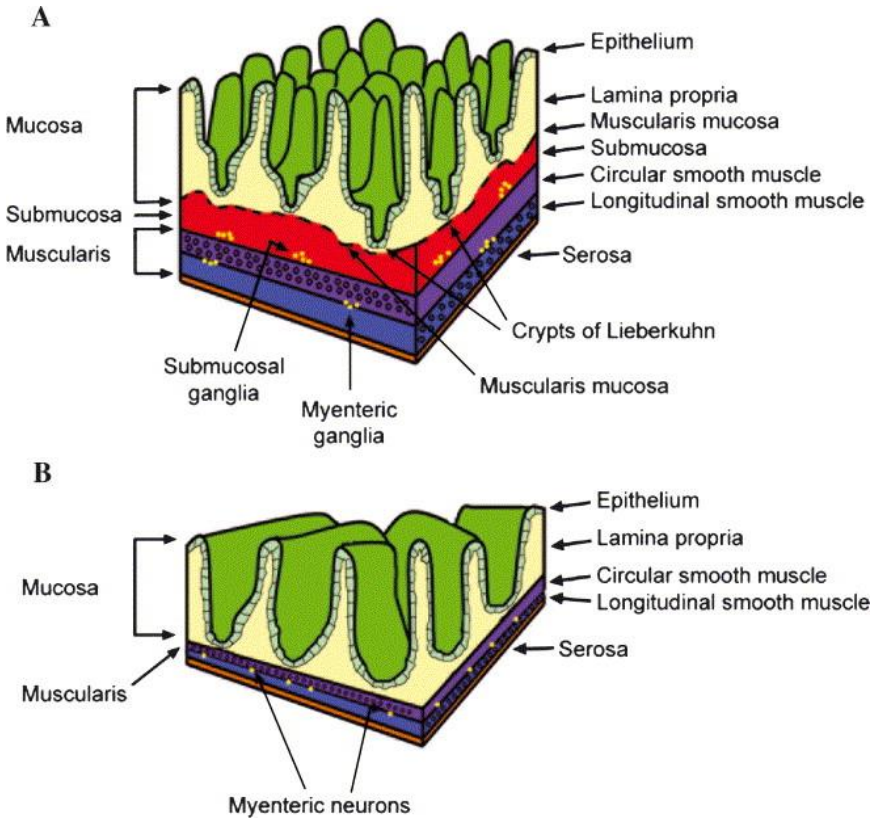

Figure 1.1. Structural differences between mammalian (A) and teleost (B) intestinal mucosa. Teleost lack crypt-villi structure and have these wide intestinal folds. This figure was reprinted from "Intestinal growth and differentiation in zebrafish" by Wallace, K.N., Akhter, S., Smith, E.M., Lorent, K. & Pack, M. (2005). *Mechanisms of Development*, **122**, 157-173. Reprinted with permission.

To form an intestinal epithelial barrier, IECs are required to form specialized cell-to-cell connections. These connections are tripartite and seen in a juxtaluminal position with the most apical component being tight junctions (TJ) followed below by adherens junctions (AJ) (Kolosov et al., 2013). The next section focuses on describing the composition and role of these apical junctional complexes in forming a functioning intestinal barrier.

1.2.1. Tight junctions

TJs have two main functions: the "fence" and "gate" functions (Rajasekaran et al., 2008). The "fence" function refers to the ability of TJs to block intramembrane diffusion of macromolecules between the apical and basolateral sides, whereas the "gate" function describes their ability to control the paracellular pathway between cells (Rajasekaran et al., 2008). As seen in Fig 1.2, TJs structurally appear as "a belt-like reticular network of anastomosing strands" (Chasiotis et al., 2012). The proteins forming the TJ complex can be classified as either transmembrane or cytosolic TJ proteins. The transmembrane TJ proteins are important in forming the connections between cells in the intercellular space influencing paracellular permeability, while cytosolic TJ proteins generally provide structural support to TJs but can also have signaling functions (Chasiotis et al., 2012).

The three most well-known classes of TJ proteins in epithelial cells (seen in Fig 1.3) are occludin, the claudin family, and zonula occludens (ZO) family (González-Mariscal et al., 2003). Occludin was the first TJ protein to be identified and is named after the latin word "occludere" meaning to occlude (González-Mariscal et al., 2003). As its name suggests, occludin's primary function is in the formation and maintenance of the TJ barrier, hence "tightening" the epithelium (Chasiotis et al., 2012). Claudins are a superfamily of proteins that make up most of the TJ complex and participate in regulating paracellular permeability (Kolosov et al., 2013). Some claudins can decrease paracellular permeability while others can increase it; hence, despite a large variety of claudin proteins, the specific combination of claudins in the TJ complex will predict its permeability and can vary between different types of tissues (Kolosov et al., 2013). Also, claudins can vary spatially in the GI tract; for example, Clelland et al. (2010) showed that the transcript level of cldn-3d (barrier forming) increased from anterior to posterior regions of the gut in the pufferfish. Whereas both occludin and claudins are transmembrane TJ proteins, ZOs are cytosolic TJ proteins providing scaffolding

and structural support to the TJ by linking claudins and occludin to the microfilamentous cytoskeleton of the cell (Chasiotis et al., 2012). Among members of the ZO family, ZO-1 is perhaps the most widely studied. ZO-1 has another role involved in intracellular signaling pathways that lead to cell proliferation, differentiation, and gene expression (Chasiotis et al., 2012).

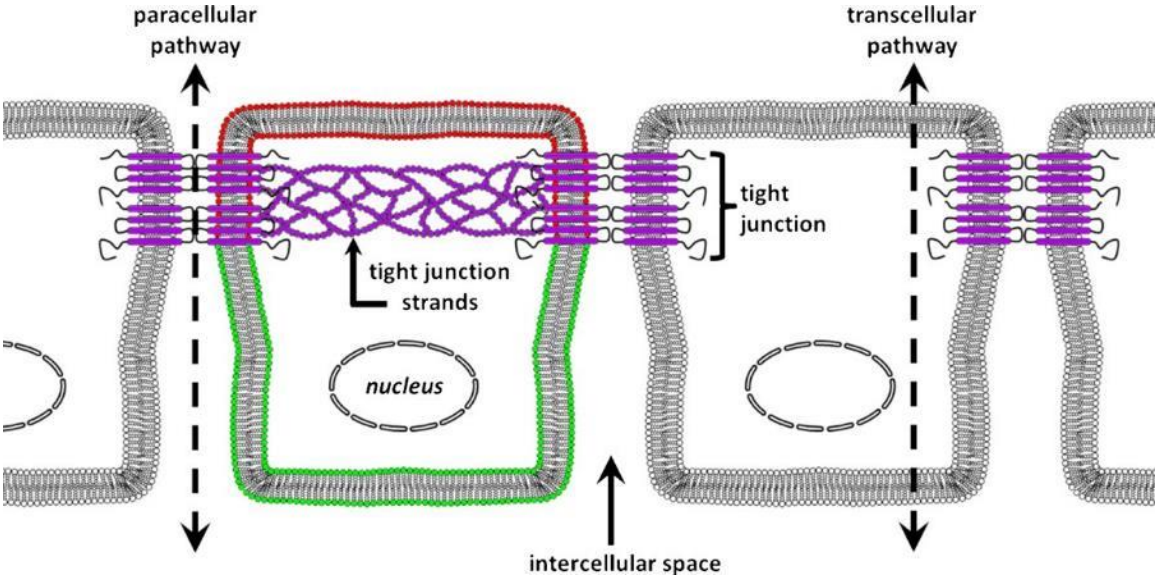

Figure 1.2. TJ have a "gate and "fence" function. TJ are seen in purple. The "Gate" function can be seen as TJ will control the paracellular pathway. The "Fence" function is also seen as TJ will block diffusion of molecules between the apical (red) and basolateral (green) side. This figure was reprinted from "Tight junctions, tight junction proteins and paracellular permeability across the gill epithelium of fishes: A review" by Chasiotis, H., Kolosov, D., Bui, P. & Kelly, S.P. (2012). *Respiratory Physiology & Neurobiology*, **184**, 269-281. Reprinted with permission.

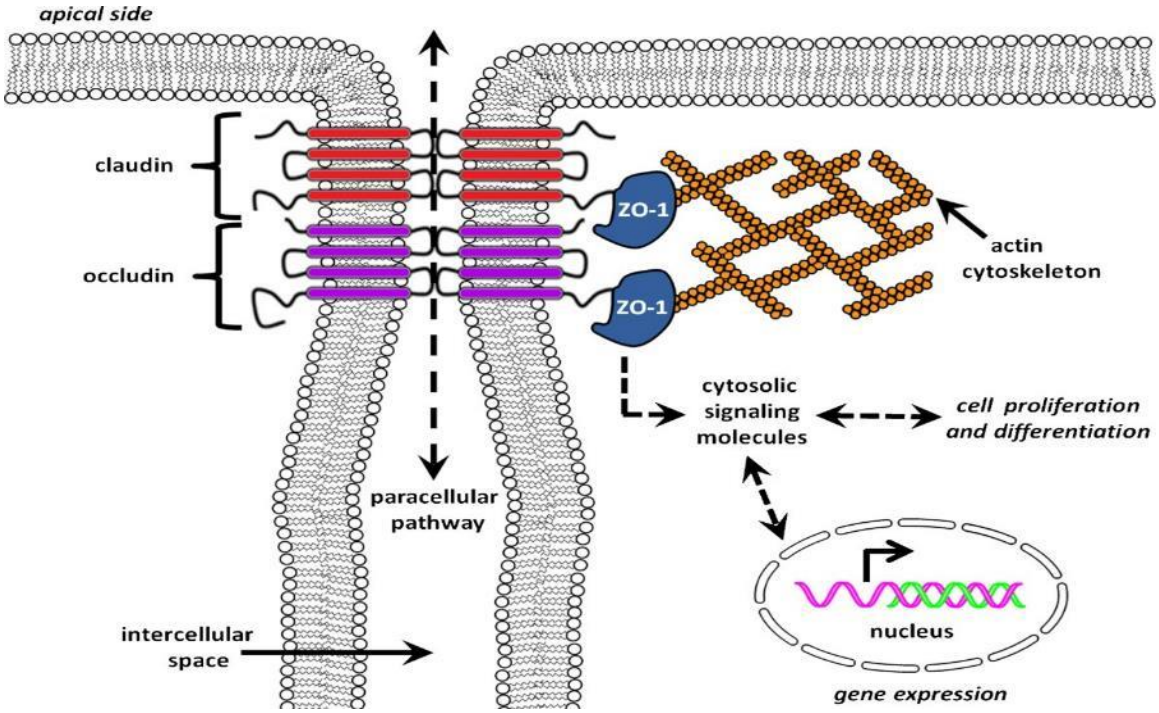

Figure 1.3. Structural composition of a TJ complex. The TJ complex with claudin (red) and occludin (purple) being important transmembrane proteins forming bridging connections within the intracellular space controlling paracellular permeability. ZO-1 (blue) binds to actin structurally supporting the TJ complex. ZO-1 can also act in a signaling pathway leading to cell proliferation, differentiation, and gene expression. This figure was reprinted from "Tight junctions, tight junction proteins and paracellular permeability across the gill epithelium of fishes: A review" by Chasiotis, H., Kolosov, D., Bui, P. & Kelly, S.P. (2012). *Respiratory Physiology & Neurobiology*, **184**, 269-281. Reprinted with permission.

1.2.2. Adherens Junctions

Below the TJs are the adherens junctions (AJs), also playing a crucial role in the formation of the intestinal barrier (Iizuka & Konno, 2011). They have roles in cell-to-cell stabilization, regulating the actin cytoskeleton, intracellular signalling, and transcriptional regulation (Hartsock & Nelson, 2008). The major transmembrane proteins of the AJs are the the Ca^{2+} dependent cadherin superfamily (Hartsock & Nelson, 2008). The most well studied cadherin is E-cadherin. E-cadherin is integral to the formation of AJs where it is required for the localization and binding of catenins such as p120-, α-, and β-catenin (Hartsock & Nelson, 2008). Catenins are intracellular proteins and stabilize the E-cadherin complex by linking to the actin cytoskeleton (Hartsock & Nelson, 2008).

1.2.3. Cytoskeleton

The cytoskeleton is essential for maintaining cell interactions in the intestinal epithelium and is suggested to be a major target of intestinal injury (Coss & Linnermans, 1996; Miller et al., 2000). Thus, the cytoskeleton is extremely important to a properly functioning biological organism and its disruption can cause severe adverse effects. The cytoskeleton is composed of actin filaments or microfilaments, microtubules, and intermediate filaments.

1.2.3.1. Actin filaments

Actin filaments are key cytoskeletal elements involved in stabilizing cell-to-cell connections, cellular shape changes, and cellular migration. Actin in cells is present as either single monomers called globular actin (G-actin) or in a polymerized form called filamentous actin (F-actin). These actin filaments themselves are the building blocks of complex actin networks (Blanchoin et al., 2014). Such networks include branched actin networks, crosslinked actin networks, parallel actin bundles and anti-parallel actin bundles. Branched actin networks have roles in force generation during cellular movement and shape changes, constantly assembling itself and polymerizing due to the presence of the Arp2/3 complex (Blanchoin et al., 2014). On the other hand, crosslinked actin networks, lacking Arp2/3 complexes, have roles in controlling and maintaining cell shape and mechanical integrity, increasing the elasticity and decreasing the viscosity of cells (Blanchoin et al., 2014). The final two actin networks are parallel actin bundles and anti-parallel actin bundles. Parallel actin bundles are found in many types of cellular protrusions such as filopodia and microvilli having roles in force generation (Blanchoin et al., 2014). Parallel actin bundles are made of filaments with barbed ends oriented in the same direction, generally facing the cell membrane (Blanchoin et al., 2014). Anti-parallel actin bundles have roles in cytokinesis and stress fiber formation important in cell-to-cell and cell-matrix adhesion (Blanchoin et al., 2014). Additionally, they form a contractile network with myosin (Blanchoin et al., 2014). The rest of this section below will focus on the various stress fiber categories.

Stress fibers are bundles of actin filaments in non-muscle cells (Tojkander et al., 2012). Typically, the filaments are crosslinked by α-actinin. Approximately 10-30 actin filaments are bundled to form a stress fiber (Pelligrin & Mellor, 2007). Stress fibers also contain non-muscle types of myosin, usually allowing the fibers to generate contractile forces. The stress fibers

are often anchored to focal adhesions. Focal adhesions are distinct sites at which cells become mechanically attached to the extracellular matrix (ECM). The ECM is synthesized by the cells and/or derived from serum proteins, such as vitronectin and fibronectin adsorbing to plastic culture surfaces (Arima & Iwata, 2015; Chen et al., 2015; Heath & Dunn, 1978; Schneider & Burridge, 1994). Stress fibers can differ in their morphology and association with focal adhesions and have been categorized into at least four types: ventral stress fibers, dorsal stress fibers, transverse actin arcs, and perinuclear actin cap fibers (Fig 1.4) (Maninova et al., 2017). Ventral stress fibers are on the basal side of the cell body and are anchored at both ends to focal adhesions. In contrast to ventral stress fibers, dorsal stress fibers or radial fibers are associated with focal adhesions at only one end. Transverse actin arcs are curved and lie parallel to the leading edge of a migrating cell. They assemble in the lamellipodium and move from the leading edge to the cell center, where they gradually disappear in front of the nucleus. The perinuclear actin cap consists of stress fibers positioned above the nucleus.

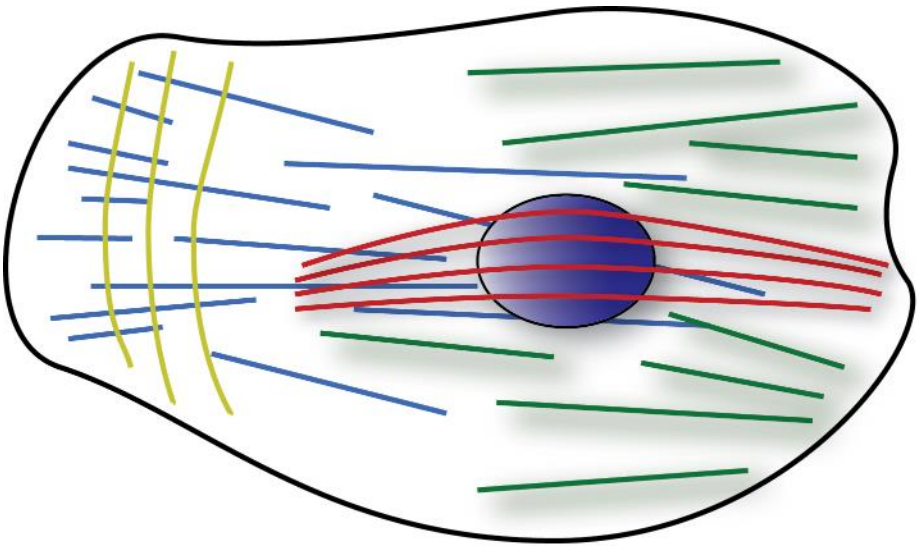

Figure 1.4. Actin stress fiber arrangements. Cell diagram demonstrating four categories of stress fibers: dorsal stress fibers in green, transverse actin arcs in yellow, ventral stress fibers in blue, and perinuclear actin cap fibers in red. The figure was adapted from Maninova et al. (2017).

1.2.3.2. Microtubules

Microtubule functions involve being the "rails" for cellular transport, drivers of chromosome separation during cellular division, flagella and cilia organization, and regulators of cell morphogenesis and polarity (Akhmanova & Steinmetz, 2015). Formation of microtubules requires the polymerization of αβ-tubulin heterodimers, comprised of α- and β-tubulin monomers on either the plus or minus end of the growing microtubule (Akhmanova & Steinmetz, 2015). It is recognized that both microtubule ends can undergo polymerization, however, the dynamic properties of the ends differ. The plus end generally polymerizes faster but is less stable and undergoes catastrophe more often than the minus end (Akhmanova & Steinmetz, 2015). New microtubule tips contain a GTP-tubulin cap, stabilizing the newly formed microtubular ends (Akhmanova & Steinmetz, 2015). In the event of the loss of a GTP-tubulin cap, microtubule shrinkage occurs (Akhmanova & Steinmetz, 2015). Additionally, microtubule end dynamics alter with the loss of a cap. The plus end depolymerizes while the minus end remains stable and continues to slowly grow (Akhmanova & Steinmetz, 2015).

In general, microtubules can be seen radiating from specific points in a cell, called microtubule-organizing centers (MTOC), localized to the minus end of microtubules. MTOCs have functions in microtubule nucleation, stabilization, and/or anchoring (Sanchez & Feldman, 2010). An example of a well-known MTOC is the centrosome, considered "the major microtubule-organizing center in the cell" (Sanchez & Feldman, 2010). However, non-chromosomal (nc) MTOCs have been discovered in differentiated cells. The complete function of nc-MTOCs remains a mystery but researchers have shown that these types of MTOCs are critical to cell function (Sanchez & Feldman, 2010).

1.2.3.3. Intermediate Filaments

Intermediate filaments are comprised of a large group of proteins with roles in maintaining cellular structural integrity. Some can be termed as "mechanical stress absorbers" (Sokolova et al., 2006). Cell types can vary in their intermediate filament composition. For example, muscle cells synthesize desmin, epithelial cells synthesize keratins, whereas mesenchymal cell types synthesize vimentin (Sokolova et al., 2006). However, all cells contain nuclear lamins (Sokolova et al., 2006).

1.2.4. Intestinal wound healing

When the intestinal epithelium is damaged, a quick and efficient recovery must occur to regain proper intestinal function and homeostasis. If not properly healed, loss of function and loss of defence to intraluminal toxins, immunogenic compounds, and bacteria can occur, all leaking through the epithelium. One form of recovery is called wound healing. The process of wound healing occurs in three steps: 1) Cells migrate quickly to close the wound. This step can be termed restitution where cell proliferation is limited (Sturm & Dignass, 2008). 2) Cells undergo proliferation to replenish the depleted cell pool (Sturm & Dignass, 2008). Finally, 3) Cells mature and differentiate to regain proper intestinal function (Sturm & Dignass, 2008). This is a simplified model of wound healing. In reality, the three steps do not happen directly in series where overlap will occur. However, this is a useful model to study the physiology of wound healing. It is known that regulatory peptides, such as growth factors and cytokines, are important mediators of wound healing acting through a TGF-β-dependent pathway. These peptides act on the basolateral side of the epithelial surface (Sturm & Dignass, 2008). Interestingly, TGF-β3 has been shown to block proliferation of various human cells by inhibiting other human growth factors such as TGFα, PDGF-BB, and VEGF, suggesting that growth factors are likely not the main drivers of early phase wound healing, being the restitution or migration step (Bhatia et al., 2016). It was found that secreted HSP90α is the likely promotility factor initiating cellular restitution or migration to close the wound (Bhatia et al., 2016). It is important to note that these wound healing studies, finding HSP90α as an important factor, were done on skin and not the intestinal epithelium. Additionally, fish intestinal wound healing and factors involved in the process are poorly understood.

1.3. POTENTIALLY HARMFUL CONDITIONS AND COMPOUNDS TO THE INTESTINAL EPITHELIUM

Several practices in aquaculture have the potential to be detrimental to fish intestinal mucosa health. Three examples are food deprivation, temperature stress, and antinutritional components in fish feed. Knowledge of how these impair cellular functions in the fish intestinal epithelium is limited but needed to improve aquaculture.

1.3.1. Food deprivation

All animals appear to have the ability to survive periods of food deprivation, but fish seem to have an exceptional ability to do this and this ability is used in some aquaculture procedures. Food deprivation arises in different ways and several terms are used to describe the cause of food deprivation, including starvation, fasting and anorexia. These definitions refer to a postabsorptive animal. A postabsorptive animal has an empty gastrointestinal tract and derives energy from the breakdown of the body's reserves. Starvation is a biological condition in which a postabsorptive animal is willing or able to eat but does not do so because food is extrinsically limited in some manner (McCue, 2010). Fasting is biological condition in which a postabsorptive animal has food available to eat but does not do so. Anorexia is a loss of appetite and can be a mechanism behind fasting. The terms starvation and fasting have been derived largely from research on mammals and birds (Wang et al., 2006) and have not always been used uniformly (Lignto & LeMaho, 2012) as under some circumstances the distinction between the two is difficult to draw (McCue, 2010). How well the terms apply to other vertebrates, such as fish, is unclear (Wang et al., 2006), and so the terms that will be used in the following brief literature review on salmon and food deprivation will be as used by the authors in the original publications.

Starvation, fasting or anorexia can arise at a number of points in the salmon life cycle. Most famously, during spawning migrations salmon fast for many months (Wang et al., 2006). As well, salmonids in northern latitudes often fast over the winter months (Pottinger et al., 2003). Young salmon metamorphose from freshwater parr to marine smolt and fasting can be part of smoltification. Some Atlantic salmon parr do not migrate to the sea during their first year but instead spend the winter under stones in streambeds and do not eat (Metcalfe & Thorpe, 1992). Finally, infection by bacteria can induce anorexia as a possible host defense mechanism (Exton, 1997; Pirhonen et al., 2003).

For several procedures in aquaculture, fish are deprived of food. In these circumstances the convention appears to be to describe food deprivation for less than 2 weeks as fasting and for longer as starvation. In general terms, starvation or fasting empties the gut and reduces oxygen consumption and production of waste (Ashley, 2007; Lines & Spence, 2012). The procedures that utilize food deprivation include transport, treatment of diseases, transfer of smolts from freshwater to seawater, and slaughter. The food deprivation appears to help fish

tolerate the stress of handling and transportation (Davis & Gaylord, 2011; Lopez-Luna et al., 2013). Additionally, emptying the gut before slaughter reduces spoilage (Lopez-Luna et al., 2014). As well, fasting is thought to improve flesh quality by enhancing flesh color (Regost et al., 2001), muscle firmness (Alvarez et al., 2008), and taste (Palmeri et al., 2009), although fasting too long can impair quality (Bermejo-Poza et al., 2017).

The first physiological system in animals to be directly affected by starvation or fasting is the GI tract (Ferraris & Carey, 2000). A common observation for fish is that intestinal tissue mass and activities of digestive enzymes decline during food deprivation (Krogdahl et al., 2005). A number of anatomical and histological changes have also been noted. The mucosal fold number and height were reduced in starved rainbow trout (MacLeod, 1978). Enterocytes declined in size and lost lipid droplets during the fasting of Atlantic salmon but the number of goblet cells increased (Baeverfjord & Krogdahl, 1996). Animal intestinal cell lines have rarely been studied, if ever, as tools to study the responses of the GI tract to starvation but could be useful.

1.3.2. Temperature stress

How the intestinal epithelium of fish responds to temperatures extremes has rarely been studied but heat stress has been found to be detrimental to the intestinal epithelial barrier in humans (Dokladny et al., 2016) and farm animals (Pearce et al., 2013). Global warming is anticipated to modulate the physiology of fish (Mazumder et al., 2015) and is a concern for aquaculture because in net pens fish cannot behaviorally thermoregulate (Hermansen & Heen, 2012). Besides responses to elevated temperatures, the effects on fish at lower temperatures are also of interest because climate change is expected to increase temperature variability, and as a result, fish will experience cold shock more frequently (Szerkeres et al., 2016).

Cells respond to temperature changes with the heat shock response (HSR), helping them protect and survive abnormal and abrupt temperature increases. A HSR is inducible not only by temperature but also by a variety of other stressors (Jolly & Morimoto, 2000). The HSR response is seen ubiquitously in nature and functions through a highly conserved set of proteins called heat shock proteins (HSPs) or chaperones. HSPs are divided into families according to their molecular size. These include small HSPs, HSP40, HSP60, HSP70, HSP90, and HSP100 (Lindquist & Craig, 1988; Jolly & Morimoto, 2000). HSP expression can be constitutive or induced by stress. HSPs vary in function by generally being molecular

chaperones and/or proteases (Mayer & Bukau, 2005). Chaperones are involved in maintaining native protein conformations while the proteases will act by degrading damaged proteins; hence, both types can help the cell survive under stressed conditions (Mayer & Bukau, 2005). The HSR is considered a genome-wide event and recent studies have shown other, less prominent but still necessary, potential functional classes of heat shock related proteins (Richter et al., 2010). They include DNA and RNA repair proteins, metabolic enzymes, regulatory proteins such as transcription factors, proteins helping with cytoskeletal stability, and proteins involved in transport and detoxification (Richter et al., 2010).

1.3.3. Antinutrionals

Plant meals and oils are being used or considered as replacements for fishmeal and fish oils because this is environmentally sustainable (Jobling, 2015). One major concern with the use of plants in feeds is that plants can contain antinutritional factors (ANF) (Jobling, 2015). As the name suggests, ANFs diminish nutritional uptake by altering the palatability of the feed, altering the digestion and absorption of the nutrients, decreasing feed utilization, and/or affecting metabolic capabilities (Jobling, 2015). One popular plant-based feed containing some ANFs is soybean meal. Such ANFs include lectins, protease inhibitors, phytic acid, saponins, phytoestrogens, antivitamins, and allergens (Francis et al., 2001). Many studies have reported that soybean meal induces enteritis in salmonids (Burrells et al., 1999; Buttle et al., 2001; Nordrum et al., 2000; van den Ingh et al., 1991). Furthermore, elevated water temperatures increase the severity of soybean-induced enteritis (Uran et al., 2008).

1.4. POTENTIALLY BENEFICIAL COMPOUNDS TO THE INTESTINAL EPITHELIUM

Searching for and identifying a compound or a group of compounds that can individually or synergistically improve gut health can promote better overall health and animal welfare. With the immense importance of animal agriculture in today's society, the threat of heat stress due to global warming is problematic on such agricultural systems by potentially decreasing animal performance productivity (e.g. milk and egg production), reducing animal reproduction, and increasing animal death events, all leading to substantial economic toll (St-Pierre et al., 2003). Hence, this section will focus on nutritional components that have been

shown to improve gut health, on a cellular and/or organismal level, under normal conditions and heat stress.

1.4.1. Nucleotides

Fundamentally, nucleotides are essential to biological life. They are the constituents of nucleic acids and are also key molecules as intermediates, mediators, allosteric regulators, coenzyme components, and agonists driving energy production and cellular metabolism (Hess & Greenberg, 2012). Under stress, nucleotide pools can become depleted; hence, exogenous supplementation of selective nucleotides can be indispensable to post heat stress recovery (Hess & Greenberg, 2012). Exogenous supplies of nucleotides, for the most part, enhance cellular proliferation (Hess & Greenberg, 2012; Rathbone et al., 1992; Rodriguez-Serrano et al., 2007; Sato et al., 1999). Additionally, nucleotide supplementation has been shown to improve cellular cytoskeleton protective mechanisms and enhance resistance against different stresses. In a study conducted with rainbow trout fingerlings, dietary nucleotides increased growth and resistance to acute stress from excessive handling and crowding (Tahmasebi-Kohyani et al., 2012). Similar results were also seen in channel catfish and sole (Palermo et al., 2013; Welker et al., 2011). In mammals, dietary nucleotides enhance cytoprotection to thioacetamide induced liver damage in rats (Torres et al., 1997). Additionally, cytoprotection was seen with adenosine and inosine in a model of tubular necrosis using rat kidney tubular cells (Modis et al., 2009). Interestingly, in a study by Glencross & Rutherford (2009) it was shown that the most effective diet strategy in reducing the effects of growth retardation of barramundi due to high water temperatures was a higher protein diet with no nucleotides and not a normal protein + nucleotide diet. On the other hand, the effects of nucleotides on the HSR have not been extensively researched and is a promising path for future studies.

1.4.2. Amino Acids

In contrast to nucleotides, many studies have focused on the protective effects of amino acids (AA) and their relations with the HSR. The most famous AA in nutritional studies is glutamine. Being extensively studied, glutamine is known to have many nutritional values fitted to improve gut health and overall health. Beneficial effects include increased cellular proliferation, decreased cellular apoptosis, enhancements in TJ protein expression and localization, all leading to significantly enhanced intestinal microstructure and increased

enterocyte migration rates (Evans et al., 2005; Larson et al., 2007; Li et al., 2004; Pohlenz et al., 2012). Furthermore, multiple studies have demonstrated that glutamine can act as an enhancer of the HSR (Chow & Zhang, 1998; Liu et al., 2015; Wischmeyer et al., 2001). Glutamine's HSR enhancing effects are mediated through the hexosamine biosynthetic pathway (HBP) (Hamiel et al., 2009). Being a key substrate of the HBP, glutamine increases HSP70 expression via augmented HBP activity generating increased O-glycosylation, nuclear translocation, and transcriptional activation of heat shock factor-1 (HSF-1) and Sp1 (Hamiel et al., 2009). Both HSF-1 and Sp1 are key transcription factors of HSPs (Hamiel et al., 2009). However, glutamine also can protect cells by other pathways such as being the precursor of protective antioxidant, glutathione or through its functions as an osmotically acting AA (Baird et al., 2013). Another important AA that elicits thermoprotective effects and is useful in improving gut barrier functions is threonine. Threonine appears to protect cells from heat stress by increasing HSP70 and HSP25 expression generating enhanced cytoprotection and decreased apoptosis (Baird et al., 2013). Similarly to glutamine, threonine's protective pathways are multifaceted (Baird et al., 2013).

1.4.3. Fatty Acids

Polyunsaturated fatty acids (PUFA) are important components influencing membrane fluidity, immune responses, and epithelial barrier function (Amasheh et al., 2009). PUFAs such as eicosapentaenoic acid (EPA), γ-linolenic acid (GLA), and docosahexaenoic acid (DHA) have been shown to generally increase fluorescein sulfonic acid permeability and decrease transepithelial electrical resistance (TEER) on a Caco-2 cell monolayer; however, in another study, EPA and linolenic acid (LA) had no effect on TEER in Caco-2 (Rosella et al., 2000), while longer incubations with LA caused an increase in TEER (Roche et al., 2001). Interestingly, EPA and DHA caused an improvement in resistance and decreased IL-4 mediated permeability in T84 (human colon carcinoma) cell monolayer (Willemsen et al., 2008).

The short chain fatty acid butyrate, produced by the intestinal microflora, also appears to have significant positive effects on the GI tract, such as being anti-inflammatory, reinforcing the intestinal barrier, and improving the oxidative status of the intestine (Canani et al., 2011).

Also, butyrate has been shown to induce HSP25 in rat IEC-18 (intestinal epithelial) cells and protected the cells against oxidative stress (Ren et al., 2001).

1.4.4. Flavonoids

Phytochemicals have generated considerable interest as compounds that can promote the intestinal mucosa health (Amashen et al., 2009). Phytochemicals constitute thousands of chemicals that are divided into multiple classes. One important class is the flavonoids.

Flavonoids consist of two aromatic rings (A and B) linked through 3 carbons. The A ring is synthesized in the acetate pathway; the B ring, the shikimate pathway. The heterocyclic C ring links the A and B rings and variations in the C ring lead to the designation of six flavonoid subclasses: flavonols, flavones, isoflavones, flavanols, anthocyanidins, and flavanones. Over 5,000 different flavonoids have been identified. Quercetin and kaempferol are two commonly studied flavonols. Apigenin is an example of a flavone. Genistein is a frequently investigated isoflavone. Flavanols or catechins include epicatechin. Examples of anthocyanidins are malvidin and cyanidin. Naringenin is a flavanone. Many flavonoids are attached to sugars to become glycosides. For example, rutin is the glycoside combining quercetin with the disaccharide rutinose, and naringin is a flavanone-7-O-glycoside between naringenin and the disaccharide neohesperidose.

Flavonoids are a broad group of secondary plant metabolites (Ross & Kasum, 2002) that are found in all foods of plant origin for humans and other animals. In plants flavonoids have different functions. Many provide protection against pathogens. Others aid pollination by attracting insects. For humans and animals, flavonoids appear to benefit health. The specific health benefits are still being debated and possible mechanisms of action are still being explored. A common action likely contributing to health benefits are the antioxidant and free-radical scavenging abilities of flavonoids.

In mammals, intestinal mucosa health appears to be improved by at least three flavonoids: epicatechin, quercetin, and naringenin. Epicatechin appears to be a gastroprotective agent against induced ulceration in rats through strengthening the mucus barrier, neutralizing gastric juices, while also increasing nitric oxide NO and HSP70 (Rozza et al., 2012). In this case it appears that NO is acting as a protective agent in the gut by increasing gastric mucosal blood flow, controlling the secretion of mucus and bicarbonate, and inhibiting the secretion of

gastric juices (Rozza et al., 2012). In some studies, quercetin appears to be a heat-sensitizing agent, inhibiting HSFs in a cell specific way (Hansen et al., 1997). On the other hand, quercetin appears to be a quite beneficial diet component under normal conditions considering its antioxidant capabilities while also enhancing intestinal barrier functions (Amasheh et al., 2008). Lastly, naringenin in addition to its antioxidant capabilities, possesses anti-inflammatory, anticarcinogenic, antidiabetic, and anti-lipidemic properties, and more recently it has been shown to have TJ modulating effects (Noda et al., 2013).

1.5. *IN VITRO* MODELS OF INTESTINAL EPITHELIAL CELLS

1.5.1. Mammalian intestinal epithelial cell lines

A large number of intestinal cell lines have been developed from mammals, allowing researchers and healthcare professionals to further study and advance intestinal epithelial barrier biology and GI tract knowledge in a cheaper, quicker, and more efficient manner. One of the most popular intestinal cell models is Caco-2, a human colon adenocarcinoma cell line (Liu *et al*., 2014). The *in vitro* use of intestinal cell lines can be very beneficial in studying cellular gut responses to stress while also allowing researchers to accumulate information that could be valuable to *in vivo* studies.

Caco-2 has been cultured in different ways to develop the most representative model of the intestinal epithelium. Most commonly Caco-2 has been grown as adherent cells on plastic surfaces treated in proprietary ways for tissue culture and configured into flasks, petri dishes, and multiwell plates. A most successful advancement has been to culture the cells on flat, porous supports. These have been used as transwell inserts in multiwell plates to divide a well into a lower basal compartment and upper apical compartment. On these porous inserts, Caco-2 cells differentiated spontaneously to form confluent monolayers that had the structural and functional characteristics of the human small intestinal epithelium (Hilgers et al., 1990). This had become a widely used *in vitro* system for studying intestinal epithelial transport.

A concern with some of the Caco-2 culture systems is the absence of a basement membrane (BM) (Vllasaliu et al., 2014). A BM, which is a specialized extracellular matrix (ECM), supports the intestinal epithelial cells *in vivo*. The intestinal BM is thin and composed of several proteins, including laminins, type IV collagen and fibronectin. These proteins are thought to play roles in intestinal cell proliferation, differentiation, and migration (Bason et al.,

1996). Thus ECM proteins have been added to some Caco-2 culture systems and found to stimulate proliferation and isomaltase activity (Bason et al., 1996). Caco-2 cells on laminin showed enhanced cell migration (Agle et al., 2010). However as cultures are maintained, endogenously synthesized and organized ECM proteins likely contribute to the differentiation and maintenance of intestinal epithelial functions.

Mammalian intestinal epithelial cell lines vary in what structures and function they express. This is illustrated with microvilli, which are specialized actin structures. Microvilli are membrane protrusions with a core of bundled actin filaments tethered laterally to the plasma membrane by proteins of the ezrin/radixin/moesin (ERM) family (Lange, 2010). Microvilli can be found in many cell types and increase cell surface area and are essential for Ca^{2+} signaling. In the intestine, enzymes involved in digestion and absorption are concentrated on the microvillar membrane. For a porcine intestinal epithelial cell line, microvilli are usually only acquired in significant number under special differentiation culture conditions, such as maintenance at confluency for several weeks on collagen coated inserts (Green & Niewold, 2011), although some intestinal epithelial cell lines, like LS174T and HT-29, have few microvilli (Bu et al., 2011; Mitchell & Ball, 2004).

Mammalian intestinal epithelial cell lines have been used to study wound healing, including identifying the roles of cellular protrusions with actin frameworks in the migration of intestinal epithelial cells in wound healing (Khurana et al., 2008). These are filopodia and lamellipodia. Filopodia are found at the leading edge of many migrating cells and are filled with tight parallel bundles of F-actin (Mattila & Lappalainen, 2008). They often protrude from the lamellipodial actin network. Very short filopodia are term microspikes. Filopodia are thought to act like antennae, allowing cells to probe their environment. Lamellipodia are cell protrusions with a branched network of F-actin and are an essential part of the machinery for cells to crawl (Krause & Gautreau, 2014). Lamellipodial protrusion is powered by actin polymerization and lamellipodia have highly dynamic, short-lived actin filaments. Behind the lamellipoda is the bulk of the protrusive region, termed the lamellum. The lamellum contains less dynamic, longer-lived actin filaments.

1.5.2. Piscine intestinal epithelial cell lines

Only one fish intestinal epithelial cell line is available for research. This is RTgutGC from the distal portion of the intestine of a female rainbow trout (Kawano et al., 2011) and its utility in research is just starting to emerge. The cell line possesses an epithelial like morphology and exhibits alkaline phosphatase activity, an indication of enterocyte differentiation (Kawano et al., 2011). Geppert et al. (2016) and Minghetti et al. (2017) explored whether RTgutGC can form a functional epithelium on permeable supports. Culturing on the permeable supports was successful and allowed Geppert et al. (2016) to study the transport of nanoparticles across the cell layer. RTgutGC in culture forms tight junctions and desmosomes (Minghetti et al., 2017). Cells become polarized in culture, evident by basolateral localization of Na^+/K^+ -ATPase and apical localization of ZO-1 (Minghetti et al., 2017). Monolayers of RTgutGC exhibit a measurable transepithelial electrical resistance (TEER) up to 50 Ω cm^2 (Geppert et al., 2016; Minghetti et al., 2017). When referencing Claude and Goodenough (1973), RTgutGC's TEER values are considered "leaky". Similar TEER values are seen *in vivo* with Atlantic salmon intestines generating values between 30 – 150 Ω cm^2 (Sundell et al., 2003). The initial characterization done by Geppert et al. (2016) and Minghetti et al. (2017) shows lots of promise for the cell line and supports the use of RTgutGC as an intestinal barrier model for fish.

1.6. HYPOTHESIS

The hypothesis underlying this thesis is that bioassays can be developed with the rainbow trout intestinal epithelial cell line, RTgutGC, for identifying potential beneficial additives and detrimental antinutritionals. The overarching goal is that such bioassays can be used in the future to screen large numbers of compounds and extracts in order to develop improved fish feeds, especially feeds that will promote gut health during periods of temperature stress.

1.7. SPECIFIC RESEARCH AIMS

Background work has been done on the responses of RTgutGC to different culture conditions as well as illustrative work with specific potential feed additives and antinutritionals. The results are organized into five chapters (Chapters 2 to 6) that address the following specific aims:

1. (Chapter 2). Are RTgutGC able to survive and maintain their cytoskeletal organization in different kinds of starvation?

2. (Chapter 3). Will RTgutGC respond to a potential phytochemical feed additive, naringenin?

3. (Chapter 4). Will the migration of RTgutGC in a wound-healing assay be influenced by antinutrionals in soybean and wheat germ meal?

4. (Chapter 5). How is the migration of RTgutGC influenced by different temperatures?

5. (Chapter 6). Will naringenin modulate the ability of RTgutGC cells to maintain their actin cytoskeleton and substrate adherence during recovery from heat stress?

CHAPTER 2

Effect of different kinds of starvation on the survival, HSP70 levels, cytoskeleton, tight junctions, and barrier functions of rainbow trout intestinal epithelial cells *in vitro*

2.1. INTRODUCTION

In the salmonid aquaculture industry, fish are exposed to many stressors, including handling of fish during transport, sorting, and stocking (Ramsay et al., 2009) and starvation (Ashley, 2007; Lines & Spence, 2012). A common practice is to deprive the fish of food for several days before any intense handling to decrease amounts of fecal materials and waste in the tanks (Ramsay et al., 2009). Also, this practice of food deprivation provides a shift in metabolic energy to more effectively respond to the stressor as less energy is needed for digestion and nutrient uptake (Beamish, 1978; Jobling, 1983). Long term food deprivation can lead to negative effects such as reduced reproductive abilities, reduced growth, reduced immunity, and lower tolerance to disease, as energy reserves are allocated to maintain vital processes (Eslamloo et al., 2017; Martin et al., 2010; Niehoff, 2000; Weber & Bosworth, 2005). Fat, protein, and carbohydrate reserves during starvation become depleted, and if not replenished, mortality is inevitable. On the other hand, short term starvation of around 4 days has been shown to be tolerable in certain fish species including rainbow trout if re-feeding occurred after the starvation period (Azodi et al., 2015). One response of interest is the expression of certain heat shock proteins (HSP) to stressors. In certain cases, it has been shown that starvation can cause the induction of HSP70 and HSP90 in larval rainbow trout undergoing starvation leading to the possibility of HSPs being a starvation bio-indicator (Cara et al., 2005). However, this response appears to be tissue specific and does not occur in all tissue types that would be directly influenced by starvation such as the intestine (Antonopoulou et al., 2013). Starvation might be conveniently studied *in vitro*: the *in vitro* advantages include being able to study a specific cell type and to do studies at less cost and with less ethical concerns compared to *in vivo*.

Most research on starvation with mammalian cell lines has focused on cancer biology, with intestinal cell lines used only occasionally. How tumor and normal cells respond to nutrient deprivation has been studied, with the aim to exploit differences for cancer therapy. Survival of human cells in subconfluent cultures was studied in a medium with vitamins and salts but lacking serum, glucose and amino acids (Izuishi et al., 2000). In this medium, normal human fibroblasts died within 24 h whereas cancer cell lines survived much longer, often up to 3 days. Follow up studies have supported the generalization that cancer cells survive nutrient deprivation much better than their normal counterparts (Kim et al., 2015; Raffaghello et al.,

2008; Song et al., 2011). This includes colorectal cancer derived cell lines (Sato et al., 2007). The starvation-resistant phenotype has been dubbed "austerity" (Izushi et al., 2000; Esumi et al., 2002).

Only one published report has appeared on the effects of starvation on fish cell lines, and again this did not include an intestinal cell line. As a minor part in the characterization of the cell line, HEW, from Haddock larvae, the ability of HEW cells to remain viable in monolayers was evaluated in media that provided different levels of nutrient deprivation (Bryson et al., 2006). The complete or normal growth medium (L15/FBS) was Leibovitz's basal medium L15 (Leibovitz, 1963), with a supplement of fetal bovine serum (FBS), which is the most commonly used undefined supplement for fish cell cultures (Bols et al., 2005). The basal medium, L15, contains amino acids, vitamins, galactose, pyruvate and salts and was used to study serum deprivation. Amino acid and vitamin deprivation was done in L15/ex, which has only the galactose, pyruvate, and the salts of L15 (Schirmer et al., 1997). L15/salts, which was referred to as simple salt solution (SSS), has no nutrients and provided complete nutrient deprivation. As judged with the indicator dyes alamar Blue, CFDA-AM, and neutral red, HEW and three other fish cell lines (CHSE-214 from Chinook salmon embryo, PHL from Pacific herring larvae, and RTG-2 from rainbow trout gonads) remained viable for at least a week in L15/salts (Bryson et al., 2006). The results imply that fish cells withstand starvation better than mammalian cells but only a limited number of cellular parameters were examined and intestinal cells were not studied.

In this study, RTgutGC, a rainbow trout intestinal cell line was used to study the effects of various kinds of starvation ranging from the lack of serum to complete starvation in a SSS over 6-7 days. The results demonstrate that cells were able to survive a 7 day starvation period but with reductions in barrier functions, wound repair, and changes in cytoskeletal structure. Additionally, increasing degrees of starvation in RTgutGC cells up regulates HSP70 protein levels.

2.2. MATERIALS AND METHODS

2.2.1. Cell cultures and culture conditions

RTgutGC, a rainbow trout epithelial cell line was used throughout the experiment. This cell line was developed in Niels C. Bols' laboratory at the University of Waterloo (Kawano et al., 2011). Medium used to culture the cells was Leibovitz's L15 with 2.05 mM L-Glutamine (Thermo Fisher Scientific) additionally supplemented with 10% fetal bovine serum (FBS, Sigma-Aldrich) and antibiotics (10,000 U/mL penicillin and 10,000 ug/mL streptomycin, P/S, Thermo Fisher Scientific) (L15/FBS). Cells were subcultured or passaged using trypsin (Thermo Fisher Scientific) every week at a 1 to 2 split and maintained at 18 ^{o}C. The cell culture vessels used were BioLite 75 cm^2 cell culture treated flasks (Thermo Fisher Scientific).

2.2.2. Starvation timeline

Once cells were seeded into culture vessel of choice, depending on the assay, cells were allowed to establish a monolayer in L15/10% FBS at 18 ^{o}C for 3-4 days. Once a confluent monolayer was established, the medium was removed, the cells were washed with Dulbecco's phosphate-buffered saline solution (DPBS, Thermo Fisher Scientific), and medium was changed to either L15/FBS (complete medium), L15 media without FBS (L15: medium containing amino acids, vitamins, inorganic salts, sodium pyruvate, and galactose), L15 media lacking amino acids and vitamins (L15/ex: medium containing only sodium pyruvate and galactose), or an inorganic salt solution (L15/salts). The range of nutritional starvation ranged from no starvation with L15/FBS, serum starvation with L15, serum, amino acid, and vitamin (SAV) starvation with L15/ex, and complete starvation with L15/salts. After the medium change, cells were left to incubate for 7 days at 18 ^{o}C in respective media conditions with one exception of the Lucifer yellow assay being performed on day 5 of starvation. All other assay end points are on day 7.

2.2.3. Cellular viability

Cellular viability was monitored by changes in cell morphology through phase contrast microscopy and with the indicator dyes, alamar Blue® (AB, Thermo Fisher Scientific) and 5' -carboxyfluorescein diacetate acetoxymethyl ester (CFDA-AM, Sigma-Aldrich). The AB assay provides a measure of metabolic activity, whereas the CFDA-AM assay provides a measure of plasma membrane integrity (Dayeh et al., 2013). The protocol used for the AB and

CFDA dyes follows closely Dayeh et al. (2013) methods. RTgutGC cells in L15/FBS were plated in 24-well plates at a density of 125,000 cells per well in replicates of 4. Plates followed an incubation timeline as described in section 2.2.2 with the four various nutritional conditions. On day 7 the media were then removed, the cells were washed with DPBS, and a solution containing 5% (v/v) AB and 4 μM CFDA-AM in DPBS was added to the cells. Plates were then incubated at room temperature for 1 hour in the dark. Using a series 4000 CytoFluor fluorescent plate reader (PerSeptive Biosystems – Thermo Fisher Scientific), results were recorded as relative fluorescent units (RFUs). The mean RFUs for the experimental wells were expressed as a percentage of the mean RFUs for control wells.

2.2.4. Cell diameter and volume

Cell size in suspension was determined by using a Scepter handheld cell counter (Millipore). RTgutGC cells in L15/FBS were plated in 12-well plates at a density of 325,000 cells per well. Plates followed an incubation timeline as described in section 2.2.2 with the four various nutritional conditions. On day 7 the media were then removed, the cells were washed with DPBS, collected into a cell suspension using trypsin, centrifuged, and resuspended in DPBS. Finally, cell size was determined with the Scepter cell counter.

2.2.5. Fluorescence microscopy of RTgutGC cytoskeleton

F-Actin

F-actin was visualized using fluorescein isothiocyanate labeled phalloidin (FITC-phalloidin, Sigma-Aldrich) and confocal microscopy. Phalloidin is a fungal toxin having an ability of binding to F-actin only in polymeric and oligomeric forms but not monomeric forms. The fluorescent conjugate of phalloidin, FITC, is used to label F-actin and can be visualized by fluorescence or laser microscopy. A 5 mg/mL stock solution of FITC-phalloidin was prepared in DMSO. RTgutGC cells in L15/FBS were plated in a 4 chamber tissue culture treated glass Falcon CultureSlide® (Corning) at a density of 150,000 cells per chamber. Slides followed an incubation timeline as described in section 2.2.2 with the four various nutritional conditions. At day 7, cells were washed with DPBS and fixed with 3% paraformaldehyde (Sigma-Aldrich) for 20 minutes at 4 ^{o}C. Following fixation, the cells were then permeabilized with 0.1% Triton X-100 (Sigma-Aldrich) for 10 minutes at room temperature. Afterwards, 5 μg/mL of FITC-phalloidin was added to the cells and allowed to incubate for 45 min at room

temperature in the dark. Cells were then washed three times with DPBS. Once dry, plastic chambers were removed from the slides and three drops of a mounting medium, Fluoroshield (Sigma-Aldrich), containing DAPI was added to the slides with a coverslip to help preserve the slide and counter stain for DNA. Confocal images were obtained with the Zeiss LSM 510 laser scanning microscope and were acquired and analyzed using a ZEN lite 2011 software.

α-tubulin

α-tubulin was visualized by indirect immunocytochemistry and confocal microscopy. RTgutGC cells in L15/FBS were plated in a 4 chamber tissue cultured treated glass Falcon CultureSlide® (Corning) at a density of 150,000 cells per chamber. Slides followed an incubation timeline as described in section 2.2.2 with the four various nutritional conditions. At day 7 cells were washed with DPBS and fixed with 3% paraformaldehyde (Sigma-Aldrich) for 20 minutes at 4 ^{o}C. Following fixation, the cells were then permeabilized with 0.1% Triton X-100 (Sigma-Aldrich) for 10 minutes at room temperature. Cells were then incubated in blocking buffer (BB) (10% goat serum, 3% bovine serum albumin, and 0.1% Triton X-100 in DPBS) for 1 hour at room temperature. At this point some chambers were incubated with primary antibodies while others were incubated with only secondary antibodies to control for nonspecific staining. The primary antibodies used were monoclonal anti-α-tubulin produced in mouse (Sigma-Aldrich) and were diluted 1:1000 in BB. Primary antibodies were incubated with the cells for 1 hour at room temperature on a rocker. Antibodies were then removed and the cells were washed three times for 3 minutes with DBPS before the addition of secondary antibodies. The secondary antibodies used were anti-mouse AlexaFluor® 488 produced in goat (Sigma-Aldrich) diluted 1:1000 in DPBS and allowed to incubate on the cells for 1 hour in the dark at room temperature on a rocker. After incubating, the antibodies were removed and cells were once again washed three times with DPBS. Once dry, plastic chambers were removed from the slides and three drops of a mounting medium, Fluoroshield (Sigma-Aldrich), containing DAPI were added with a coverslip to help preserve the slide and counter stain for DNA. Confocal images were obtained with the Zeiss LSM 510 laser scanning microscope and were acquired and analyzed using a ZEN lite 2011 software.

2.2.5. Fluorescence microscopy of RTgutGC tight junction associated protein, ZO-1

ZO-1 was visualized by indirect immunocytochemistry (ICC) and confocal microscopy. The staining protocol was the same as used for α-tubulin but differed in primary and secondary antibodies. The primary and secondary antibodies used were polyclonal anti-ZO-1 produced in rabbit (Thermo Fisher Scientific) diluted 1:100 in BB and anti-rabbit AlexaFluor® 488 produced in goat (Sigma-Aldrich) diluted 1:1000 in DPBS.

2.2.6. Measurement of epithelial barrier function

To evaluate tight junction integrity of the RTgutGC barrier, transepithelial electrical resistance (TEER) and Lucifer Yellow CH dilithium salt (LY) permeability were measured with the use of Transwell® permeable supports with 1 μm pore sizes (Corning). Cells were plated in a 24-well Transwell® supports system at a density of 120,000 per Transwell® with L15/FBS medium. The plates were then incubated for 7 days at 18 ^{o}C allowing the cells to form a barrier. Cells were washed with DPBS and medium was changed in both apical and basolateral wells to one of the four nutritional conditions described in section 2.2.2. TEER was measured over time using an EVOM with the STX2 chopstick electrode (World Precision Instruments). The unit area resistance (Ω cm^2) was then calculated. To measure barrier permeability by LY, 24-well plates with Transwell® permeable supports were also used. Cells were plated at the same density as above and allowed to incubate for 7 days at 18 ^{o}C in L15/FBS. As with the TEER set up, cells were then washed and the various four nutritional conditions were administered. After 5 days, the medium was removed and the cells were washed with DPBS. Then 0.1 mg/mL of LY in DPBS was added to the apical wells and allowed to incubate for 60 min in the dark. The Transwell® supports were then removed and the amount of LY in the basal compartment was quantified using a fluorescent plate reader with results recorded as RFUs. The data were then expressed as percent permeability being the percent difference of the blank with no cells on the Transwell® supports.

2.2.8. HSP70 detection

HSP70 was visualized by Western blotting. RTgutGC cells were plated in 6-well plates with L15/FBS at a density of 1,000,000 cells per well. Cells then followed an incubation timeline as described in section 2.2.2 with the four various nutritional conditions. After day 7, the cells were lysed by adding 200 μL RIPA lysis buffer containing a protease inhibitor cocktail

(Qiagen) directly to the plates. The cells were scraped off, transferred to microcentrifuge tubes, and allowed to sit on ice for 30 minutes. Tubes were then centrifuged at 10,000 x g for 1 minute and protein in supernatant was collected. Protein concentrations were determined using a Pierce BCA protein assay kit (Thermo Fisher Scientific). SDS-PAGE was performed using a Mini-PROTEAN tetra system (Bio-Rad) with premade 1 mm thick handcast gels. Loaded gels were run at 120 volts for 1 ½ hours. The transfer step onto a nitrocellulose membrane was performed in a Mini-Trans Blot Cell system (Bio-Rad) running at 150 milliamps for 1 hour. Equal protein loading was visualized by a 0.1 % Ponceau S stain in 5% (w/v) acetic acid. Before probing the membrane with rabbit anti-salmon HSP70 (Fish) polyclonal antibodies, binding only to the inducible form of HSP70 (SPC-314B, StressMarq), a 1 hour blocking step using 5% skim milk (w/v) in 1x TBS-T was performed. All antibodies were diluted in 5% skim milk (w/v) in 1x TBS-T. Rabbit anti-Salmon HSP70 (Fish) polyclonal antibodies were diluted 1:1000. To detect actin as a reference protein, rabbit anti-actin antibodies (Sigma Aldrich) were used and diluted 1:600. The secondary antibody used was goat anti-rabbit IgG conjugated to alkaline phosphatase (Sigma Aldrich) diluted 1:5000. Protein bands were detected by NBT/BCIP and membranes were scanned with a printer scanner.

2.2.9. Evaluating the effect of nutritional deprivation on wound healing and restitution

The ability of RTgutGC cells to heal a wound under different kinds of nutritional deprivation was investigated in a fence assay that utilized 2-well culture inserts from Ibidi GmbH, Planegg / Martinsried, Germany. The inserts were placed inside the wells of a 24 well plate to create two smaller wells. Approximately 50,000 cells in L15/FBS were seeded into each of the two insert wells, which were separated from each other by a rubber divider. The cultures were incubated at 18 °C and after 3 days monolayers had formed. At this time, the cultures were rinsed with DPBS, and the rubber divider removed to create a 500 μm gap between the monolayers. Immediately, L15/FBS, L15, L15/ex or L15/salts was added to the cultures and phase contrast microscopy pictures taken to document the size of gap or wound at time zero. The cultures were incubated at 18 °C for up to 7 days and the gap photographed every day to document the movement of cells into the wound. Two cellular processes contribute to wound healing, proliferation and migration (Iizuka & Konno, 2011). As L15/FBS is the routine growth medium for RTgutGC, the removal of the barrier or fence between the

wells and the addition of L15/FBS began a wound-healing assay. As RTgutGC do not proliferate in L15 (Kawano et al., 2011) and showed no signs of proliferation (mitotic figures) in the more nutritionally depleted L15/ex and L15/salts, the addition of these media after removal of the barriers assayed cell migration or restitution.

2.2.10. Statistical Analyses

Variables were expressed as the mean ± standard deviation. Statistical analysis was done by a one-way ANOVA and Tukey post hoc test or a two-tail unpaired student's T-test. Statistical significance was defined as $p < 0.05$.

2.3. RESULTS

2.3.1. Effect of nutritional deprivation on cell adherence, morphology and plasma membrane integrity

As viewed under the phase contrast microscope, confluent monolayers of RTgutGC cells remained adherent to the plastic surfaces of culture plates for at least 7 days despite nutrient deprivation of serum (L15), serum, amino acids and vitamins (L15/ex), and all nutrients (L15/salts). The monolayers were established in L15/FBS, and as monolayers became confluent, cells began to acquire a cobblestone shape (day 0) (A, Fig. 2.2). When the monolayers were maintained for a further 7 days in L15/FBS, L15, L15/ex and L15/salts, most cells became polygonal (B-E, Fig. 2.2). In L15/ex and L15/salts, the cells were larger and flatter. The polygonal shape was most prominent in L15/salts as phase dark lines often demarcated the periphery of cells (B-E, Fig. 2.2). As a measure of the integrity of the plasma membrane, the ability of the monolayers to retain esterase activity was measured with CFDA-AM and found to drop approximately 25 % in nutritionally deprived cultures (A, Fig. 2.1). However, little difference was found between cultures in L15, L15/ex and L15/salts. Overall the results suggest that most cells in RTgutGC monolayers at the start of the starvation remain viable after 7 days in nutritionally deprived media.

2.3.2. Effect of nutritional deprivation on energy metabolism

Energy metabolism was impaired after 7 days of nutritional deprivation, with the magnitude of the impairment increasing with the severity of the nutritional deprivation (B, Fig. 2.1). Energy metabolism was evaluated by the ability of cells to reduce alamar Blue (resazurin) to resorufin and was recorded as RFUs. Compared to the metabolism by cultures in the normal growth medium (L15/FBS), the metabolism by cells starved of serum (L15), of serum, amino acids, and vitamins (L15/ex), and of all nutrients (L15/salts) showed decreases of approximately 35%, 45%, and 87 % respectively.

2.3.3. Effect of nutritional deprivation on F-actin organization

Staining for F-actin with fluorescently labelled phalloidin showed stress fibers in RTgutGC but the staining intensity and distribution of stress fibers changed with nutrient deprivation (A, Fig 2.3). Shortly after RTgutGC monolayers developed in cultures (day 0), the cells had many short stress fibers running parallel to one another but with continued

maintenance in L15/FBS for 7 days the stress fibers became fewer and less intensely stained (A & B, Fig. 2.3). By contrast if L15/FBS was removed and the cells maintained a further 7 days in L-15 without serum, the stress fibers appeared longer and more numerous than at day 0 (C, Fig. 2.3). Furthermore, when monolayers were maintained for 7 days in either L15/ex or L15/salts, the stress fibers became much more intensely stained (D & E, Fig. 2.3). The stress fibers appeared thicker and many cells now had circumferential actin fibers, especially in L15/salts (E, Fig. 2.3). Therefore, depriving intestinal epithelial cells for 7 days of serum (L15), serum, amino acids and vitamins (L15/ex) or of all nutrients (L15/salts) elicited the development of prominent stress fibers.

2.3.4. Effect of nutritional deprivation on microtubule organization

Immunocytochemical staining for α tubulin revealed in each cell a network of cytoplasmic fibers that radiated out from a single, intensely stained region, which was next to the nucleus and is interpreted to be a microtubule organizing centre (MTOC), but α tubulin staining was changed by nutritional deprivation (Fig 2.4). For cells in L15 either with or without FBS, α tubulin organization was similar, although MTOCs appeared to become a little smaller after 7 days of culturing the cells in monolayers (B-D, Fig 2.4). By contrast, for cells in L15/ex and L15/salts for 7 days, the α tubulin network appeared to have fewer fibers but the fibers were thicker and longer. As well, the MTOCs were larger and more intensely stained (E & F, Fig 2.4). These changes were most pronounced for cells in no nutrients (F, Fig 2.4). Therefore intestinal epithelial cells deprived of serum, amino acids and vitamins (L15/ex) or of all nutrients (L15/salts) were able to maintain microtubule networks for at least 7 days but the nutrient deprivation altered the organization of α tubulin in microtubule fibers and in MTOCs.

2.3.5 Effect of nutritional deprivation on zonula occludens-1 (ZO-1) organization

ZO-1 (tight junction protein-1) was detected in RTgutGC by immunocytochemical staining, with nutritional deprivation causing a slight change in the staining pattern (Fig 2.5). Shortly after RTgutGC monolayers developed in cultures (day 0), cells showed diffuse cytoplasmic staining for ZO-1 (B, Fig. 2.5), but with continued maintenance in either L15/FBS, L15, L15/ex or L15 salts for 7 days ZO-1 now appeared at the cell periphery (C-F, Fig. 2.5).

However, in L15, L15/ex and L15 salts, the cytoplasmic staining was less and the staining at the periphery was thinner and more irregular (D-F, Fig. 2.5).

2.3.6. Starvation increases HSP70 levels in RTgutGC

HSP70 protein levels were measured by Western immunoblotting. After 7 days, increases in nutritional starvation (L15/FBS → L15 → L15/ex → L15/salts) caused a respective increase in HSP70 protein levels (Fig 2.6). No changes in the actin control bands were observed with increasing starvation.

2.3.7. Effect of nutritional deprivation on epithelial barrier functions

The ability of an RTgutGC monolayer to maintain a functioning barrier under different kinds of nutritional deprivation over time was evaluated by TEER (A, Fig 2.7). Initial day 0 readings of cells in the 4 different media ranged between 23.7 - 28.0 Ω cm^2. On day 1, differences in TEER were seen in L15/FBS and L15/salts (data not shown). L15/FBS cells' resistance increased to 38.0 ± 1.1 Ω cm^2 (compared to initial 27.3 ± 1.5 Ω cm^2 day 0 reading), whereas the resistance of cells in L15/salts decreased to 17.5 ± 1.1 Ω cm^2 (compared to initial 26.4 ± 2.4 Ω cm^2 day 0 reading). No day 1 differences in TEER were seen with cells in L15 or L15/ex. Over time, slight variations in TEER were observed with cells in L15/FBS. On day 7, the cells reached a TEER value of 41.2 ± 0.5 Ω cm^2. Cells in L15/salts reached a final TEER value of 17.5 ± 2.2 Ω cm^2 on day 7. Cells in L15 or L15/ex had a slower decrease in TEER over time compared to cells in L15/salts before eventually catching up to L15/salts values on day 5 (data not shown). Final TEER values for cells in L15 or L15/ex on day 7 were 15.3 ± 1.8 Ω cm^2 and 16.2 ± 2.5 Ω cm^2 respectively.

RTgutGC monolayers under different degrees of nutritional deprivation for 5 days had varying capacities to act as a barrier to the penetration of Lucifer yellow (LY) from the top chamber to the bottom chamber of two chamber culture systems (B, Fig 2.7). Consistently, the monolayers were most permeable in L15/salts, with only about 30 % of the LY remaining in the top chamber after 1 h, and least permeable in L15/FBS, with approximately 75 % of the dye remaining in the top chamber. The permeabilities of monolayers in L15 and L15/ex fell between these two extremes and were not consistently different from each other or from the extremes.

2.3.8. Effect of nutritional deprivation on wound healing and restitution

Nutritional deprivation profoundly influenced the healing of a 500 μm gap or wound in RTgutGC monolayers (Fig 2.8). In L15/FBS, cells filled the gap within 5 days (data not shown). Thus L15/FBS supported wound healing. In L15 and L15/ex, cells entered the gap but the wound was still incompletely healed after 7 days (B & C, Fig 2.8). Thus these media supported partial restitution. By contrast, in L15/salts, cells failed to enter the gap, and even after 7 days, the wound remained completely open (E, Fig. 2.8). Thus L15/salts failed to support restitution.

2.3.9. Effect of nutritional deprivation on trypsinization and replating of cells

The responses to trypsin by cell monolayers that had been nutritionally deprived for 7 days either in L15, L15/ex, or L15/salts were compared to the responses of cell monolayers in L15/FBS for 7 days (control). Within minutes of the trypsin addition, cells began to round up and draw away from their neighbors, but cells that had been in L15/ex and L15/salt appeared to round up more slowly and to be less round (data not shown). Repeatedly pipetting L15/FBS into these cultures dislodged the cells to create a cell suspension. Greater than 90 % of these cells excluded Trypan blue, with no obvious relationship between nutrient deprivation and Trypan blue staining (data not shown). The mean volume for cells that had been in L15/salts (3.1 ± pL, n=3) was approximately 40% of the volume for cells that had been in L15/FBS (1.8 ± 0.1 pL, n=3) but cell diameter in L15/salts (15.0 ± 0.3 μm, n=3) was only about 15% less than the cell diameter in L15/FBS (17.9 ± 1.6 μm, n=3) (Fig 2.9). When resuspended in L15/FBS and added to new culture vessels, the cells attached within minutes. Lamellopodia began to extend out from the cells and within a few hours the cells became completely spread onto the plastic culture surface. Spreading was a little slower for the cells that had been nutritionally deprived in L15/ex and L15/salts (data not shown). Overall, cells nutritionally deprived for 7 days were still able to disassemble their cytoskeleton as illustrated by their rounding during trypsinization and reassemble their cytoskeleton as illustrated by their attachment and spreading onto the plastic surface of culture vessels.

2.3.10. Recovery from complete nutrient deprivation of cell culture propagation and wound healing

When cultures in L15/salts for 7 days were passaged with trypsin to new vessels (1 to 2 split) with new medium (L15/FBS), the cells proliferated to eventually form monolayers. These monolayers also could be subsequently split 1 to 2 and again be grown to confluency in L15/FBS. As noted in section 2.3.8, a gap in a monolayer in L15/salts remained undiminished for at least 7 days. Yet when L15/FBS was added at this point, cells began migrating into the gap and the wound healed within the next 7 days (data not shown). Therefore, adding L15/FBS to cell cultures that had been deprived of all nutrients (L15/salts) for 7 days restored their capacity to be continuously propagated and to heal wounds.

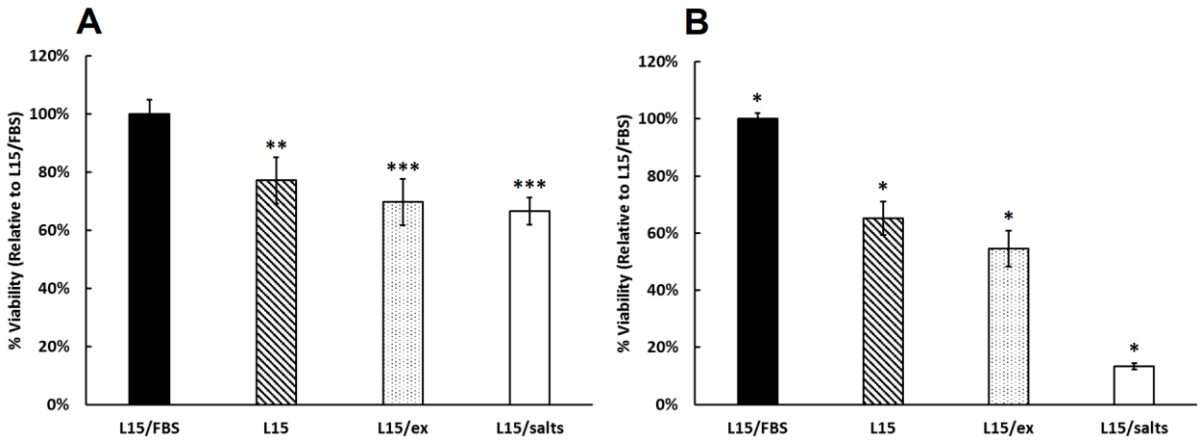

Figure 2.1. Effect of nutritional deprivation on the ability of RTgutGC monolayer cultures to retain plasma membrane integrity and energy metabolism. RTgutGC monolayer cultures were established in L15/FBS and then switched either to L15, L15/ex or L15/salts. After 7 days, esterase activity was measured with CFDA-AM as an indication of plasma membrane integrity (A) and the reduction of alamar Blue (AB), as an indication of energy metabolism (B). In both cases the results were recorded as relative fluorescent units (RFUs). For graphic presentation, RFUs were expressed as a percentage of the RFUs for control cultures (7 days in L15/FBS), and the means with standard deviations (n=3) are presented. For statistical analysis, RFUs were subjected to a one-way ANOVA and Tukey post hoc test (*$p < 0.05$, **$p < 0.01$, ***$p < 0.001$). For CFDA-AM, all nutritionally deprived cultures are different from the control but not different from each other (A); for AB, all pair wise combinations were significantly different from each other.

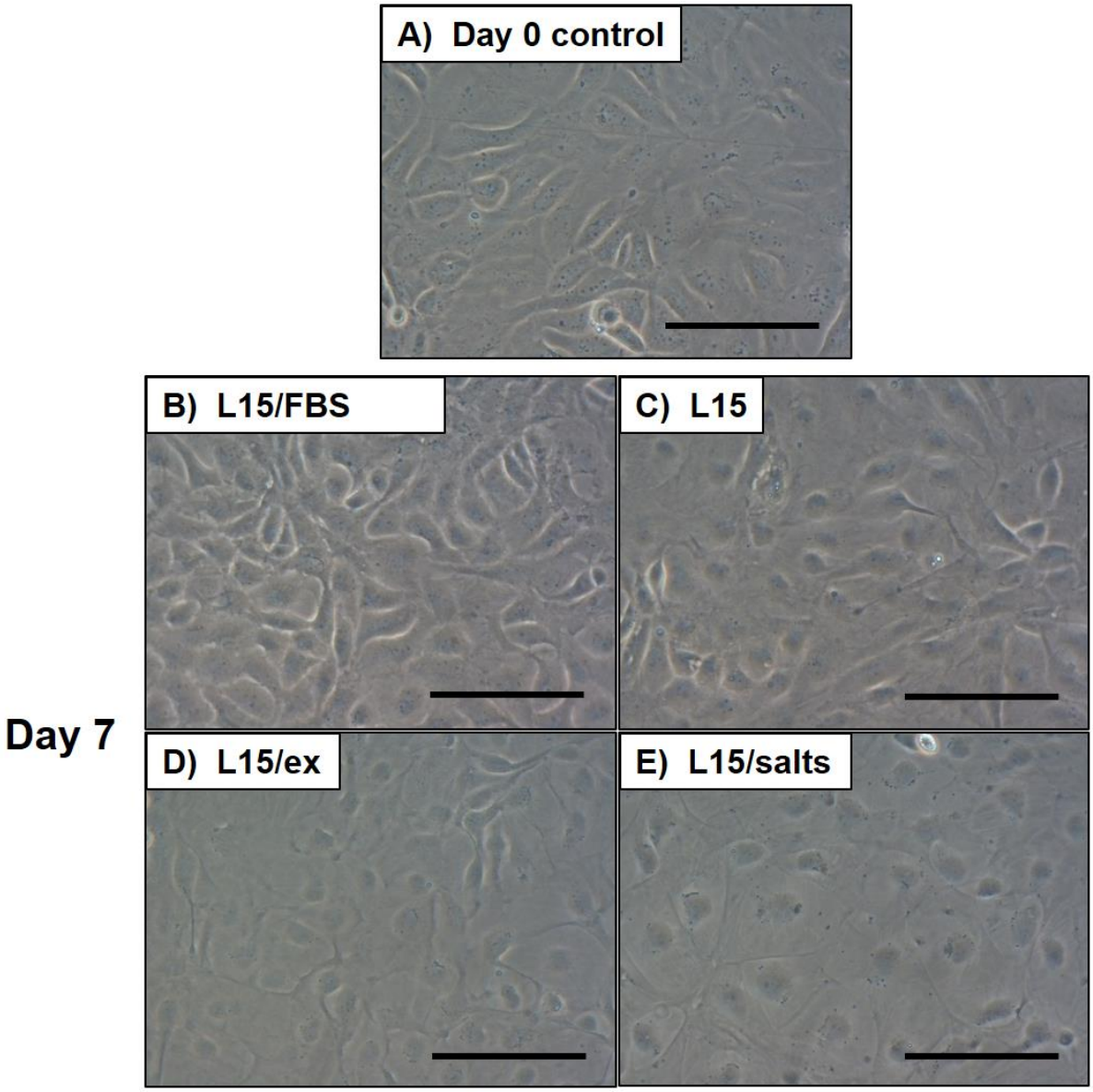

Figure 2.2. Phase-contrast microscopic observation of RTgutGC under various degrees of starvation. Starvation end point was 7 days in respective conditions. (A) Day 0 control after establiment. (B) Cells in L15/FBS after 7 days at 18 ^{o}C. (C) Cells in L15 after 7 days at 18 ^{o}C. (D) Cells in L15/ex after 7 days at 18 ^{o}C. (E) Cells in L15/salts after 7 days at 18 ^{o}C. Pictures were taken under 400x. Scale bar = 100 μm.

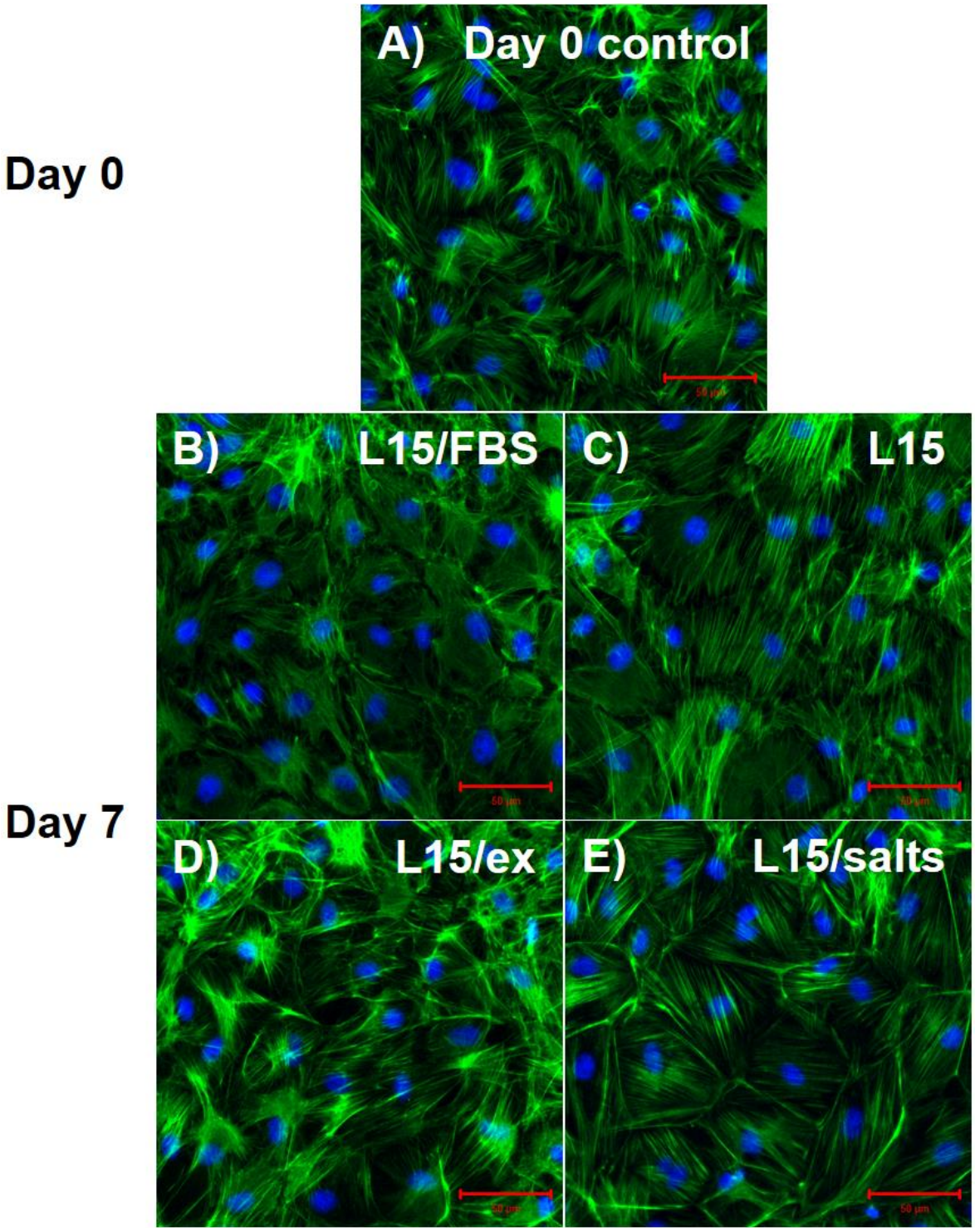

Figure 2.3. F-actin arrangement after 7 days under various nutritional conditions. (A) Day 0 control. (B) F-actin arrangement after 7 days in L15/FBS. (C) F-actin arrangement after 7 days in L15. (D) F-actin arrangement after 7 days in L15/ex. (E) F-actin arrangement after 7 days in L15/salts. F-actin was visualized by FITC-phalloidin, staining green. The cells' nuclei were visualized by DAPI, staining blue. Scale bar = 50 μm

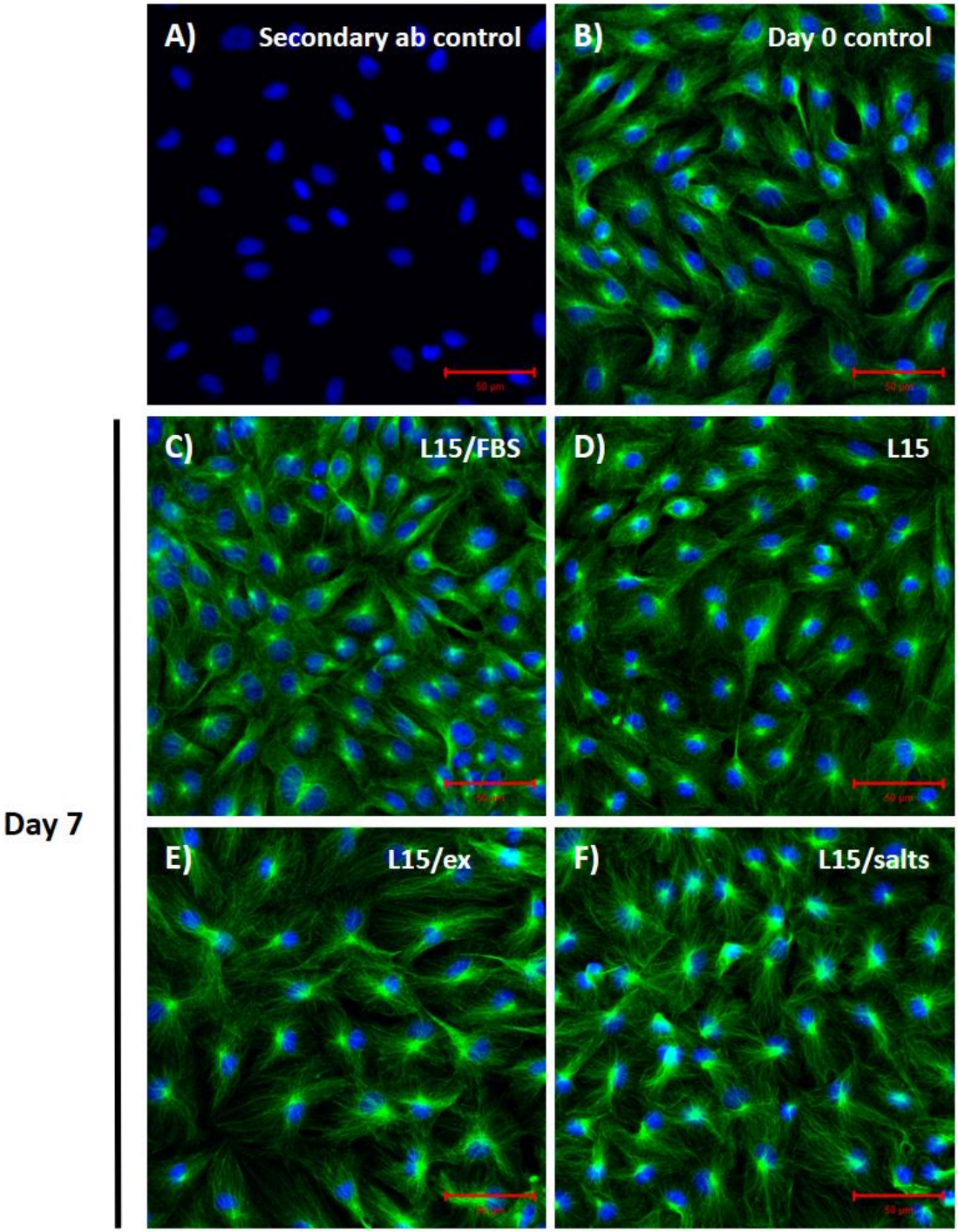

Figure 2.4. α-tubulin arrangement after 7 days under various nutritional conditions. (A) Secondary antibody control to ensure that no nonspecific binding of the secondary antibody occurred. (B) Day 0 control. (C) α-tubulin arrangement after 7 days in L15/FBS. (D) α-tubulin arrangement after 7 days in L15. (E) α-tubulin arrangement after 7 days in L15/ex. (F) α-tubulin arrangement after 7 days in L15/salts. α-tubulin is visualized in green by the incubation of a primary monoclonal anti- α-tubulin antibody produced in mouse and a secondary anti-mouse AlexaFluor® 488 antibody produced in goat. The cells' nuclei, stained blue, were visualized by DAPI. Scale bar = 50 μm.

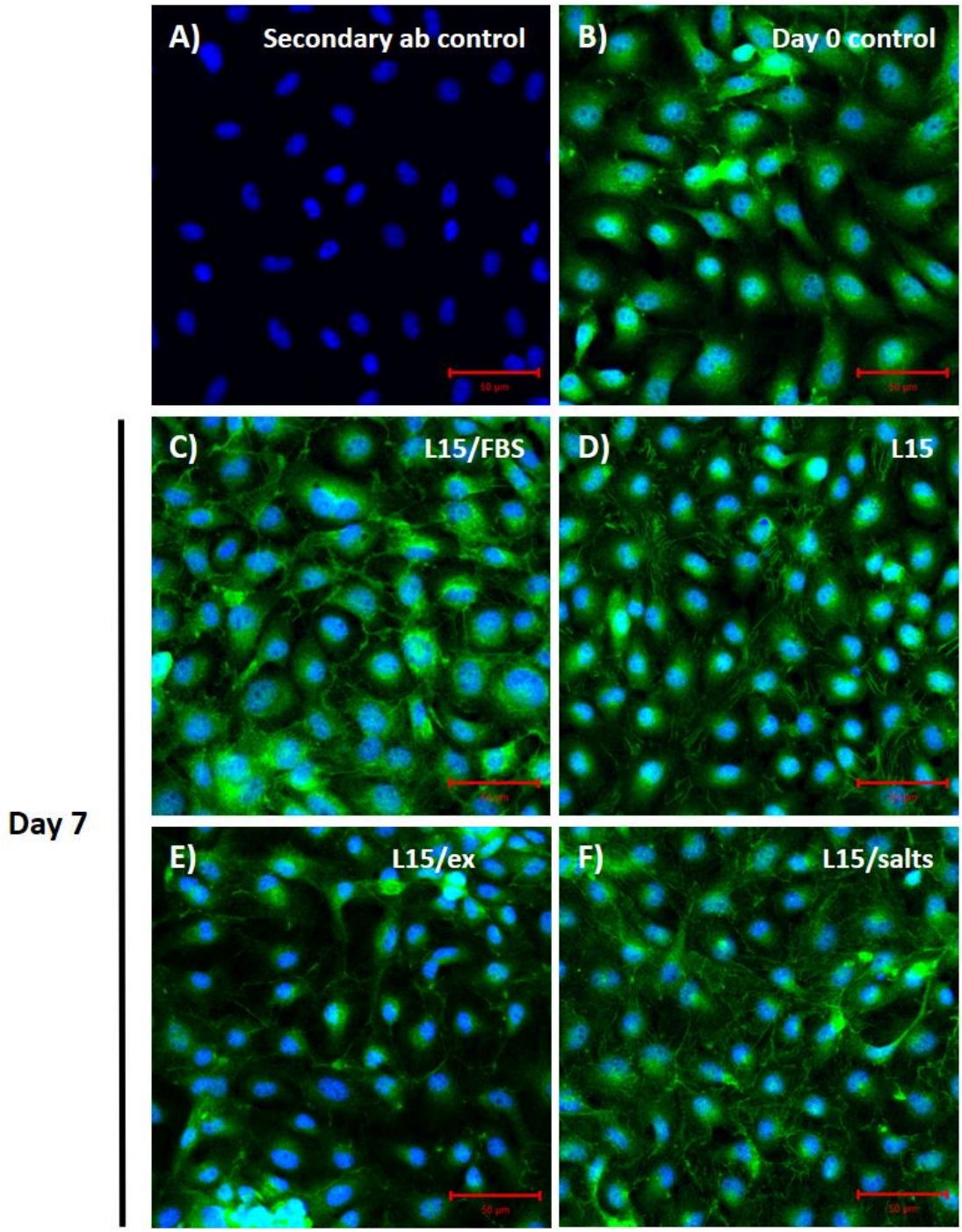

Figure 2.5. ZO-1 localization after 7 days under various nutritional conditions. (A) Secondary antibody control to ensure that no nonspecific binding of the antibody occurred. (B) Day 0 control. (C) ZO-1 localization after 7 days in L15/FBS. (D) ZO-1 localization after 7 days in L15. (E) ZO-1 localization after 7 days in L15/ex. (F) ZO-1 localization after 7 days in L15/salts. ZO-1 is visualized in green by the incubation of a primary polyclonal anti- ZO-1 antibody produced in rabbit and secondary anti-rabbit AlexaFluor® 488 antibody produced in goat. The cells' nuclei, stained blue, were visualized by DAPI. Scale bar = 50 µm

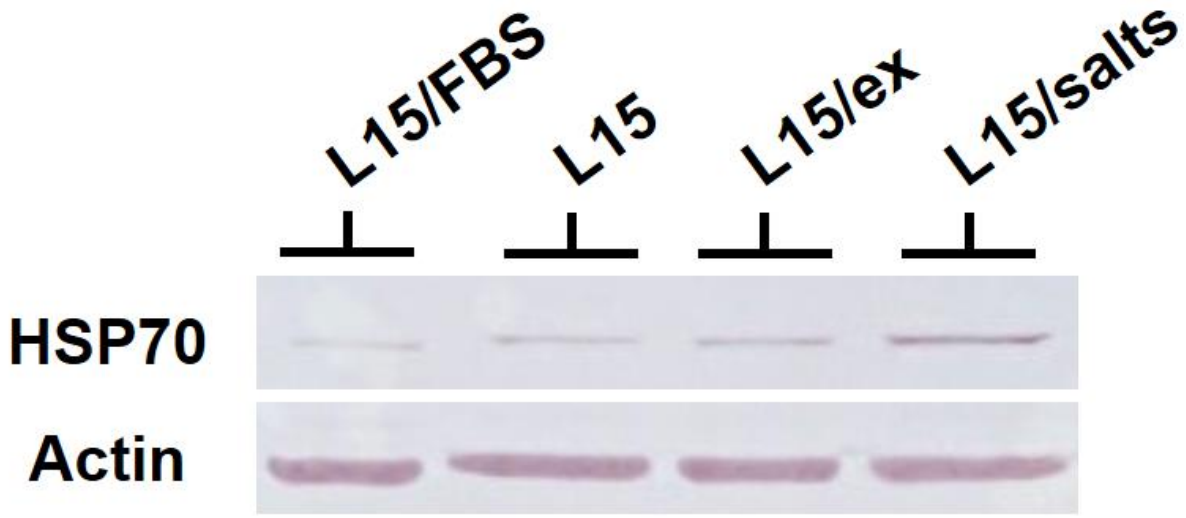

Figure 2.6. HSP70 protein levels after 7 days under four different nutritional conditions. RTgutGC cells were incubated in either L15/FBS, L15, L15/ex, or L15/salts for 7 days at 18 ^{o}C. HSP70 levels were visualized by Western blotting. Actin was used as a control to HSP70.

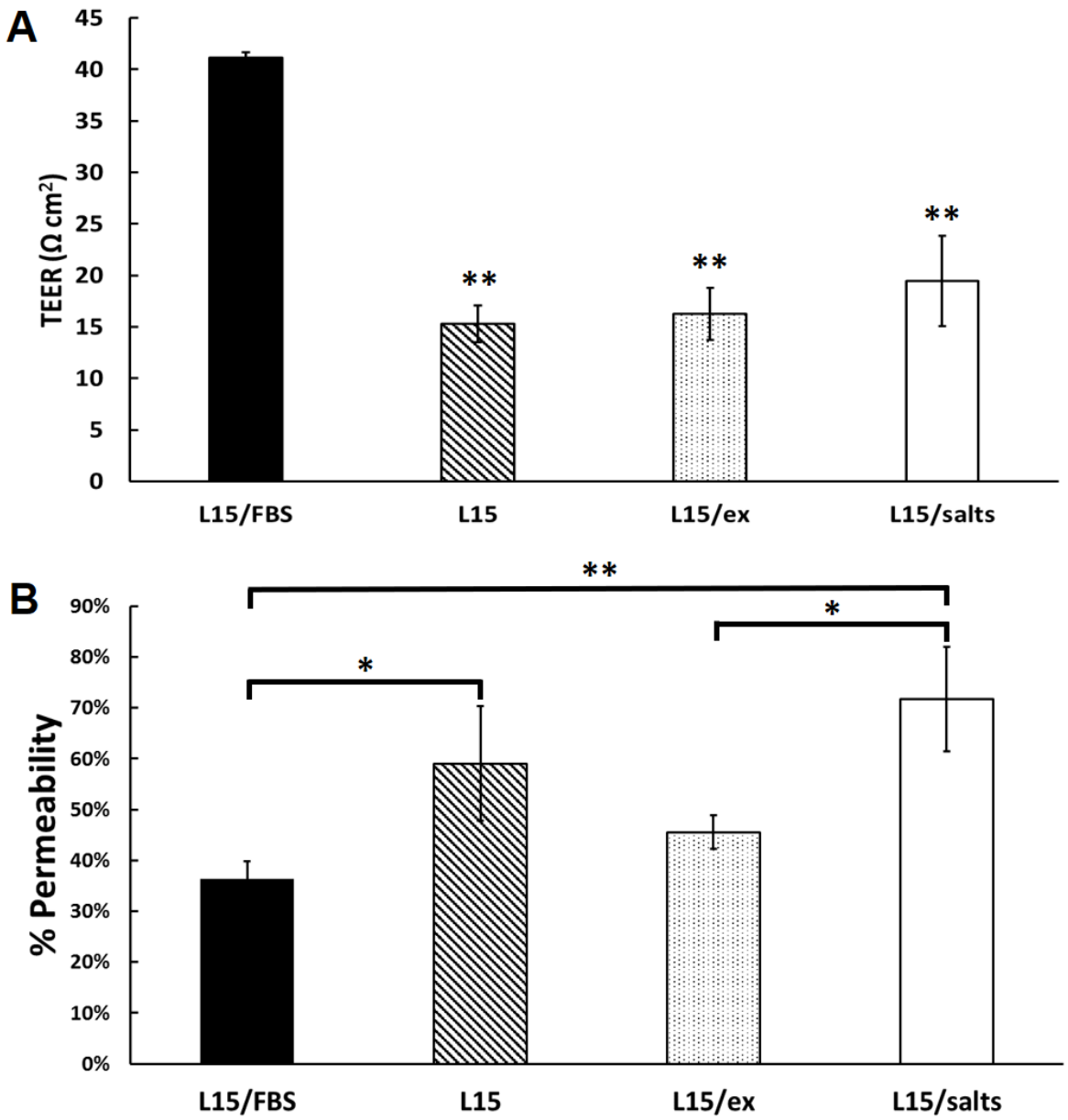

Figure 2.7. Effects of different degrees of nutritional starvation on the barrier function of RTgutGC. (A) Transepithelial electrical resistance (TEER) in either L15/FBS, L15, L15/ex, or L15/salts after 7 days at 18 ^{o}C. Initial TEER readings on day 0 were approximately 24-28 Ω cm^2. Statistical significance (**$p < 0.01$) was reached when compared to L15/FBS. (B) Day 5 measurements of Lucifer yellow (LY) permeability in either L15/FBS, L15, L15/ex, or L15/salts. Values are means ± standard deviation. Asterisks indicate significant differences: *$p < 0.05$, **$p < 0.01$.

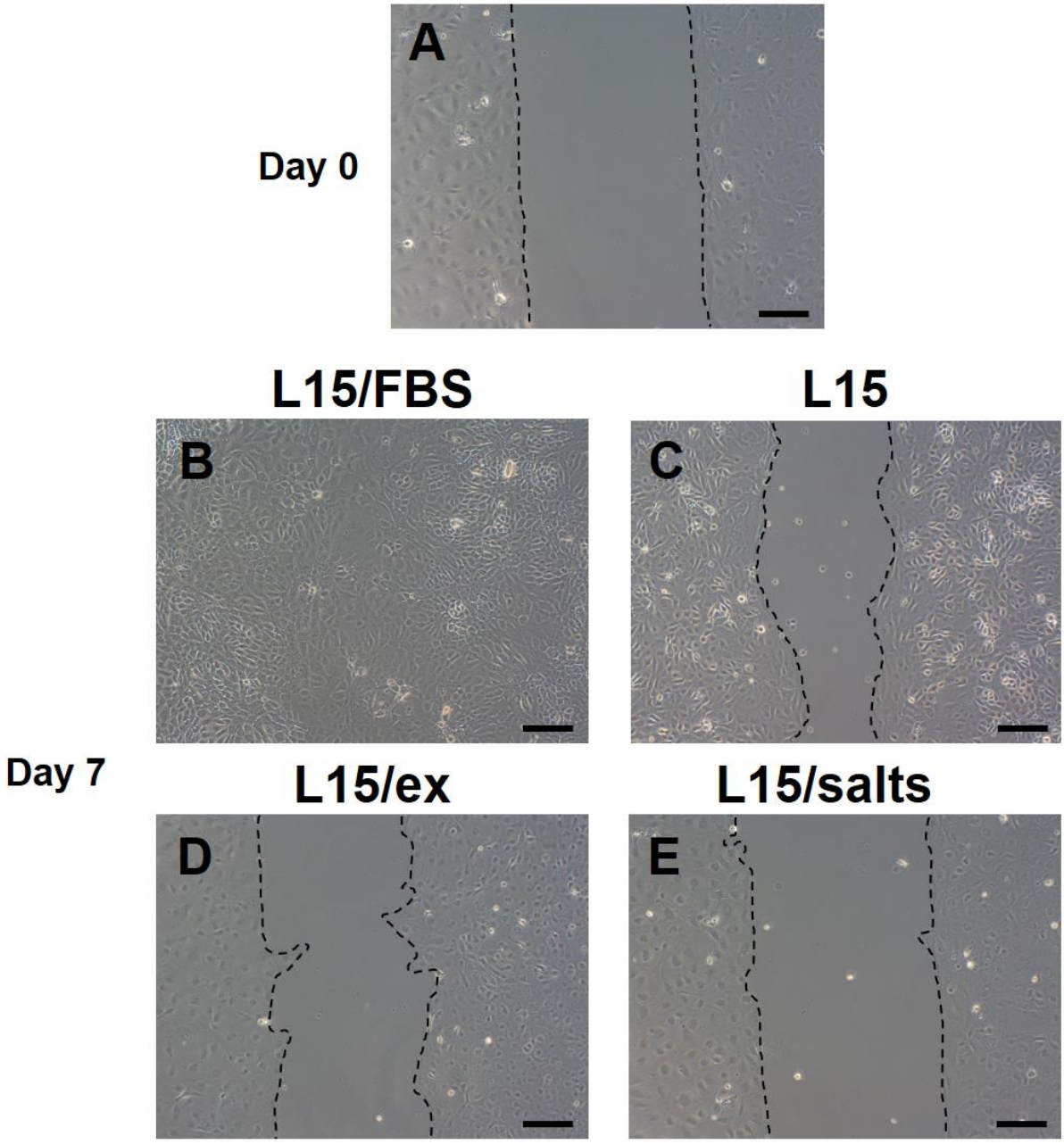

Figure 2.8. RTgutGC cells' ability to migrate into a cell free gap under different degrees of starvation. (A) Day 0 of migration after 3 day establishment period. (B) Day 7 migration time point of cells in L15/FBS medium (complete media). (C) Day 7 migration time point of cells in L15 medium (serum starvation). (D) Day 7 migration time point of cells in L15/ex (serum, amino acid, and vitamin starvation). (E) Day 7 migration time point of cells in L15/salts (complete starvation). Cell monolayer borders are traced in black to better visualize restitution. Phase contrast pictures were taken at a 100x magnification. Scale bar = 100 μm.

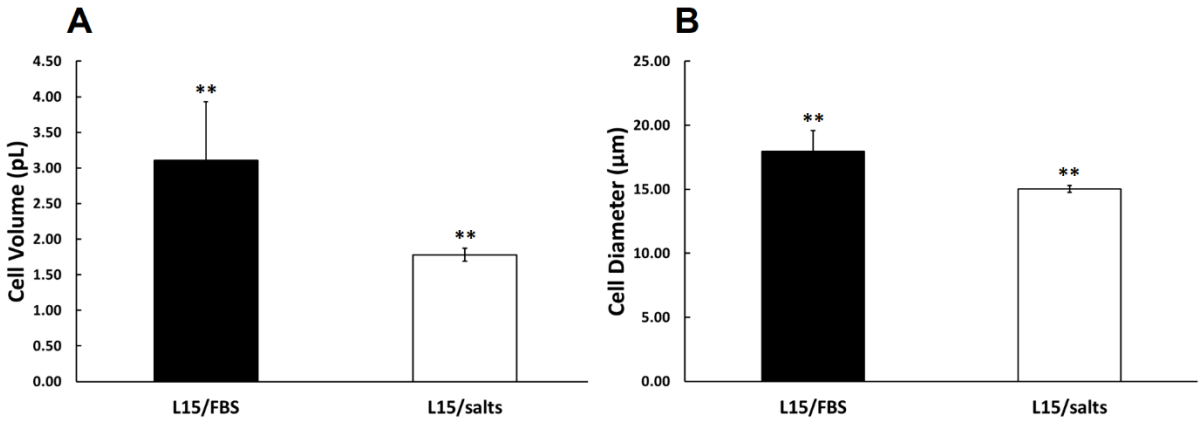

Figure 2.9. Effects of starvation on the cell volume and diameter of RTgutGC cells after 7 days. (A) Volume (pL) of cells either in a full nutritional condition (L15/FBS) or deprived of any nutrients (L15/salts) after 7 days. (B) Diameter (µm) of cells either in a full nutritional condition (L15/FBS) or deprived of any nutrients (L15/salts) after 7 days. For both (A) and (B), values are means ± standard deviation. **$p < 0.01$ by a two-tail unpaired student's T-test.

2.4. DISCUSSION

Rainbow trout intestinal epithelial cells, RTgutGC, were able to survive for at least 7 days under three kinds of nutrient deprivation or starvation: serum starvation(L15), serum, amino acid and vitamin starvation (L15/ex), and complete starvation (L15/salts). Nutrient deprivation caused changes in cellular functions and organizations, with the most pronounced changes arising from complete starvation. In L15/salts for 7 days, the cells underwent a diminishment in metabolism, a reorganization of the cytoskeleton and ZO-1, and a loss of barrier functions and of restitution (cell migration). The addition of growth medium (L15/FBS) supported the restoration in starved intestinal epithelial cells of energy metabolism, cytoskeletal organization, and cell migration.

2.4.1. Effect of nutritional deprivation on cell adherence, morphology and plasma membrane integrity

Despite nutrient deprivation for 7 days, rainbow trout intestinal epithelial cells were able to remain adherent in monolayers but within the monolayers the cellular morphology became larger, flatter, and more polygonal with a decline in esterase activity. Esterase activity was measured by the conversion of CFDA-AM to carboxyfluorescein (CF) and recorded as relative fluorescent units (RFUs). The fewer RFUs suggests that some cells in the monolayer had lost their plasma membrane integrity, causing esterase activity and CF to be removed from the monolayer during rinsing. The magnitude of the RFU diminishment might represent approximately how many cells were lost from the monolayer. However, visually the monolayer seemed intact so any space left by dying cells likely was covered over by the enlargement of the remaining adherent cells. These cells were viable as judged by their continued adherence, esterase activity, and recovery upon refeeding, as will be discussed later.

Only a few other studies have examined the ability of cell lines to persist as monolayers during nutrient deprivation, so whether the ability of RTgutGC to survive starvation is a property generally found with fish cells or unique to the intestine needs to be explored further. In L15/ex, rainbow trout gill epithelial cells, RTgill-W1, and American eel brain endothelial cells, eelB, survived for at least 4 and 7 days respectively with no decline in CF RFUs or obvious change in morphology (Schirmer et al., 1997; Bloch et al., 2017). In L15/salts, the Chinook salmon embryo cells, CHSE-214 remained adherent for more than a week, whereas the human choriocarcinoma cells, JEG-3, did not (Bryson et al., 2006). Shortly after being

placed in L15/salts, the haddock embryo cells, HEW, developed long cytoplasmic extensions but over time in L15/salts the cells flattened out again into a monolayer, although CF readings declined by approximately 25 % (Bryson et al., 2006). The retention of all esterase activity by some cell lines (eelB) and loss of some activity by others (RTgutGC) could reflect differences in their physiology but could be due to methodological differences. The RFUs for cultures after 7 days in L15/ex was expressed relative to the RFUs at the start of starvation for eelB (Bloch et al., 2017) but relative to control cultures after 7 days in L15/FBS for RTgutGC. For the latter method, a % drop in RFU could be due to the growth of cells in L15/FBS rather than just the loss of esterase activity from the monolayer. This might explain why the decline was similar in all three types of nutrient deprivation (L15, L15/ex and L15/salts) with RTgutGC.

2.4.2. Effect of nutritional deprivation on energy metabolism

Relative to cultures in the normal growth medium (L15/FBS), RTgutGC in L15, L15/ex or L15/salts for 7 days reduced less AB, which was recorded as fewer RFUs and interpreted as diminished energy metabolism. The decline of 45 % for RTgutGC in L15/ex contrasts with previous studies on RTgill-W1 and eelB in L15/ex for 4 to 7 days. With these cell lines little or no diminishment in energy metabolism was observed (Schirmer et al., 1997; Bloch et al., 2017). Likewise, no diminishment in AB reduction was observed in HEW cells after 7 days in L15/salts (Bryson et al., 2006), whereas the diminishment was approximately 85 % for RTgutGC. The differences could arise from methodology dissimilarities. Firstly, the rinsing of the cultures to initiate nutrient deprivation might have been more thorough with RTgutGC cultures. Secondly the RFUs for cultures after a period in L15/ex or L15/salts was expressed relative to the RFUs at the start of starvation for RTgill-W1, eelB and HEW (Bloch et al., 2017; Schirmer et al., 1997) but relative to control cultures after 7 days in L15/FBS for RTgutGC. A % decline in AB reduction by RTgutGC during nutritional deprivation could be due to the increase in cell number in L15/FBS and a proportional increase in energy metabolism rather than diminished energy metabolism in L15 or L15/ex. Alternatively, energy metabolism in RTgutGC might be more sensitive to down regulation or disruption by starvation than in the other cell lines.

Three different mechanisms, working separately or in some combination, can be advanced to explain why RTgutGC undergoing nutritional deprivation showed a decline in energy metabolism. Firstly, RTgutGC more so than other cell lines might sense and respond

to nutritional deprivation by shutting down energy metabolism, even before the internal energy substrates or energy machinery have been diminished significantly. The cells might downregulate their cellular metabolic rate to a new hypometabolic steady state as has been proposed as a mechanism for cells surviving hypoxia and hypothermia (Boutilier, 2001). Secondly, during starvation the intracellular pool of substrates and co-factors necessary for energy metabolism might decline more rapidly with RTgutGC and become limiting earlier. A third possibility is that the machinery for energy metabolism degenerates during starvation through the inability of cells to repair or replenish organelles, such as mitochondria, and this degeneration is more rapid in RTgutGC.

2.4.3. Effects of nutritional deprivation on F-actin

Considerable changes in F-actin arrangement were observed under various degrees of nutritional starvation. Additionally, a lack of nutritional starvation (L15/FBS) promoted the loss of stress fibers after 7 days, whereas serum starvation in L15 retained stress fibers in the cells, where they appeared more organized. Past studies have shown that cells under serum starvation retain stress fibers with observable increases in F-actin and stress fiber thickness (Boraldi et al., 2008; Paddenberg et al., 2001; Schmitz & Bereiter-Hahn, 2002). Stress fiber thickening was also seen in the presence of SAV and complete starvation (L15/ex and L15/salts respectively). Conversely, the presence of certain growth factors, such as LPA, bombesin, PDGF, and EGF, in serum is thought to coordinate the assembly of focal adhesions and stress fibers by interactions with the small GTP-binding protein rho and that the removal of serum results in the loss of stress fibers (Ridley & Hall, 1992). Since serum promotes cellular growth and proliferation, actin will be in a state of change, constantly being disassembled and reassembled, hence leading to the possibility of fixing the cells at a state of actin reorganization. Moreover, it has been recently suggested that highly proliferative and motile cells can lack stress fibers, where the onset of cell softening due to a decrease in stress fibers, preceded by a stiffening state, is a characteristic of cancer cell invasion (Tavares et al., 2017). This study's data suggest that cells undergoing serum starvation and further complete starvation retain stress fibers in a more organized manner. Stress fibers are generally anchored to focal adhesions, and can be categorized by morphology and association to focal adhesions as four different types: ventral stress fibers, dorsal stress fibers, transverse actin arcs, and

perinuclear actin cap fibers (Maninova et al., 2017). It is possible that the various regimens of starvation in the current study caused a shift in the type of stress fibers observed.

2.4.4. Effects of nutritional deprivation on microtubules

In addition to F-actin, cytoskeletal microtubular changes were observed after the various starvation regimens. Increasing degrees of nutritional starvation in RTgutGC generate less dense but thicker arrays of α-tubulin with larger MTOCs. Reductions in microtubular densities have been linked to tubulin folding cofactors B expression in murine microglial cells (Fanarraga et al., 2009). Microtubules, being dynamic structures constantly polymerizing and depolymerizing, show fast growth at their "plus" ends and slower dimer addition at their "negative" ends. These highly dynamic properties are controlled by microtubule binding proteins called tubulin folding cofactors (Szymanski, 2002). Hence, alterations in expression or function of these proteins, possibly in the case of starvation, would impart changes to microtubular networks. Larger MTOCs in starvation conditions could be due to the appearance of non-chromosomal (nc) MTOCs. These nc-MTCOs have a lesser role in cellular division but impart important functions in differentiated cells (Sanchez & Feldman, 2010). To confirm the appearance of nc-MTOCs, future studies will have to be done.

2.4.5. Effects of nutritional deprivation on barrier functions

To measure the integrity of an RTgutGC monolayer and tight junctions under different kinds of starvation, TEER and LY assays were used in conjunction with immunofluorescence of an important tight junctional scaffolding protein, ZO-1. TEER is an indicator of the ionic conductance of the paracellular pathway in the epithelial monolayer, whereas LY is an indicator of paracellular water flow and pore size as it has low permeability and can only pass through monolayers by paracellular diffusion (Rastogi et al., 2013; Srinivasan et al., 2015). Both assays indicated that RTgutGC cells were unable to maintain an effective barrier in the absence of serum. This was particulary evident in complete starvation conditions (L15/salts). Interestingly, LY permeability did not increase after SAV starvation (L15/ex). Nonetheless, a reduction in monolayer resistance measured by TEER was observed. FBS has many constituents, including low-molecular-weight nutrients, hormones and polypeptide growth factors (Ham, 1981), and might be contributing to the maintenance of a functional epithelial barrier in two fundamentally different ways. The FBS components might be acting generally

on the cells to keep a contiguous layer of viable epithelial cells so that the paracellular space between cells can be sealed. In the absence of FBS, RTgutGC monolayers remained viable for at least seven days in L15, L15/ex or L15/salts when measured by the viability indicator CFDA-AM. Yet the decline in TEER values for monolayers in L15, L15/ex and L15/salts might be due to the death of only a few cells, which are sufficient in number to break up the contiguous cell layer and the functional barrier. Nutrients and polypeptide growth factors in FBS might be preventing this small amount of cell death. Alternatively or additionally, the components of FBS might be regulating specifically the synthesis, assembly and turnover of tight junction components so that epithelial cells remain sealed. For example, bovine serum albumin (BSA) has been reported to stabilize tight junctions in Caco-2 (Hashimoto et al., 1995).

2.4.6. Effects of nutritional deprivation on ZO-1

In the presence of serum, ZO-1 was strongly localized at the cells' periphery indicating strong interactions with junctional complexes. In the absence of serum, ZO-1 appeared to have a weaker localization at cells' periphery and was disorganized in L15 and L15/salts. In the day 0 control, ZO-1 was completely localized in the cytoplasm and not at the periphery, an indication that tight junction complexes have yet to form. Balda and Matter (2000) demonstrated that ZO-1 expression increases upon serum stimulation in MDCK cells and that overexpressing ZO-1 resulted in a significantly higher TEER value for the cell line. Conversely, multiple studies suggest that serum can increase permeability (decreasing TEER) of multiple different cell lines by the reduction in ZO-1 expression and/or reduction in the distribution of ZO-1 to the cells' periphery with decreases in co-localization and association to occludin (Bian et al., 2009; Chang et al., 1997; Colgan, 2008). Nonetheless, the results suggest that the proper maintenance of an RTgutGC barrier requires serum, whereas the removal of serum disrupts this barrier by ZO-1 disorganization. ZO-1 is an important scaffolding protein that structurally supports tight junction proteins, such as occludin, to the actin cytoskeleton. As ZO-1 directly binds and supports occludin, a critical transmembrane protein in controlling the paracellular pathway, it is possible for ZO-1 to control the paracellular pathway through occludin interactions (Balda and Matter, 2000; Chasiotis et al., 2012). ZO-1 also has additional roles in some signalling pathways involved in cell proliferation (Chasiotis et al., 2012).

2.4.7. Effects of nutritional deprivation on HSP70 levels

HSPs are multifaceted with diverse roles and highly conserved proteins that see increases in expression under stress, such as hyperthermia, UV radiation, oxidative stress, and nutritional deprivation (Jolly & Morimoto, 2000). Increased levels of HSP70 were observed with increases in nutritional starvation over 7 days by Western blotting. This observation with RTgutGC provides *in vitro* evidence that nutritional starvation is a stressor that fish intestinal epithelium cells respond to by increasing the expression of HSP70. Observations of HSP, including HSP70, expression increasing during food deprivation have also been made *in vivo* with fish (Antonopoulou et al., 2013; Cara et al., 2005; Gronquist & Berges, 2013). However, this response is variable *in vivo* with fish and not always indicative of stress from starvation (Gronquist & Berges, 2013). Whether the increase in HSP70 protein expression play specific roles or influences to the starvation responses seen in RTgutGC is unknown and is a potential path for future studies.

2.4.8. Effect of nutritional deprivation on wound healing and restitution

Wound healing by RTgutGC was slower without serum (L15 and L15/ex) than in L15/FBS and stopped completely in the absence of any nutrients (L15/salts). Previously RTgutGC cells were found not to grow without serum (Kawano et al., 2010), so in L15 and L15/ex, healing was likely slower because filling in the gap would have been only due to cell migration or restitution. By contrast in L15/FBS, both proliferation and migration would occur and account for the faster healing. Surprisingly, in L15/ex RTgutGC cells were able to migrate into a gap but not to completely close it. Thus RTgutGC can at least start restitution without serum, amino acids, and vitamins and only an energy source (L15/ex). The lack of any cell migration in L15/salts might be a way for the cells to reduce ATP demand to match reduced ATP production.

2.4.9. Summary

Overall, RTgutGC cells were able to survive starvation over 7 days but with the impairment of barrier function and wound repair. Due to the complexity and variability of a starvation response *in vivo* and the necessity of good aquaculture practice to ensure healthy fish, the RTgutGC cell line is a useful tool to study the cellular responses involved in nutritional starvation. Future studies should focus on molecular aspects of this stress response, whether

HSPs play a role in mitigating this nutritional stress, cell cycle progression and/or arrest, and the underlying cellular metabolic response to starvation.

CHAPTER 3

Effect of naringenin on rainbow trout intestinal epithelial cells

3.1. INTRODUCTION

Understanding the interaction between the rainbow trout intestinal epithelium and feed additives, especially phytochemicals, will aid the development of feeds that better promote intestinal fish health. The use of intestinal cell cultures is one approach for identifying interactions. For example, the human Caco-2 cell line has been used to study the impact of flavonoids on tight junctions (TJ) and epithelium barrier functions. Quercetin increased the expression of Claudin-4 in Caco2 while also increasing Claudin-4 localization within the tight junction and in subjunctional regions (Amasheh et al., 2008).

One phytochemical of interest is the flavanone naringenin, mainly found in citrus fruits such as grapefruit. In addition to its antioxidant capabilities, naringenin possesses anti-inflammatory, anticarcinogenic, antidiabetic, and anti-lipidemic properties, and has been shown to have TJ modulating effects (Leonardi et al., 2010; Mulvihill et al., 2009; Noda et al., 2013; Park et al., 2012; Wang et al., 2012). In a monolayer of Caco-2 cells, naringenin was seen to increase TJ function through cytoskeletal association, localization, and expression of ZO-1, occludin, claudin-1, and claudin-4 (Noda et al., 2013). Naringenin was also seen to increase HSP70 expression in Caco-2 cells (Noda et al., 2013). In teleost systems, *in vitro* naringenin administration in goldfish scale fibroblast GAKS cells suppressed *Edwardsiella tarda* infection by inhibiting NanA sialidase, an important enzyme for the initial adhering process in *E. tarda* infection (Shinyoshi et al., 2016). Additionally, feed additives containing citrus oils reduced *Aeromonas salmonicida* infection in rainbow trout (Menanteau-Ledouble et al., 2015). Fish feeds containing citrus extracts are starting to emerge in popularity with the aquaculture industry in Japan (Fukada et al., 2014).

Very little is known of the interaction of naringenin and the intestinal epithelium in teleost systems either *in vivo* or *in vitro*. Hence, this chapter focuses on such interaction at a cellular level with the use of a rainbow trout intestinal epithelial cell line, RTgutGC.

3.2. MATERIALS AND METHODS

3.2.1. Cell cultures and culture conditions

RTgutGC, a rainbow trout epithelial cell line was used throughout the experiment. This cell line was developed in Niels C. Bols' laboratory at the University of Waterloo, Canada (Kawano et al., 2011). Medium used to culture the cells was Leibovitz's L15 with 2.05 mM L-Glutamine (Thermo Fisher Scientific) additionally supplemented with 10% fetal bovine serum (FBS, Sigma-Aldrich) and antibiotics (10,000 U/mL penicillin and 10,000 μg/mL streptomycin, P/S, Thermo Fisher Scientific) (L15/FBS). Cells were subcultured or passaged using trypsin (Thermo Fisher Scientific) every week at a 1 to 2 split and maintained at 18 ^{o}C. The cell culture vessels used were BioLite 75 cm^2 cell culture treated flasks (Thermo Fisher Scientific).

3.2.2. Naringenin dosing timeline

Cells were first allowed to establish a confluent monolayer in L15/FBS at 18 ^{o}C for 3-4 days. Afterwards, the medium was removed, the cells were washed with Dulbecco's phosphate-buffered saline solution (DPBS, Thermo Fisher Scientific), and exposed to varying concentrations of naringenin (Sigma-Aldrich) either in L15/FBS, in L15 lacking serum (L15), or in a simple salt solution of L15 (L15/salts). The naringenin concentrations used were 10, 30, 50, 75, and 100 μM diluted from a 200x stock solution of the reagent dissolved in DMSO. Final DMSO concentration in control and media-naringenin solutions was always 0.5% (v/v). The selected naringenin concentration range is based on concentrations used on fish and mammalian cells found in the literature (Menanteau-Ledouble et al., 2015; Noda et al., 2013). The cells were left to incubate in a naringenin containing solution for 24 h to 96 h at 18 ^{o}C depending on the assay.

3.2.3. Cellular viability

Cellular viability was monitored by changes in cell morphology through phase contrast microscopy and with the indicator dyes, Alamar Blue® (AB, Thermo Fisher Scientific) and 5'-carboxyfluorescein diacetate acetoxymethyl ester (CFDA-AM, Sigma-Aldrich). AB provides a measure of metabolic activity while CFDA-AM provides a measure of plasma membrane integrity (Dayeh et al., 2013). The protocol used for the AB and CFDA-AM dye assays follows

closely Dayeh et al. (2013) methods. RTgutGC cells in L15/FBS were added to a 24-well plate at a plating density of 125,000 cells per well in replicates of 4. Plates were dosed with 10, 30, and 100 μM of naringenin as in section 3.2.2 for 24 h. After the incubation, the medium was then removed, the cells were washed with DPBS, and a solution containing 5% (v/v) AB and 4 μM CFDA-AM in DPBS was added to the cells. Plates were then incubated at room temperature for 1 hour in the dark. Using a series 4000 CytoFluor fluorescent plate reader (PerSeptive Biosystems - ThermoFisher Scientific), results were recorded as relative fluorescent units (RFUs). The mean RFUs for the experimental wells were expressed as a percentage of the mean RFUs for control wells.

3.2.4. Fluorescence microscopy of RTgutGC F-actin

F-actin was visualized using fluorescein isothiocyanate labeled phalloidin (FITC-phalloidin, Sigma-Aldrich) and confocal microscopy. Phalloidin is a fungal toxin having an ability of binding to F-actin only in polymeric and oligomeric forms but not monomeric forms. The fluorescent conjugate of phalloidin, FITC, is used to label F-actin and can be visualized by fluorescence or laser microscopy. A 5 mg/mL stock solution of FITC-phalloidin was prepared in DMSO. RTgutGC cells in L15/FBS were plated in a 4 chamber tissue culture treated glass Falcon CultureSlide® (Corning) at a density of 150,000 cells per chamber. Slides were dosed with 10, 30, and 100 μM of naringenin as seen in section 3.2.2 for 24 h. After the incubation, cells were washed with DPBS and fixed with 3% paraformaldehyde (Sigma-Aldrich) for 20 minutes at 4 ^{o}C. Following fixation, the cells were then permeabilized with 0.1% Triton X-100 (Sigma-Aldrich) for 10 minutes at room temperature. Afterwards, 5 μg/mL of FITC-phalloidin was added to the cells and allowed to incubate for 45 min at room temperature in the dark. Cells were then washed three times with DPBS and the slides were allowed to dry. Once dry, plastic chambers were removed from the slides and three drops of a mounting medium, Fluoroshield (Sigma-Aldrich), containing DAPI was added to the slides with a coverslip to help preserve the slide and counter stain for DNA. Confocal images were obtained with the Zeiss LSM 510 laser scanning microscope and were acquired and analyzed using a ZEN lite 2011 software.

3.2.5. Fluorescence microscopy of RTgutGC tight junction

RTgutGC cells in L15/FBS were plated in a 4 chamber tissue culture treated glass Falcon CultureSlide® (Corning) at a density of 150,000 cells per chamber. Slides were dosed 24 h with 10, 30, and 100 μM of naringenin as in section 3.2.2. After the incubation, cells were washed with DPBS and fixed with 3% paraformaldehyde (Sigma-Aldrich) for 20 minutes at 4 ^{o}C. Following fixation, the cells were then permeabilized with 0.1% Triton X-100 (Sigma-Aldrich) for 10 minutes at room temperature. Cells were then incubated in blocking buffer (BB) (10% goat serum, 3% bovine serum albumin, and 0.1% Triton X-100 in DPBS) for 1 hour at room temperature. At this point some chambers were incubated with primary antibodies while others were incubated with only secondary antibodies to control for nonspecific staining. The primary antibodies used were polyclonal anti-ZO-1 and anti-Claudin-3 both produced in rabbit (ThermoFisher Scientific) and were diluted 1:100 and 1:50 respectively in BB. Primary antibodies were incubated on cells for 1 hour at room temperature on a rocker. Antibodies were then removed and cells were washed three times for 3 minutes with DBPS before the addition of secondary antibodies. The secondary antibodies were anti-rabbit AlexaFluor® 488 produced in goat (Sigma-Aldrich) diluted 1:1000 in DPBS and allowed to incubate on the cells for 1 hour in the dark at room temperature on a rocker. After incubating, the antibodies were removed and cells were once again washed three times with DPBS and allowed to dry. Once dry, plastic chambers were removed from the slides and three drops of a mounting medium, Fluoroshield (Sigma-Aldrich), containing DAPI was added to the slides with a coverslip to help preserve the slide and counter stain for DNA. Confocal images were obtained with the Zeiss LSM 510 laser scanning microscope and were acquired and analyzed using a ZEN lite 2011 software.

3.2.6. Measurement of epithelial barrier function

To evaluate TJ integrity of the RTgutGC barrier, transepithelial electrical resistance (TEER) and Lucifer Yellow CH dilithium salt (LY) permeability were measured with the use of Transwell® permeable supports with 1 μm pore sizes (Corning). Cells were plated in a 24-well Transwell® supports system at a density of 120,000 cells per Transwell® with L15/FBS medium. The plates were then incubated for 7 days at 18 ^{o}C allowing the cells to form a barrier. Cells were washed with DPBS and varying concentrations (10, 30, and 100 μM) of naringenin

in L15 medium were administered to the apical wells. Basolateral wells only contained L15 medium. TEER was measured overtime using an EVOM with the STX2 chopstick electrode (World Precision Instruments). The unit area resistance (Ωcm^2) was then calculated. To measure barrier permeability by LY, 24-well plates with Transwell® permeable supports were also used. Cells were plated at the same density as above and allowed to incubate for 7 days at 18 ^oC in L15/FBS. As with the TEER set up, cells were then washed and naringenin (10, 30, and 100 μM) was administered. After 4 days, naringenin was removed and the cells were washed with DPBS. Then 0.1 mg/mL of LY in DPBS was added to the apical wells and allowed to incubate for 60 min in the dark. The Transwell® supports were then removed and the amount of LY in the basal compartment was quantified using a fluorescence plate reader with results recorded as RFUs. The data were then expressed as percent permeability being the percent difference compared to blank Transwell® supports containing no cells.

3.2.7. HSP70 detection

HSP70 was visualized by Western blotting. RTgutGC cells were plated in 6-well plates with L15/FBS at a density of 1,000,000 cells per well. Plates were dosed for 96 h with 10, 30, and 100 μM of naringenin as in section 3.2.2. After the incubation, the cells were lysed by adding 200 μL of RIPA lysis buffer containing a protease inhibitor cocktail (Qiagen) directly to the plates. The cells were scraped off, transferred to microcentrifuge tubes, and allowed to sit on ice for 30 minutes. Tubes were then centrifuged at 10,000 x g for 1 minute and protein in the supernatant was collected. Protein concentrations were determined using a Pierce BCA protein assay kit (ThermoFisher Scientific). SDS-PAGE was performed using a Mini-PROTEAN tetra system (Bio-Rad) with premade 1 mm thick handcast gels. Loaded gels were run at 120 volts for 1½ hours. The transfer step onto a nitrocellulose membrane was performed in a Mini-Trans Blot Cell system (Bio-Rad) running at 150 milliamps for 1 hour. Equal protein loading was visualized by a 0.1 % Ponceau S stain in 5% (w/v) acetic acid. Before probing the membrane with rabbit anti-salmon HSP70 (Fish) polyclonal antibodies (SPC-314B, StressMarq), a 1 hour blocking step using 5% skim milk (w/v) in 1x TBS-T was performed. All antibodies were diluted in 5% skim milk (w/v) in 1x TBS-T. Rabbit anti-Salmon HSP70 (Fish) polyclonal antibodies were diluted 1:1000. To detect a reference protein, rabbit anti-β-actin antibodies (Sigma Aldrich) were used and diluted 1:600. The secondary antibody used

was goat anti-rabbit IgG conjugated to alkaline phosphatase (Sigma Aldrich) diluted 1:5000. Protein bands were detected by NBT/BCIP. Membranes were scanned and bands quantified by densitometry using a Bio-Rad ChemiDoc MP imaging system without chemiluminescense option. The data were then normalized to the actin bands and expressed relatively to the control.

3.2.8. Evaluating the effect of naringenin on restitution

The influence of naringenin on the migration of RTgutGC into a wound or gap was investigated in L15, and because L15 does not support RTgutGC proliferation (Kawano et al., 2011), this constituted a restitution assay. The assay was set up in 12-well culture inserts from Ibidi GmbH, Planegg / Martinsried, Germany as described in Chapter 2. After monolayers had been established in L15/FBS, medium was changed to just L15. Twenty-four hours later the inserts were removed to create the gap and concentrations of 30, 50, and 75 μM of naringenin were added. Phase contrast microscopy pictures were immediately taken to establish a day 0 time point. Cultures were incubated at 18 ^{o}C over the course of 6-7 days and monitored daily and with some exceptions photographed daily. Photographs of the gaps were analyzed with the ImageJ software. At four sites on a gap, the area without cells was calculated at day zero ($A_{day\ 0}$) and at some later period ($A_{day\ x}$), usually 6-7 days. Subtracting $A_{day\ x}$ from $A_{day\ 0}$ gave the gap area that had become covered with cells. The area of the gap that had become covered by cells was expressed as a percentage of the initial gap area (see formula below).

$$\textbf{\% migration} = (A_{day\ 0} - A_{day\ x})/A_{day\ 0} \times 100\%$$

For graphical presentation, the % cell migration was plotted on the Y axis. For statistical analysis, the areas without cells were used as described in section 3.2.10. Three independent experiments were done.

3.2.9. Forskolin and H89

Forskolin (Sigma-Aldrich) is an adenylyl cyclase activator while H89 (Sigma-Aldrich) is a potent protein kinase A inhibitor. Experiments that use these compounds include phase-contrast microscopy, F-actin visualization by FITC-phalloidin, and cell restitution assays.

Protocols for phase-contrast microscopy and F-actin visualization were similar to described above (section 3.2.3 & 3.2.4). As the case for cellular restitution, specialized 2-well culture inserts were used and followed a similar protocol as above (section 3.2.8).

3.2.10. Statistical analyses

Variables were expressed as the mean ± standard deviation or standard error of the mean (western blot densitometric analysis). Statistical analysis was done by a one-way ANOVA and Dunnet post hoc test. Statistical significance was defined as $p < 0.05$.

3.3. RESULTS

3.3.1. Effects of naringenin on cell morphology by phase-contrast microscopy

Visible morphological changes of RTgutGC cells were observed after a 24h incubation with naringenin in L15/salts (Fig 3.1). After 24 h, the control cell population had an epithelial like shape in a tightly packed monolayer (A, Fig 3.1). 10 μM naringenin did not significantly change cell morphology (B, Fig 3.1). Cells incubated with 30 and 100 μM naringenin had a more flattened morphology and appeared more ruffled with a distinct darker cell border (C and D, Fig 3.1). These effects were more pronounced with 100 μM naringenin. When incubated in L15 with naringenin for 24 h, visible morphological changes only occurred with 100 μM naringenin and not 10 or 30 μM naringenin (Fig 3.2). RTgutGC cells obtained a more wrinkled and wavy appearance in 100 μM naringenin with L15. A 24 h incubation of naringenin with L15/FBS medium did not generate significant or observable differences (Fig. 3.3).

3.3.2. Effects of naringenin cellular viability

10 and 30 μM naringenin appeared to have no effect on the metabolic activity of cells in L15/FBS (A, Fig 3.4). However, 100 μM naringenin caused a slight 6% but statistically significant decrease ($p < 0.01$) in cells' metabolic activity (A, Fig 3.4). Increasing concentrations of naringenin slightly decreased plasma membrane integrity in a dose dependent manner (B, Fig 3.4). 10 μM naringenin caused a 9% decrease, 30 μM naringenin caused an 11% decrease, and 100 μM naringenin caused a 16% decrease in plasma membrane integrity compared to the control (B, Fig 3.4). All values obtained were statistically significant compared to the control ($p < 0.01$).

Similar to when using L15/FBS as the medium, a significant drop of 59% in cellular metabolic activity was only observed with 100 μM naringenin in L15 medium (A, Fig 3.5). 10 and 30 μM naringenin in L15 did not significantly decrease the cells' metabolic activity. On the other hand, all three concentrations of naringenin caused a significant decrease ($p < 0.01$) in the cells' plasma membrane integrity, however, this decrease was more pronounced with 100 μM naringenin (B, Fig 3.5). 10 μM naringenin caused an 11% reduction, 30 μM naringenin caused a 12% reduction, and 100 μM naringenin a 31% reduction in plasma membrane integrity compared to the control.

In L15/salts medium, increasing concentrations of naringenin caused a dose dependent decrease in metabolic activity, where 10 μM naringenin caused a 12% reduction, 30 μM naringenin caused a 19% reduction, while a 50% reduction in metabolic activity with 100 μM naringenin was observed compared to the control (A, Fig 3.6). Increasing concentrations of naringenin had no negative effects on the plasma membrane integrity of cells in L15/salts where even slight but statistical significant increases of 15%, 9%, and 6% were observed with 10, 30, and 100 μM naringenin respectively (B, Fig 3.6).

3.3.3. Naringenin increases circumferential actin bundle formation with decreases in stress fibers

Naringenin prescence caused visible effects on F-actin arrangement in RTgutGC cells. Control populations of RTgutGC in both L15/FBS and L15/salts medium had numerous arrays of linear stress fibers oriented parallel and perpendicular to the cells' long axis (A, Fig 3.7 and 3.8). The addition of 10, 30, and 100 μM naringenin for 24 h in L15/FBS did not generate a large difference in F-actin arrangement and structure. The cell population incubated with 10, 30, and 100 μM naringenin in L15/FBS retained a similar stress fiber arrangement as seen in the control (Fig 3.7). On the other hand, the incubation of RTgutGC cells with naringenin in L15/salts caused a dose-response disorganization of F-actin, mainly noted by a diffuse staining pattern with short actin fibers and small punctations accumulating in the cytoplasm with the loss of stress fibers (Fig 3.8). Additionally, accumulation in circumferential actin bundles is seen with increasing concentrations of naringenin in L15/salts (Fig 3.8). The intensity of the staining of these bundles increased in the cell population incubated with 100 μM naringenin (D, Fig 3.8).

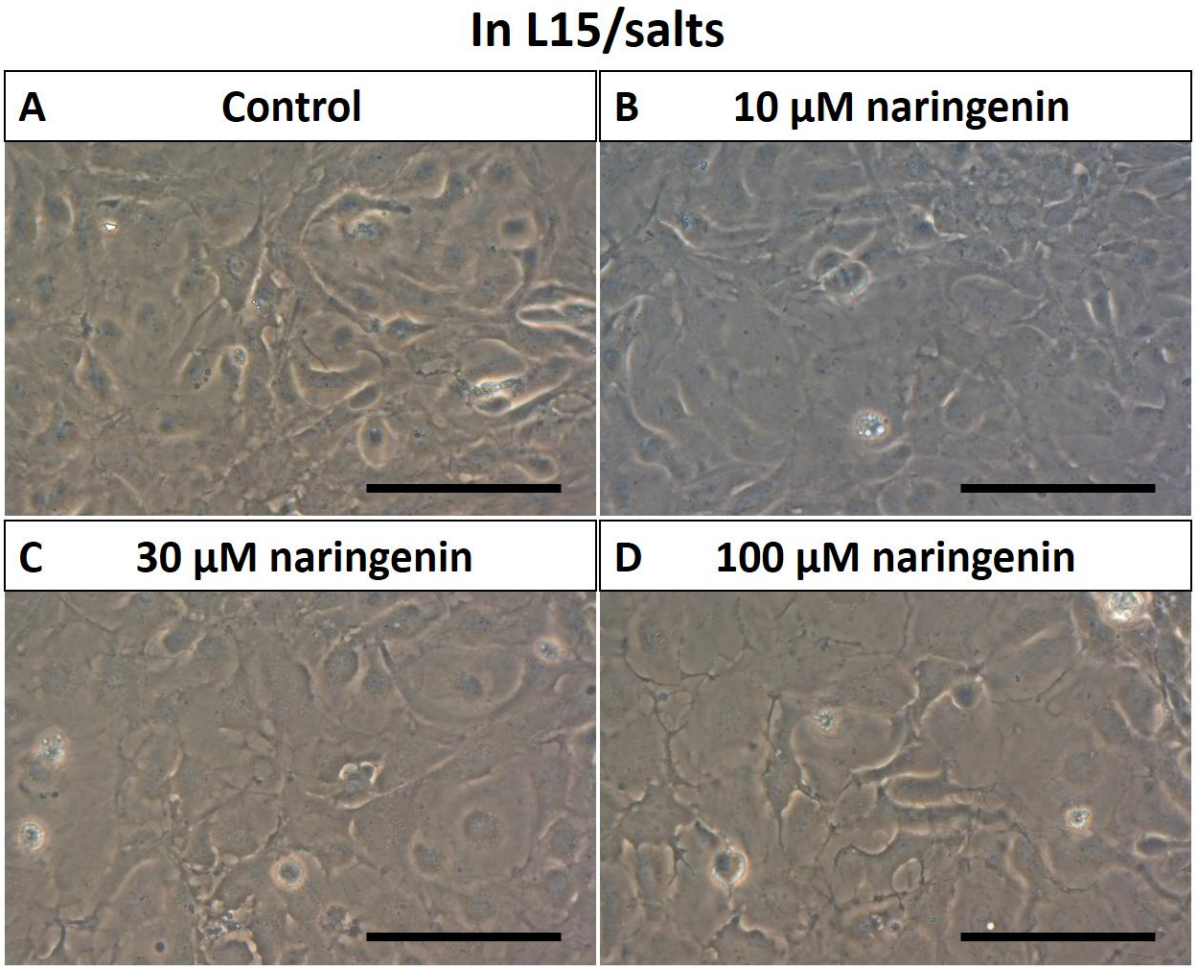

Figure 3.1. Phase-contrast observations of RTgutGC with naringenin in L15/salts. Cells were incubated for 24 h with different concentrations of naringenin (10, 30, and 100 µM) in L15/salts medium. Pictures represent magnification at 400x field with a scale bar of 100 µm.

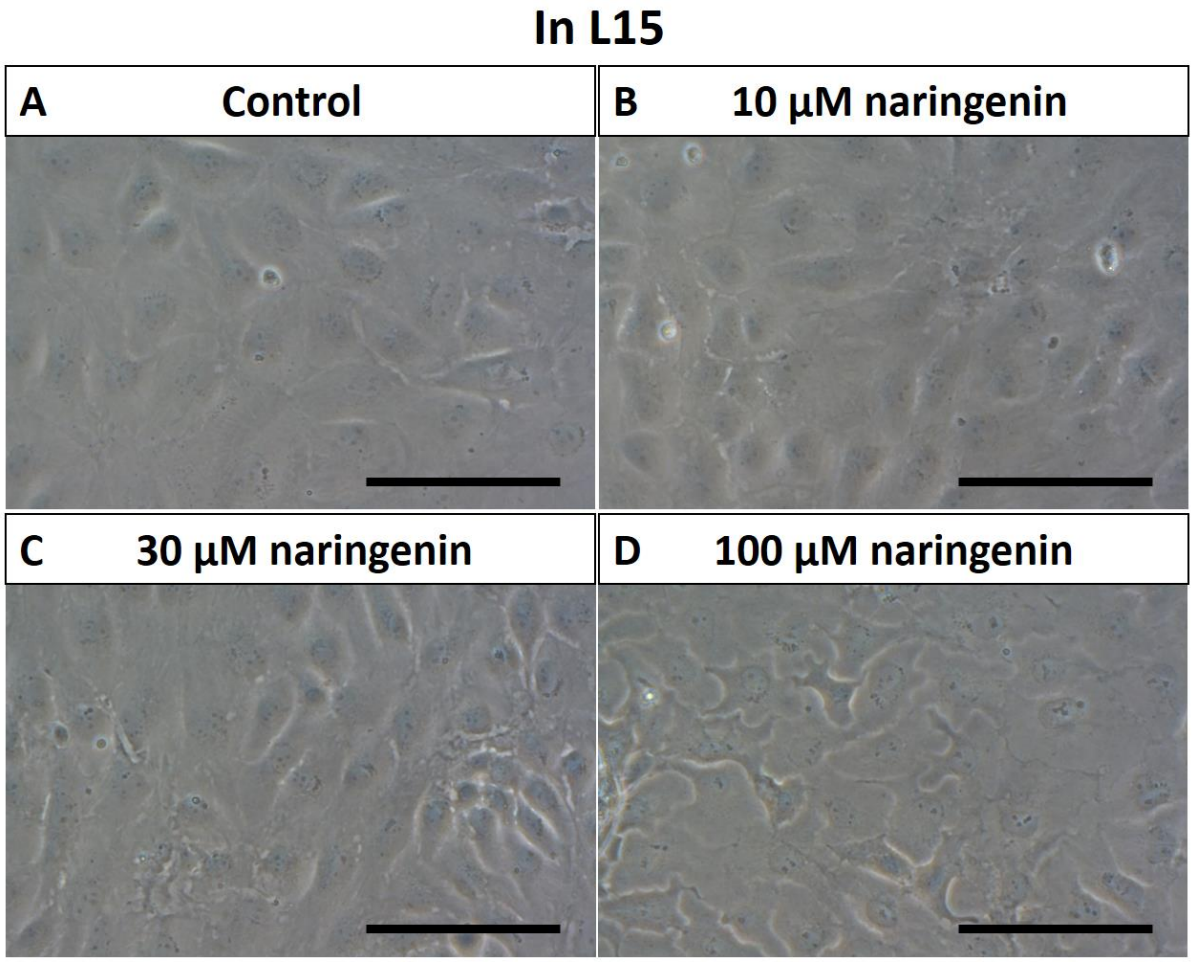

Figure 3.2. Phase-contrast observations of RTgutGC with naringenin in L15. Cells were incubated with different concentrations of naringenin (10, 30, and 100 µM) for 24 h in L15. Pictures represent magnification at 400x field with a scale bar of 100 µm.

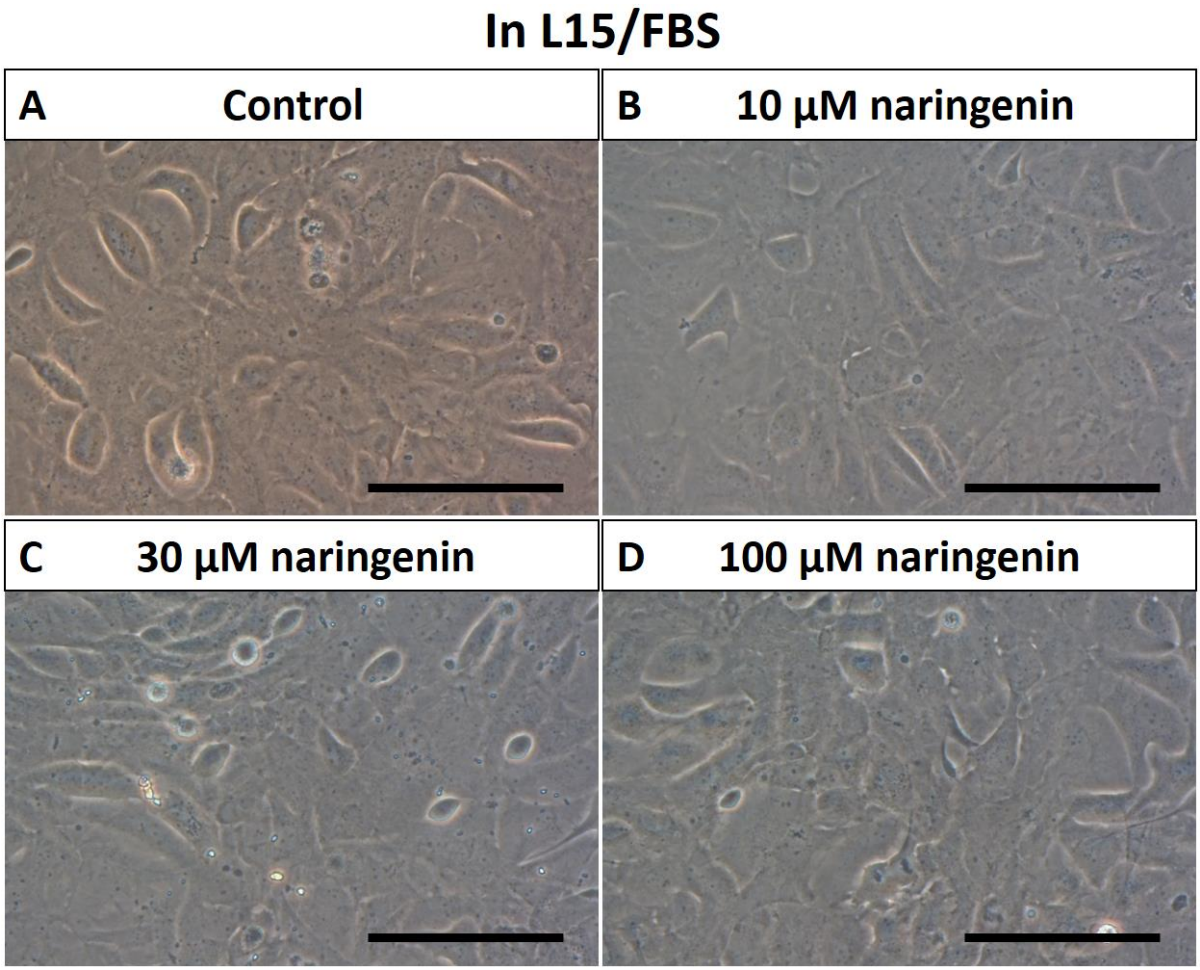

Figure 3.3. Phase-contrast observations of RTgutGC with naringenin in L15/FBS. Cells were incubated with different concentrations of naringenin (10, 30, and 100 µM) for 24 h in L15/FBS. Pictures represent magnification at 400x field with a scale bar of 100 µm.

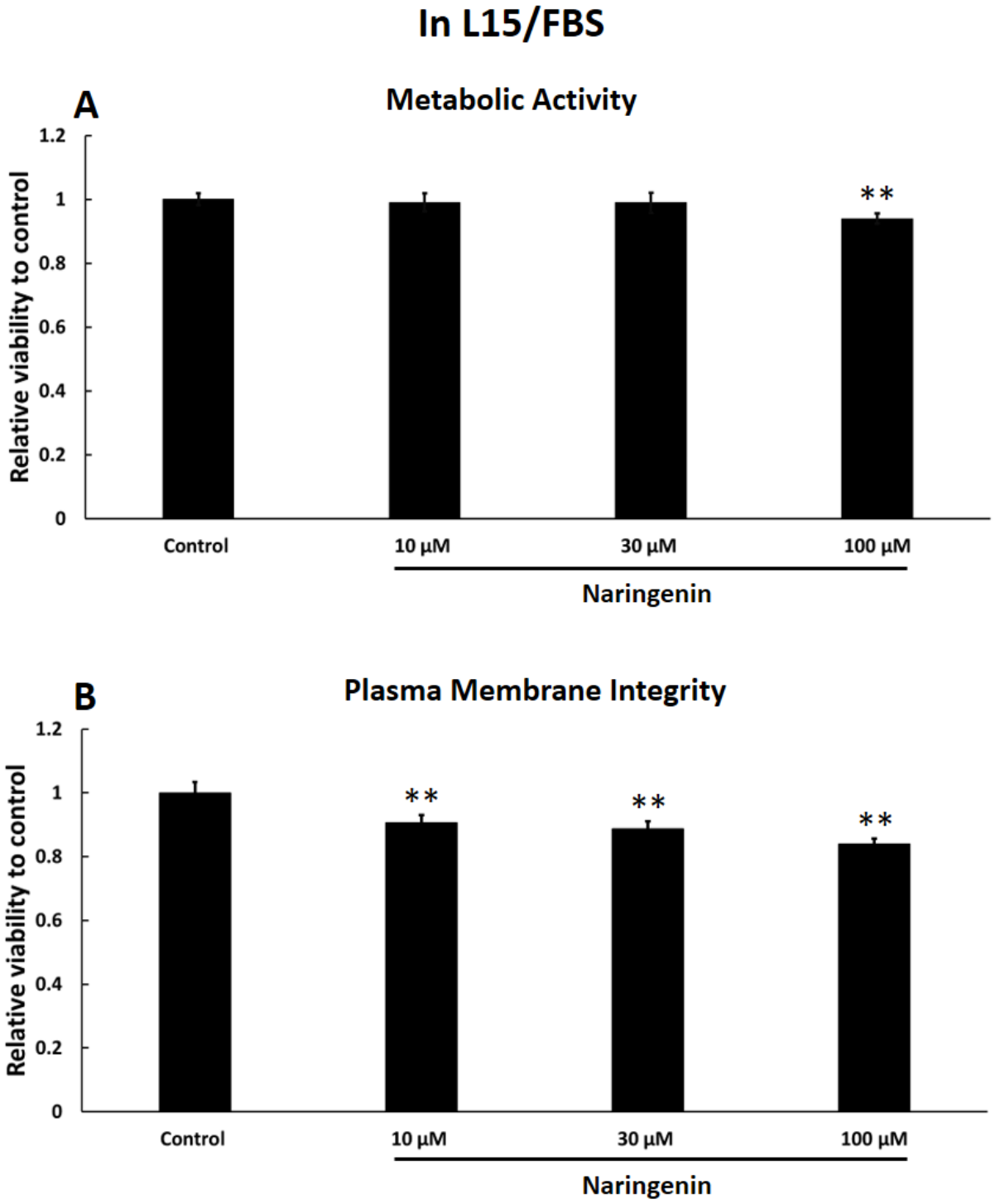

Figure 3.4. Cellular viability of RTgutGC with naringenin in L15/FBS. (A) Cells' metabolic activity measured by alamarBlue reduction. (B) Cells' plasma membrane integrity measured by CFDA-AM conversion to CF and its retainement in the cells. Both indicators of cellular viability were measured after a 24 h 18 ^{o}C incubation period with naringenin. Values are means ± standard deviation. Asterisk indicates significant difference when compared to the control: **$p < 0.01$.

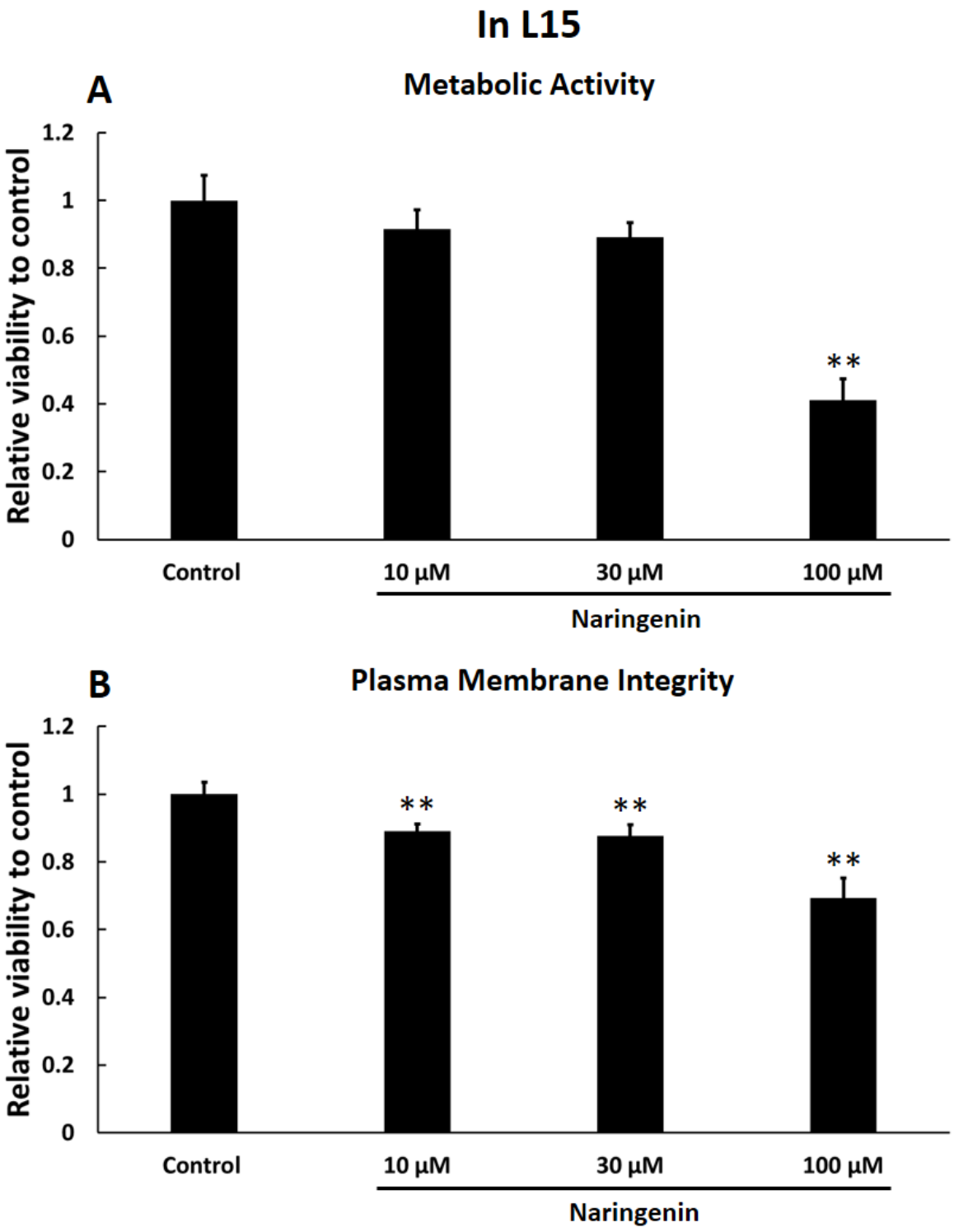

Figure 3.5. Cellular viability of RTgutGC with naringenin in L15. (A) Cells' metabolic activity measured by alamarBlue reduction. (B) Cells' plasma membrane integrity measured by CFDA-AM conversion to CF and its retainement in the cells. Both indicators of cellular viability were measured after a 24 h 18 ºC incubation period with naringenin. Values are means ± standard deviation. Asterisk indicates significant difference when compared to the control: **$p < 0.01$.

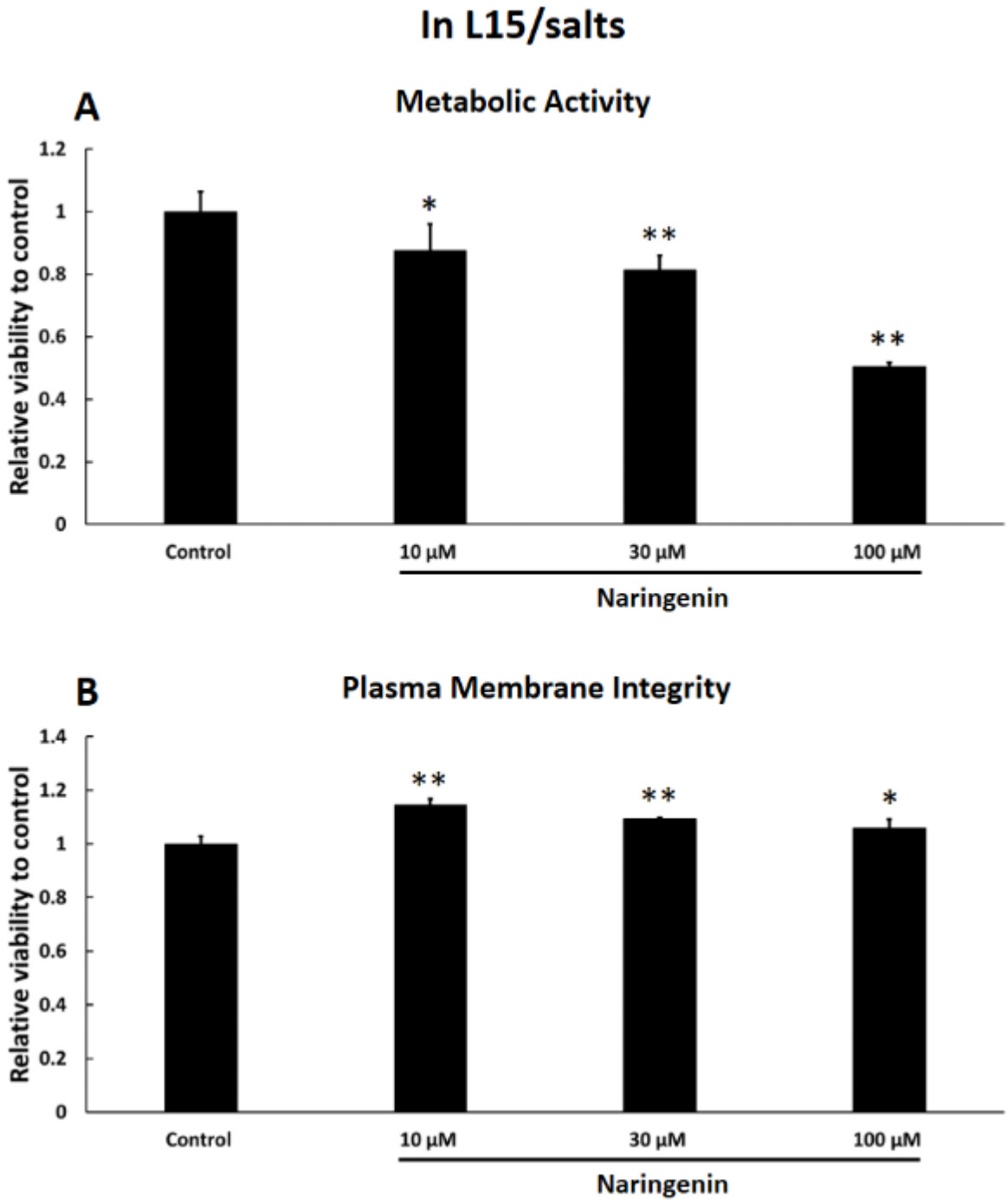

Figure 3.6. Cellular viability of RTgutGC with naringenin in L15/salts. (A) Cells' metabolic activity measured by alamarBlue reduction. (B) Cells' plasma membrane integrity measured by CFDA-AM conversion to CF and its retainement in the cells. Both indicators of cellular viability were measured after a 24 h 18 ^{o}C incubation period with naringenin. Values are means ± standard deviation. Asterisks indicate significant differences when compared to the control: *$p < 0.05$, **$p < 0.01$.

3.3.4. Naringenin increases barrier function without altering claudin 3 and ZO-1

TEER measurements on day 3 post naringenin administration showed that increasing concentrations of naringenin significantly increased resistance readings compared to the control (Fig 3.9). 10, 30, and 100 μM naringenin increased TEER 1.3, 1.75, and 1.9-fold respectively when compared to the control. Using LY as a measurement of epithelial barrier permeability, cells incubated with 100 μM naringenin showed a significant decrease of 39% in permeability (Fig 3.10).

Claudin 3 and ZO-1 visualization by ICC staining were both positive in RTgutGC cells (B and D, Fig 3.11). A secondary antibody control (cells are only stained with secondary antibodies and lack primary antibodies) showed no nonspecific antibody binding (A, Fig 3.11). 100 μM naringenin had no effect on claudin 3 (B-C, Fig 3.11) or ZO-1 (D-E, Fig 3.11) formation and localization.

3.3.5. Effect of naringenin on HSP70 levels

Exposure of RTgutGC cells to naringenin for 24 h had no effect on HSP70 levels as judged by western blotting (Fig 3.12). In cell extracts from all cultures, the antibody to the salmonid HSP70 stained a band at approximately 70 kDa. Relative to control cultures, the band staining was similar for cultures that had been exposed to concentrations of up to 100 μM naringenin in either L15/FBS (A, Fig 3.12) or L15/salts (B, Fig 3.12). The actin reference band was also unchanged. Densitometry of the HSP70 band confirmed that naringenin had no effect on HSP70 levels (C, Fig 3.12).

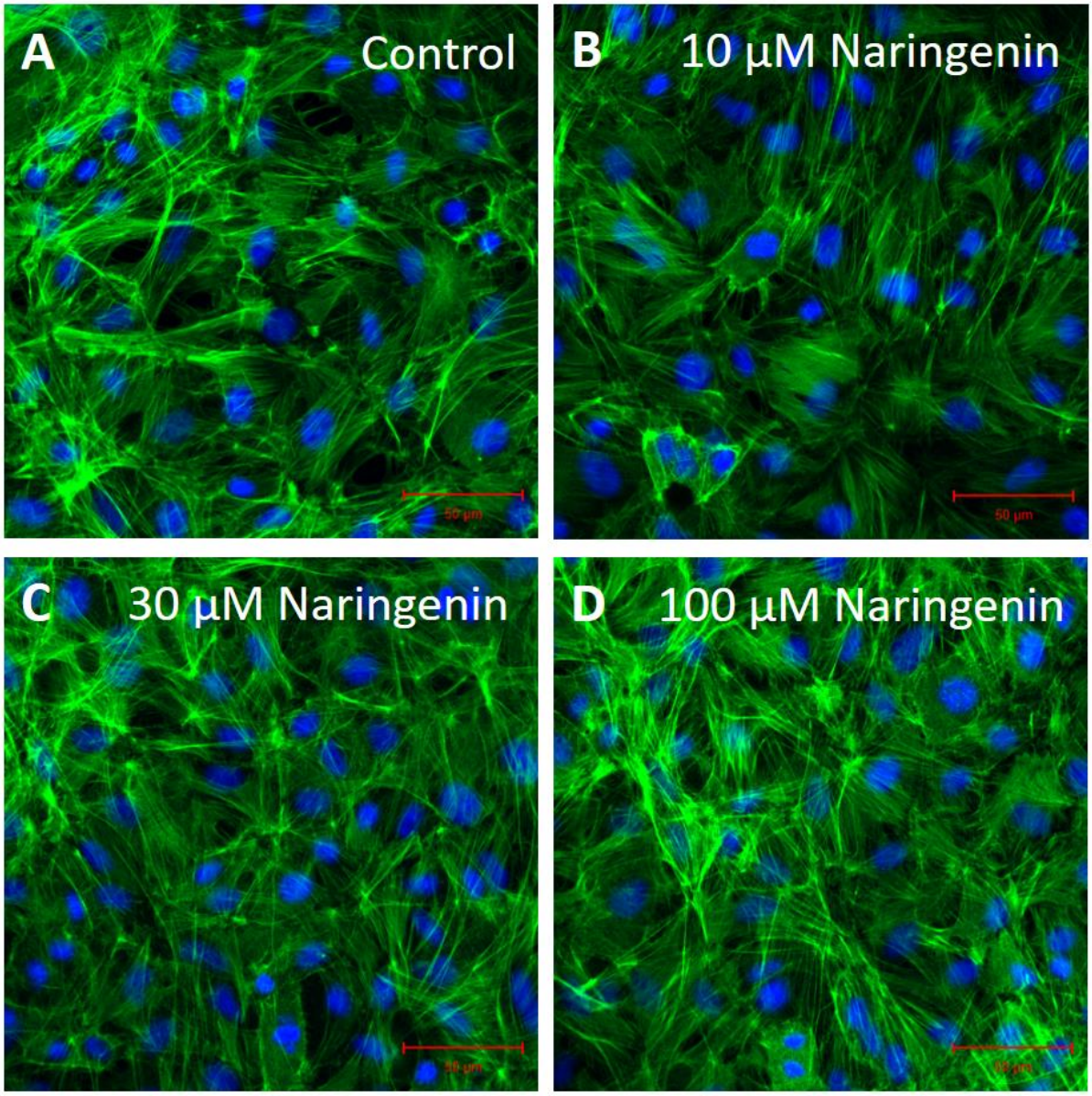

Figure 3.7. F-actin arrangement under the influence of naringenin in L15/FBS medium. F-actin is visualized in green by FITC-phalloidin, while the nuclei are visualized in blue by DAPI. Staining occurred after a 24 h incubation period at 18 ºC with naringenin. Scale bar = 50 µm.

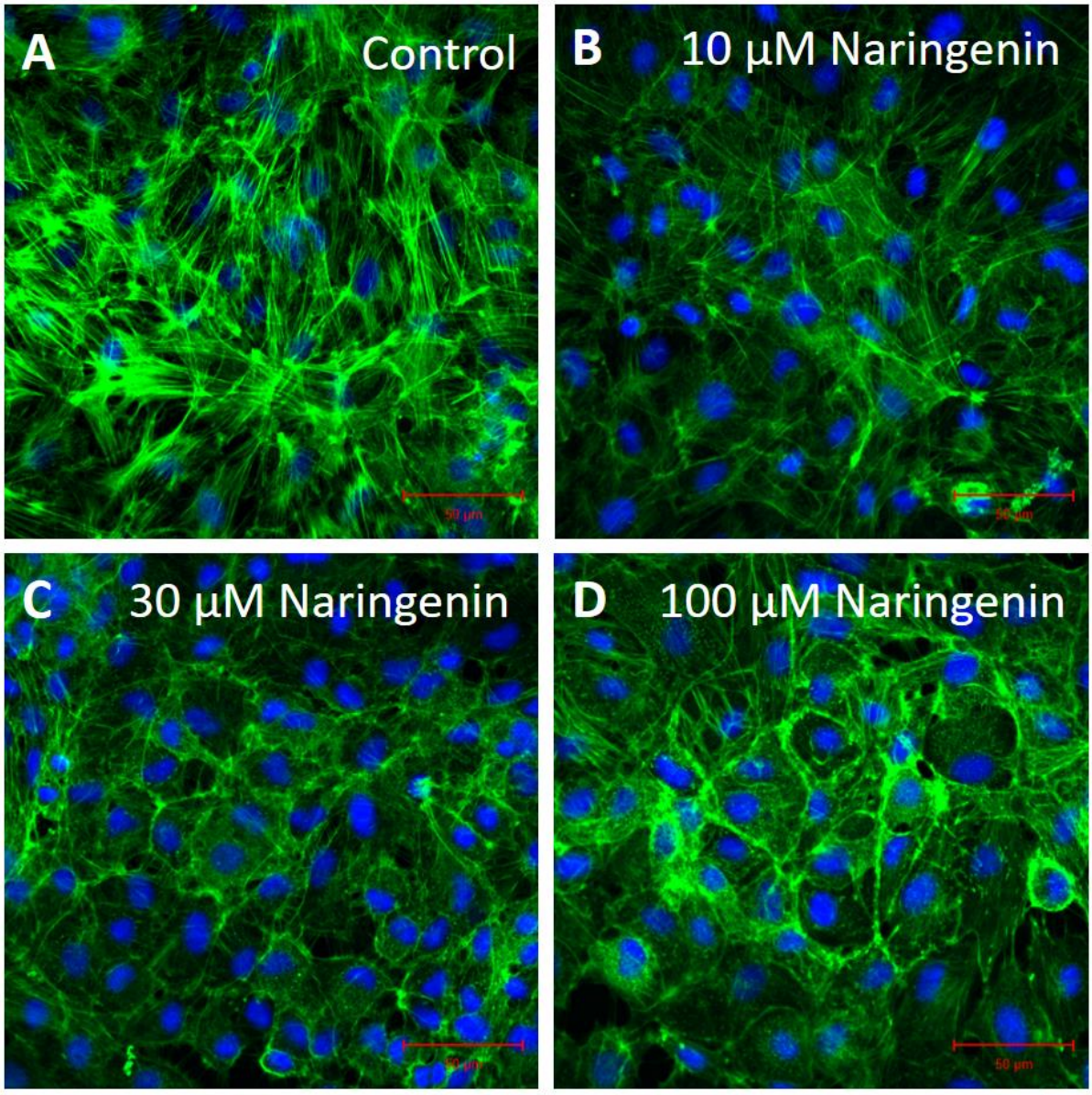

Figure 3.8. F-actin arrangement under the influence of naringenin in L15/salts medium. F-actin is visualized in green by FITC-phalloidin, while the nuclei are visualized in blue by DAPI. Staining occurred after a 24 h incubation period at 18 ^{o}C with naringenin. Scale bar = 50 µm.

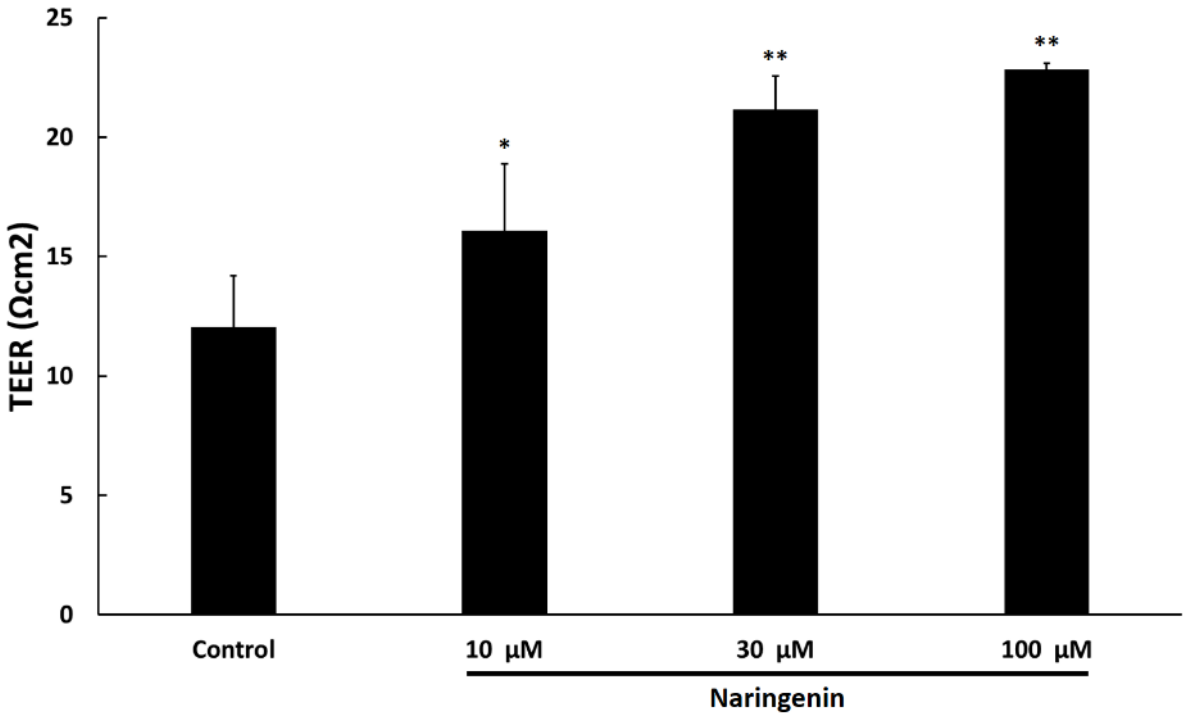

Figure 3.9. Measured TEER under various concentrations of naringenin. Cells were grown on Transwell® supports for 7 days. Once a barrier was formed, naringenin (10, 30, and 100 µM) was added apically to the cells in L15 medium. This figure represents TEER measurements on day 3 post naringenin administration. Values are means ± standard deviation. Asterisks indicate significant differences when compared to the control: *$p < 0.05$, **$p < 0.01$.

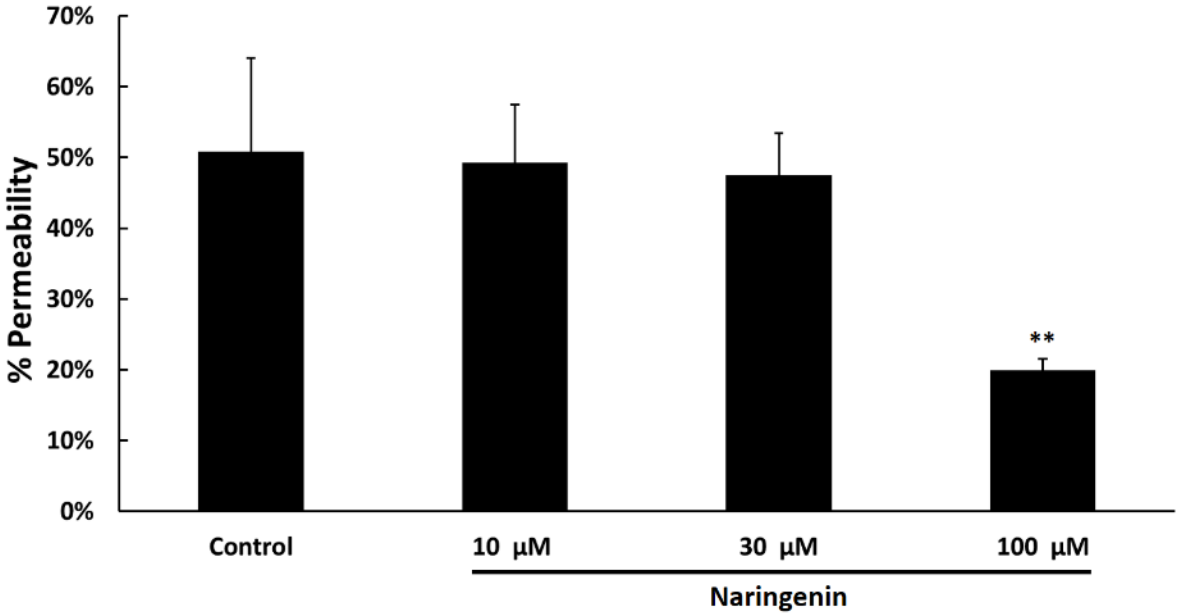

Figure 3.10. Measured LY as an indicator of barrier permeability under various concentrations of naringenin. Cells were grown on Transwell® supports for 7 days. Once a barrier was formed, naringenin (10, 30, and 100 µM) was added apically to the cells in L15 medium. LY was added to the apical side of the supports on day 4 post naringenin administration. % permeability was calculated as the % difference from a no cell (blank) support. Values are means ± standard deviation. Asterisk indicates significant difference when compared to the control: $^{**}p < 0.01$.

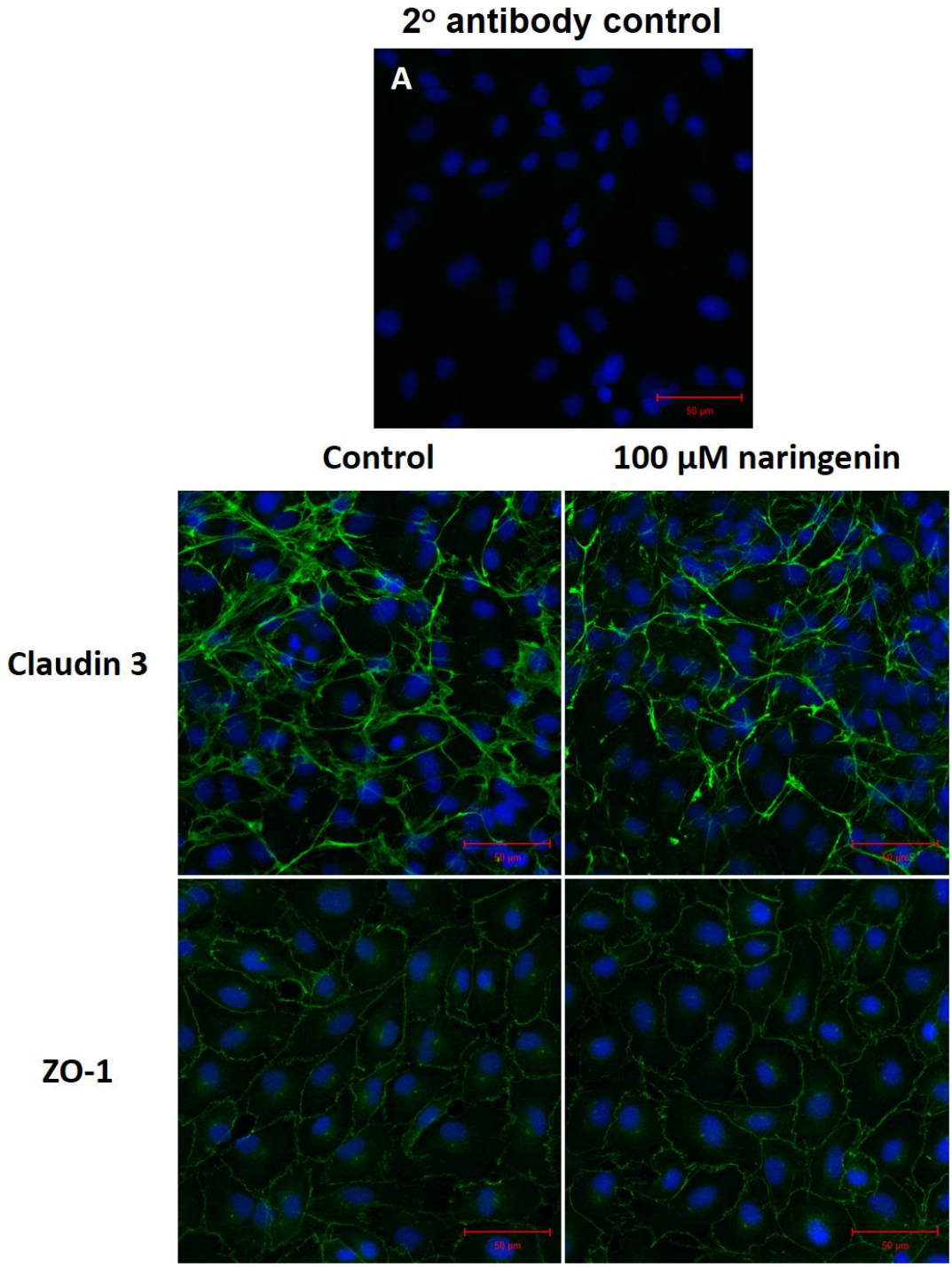

Figure 3.11. Claudin 3 and ZO-1 visualization in the presence of naringenin. (A) Secondary antibody control for nonspecific binding. (B) Claudin 3 (green) of cells incubated in L15 medium without naringenin. (C) Claudin 3 (green) of cells incubated in L15 medium with 100 µM naringenin. (D) ZO-1 (green) of cells incubated in L15 medium without naringenin. (E) ZO-1 (green) of cells incubated in L15 medium with 100 µM naringenin. Nuclei are stained blue by DAPI. Scale bar = 50 µm.

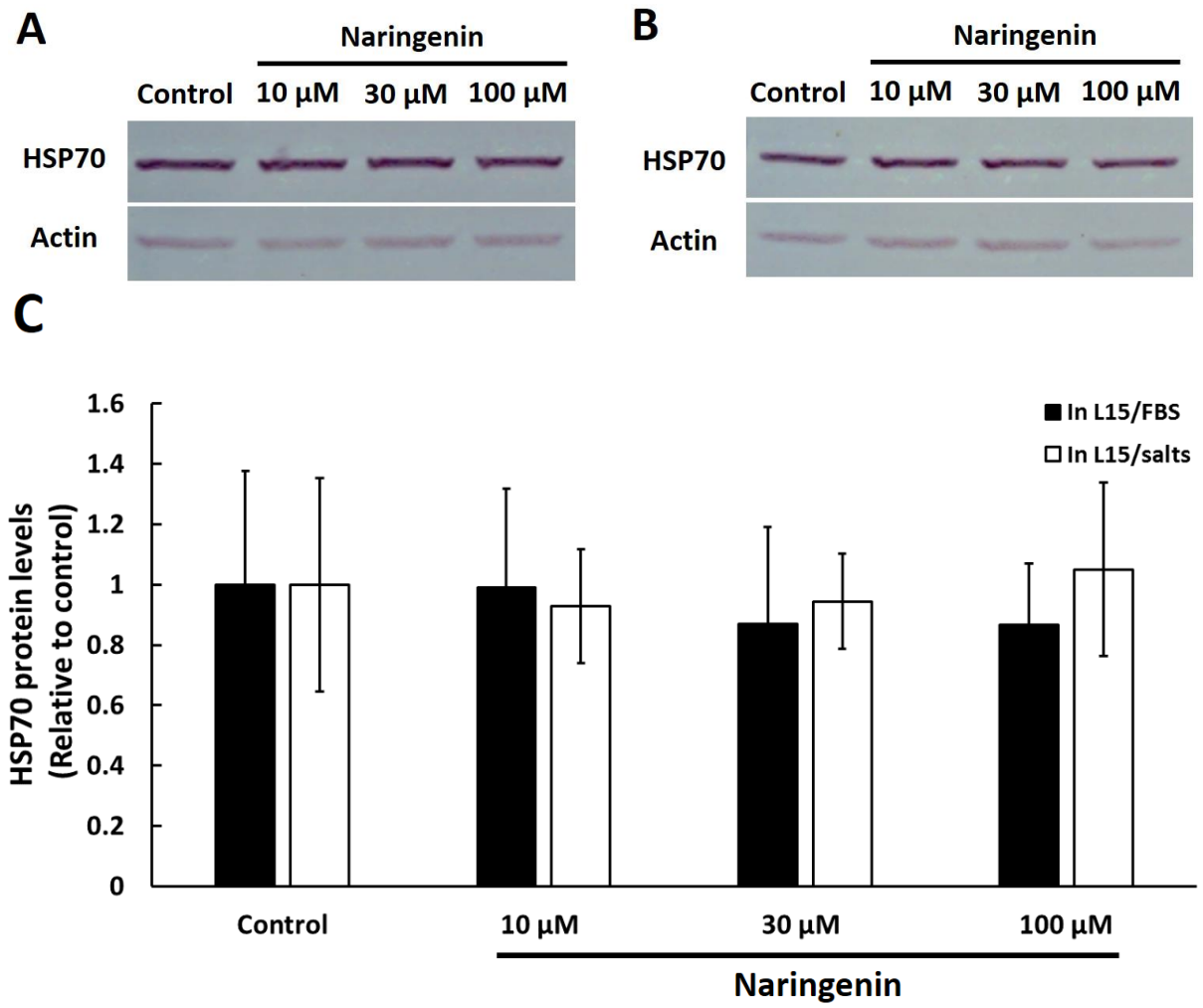

Figure 3.12. Effect of naringenin on HSP70 levels in cells. RTgutGC cultures in either L15/FBS (A) or L15/salts (B) were exposed to increasing concentrations of naringenin. After 24 h, cell extracts were prepared and subjected to SDS PAGE and western blotting with a polyclonal antibody to salmonid HSP70 and polyclonal antibody to β-actin. Densitometry of the HSP70 bands normalized to the actin bands (C) was done and values are expressed relative to the control. Values are means ± standard error of the mean.

3.3.6. Naringenin decreases restitution or migratory abilities of RTgutGC cells

Phase-contrast microscopy on day 7 post naringenin administration showed decreased restitution abilities for cells to close the cell free gap with increasing concentrations of naringenin (Fig 3.13). Restitution was almost completely halted with 75 µM naringenin (E, Fig 3.13). Using imageJ to quantify the amount of migration over time, migration is seen to slow down with increasing concentrations of naringenin (A, Fig 3.14). At day 7, 50 and 75 µM naringenin significantly halted migration by 43% and 93% respectively (B, Fig 3.14).

Concentrations of 30 and 50 μM naringenin changed f-actin organization in the migrating cells (C and D, Fig 3.15). Less f-actin was organized in the direction of migration by an increase in circumferential actin bundles. Also, a decrease in actin stress fibers was observed.

3.3.7. Naringenin and forskolin induce similar morphological and F-actin arrangements

It was hypothesized that naringenin might be conferring changes to the cells through the cAMP-PKA pathway; hence, an adenynyl cyclase activator called forskolin was used to compare F-actin arrangement changes seen with naringenin. Phase-contrast microscopy of RTgutGC cells incubated with 100 μM naringenin show a more flattened morphology with distinct cell borders (B, Fig 3.16). Cells in 10 and 30 μM forskolin retain a flattened characteristic but with less defined cell borders (C and D, Fig 3.16). Also, cells incubated with forskolin appear to display cell extensions or protrusions.

As seen in section 3.3.3, F-actin arrangement drastically changes when cells are incubated with 100 μM naringenin where more actin bundles are seen at the cells' periphery with decreases in stress fibers (B, Fig 3.17). A very similar f-actin arrangement was seen in cells incubated with 10 and 30 μM forskolin (C and D, Fig 3.17).

3.3.8. Effects of naringenin with forskolin and H89 on the restitution abilities of RTgutGC

To further test the hypothesis that naringenin might be exerting F-actin changes through the cAMP-PKA pathway, a restitution study was done with two cAMP-PKA modulators, forskolin and H89. On day 4 of restitution, 75 μM naringenin halted migration as demonstrated before (C, Fig 3.18). The addition of 5 μM H89, a potent protein kinase A inhibitor, appeared to have no effect in diminishing the halt in migration due to naringenin (E, Fig 3.18). Forskolin, an adenylyl cyclase activator, and H89, either alone or in combination, had no effect on cell migration (D, E, and G, Fig 3.18). Interestingly, cells migrating with forskolin addition obtained prominent cell protrusion in the direction of cell migration (Fig 3.19). When quantification was performed on the pictures, naringenin significantly halted migration by 63% (Fig 3.20). As seen with phase-contrast microscopy, H89 did not diminish the inhibitory effects of naringenin on cell migration as a significant 76% drop in migration occurred. Again,

forskolin and H89 (either on their own or in combination) had no effect on cell migration (Fig 3.20).

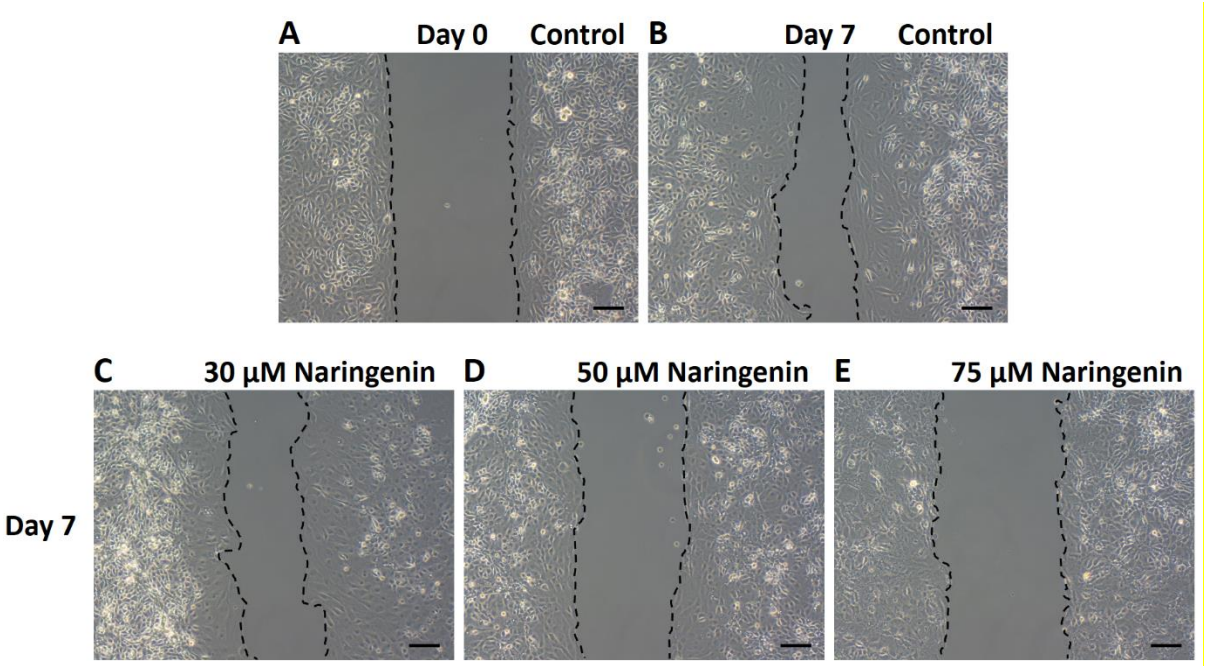

Figure 3.13. Phase-contrast microscopy of RTgutGC restitution under the influence of naringenin. (A) Day 0 of restitution. (B-E) Day 7 of restitution under the influence of 30, 50, and 75 µM naringenin in L15. Cell monolayer borders are traced in black to better visualize restitution. Pictures represent magnification at 100x field with a scale bar of 100 µm.

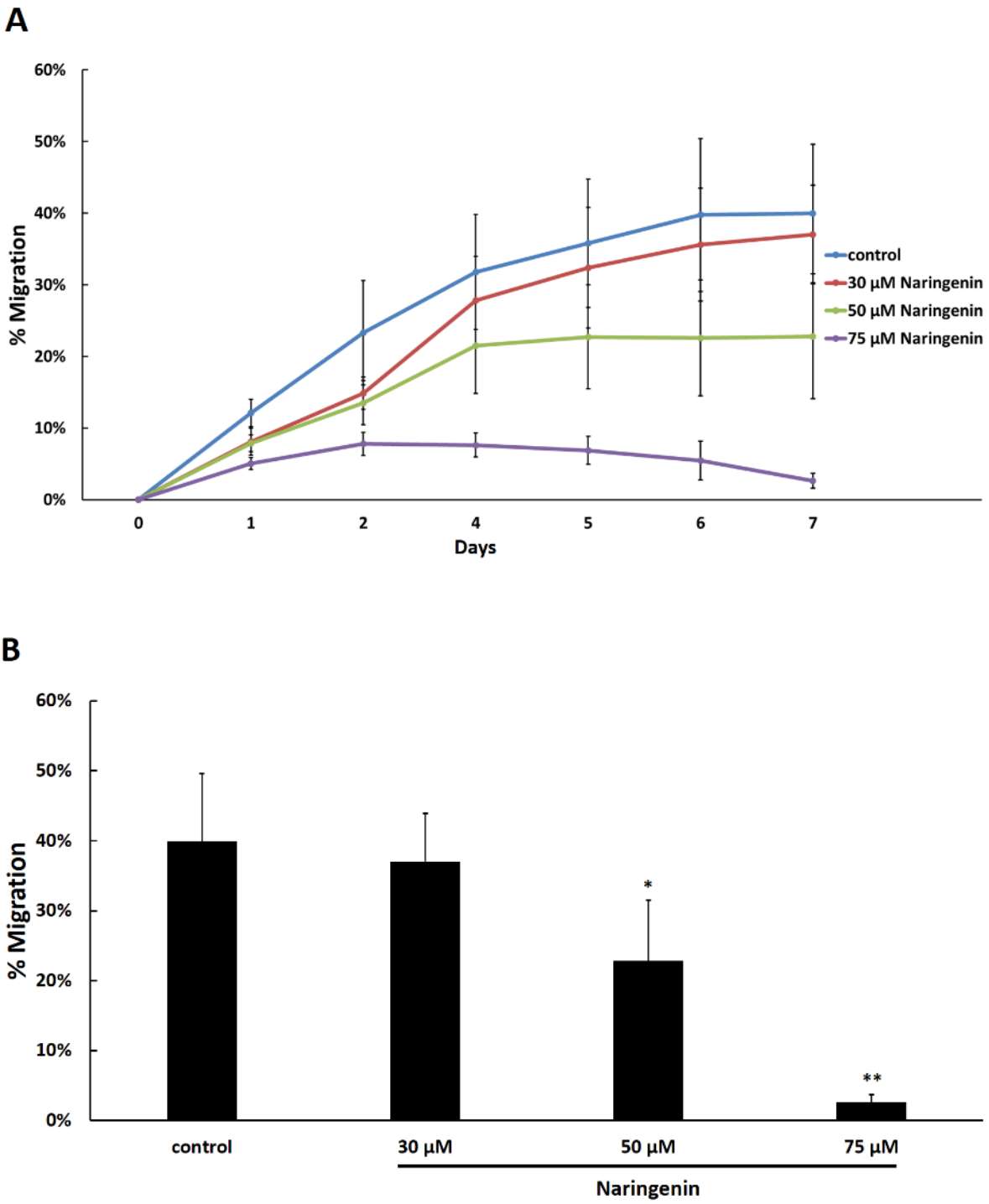

Figure 3.14. Graphical demonstration of the influence of naringenin on cell restitution. (A) Restitution capacity of RTgutGC when incubated with 30, 50, and 75 µM of naringenin in L15 medium measured as % migration over days. (B) Day 7 restitution capacity of RTgutGC incubated with naringenin. Values are means ± standard deviation. Asterisks indicate significant differences when compared to the control: *$p < 0.05$, **$p < 0.01$.

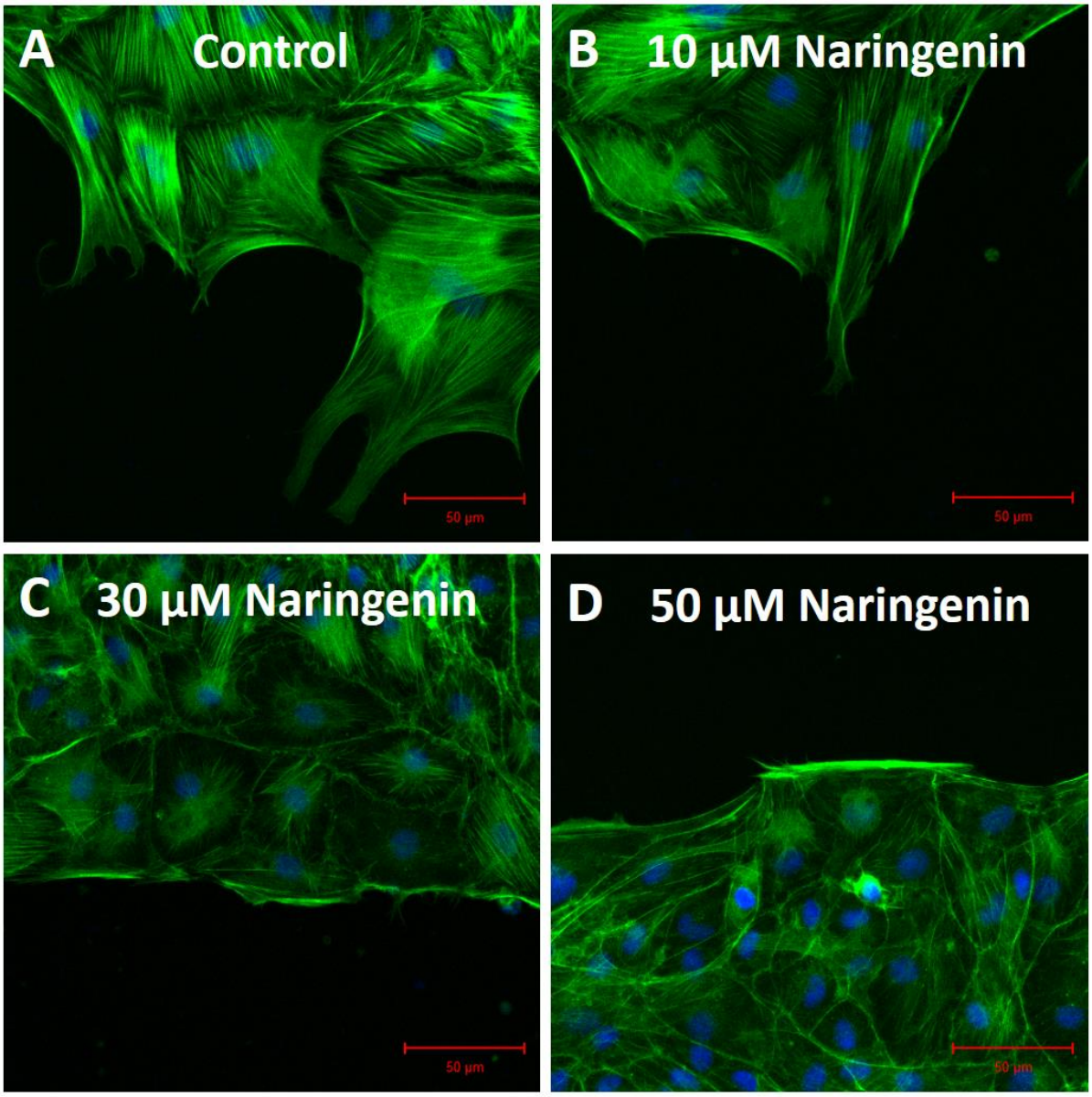

Figure 3.15. F-actin arrangement during migration under the influence of naringenin. F-actin is stained as green by FITC-phallodin, while the nuclei are stained as blue by DAPI. (A) F-actin of migrating control cells in L15 medium. (B) F-actin of migrating cells incubated with 10 µM naringenin. (C) F-actin of migrating cells incubated with 30 µM naringenin. (D) F-actin of migrating cells incubated with 50 µM naringenin. Scale bar = 50 µm.

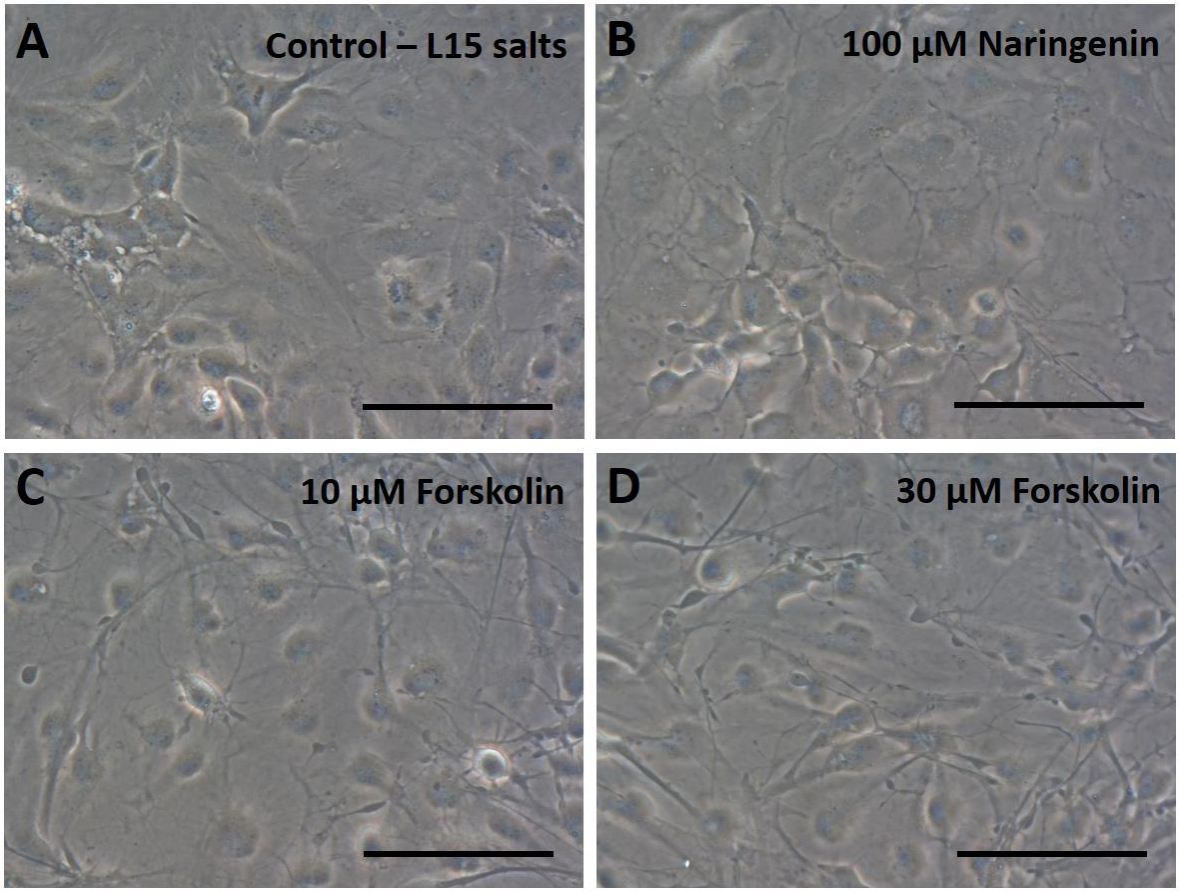

Figure 3.16. Phase-contrast microscopy of RTgutGC cells incubated in either naringenin or forskolin. (A) Cells incubated in L15/salts without naringenin or forskolin for 24 h. (B) Cells incubated in L15/salts with 100 µM naringenin for 24 h. (C) Cells incubated in L15/salts with 10 µM forskolin for 24h. (D) Cells incubated in L15/salts with 30 µM forskolin for 24 h. Pictures represent magnification at 400x field with a scale bar of 100 µm.

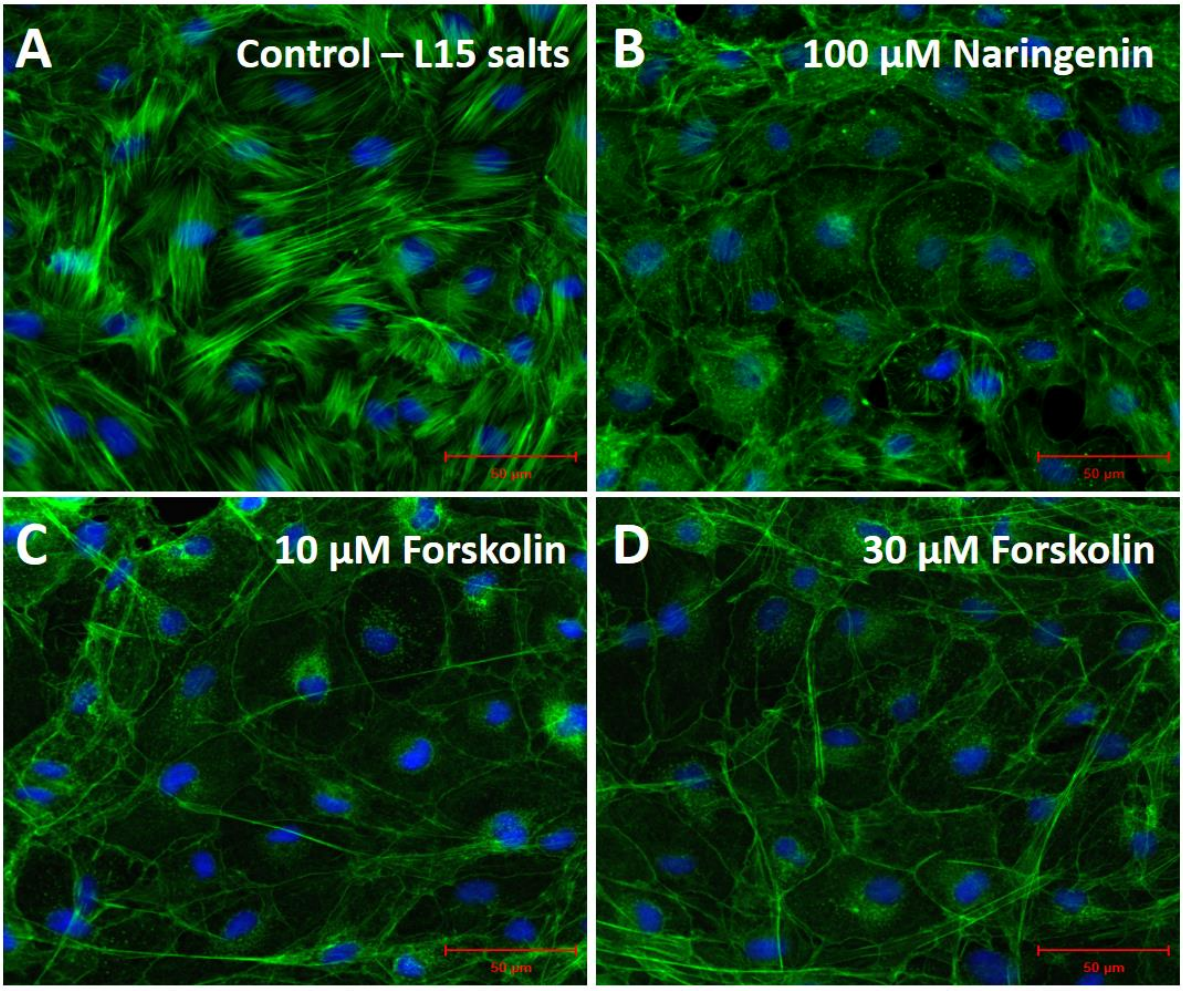

Figure 3.17. F-actin arrangement of RTgutGC cells incubated with naringenin or forskolin. FITC-phalloidin was used to stain F-actin as green. (A) Cells incubated in L15/salts without naringenin or forskolin for 24 h. (B) Cells incubated in L15/salts with 100 µM naringenin for 24 h. (C) Cells incubated in L15/salts with 10 µM forskolin for 24h. (D) Cells incubated in L15/salts with 30 µM forskolin for 24 h. Nuclei are stained blue by DAPI. Scale bar = 50 µm.

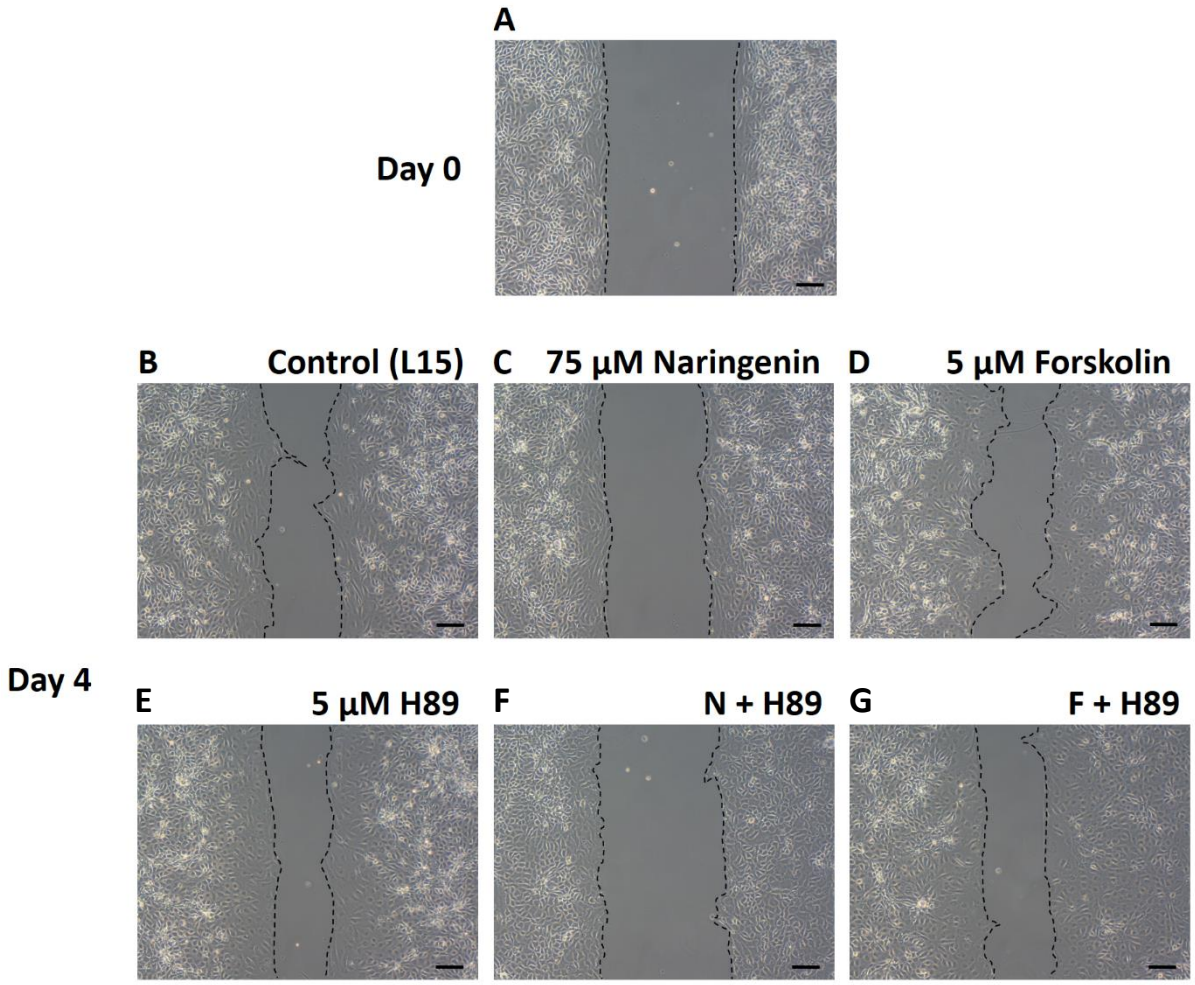

Figure 3.18. Phase-contrast microscopy of RTgutGC restitution under the influence of naringenin, forskolin, H89, and their combinatorial uses. (A) Day 0 of restitution. (B-G) Day 4 of restitution in various components. N + H89 is 75 µM naringenin with 5 µM H89 while F + H89 represents 5 µM forskolin with 5 µM H89. All compounds were incubated with the cells in L15 medium. Cell monolayer borders are traced in black to better visualize restitution. Pictures represent magnification at 100x field with a scale bar of 100 µm.

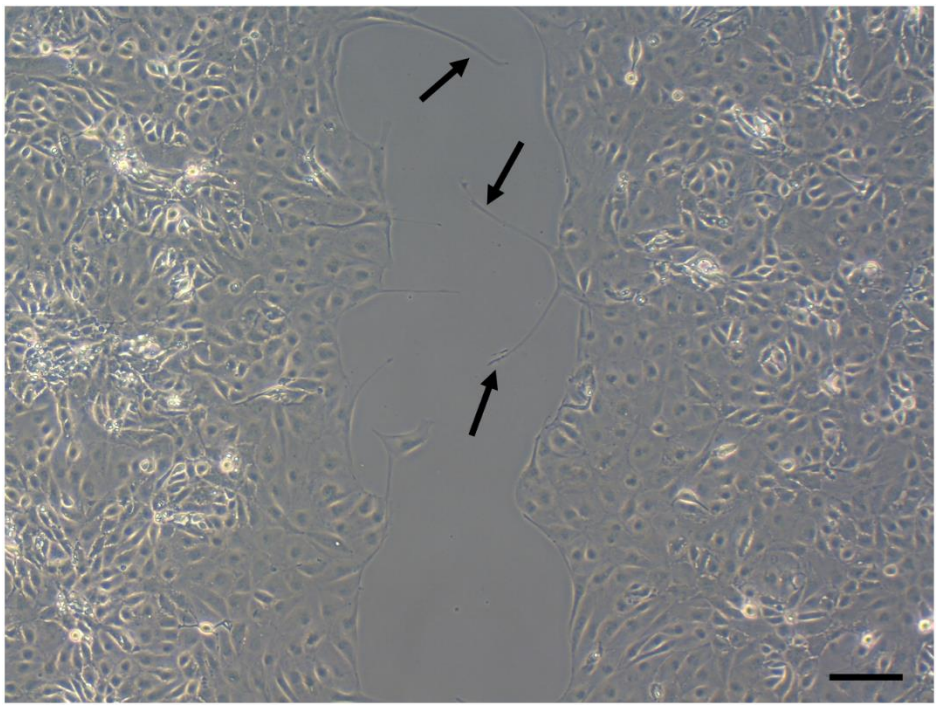

Figure 3.19. Cell protrusions induced by 5 µM forskolin. Arrows indicate cell protrusions that were only seen during migration in the presence of forskolin**.** Scale bar = 100 µm

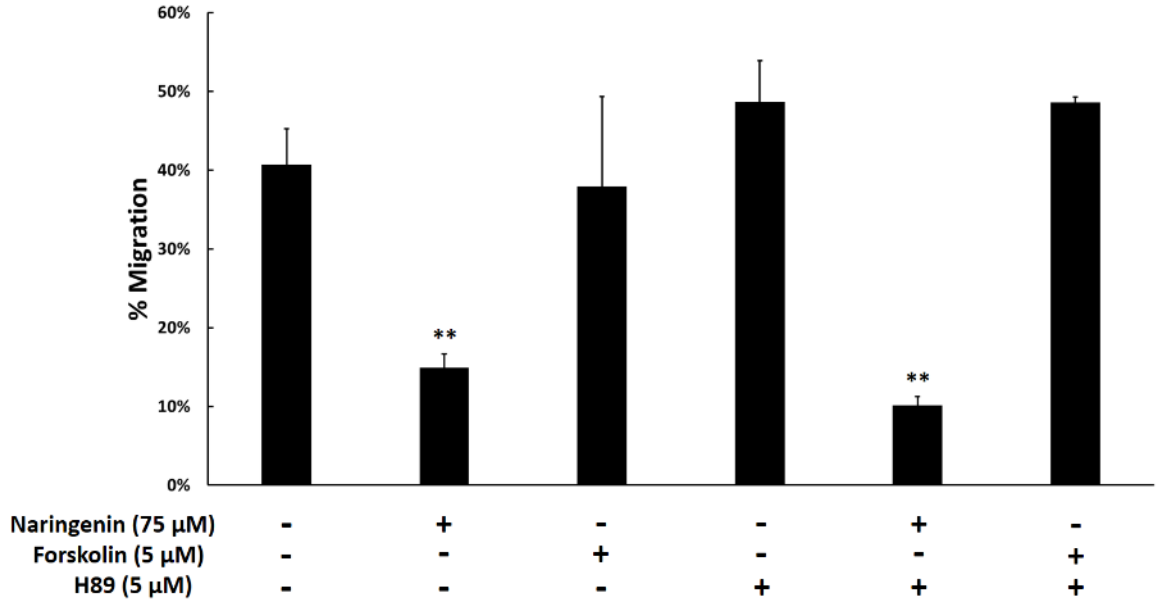

Figure 3.20. Day 4 RTgutGC restitution capacity under the influence of naringenin, forskolin, H89, and their combinatorial use. Cells were incubated with 75 µM naringenin, 5 µM forskolin, 5 µM H89, 75 µM naringenin with 5 µM H89, or 5 µM forskolin with 5 µM H89 all in L15 medium. Cell restitution was monitored over 7 days. This figure represents the percent migration on day 4 calculated from the phase-contrast microscopic pictures. Values are means ± standard deviation. Asterisk indicates significant difference when compared to the control: **$p < 0.01$.

3.4. DISCUSSION

Flavonoids such as naringenin are known to exert potential health promoting effects by interactions with cellular and molecular events. Some examples include suppressed protein aggregation and apoptosis from the induction of the endoplasmic reticulum chaperone GRP78, increased intestinal barrier function through the increased expression of the TJ protein ZO-2, occludin, claudin 1, and claudin 4, increases in HSP70 protein expression, and overall, naringenin possesses anti-inflammatory, anticarcinogenic, antidiabetic, anti-lipidemic, and antioxidant properties (Leonardi et al., 2010; Mulvihill et al., 2009; Noda et al., 2013; Park et al., 2012; Wang et al., 2012; Yamagishi et al., 2012). More recently naringenin was shown to be cardioprotective by activating mitoBK channels and had antiviral properties against the dengue virus (Frabasile et al., 2017; Testai et al., 2017). Studies on naringenin are predominantly in mammalian systems with very few elucidating the interactions of this flavanone in teleost. In the present study, a rainbow trout intestinal epithelial cell line, RTgutGC, was used as an *in vitro* model to investigate the influence of naringenin on various cellular functions.

Higher concentrations (30 and 100 μM) of naringenin in L15/salts slightly changed the morphology of RTgutGC with more cells acquiring a flattened morphology with some membrane ruffling and more distinct cell borders. This was matched with a decrease in metabolic activity but not plasma membrane integrity of cells exposed to 100 μM of naringenin in L15/salts. A significant reduction in metabolic activity and plasma membrane integrity was additionally observed at 100 μM of naringenin in L15 media. However, when cells were incubated in L15/FBS this effect was less prominent. Plasma membrane integrity was less compromised by naringenin presence compared to the cells' metabolic activity. In fact, plasma membrane integrity slightly increased when narningenin was incubated with cells in L15/salts, a condition completely deprived of nutrients, whereas a small but significant decrease was observed in L15 and L15/FBS, two nutritionally rich conditions. It appears that under suboptimal conditions, in this case the cells being starved of essential nutrients in L15/salts, naringenin exerts cytotoxic effects towards the cells' metabolic activity. Under starvation, cells divert certain cellular pathways to ensure cell survival by degradation systems recycling cytosolic proteins and RNA through a process called autophagy (Kuma & Mizushima, 2010). Under such state, it is possible that cells are unable to properly metabolise naringenin and retain

toxic metabolites (Khan et al., 2014). The presence of glutamine in L15/FBS might also exert protective effects on cells through induced HSP expression and the synthesis of glutathione, while also suppressing apoptosis and cytokine pathways (Evans et al., 2005; Kawano et al., 2011; Roth, 2008). Additionally, albumins in serum are known to bind polyphenols such as naringenin possibly making it less available to the cells (Khan et al., 2014).

Noda et al., 2013 demonstrated that naringenin increased Caco-2's barrier by the increased expression of the TJ protein ZO-2, occludin, claudin 1, and claudin 4. Additionally, naringenin mediated increases of claudin 4 in Caco-2 involved interactions with the transcription factor Sp1, known to bind to the human HSP70 promoter site, possibly explaining increased HSP70 protein expression with naringenin in Caco-2 (Morgan, 1989; Noda et al., 2013). In contrast to what was discovered in Caco-2 cells (Noda et al., 2013), naringenin did not increase HSP70 protein expression in RTgutGC cells. As seen with Caco-2 cells, naringenin increased the RTgutGC barrier by TEER and LY measurements. However, in this current study, no visible differences in claudin 3 and ZO-1 were observed in RTgutGC cells incubated with naringenin This indicates a possible alternate mechanistic action of naringenin enhancing barrier functions in RTgutGC cells. Also, TJs comprise of a large variety of dynamic proteins upon which naringenin might act, other than claudin 3 and ZO-1. Claudins can vary in roles with protein combinations in TJ resulting in a more "leaky" or "tighter" barrier (Kolosov et al., 2013). In fish, claudin 3 is considered one of the main barrier forming TJ proteins (Clelland et al., 2010). ZO-1 is a cytosolic TJ protein providing scaffolding and structural support to the TJ by linking claudins and occludin to the actin cytoskeleton of the cell (Chasiotis et al., 2012). In RTgutGC cells, naringenin promoted a circumferential actin arrangement with a decrease in stress fibers. The appearance of circumferential actin bundles usually indicates stronger interactions with TJ and cell adhesion proteins, generating stronger cell-to-cell contacts by actin stabilizing those structures (Noda et al., 2010), possibly explaining the barrier increase observations with naringenin. Moreover, Yukiura et al. (2015) demonstrated that the loss of circumferential actin bundles followed by an increase of stress fibers lead to an increase in cell permeability.

RTgutGC cells' ability to migrate into a cell free space diminished with the addition of naringenin. This took place with the loss of actin fibers oriented in the direction of migration suggesting loss of lamellipodia and filopodia structure. Naringenin promoted the loss of stress

fibers that occurred concomitantly with the formation of circumferential actin bundles. Stress fibers connected to focal adhesion points play an important role in cellular migration of certain cell types and their loss can lead to decreases in migratory capacity (Dourdin et al., 2001; Vallenius, 2013).

Modulation of F-actin rearrangement and proper cytoskeletal organization is regulated by the cAMP-dependent protein kinase (PKA) pathway (Howe, 2004; Gerits et al., 2007). The complete function and role of the cAMP-PKA pathway on actin organization and its influences on migratory and barrier integrity are far from understood. It is reported that PKA activation causes loss of stress fibers and decreases in migratory capabilities, while downregulation of PKA is required for stress fiber formation (Kim et al., 2000; Whelan & Senger, 2003; Zimmerman et al., 2012). However, in other cases, activation of PKA is considered important for proper cell migration (Glenn & Jacobson, 2003; Nadella et al., 2009; Plopper et al., 2000; Spurzem et al., 2002). Additionally, there is evidence that high levels of cAMP and activation of the PKA pathway can lead to enhanced barrier functions (Fukuhara et al., 2005; Li et al., 2015; Stelzner et al., 1989). It would appear that there is no simple positive/negative effect of cAMP-PKA activation or inhibition to actin organization promoting proper cell migration or barrier functions; rather it being an intricate balance of molecular functions (Howe, 2004).

In this current study similarities in F-actin arrangement were observed with naringenin and with forskolin, an adenylyl cyclase activator. In mammalian cells, forskolin has been shown to increase cell-to-cell contacts with increased circumferential actin bundles, increased barrier functions, and decreased migration, all traits that were similarly seen in RTgutGC cells incubated with naringenin (Fukuhara et al., 2005; Stelzner et al., 1989; Yukiura et al., 2015; Zimmerman et al., 2012). Additionally, there is evidence supporting the idea that naringenin increases intracellular cAMP levels and activates PKA (Yang et al., 2008). This lead us to believe that naringenin might be generating changes in RTgutGC F-actin by the cAMP-PKA pathway. Hence, a cell migration experiment was conducted to observe and compare the effects of naringenin, forskolin, and with the addition of H89, a PKA inhibitor, on RTgutGC cells. As expected naringenin significantly halted migration; however, the addition of H89 with naringenin did not recover migration indicating that naringenin might not involve PKA activation in RTgutGC cells. An interesting result was that forskolin treated cells, and also with the addition of H89, did not exhibit any changes in migration. Despite the high level of

conservation in the PKA family, there exist some residues where no overlap is seen when comparing human residues to bony fish (Søberg et al., 2013). It is possible that there exist some functional differences in cAMP-PKA in fish compared to mammals. Additionally, studies suggest there may be a dual role of cAMP, where high nonphysiological concentrations can inhibit migration, whereas low concentrations may stimulate migration (Spurzem et al., 2001). However, since intracellular cAMP levels were not measured in this study, it cannot be confirmed that forskolin acted in the intended way. Experiments focusing on the role of cAMP and PKA in RTgutGC with naringenin are a promising path for future work.

In summary, low concentrations of naringenin could be a beneficial feed additive to promote barrier integrity without affecting cellular migration and metabolism. In this study, a concentration of 30 μM was shown to be most beneficial to RTgutGC cells where it increased barrier integrity, did not halt migratory abilities of the cells, and did not significantly decrease the cells' metabolic activity or plasma membrane integrity in full nutritional conditions. However, more studies will have to be done to explore whether the results correlate to *in vivo* conditions and the underlying mystery to naringenin's cellular and molecular actions in RTgutGC cells whether actin on the cAMP-PKA pathway or not.

CHAPTER 4

Effect of plant antinutritionals and sodium butyrate on rainbow trout epithelial cell restitution

4.1. INTRODUCTION

Aquaculture is considered one of the fastest growing food production sectors in the world (FAO, 1997; FAO, 2016; Francis et al., 2001). It comes as no surprise that the aqua-feed industry, sustaining this growth, is also one of the largest and fastest growing agricultural industries (FAO, 1997; FAO, 2016; Francis et al., 2001). Fishmeal was a popular food source in aquaculture, especially for salmon and trout; however, the high use and demand of fish feed led to it being a potential limited global resource in the future (Sargent & Tacon, 1999; Naylor et al., 2000). Accordingly, the Second International Symposium on Sustainable Aquaculture (1998) in Oslo, Norway recommended the use of an alternate protein source to fishmeal (Francis et al., 2001). Plant-derived protein sources showed promise to replace fishmeal and are now currently in use in many aquaculture practises (Francis et al., 2001; Teves & Ragaza, 2016). However, many plant-protein sources come with a handful of unwanted compounds called antinutritionals or antinutritional factors (ANFs) such as protease inhibitors, lectins, saponins, and tannins (Francis et al., 2001; Teves & Ragaza, 2016).

An important organ system critical to proper fish health is the gastrointestinal (GI) tract. To maintain a proper functioning, homeostatic intestinal system, a variety of intestinal cells are constantly dividing, growing, and differentiating. However, intestinal damage can occur during fish husbandry (Beck & Peatman, 2015). To heal from this damage, cells undergo intestinal wound healing (Nakamura et al., 2013). The process can be broken down into three main steps: 1) Intestinal epithelial cells migrate into the wound quickly sealing it, a process called restitution. Cellular proliferation is very limited during this step (Sturm & Dignass, 2008). 2) The cells undergo proliferation to restore the decreased cell pool, and 3) growth and differentiation occurs to regain proper intestinal function (Sturm & Dignass, 2008). With the GI tract being the first organ system coming in contact with nutrients and absorbing such nutrients, it is important to understand the interaction of fish feed components with the intestinal system. However, next to nothing is known about the impacts of ANFs on salmon and rainbow trout intestinal health and restitution.

This study is the first to show negative impacts of a variety of ANFs on rainbow trout intestinal epithelial cell (RTgutGC) migration. The ANFs used in this study include the two soybean protease inhibitors: Bowman-Birk inhibitor (BBI) and Kunitz inhibitor (KI), and two lectins: soybean agglutinin (SBA) and wheat germ agglutinin (WGA). *In vivo* studies suggest

that rainbow trout are particularly sensitive to the soybean protease inhibitors (Francis et al., 2001). An additional component of interest studied was the short chain fatty acid butyrate, not considered an ANF, but growing in popularity as a fish feed additive. The results show that BBI, WGA, and butyrate significantly decreased RTgutGC migration, KI only slightly decreased migration, and SBA had no effect on migration.

4.2. MATERIALS AND METHODS

4.2.1. Cell culture and culture conditions

The cell line used was RTgutGC, a rainbow trout intestinal epithelial cell line (Kawano et al., 2011). To maintain the cells, Leibovitz's L15 medium with 2.05 mM L-Glutamine (Thermo Fisher Scientific) supplemented with 10% fetal bovine serum (FBS, Sigma-Aldrich) and antibiotics (10,000 U/mL penicillin and 10,000 μg/mL streptomycin, P/S, Thermo Fisher Scientific) (L15/FBS) was used. Subculturing with the use of trypsin (Thermo Fisher Scientific) occurred every week passaging the cells at a ratio of 1 to 2. Cells were kept at 18 ^{o}C in BioLite 75 cm^2 cell culture treated flasks (Thermo Fisher Scientific).

4.2.2. Feed additives and antinutritional factors

Components used were 2, 5, and 8 mM sodium butyrate (Sigma-Aldrich), 25, 50, and 100 μg/mL trypsin-chymotrypsin inhibitor from *Glycine max* (Bowman-Birk inhibitor, BBI, Sigma-Aldrich), 25, 50, and 100 μg/mL trypsin inhibitor from *Glycine max* (Kunitz inhibitor, KI, Sigma-Aldrich), 50, 100, and 200 μg/mL lectin from *Glycine max* (soybean agglutinin, SBA, Sigma-Aldrich), and 0.25, 0.75, 1.5, 2.25, and 2.5 μg/mL lectin from *Triticum vulgaris* (wheat germ agglutinin, WGA, Sigma-Aldrich). Concentrations were determined by preliminary experiments and past cytotoxicity data not shown in this section. All components were diluted in L15 media when added to the cells.

4.2.3. Evaluating plant antinutritionals and butyrate for effects on restitution

The influence of several plant antinutrionals and sodium butyrate on the migration of RTgutGC into a wound or gap was investigated in a restitution assay. The assay was set up in 2-well culture inserts from Ibidi GmbH, Planegg / Martinsried, Germany as described in Chapter 2 (section 2.2.9) and performed at 18 °C. After monolayers had been established in L15/FBS, the medium was changed to just L15, which supports migration but not proliferation (Chapter 2). Twenty-four hours later the inserts were removed to create the gap and the components of interest, described in section 4.2.2, were then added. Phase contrast microscopy pictures were taken of the gaps immediately and for up to 6-7 days afterwards. Photographs of the gaps were analyzed with ImageJ and the results expressed as % cell migration as

described in Chapter 3 (section 3.2.8). Three independent experiments were done for each test agent and statistical analysis was done as described in section 4.2.5.

4.2.4. FITC labelled phalloidin staining for F-actin

Similar to 4.2.3 above, specialized 2-well culture inserts were used to create a 500 μm gap to monitor cellular migration. The protocol followed 4.2.3 except inserts were placed in a 4 chamber tissue culture treated glass Falcon CultureSlide® (Corning) instead of a 24-well plate, and day 3 was used as the endpoint. On day 3 of migration in precense of the component of interest, cells were washed with DPBS and fixed with 3% paraformaldehyde (Sigma-Aldrich) for 20 minutes at 4 ^{o}C. Following fixation, the cells were then permeabilized with 0.1% Triton X-100 (Sigma-Aldrich) for 10 minutes at room temperature. Afterwards, 5 μg/mL of FITC-phalloidin in DPBS was added to the cells and allowed to incubate for 45 min at room temperature in the dark. Cells were then washed three times with DPBS and the slides were allowed to dry. Once dry, plastic chambers were removed from the slides and three drops of a mounting medium, Fluoroshield (Sigma-Aldrich), containing DAPI was added to the slides with a coverslip to help preserve the slide and counter stain for DNA. Confocal images were obtained with the Zeiss LSM 510 laser scanning microscope and were acquired and analyzed using a ZEN lite 2011 software.

4.2.5. Statistical analyses

Variables were expressed as the mean ± standard deviation. Statistical analysis was done by a one-way ANOVA and Dunnet post hoc test. Statistical significance was defined as $p < 0.05$.

4.3. RESULTS

4.3.1. BBI reduces migration in RTgutGC cells

When observing the migratory trend over time, it was seen that increasing concentrations of BBI caused migration to plateau on day 2 at lower respective percentages (A, Fig 4.1). When observing the total migration on day 7, 100 μg/mL BBI significantly decreased percent migration to 13 ± 3% in RTgutGC cells when compared to the L15 control at 23 ± 7% (B, Fig 4.1 and Fig 4.2). 25 and 50 μg/mL BBI plateaued on day 2 (A, Fig 4.1). Total percent migration on day 7 for 25 and 50 μg/mL BBI a similar respective value of 19 ± 2% and 19 ± 6% cell migration (B, Fig 4.1 and Fig 4.2).

4.3.2. SBA has no effect on RTgutGC migration and F-actin arrangement

Over 7 days, 50, 100, and 200 μg/mL SBA had no observable or influence on migration of RTgutGC cells (Fig 4.3 and 4.4). Over time, a similar trend was seen at all concentrations relative to the control (A, Fig 4.3) with the total percent migration on day 7 for 50, 100, and 200 μg/mL SBA at 39 ± 5%, 40 ± 5%, and 38 ± 8%, respectively, compared to 37 ± 8% for the L15 only (0 μg/mL SBA) control (B, Fig 4.3).

F-actin visualization by FITC-phalloidin and confocal microscopy revealed no observable differences in F-actin arrangements (Fig 4.5). Cells in all conditions had similar stress fiber organization with most bundles parallel to the direction of migration.

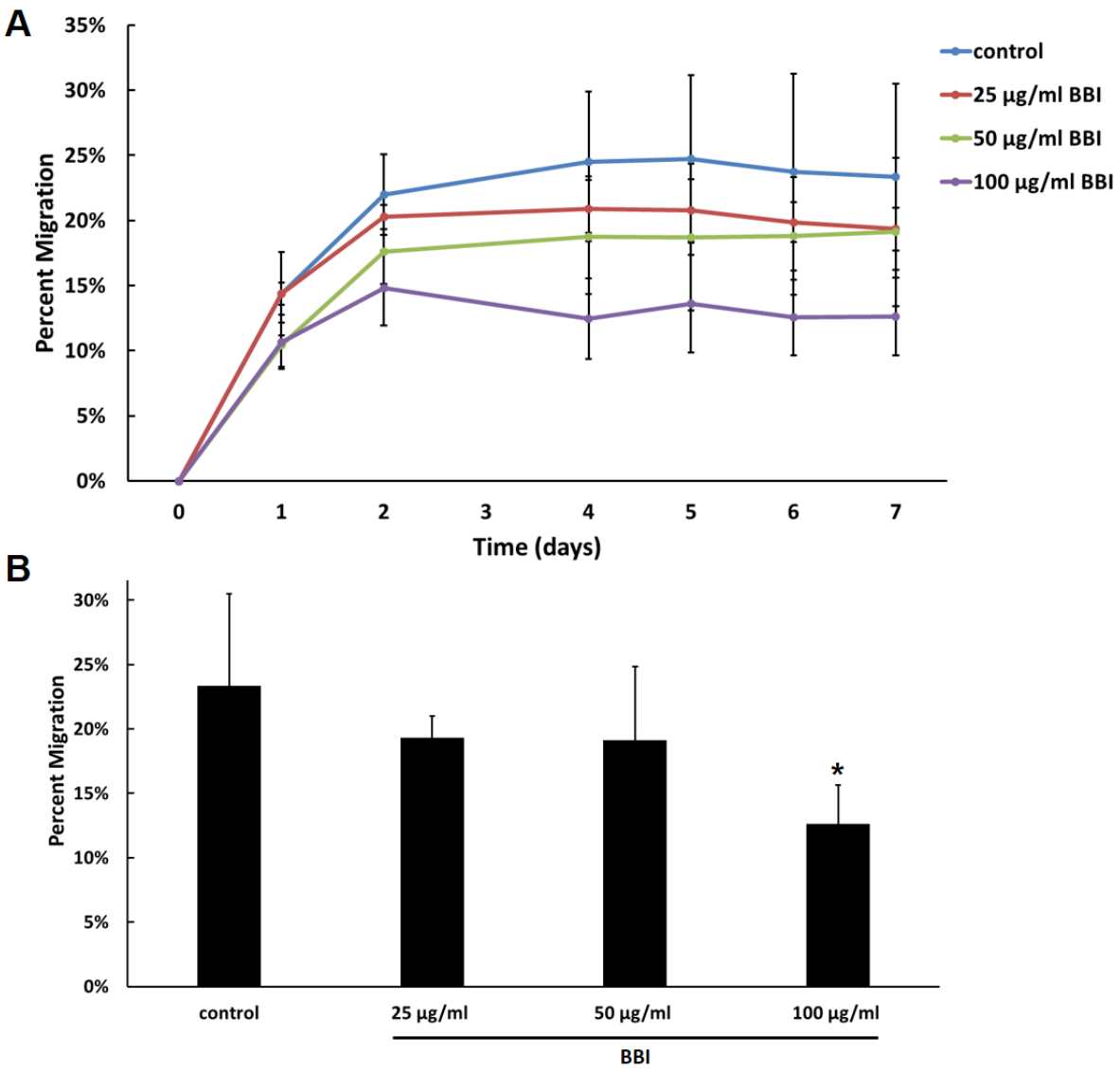

Figure 4.1. RTgutGC migration over time under the influence of Bowman Birk inhibitor (BBI). (A) Migratory capacity of RTgutGC over 7 days when incubated with 0, 25, 50, and 100 µg/mL of BBI in L15 medium measured as percent migration into a cell free gap. (B) Bar graph of the day 7 migratory capacity of RTgutGC cells incubated with 0, 25, 50, and 100 µg/mL of BBI in L15 medium. Values are means ± standard deviation. Asterisk indicates significant difference when compared to the control: *$p < 0.05$.

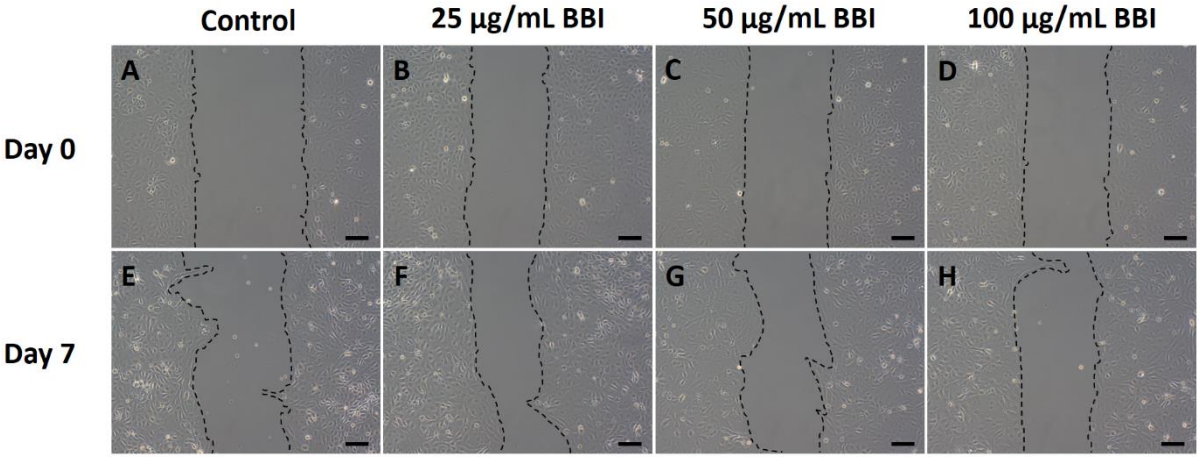

Figure 4.2. Phase-contrast microscopy of RTgutGC restitution under the influence of Bowman Birk inhibitor (BBI). (A – D) Day 0 pictures after establishment of control, 25, 50, and 100 µg/mL BBI in L15 medium. (E – H) Day 7 pictures of control, 25, 50, and 100 µg/mL BBI in L15 medium. Cell monolayer borders are traced in black to better visualize restitution. Scale bar = 100 µm.

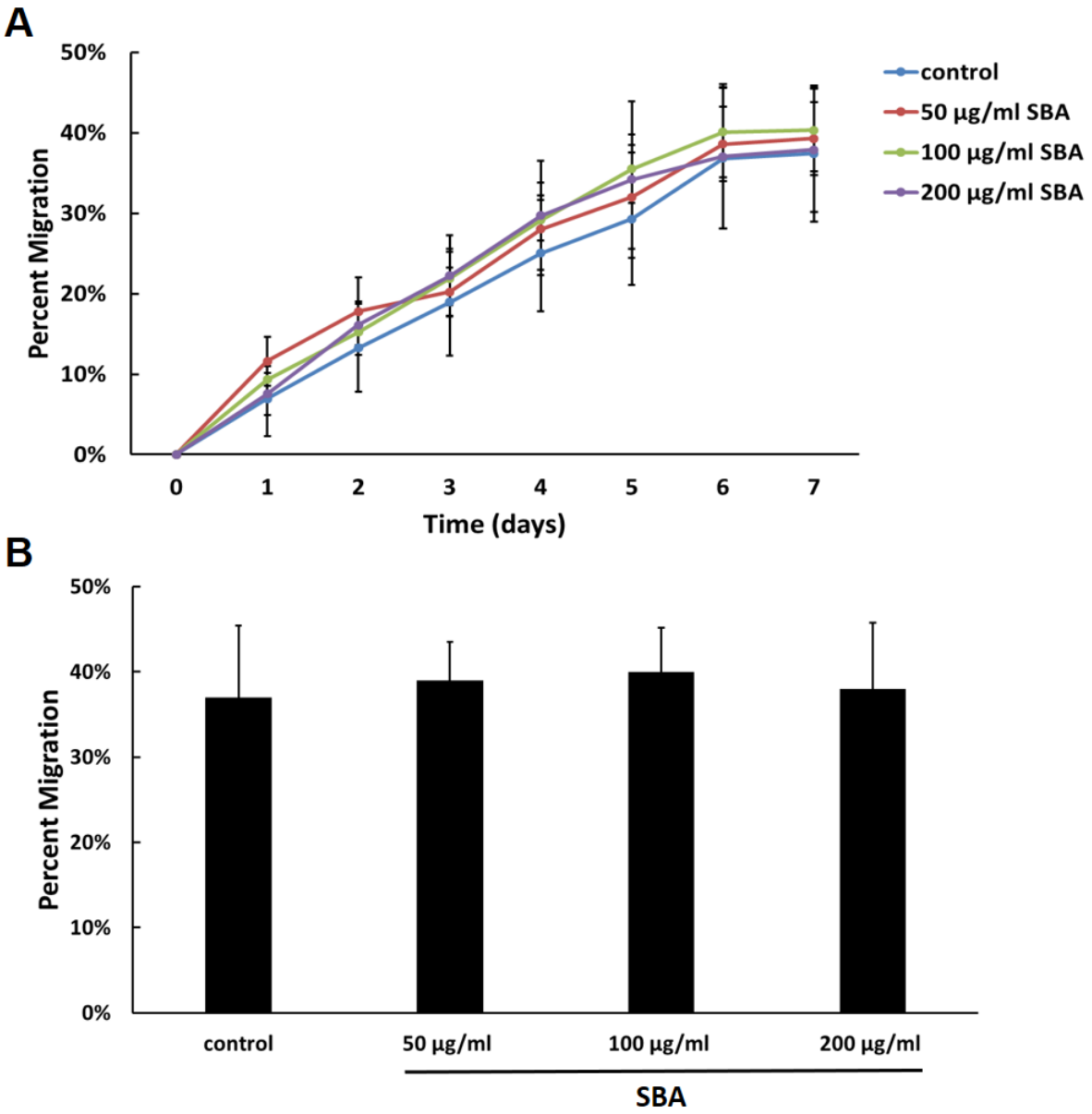

Figure 4.3. RTgutGC migration over time under the influence of soybean agglutinin (SBA). (A) Migratory capacity of RTgutGC over 7 days when incubated with 0, 50, 100, and 200 µg/mL of SBA in L15 medium measured as percent migration into a cell free gap. (B) Bar graph of the day 7 migratory capacity of RTgutGC cells incubated with 0, 50, 100, and 200 µg/mL of SBA in L15 medium. Values are means ± standard deviation.

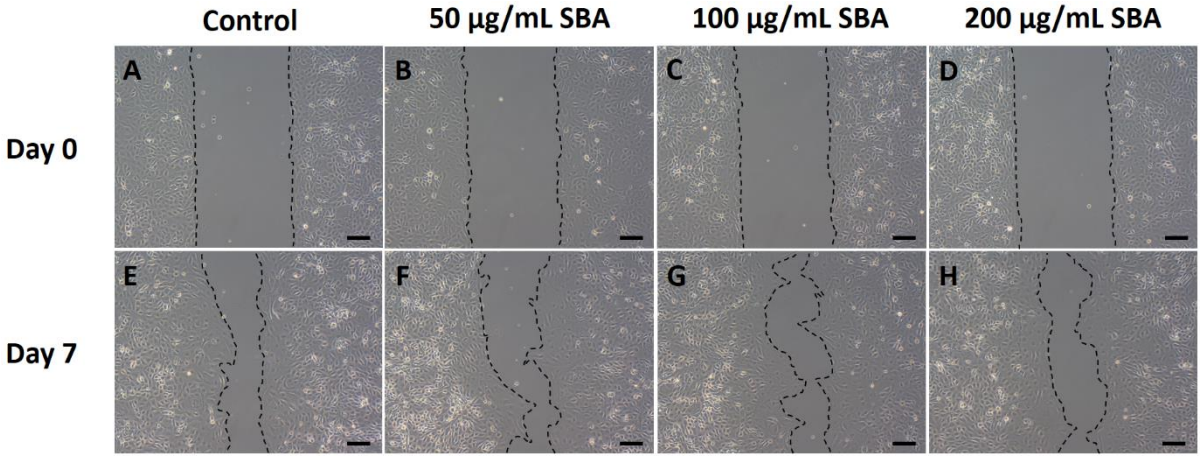

Figure 4.4. Phase-contrast microscopy of RTgutGC restitution under the influence of soybean agglutinin (SBA). (A – D) Day 0 pictures after establishment of control, 50, 100, and 200 µg/mL SBA in L15 medium. (E – H) Day 7 pictures of control, 50, 100, and 200 µg/mL SBA in L15 medium. Cell monolayer borders are traced in black to better visualize restitution. Scale bar = 100 µm.

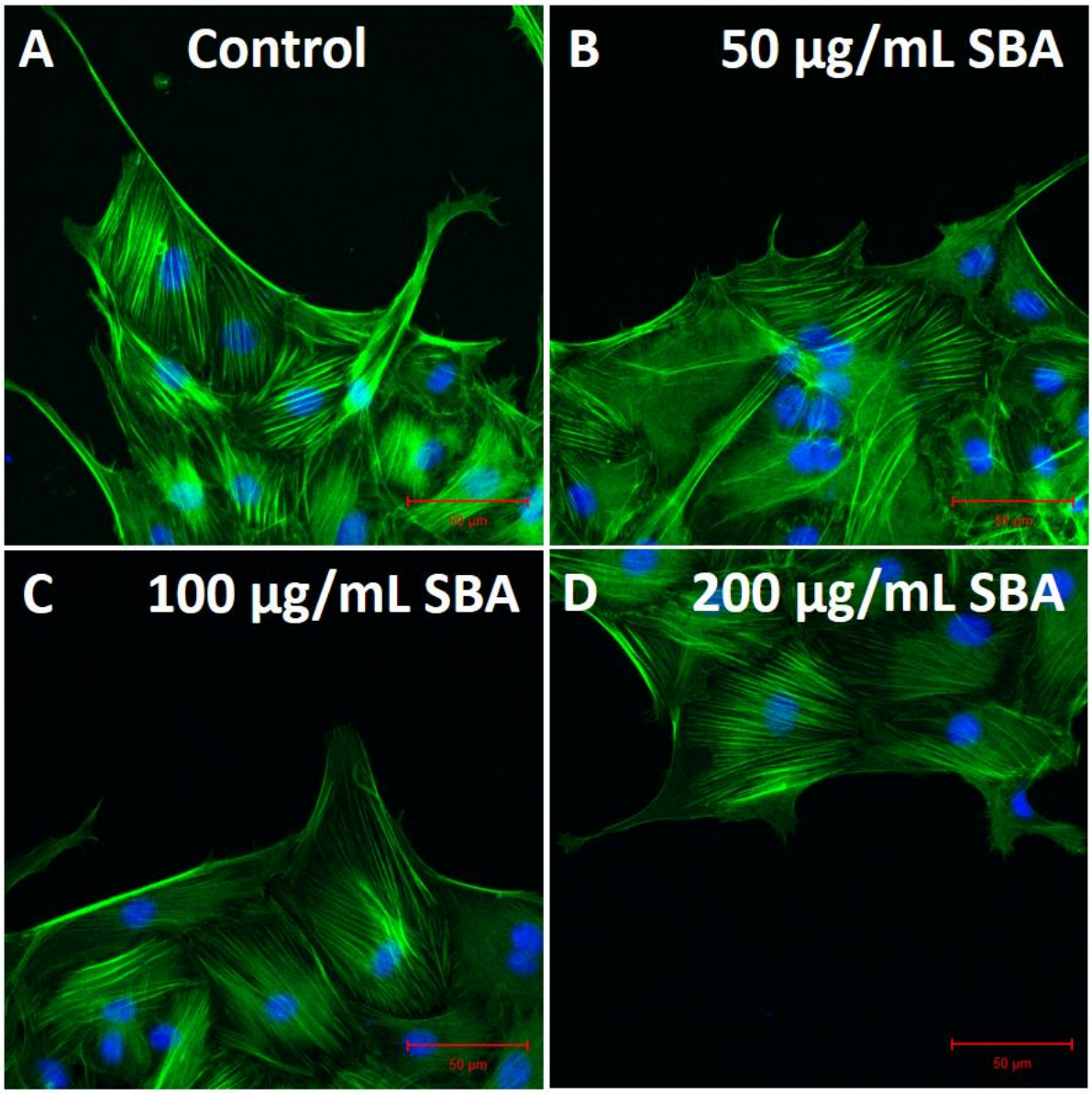

Figure 4.5. F-actin arrangement in RTgutGC after 3 days of migration under the influence of soybean agglutinin (SBA). F-actin is stained as green by FITC-phalloidin, while the nuclei is stained as blue by DAPI. (A) F-actin of migrating control cells in L15 medium. (B) F-actin of migrating cells incubated with 50 µg/mL SBA. (C) F-actin of migrating cells incubated with 100 µg/mL SBA. (D) F-actin of migrating cells incubated with 200 µg/mL SBA. Scale bar = 50 µm.

4.3.3. WGA reduces migration in RTgutGC and promotes stress fiber disorganization

Over a period of 6 days, 0.75 and 2.25 μg/mL WGA halted migration in RTgutGC cells, whereas 0.25 μg/mL WGA had no effect on migration (Fig 4.6 and 4.7). An incubation of 0.75 μg/mL WGA significantly ($p < 0.01$) halted the migration of RTgutGC at around 13% ± 3%, whereas the control and 0.25 μg/mL WGA showed an increasing trend in migration where on day 6 they reached a total percent migration of 49 ± 16% and 52 ± 6% respectively (Fig 4.6). An incubation of 2.25 μg/mL WGA completely inhibited migration of RTgutGC cells (Fig 4.6). Values remained close to 0% and entered negative values on day 4 as the cell free gap enlarged (Fig 4.6 and 4.7). On day 6, the total percent migration of cells incubated with 2.25 μg/mL WGA was -11 ± 4% (Fig 4.6).

With increasing concentrations of WGA, cell morphology changed (Fig 4.7 and 4.8). The most observable and intense change in cell morphology was seen with 2.25 μg/mL WGA (Fig. 4.8). Cells incubated with 2.25 μg/mL WGA had a somewhat fibroblastic, thinner morphology with gaps in the monolayer compared to control cells (Fig 4.8). Control cells demonstrated an epithelial, cobblestone-like morphology without any visible gaps between cells (Fig 4.8). Additionally, cells incubated with 2.25 μg/mL WGA obtained small vacuoles near the center of the cell.

Actin in the control cell population after 3 days of migration showed stress fibers in the cells oriented to the direction of migration in the leading cells (A, Fig 4.9). When incubated with 0.75 μg/mL WGA, the cell population still retained stress fibers but some cells demonstrated a loss of stress fibers with some actin bundles being peripherally organized (B, Fig 4.9). Additionally, some cells have finger like actin protrusions appearing similar to filipodia (B, Fig 4.9). In 1.5 μg/mL WGA small stress fibers were still visible but the cell population predominantly had actin oriented to the periphery (C, Fig 4.9). When incubated in 2.5 μg/mL WGA, cells appeared to have actin orientated to the cells' periphery and diffused in the cytoplasm. No stress fibers were observed orientated in the direction of migration.

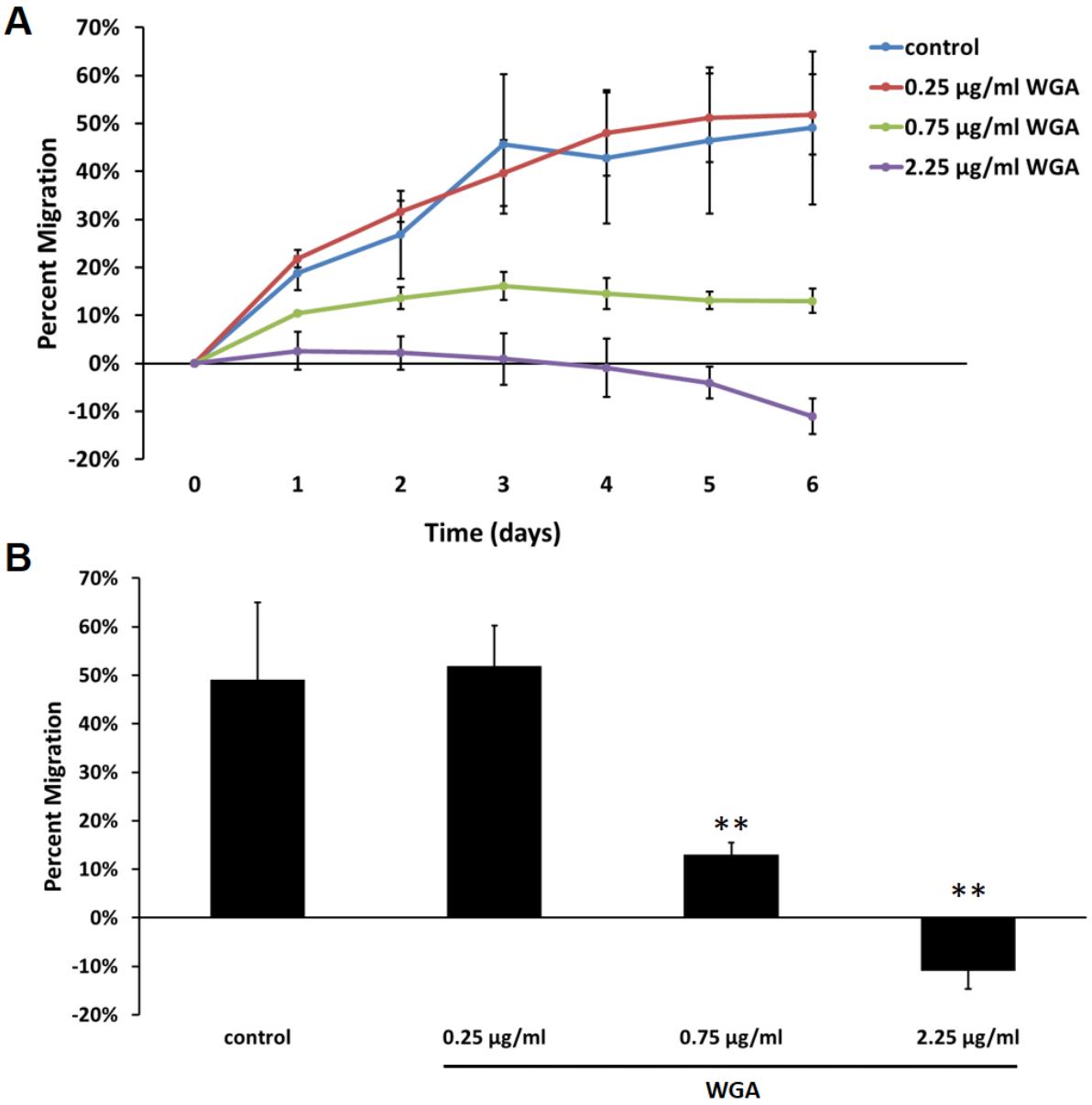

Figure 4.6. RTgutGC migration over time under the influence of wheat germ agglutinin (WGA). (A) Migratory capacity of RTgutGC over 6 days when incubated with 0.25, 0.75, and 2.25 µg/mL of WGA in L15 medium measured as percent migration into a cell free gap. (B) Bar graph of the day 6 migratory capacity of RTgutGC cells incubated with 0, 0.25, 0.75, and 2.25 µg/mL of WGA in L15 medium. Values are means ± standard deviation. Asterisks indicate significant difference when compared to the control: **$p < 0.01$.

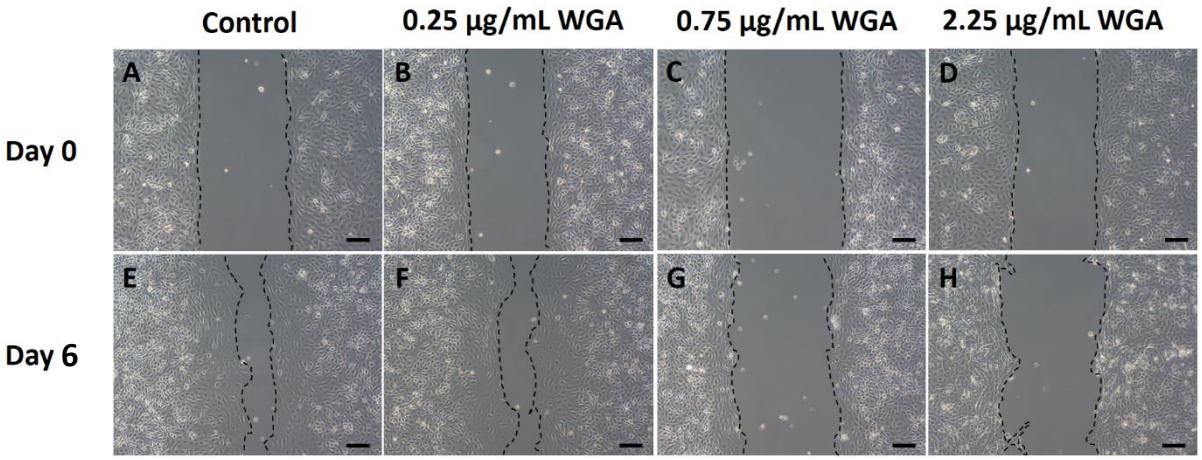

Figure 4.7. Phase-contrast microscopy of RTgutGC restitution under the influence of wheat germ agglutinin (WGA). (A – D) Day 0 pictures after establishment of control, 0.25, 0.75, and 2.25 µg/mL of WGA in L15 medium. (E – H) Day 6 pictures of control, 0.25, 0.75, and 2.25 µg/mL of WGA in L15 medium. Cell monolayer borders are traced in black to better visualize restitution. Scale bar = 100 µm.

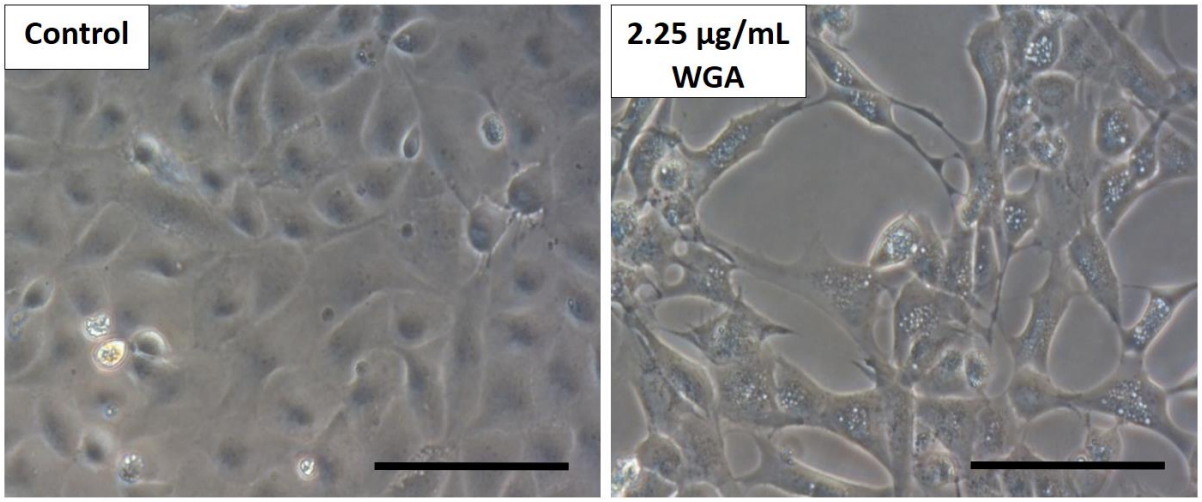

Figure 4.8. Phase contrast observations of the effects 2.25 µg/mL wheat germ agglutinin (WGA) has on RTgutGC cells after an incubation period of 4 days. The control represents RTgutGC cells incubate in L15 medium for 4 days. The treated cells were exposed to 2.25 µg/mL WGA in L15 medium for 4 days. Scale bar = 100 µm.

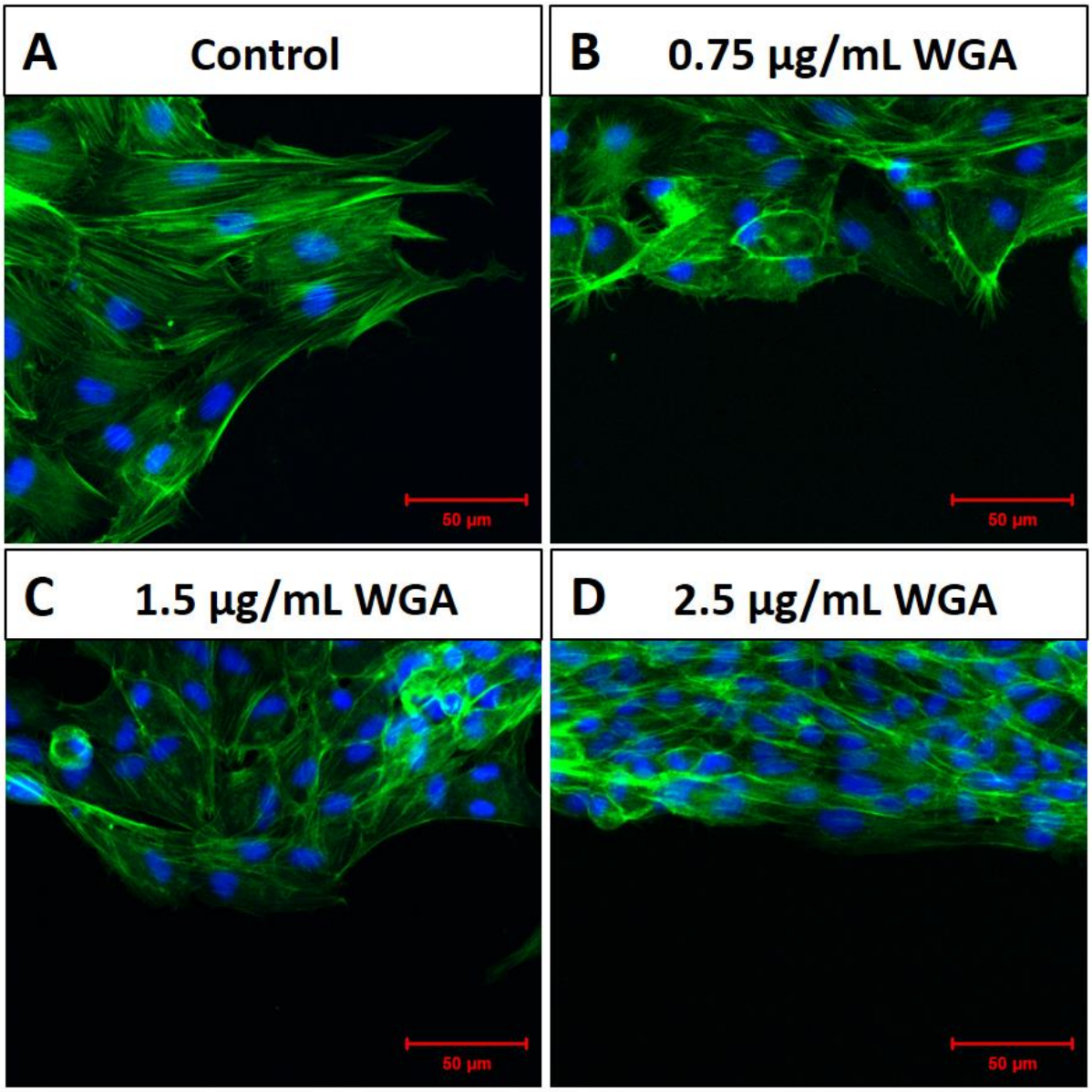

Figure 4.9. F-actin arrangement in RTgutGC after 3 days of migration under the influence of wheat germ agglutinin (WGA). F-actin is stained as green by FITC-phalloidin, while the nuclei is stained as blue by DAPI. (A) F-actin of migrating control cells in L15 medium. (B) F-actin of migrating cells incubated with 0.75 µg/mL WGA. (C) F-actin of migrating cells incubated with 1.5 µg/mL WGA. (D) F-actin of migrating cells incubated with 2.5 µg/mL WGA. Scale bar = 50 µm.

4.3.4. Butyrate reduces migration in RTgutGC cells

Overtime, increasing concentrations of butyrate (2, 5, and 8 mM) appeared to decrease cellular migration in RTgutGC (A, Fig 4.10 and Fig 4.11). Cellular migration in 2 and 5 mM butyrate plateaued on day 4. This is similar to the control, as migration also plateaued on day 4, but the percent migration of 2 and 5 mM butyrate is lower than the control on day 4. 8 mM butyrate caused cellular migration to plateau sooner on day 2 or 3 (A, Fig 4.10). On day 7, the total percent migration of cells in 8 mM butyrate was significantly less (18 ± 6%) compared to the control (39 ± 11%) (B, Fig 4.10). No significant difference in migration compared to the control was observed on day 7 for cells in 2 or 5 mM butyrate with their total percent migration respectively being 32 ± 6% and 29 ± 10% (B, Fig 4.10 and Fig 4.11).

In addition to changes in cellular migration, butyrate caused significant changes in morphology of RTgutGC cells in a monolayer (Fig 4.12). At 2, 5, and 8 mM butyrate clear vesicles can be observed. Vesicle formation was first seen on day 2 in all concentrations. These vesicles increase in numbers with increasing concentration of butyrate. For the most part, the vesicles appear to be located in-between or on the periphery of the cells (Fig 4.12).

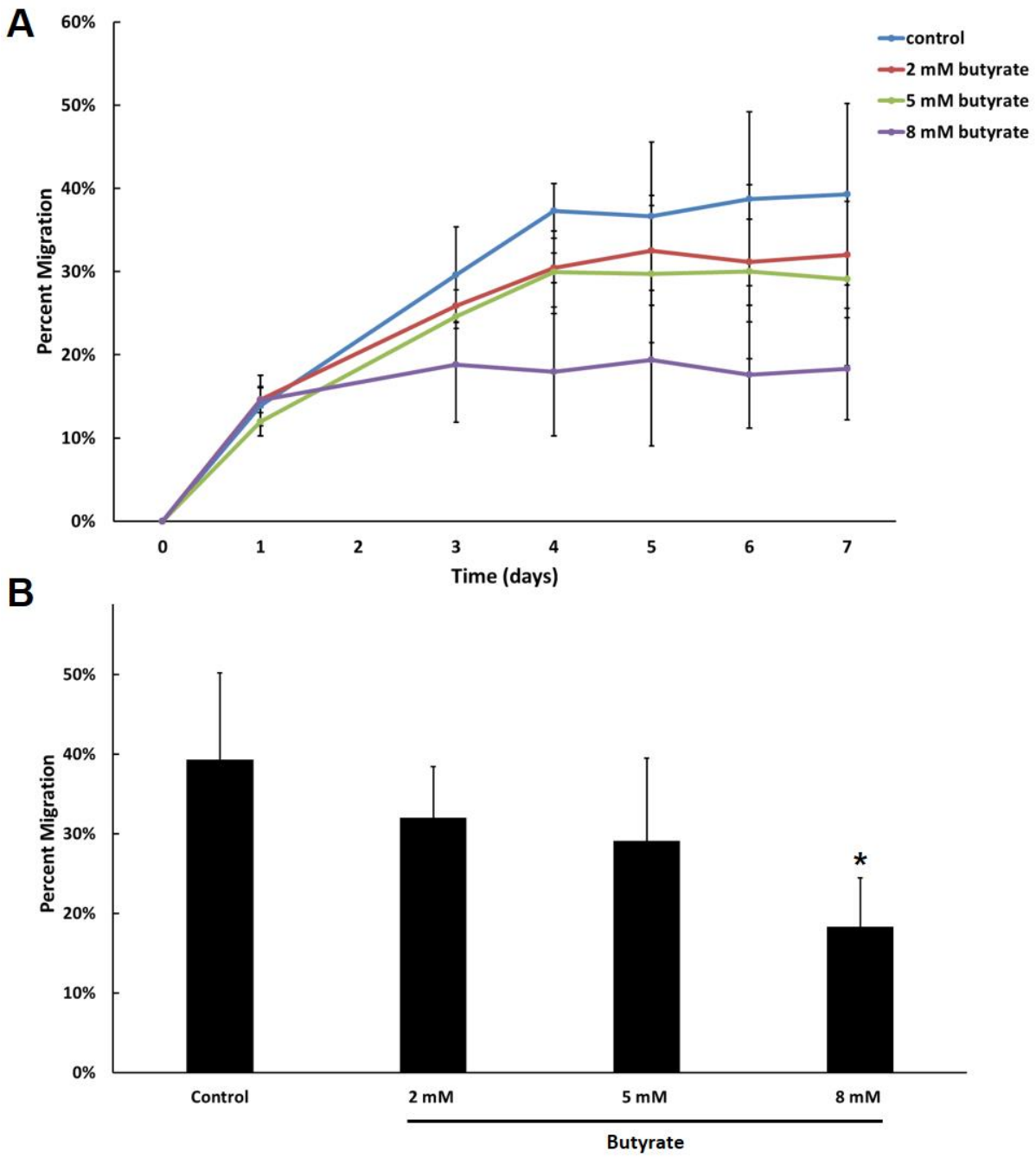

Figure 4.10. RTgutGC migration over time under the influence of butyrate. (A) Migratory capacity of RTgutGC over 7 days when incubated with 0, 2, 5, and 8 mM of butyrate in L15 medium measured as percent migration into a cell free gap. (B) Bar graph of the migratory capacity of RTgutGC cells over 7 days with 0, 2, 5, and 8 mM of butyrate in L15 medium. Values are means ± standard deviation. Asterisk indicates significant difference when compared to the control: *$p < 0.05$.

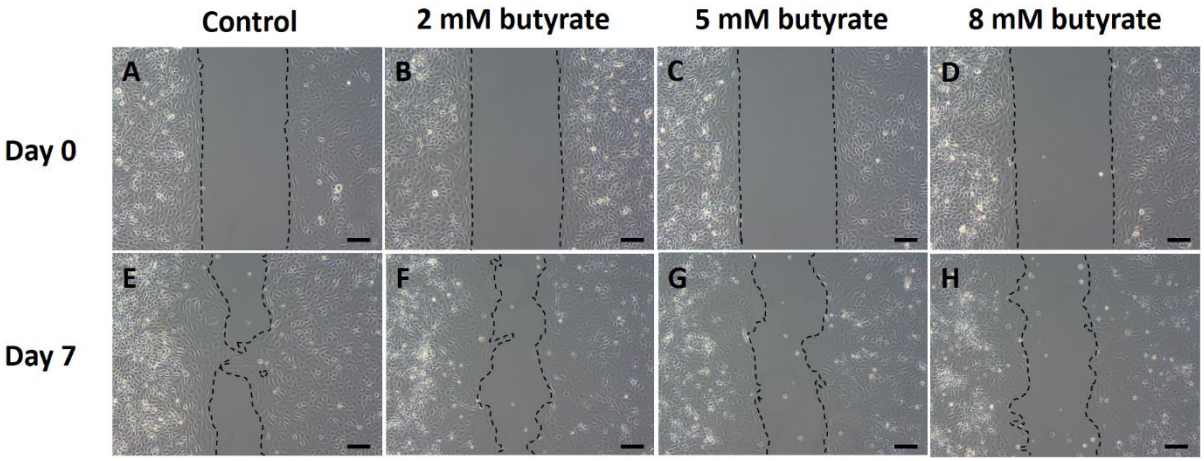

Figure 4.11. Phase-contrast microscopy of RTgutGC restitution under the influence of butyrate. (A – D) Day 0 pictures after establishment of the gap in control, 2, 5, and 8 mM butyrate exposed monolayers in L15 medium. (E – H) Day 7 pictures of control, control, 2, 5, and 8 mM butyrate in L15 medium. Cell monolayer borders are traced in black to better visualize restitution. Scale bar = 100 μm.

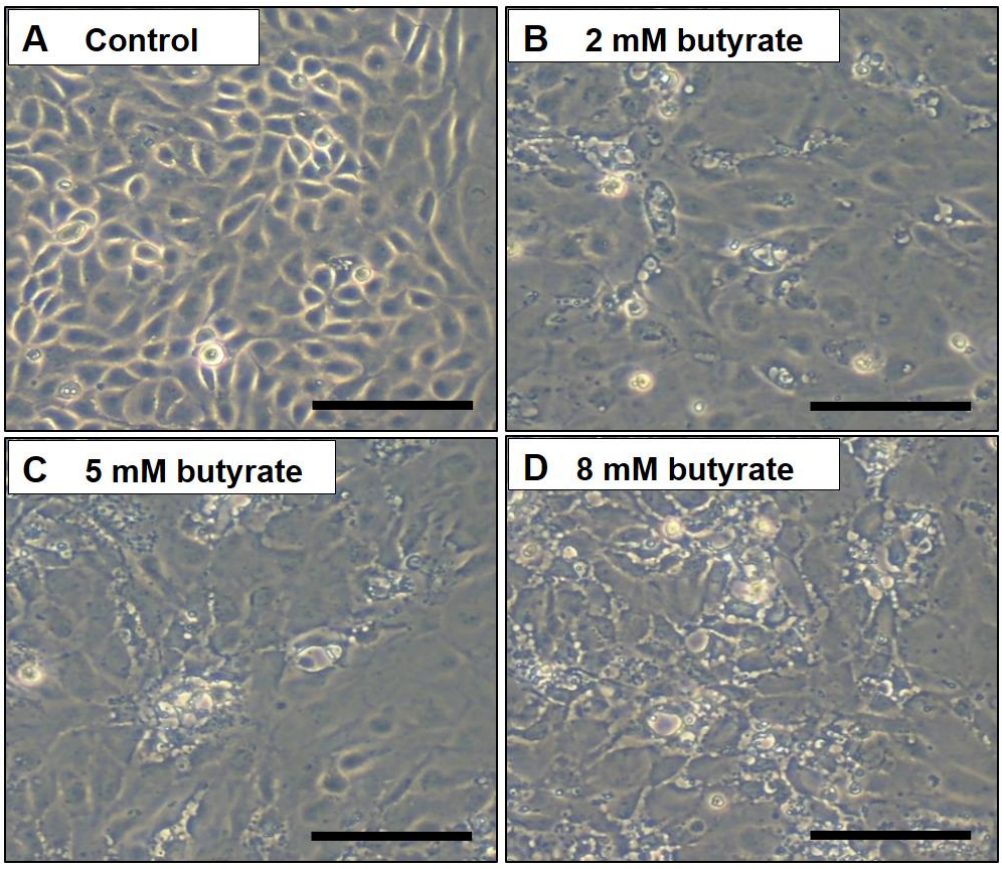

Figure 4.12. Phase contrast observation of RTgutGC in L15 incubated with 2, 5, and 8 mM of butyrate causing vesicle formation. (A) RTgutGC cells in L15 control without any butyrate for 6 days. (B) RTgutGC cells incubated with 2 mM of butyrate in L15 for 6 days. (C) RTgutGC cells incubated with 5 mM of butyrate in L15 for 6 days. (D) RTgutGC cells incubated with 8 mM of butyrate in L15 for 6 days. Scale bar = 100 μm.

4.3.5. KI effects on RTgutGC migration

Over time, a concentration of 25 μg/mL of KI appeared to slightly enhance migration of RTgutGC cells, whereas a concentration of 50 and 100 μg/mL KI slightly inhibited migration (Fig 4.13 and Fig 4.14). At all concentrations, migration was not completely inhibited or halted as an increase in percent migration over time can be seen with all concentrations. The final percent migration reached on day 7 for 25, 50, and 100 μg/mL KI was 38 ± 6%, 27 ± 4%, and 24 ± 1% respectively (A, Fig 4.13). However, when compared to the percent migration of the control (32 ± 10%) the differences were not statistically significant. However, the percent migration of RTgutGC cells incubated with 100 μg/mL KI (19 ± 0.004%) was statistically less than the control (25 ± 4%) on day 3 (A, Fig 3.13).

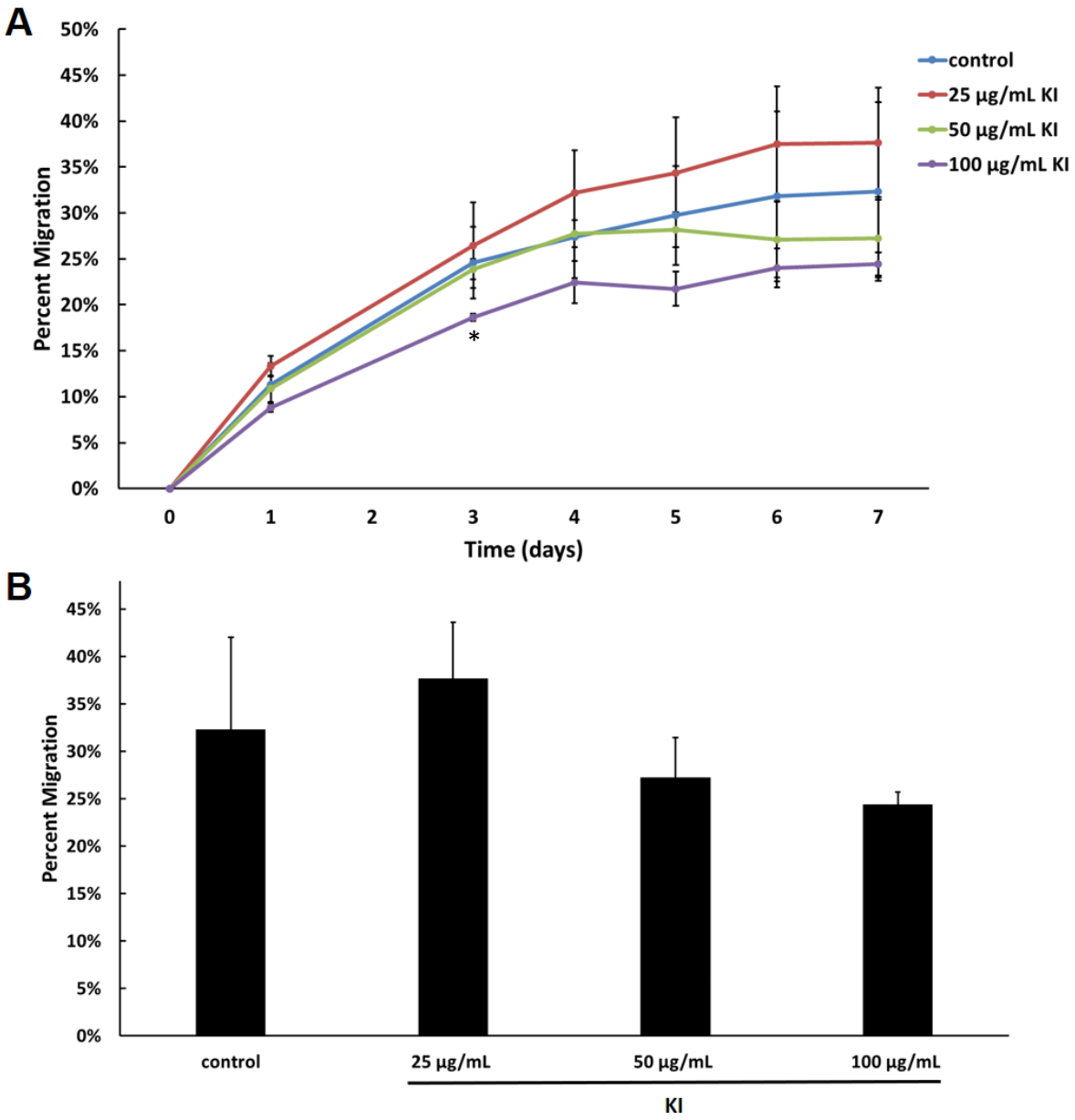

Figure 4.13. RTgutGC migration over time under the influence of Kunitz inhibitor (KI). (A) Migratory capacity of RTgutGC over 7 days when incubated with 0, 25, 50, and 100 µg/mL of KI in L15 medium measured as percent migration into a cell free gap. (B) Bar graph of the day 7 migratory capacity of RTgutGC cells incubated with 0, 25, 50, and 100 µg/mL of KI in L15 medium. Values are means ± standard deviation. Asterisks indicate significant difference when compared to the control: *$p < 0.05$.

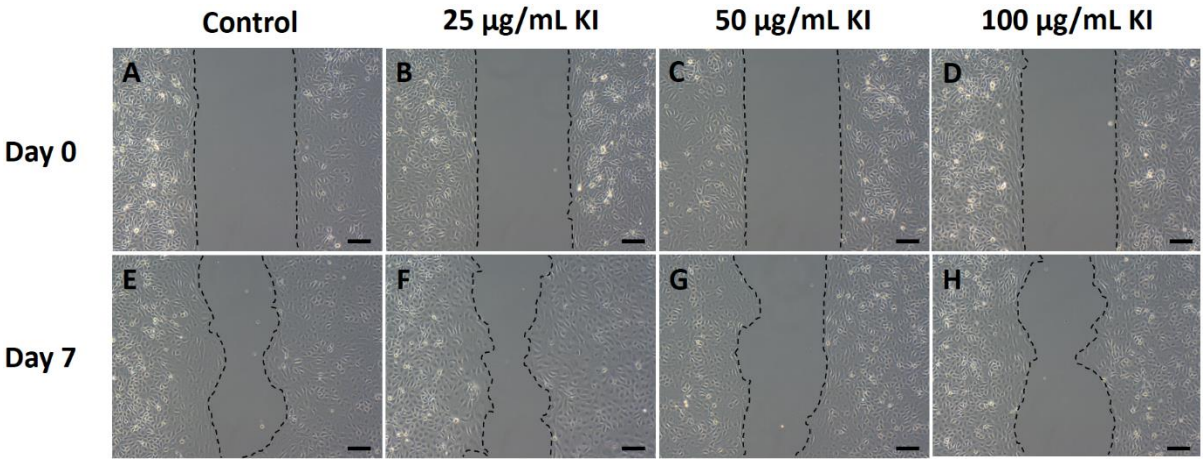

Figure 4.14. Phase-contrast microscopy of RTgutGC restitution under the influence of Kunitz inhibitor (KI). (A – D) Day 0 pictures after establishment of control, 25, 50, and 100 µg/mL of KI in L15 medium. (E – H) Day 7 pictures of control, control, 25, 50, and 100 µg/mL of KI in L15 medium. Cell monolayer borders are traced in black to better visualize restitution. Scale bar = 100 µm.

4.4. DISCUSSION

Several antinutritionals potentially found in fish feeds were assayed by observing their effects on cellular restitution or migration of a rainbow trout intestinal epithelial cell line RTgutGC. The results showed the differential effects of various antinutritionals on restitution *in vitro* and demonstrated the potential use of RTgutGC as a model intestinal cell line to assay fish feed components.

4.4.1. BBI reduces migration in RTgutGC cells

For the first time, BBI was shown to decrease the migratory capacity of intestinal cells. Found in the seeds of soybean and many other plants, BBI is a small water-soluble protein with proteolytic activities inhibiting a wide array of proteases and protein kinases such as trypsin, chymotrypsin, elastase, cathepsin G, chymase, serine-protease-dependent matrix metalloproteinases, mitogen activated protein kinase and PI3 kinase (Losso, 2008). Cytoskeletal rearrangement occurring during cellular migration likely requires the action of these proteolytic enzymes (Lotz et al., 2000). Hence, the inhibitory abilities of BBI on proteolytic enzymes leading to less cytoskeletal rearrangement might be a cause of the observed decreases in cellular migration. However, BBI did not change cellular morphology of RTgutGC cells suggesting that any action on the actin cytoskeleton must be rather specific for cytoskeletal changes involved in cell migration.

4.4.2. SBA has no effect on RTgutGC migration and F-actin arrangement

SBA is a lectin found in soybean. It is an ANF as it has been shown to bind to the brush border of the small intestine of fish, including Atlantic salmon, disrupting small intestine metabolism and morphologically damaging the villi (Francis et al., 2001). The results show that SBA neither increased or decreased migration of RTgutGC cells. This is contrary to past reports showing inhibitory restitution effects of SBA on mammalian cells (Draaijer et al., 1989; Gordon & Wood, 2009) and with the general consensus that SBA is an antinutritional component in fish feed (Francis et al., 2001; Hart et al., 2010). The monolayer and morphology of RTgutGC cultures treated with SBA appeared to be same as in control cultures. Additionally, SBA had no effect on F-actin arrangement in RTgutGC cells. Control and treated cells all demonstrated similar stress fibers at the leading cell edge oriented in the direction of

migration. The null effects of SBA on F-actin were also observed in human Caco-2, where the pattern of F-actin staining remained unchanged (Draaijer et al., 1989). However, SBA increased the amount of G-actin in Caco-2 (Draaijer et al., 1989) and disrupted rat corneal endothelial monolayer due to cell-cell alterations (Gordon & Wood, 2009).

4.4.3. WGA reduces migration in RTgutGC and promotes actin stress fiber disorganization

As with SBA, WGA, found in wheat, can bind to the intestinal surface of the gut generating adverse effects (de Punder & Pruimboom, 2013). The results showed that WGA had a profound effect on RTgutGC cells, including impeding cell migration. Cells lost connections with each other, appeared more spindle like in shape, and accumulated vesicles. WGA also caused a visible major disorganization of F-actin and actin stress fibers. Stress fibers anchored to focal adhesions play a role in migration for certain cell types, where it has been shown that decreases in stress fibers can lead to reductions in cellular migration (Dourdin et al., 2001; Vallenius, 2013). It has been reported that the incubation of WGA with a human intestinal cell line also caused changes in F-actin organization by a calcium-dependent mechanism (Sjölander & Magnusson, 1988). Whether WGA acts in a similar manner in RTgutGC cells is unknown but a potential path for future studies. Additionally, WGA has been reported to act on microtubules in the gill of Tilapia (Tsai & Hwang, 1998); hence, microtubule effects also present a potential path of study.

4.4.4. Butyrate reduces migration in RTgutGC cells

Not considered an ANF, short chain fatty acids, such as butyrate, produced by intestinal microflora are important to normal intestinal biology (Peng et al., 2007). Butyrate is also gaining popularity as fish feed additive. The highest concentration of butyrate in the current study (8 mM) significantly reduced the migration of RTgutGC cells. Although many effects of butyrate on mammalian intestinal epithelial cell lines have been documented, influences on cell migration has not been noted. Incubated with a human intestinal cell line, Caco-2, butyrate shows a paradoxical action on intestinal barrier function (Peng et al., 2007). Low concentrations (2 mM) led to improvements in barrier function from increased TEER and decreased monolayer permeability, whereas a higher concentration (8 mM) impaired barrier

functions as seen by reductions in TEER and increases in permeability (Peng et al., 2007). This disruption in barrier function at a higher concentration of butyrate was due the loss of monolayer integrity from cells undergoing apoptosis (Peng et al., 2007). Similar cases of apoptosis induction by butyrate in mammalian cell lines were seen by other groups (Daehn et al., 2006; Fung et al., 2011; Ruemmele et al., 2003). Whether apoptosis is induced in RTgutGC remains to be investigated. However, butyrate did cause the cell morphology to change (large vesicle formation), with the change being more pronounced as the concentrations of sodium butyrate increased. Future studies could assess the apoptosis pathway, RTgutGG barrier functions under the influence of butyrate, and whether butyrate could induce change in RTgutGC's cytoskeleton.

4.4.5. KI effects on RTgutGC migration

As with BBI, KI is a protease inhibitor. However, it is considered less stable due to it being more heat and acid sensitive than BBI (Francis et al., 2001). The results show that KI had a slight stimulatory effect on RTgutGC migration at the lowest concentration (25 μg/mL), whereas slight inhibition was observed at higher concentrations (50 and 100 μg/mL). However, none of the effects were statistically significant. The effects of KI on intestinal restitution or *in vitro* migration is poorly understood and lacks documentation. One can hypothesize that BBI and KI should affect RTgutGC migration in the same manner. Both inhibit proteases that might be important in cytoskeletal rearrangement during cellular migration. However, the data suggest that KI exerts weaker effects on cellular migration than to the other soybean protease inhibitor BBI. In contrast, with the use of HRA human ovarian cancer cells, Kobayashi et al. (2004) demonstrated that a concentration near the IC50 of KI was sufficient to supress HRA cell invasion, whereas BBI did not suppress invasion. Yet cancer cell invasion can differ from intestinal restitution. In more relatable study, though no concerning restitution, an *ex vivo* methodology was used to study the effects of different ANFs on glucose uptake and permeability of mid and distal Atlantic salmon intestinal tissue. KI in the presence of bile resulted in increased glucose uptake suggesting the possibility of KI altering intestinal permeability and function (Bakke et al., 2014). The effects of KI on RTgutGC barrier function are unknown.

4.4.6. Summary and concluding thoughts

Overall, RTgutGC proved to be a useful rainbow trout intestinal model to study the effects of various ANFs on intestinal restitution. With the lack of *in vivo* and *in vitro* restitution studies involving ANFs, this study provided evidence for the first time that BBI, WGA, and butyrate can reduce *in vitro* intestinal restitution. The findings could shed light on the effects of ANFs on the intestine and their impacts on aquaculture. Complementary *in vivo* studies of the effects of ANFs on barrier functions would also prove useful to understand the impact of these compounds.

CHAPTER 5

Rainbow trout intestinal epithelial cell migration into a wound at hypo-, normo-, and hyper-thermic temperatures and the development of thermotolerance

5.1. INTRODUCTION

Intestinal wound healing is essential for the maintenance of gut homeostasis (Iizuka & Konno, 2011) but little is known about wound healing in the fish intestine or how intestinal wound healing of animals in general is influenced by temperature. For mammals, several intestinal cell lines have been used to study the mechanism and regulation of wound healing (Meir et al., 2016) but not how heat might modulate the process. However, an elevated temperature exposure inhibited the migration of a human T lymphocyte cell line and heat shock protein 70 (HSP70) had a role in the recovery of cell movement (Simard et al., 2011). Additionally, HSP70 and HSP90α have been implicated in the migration of human keratinocytes and breast cancer cells (Bhatia et al., 2016; Sims et al., 2011). For fish, temperature is a critical factor, regulating all aspects of cellular physiology, and both low and high temperatures are of interest.

A strength of fish cell lines is that they can be more conveniently used than fish to study the responses of cells over a wide temperature range (Bols et al., 1992). Fish cell cultures can be studied at normothermic, hyperthermic, and hypothermic temperatures, but these temperatures vary with the species. Temperatures that support the proliferation of cells from a species constitute the normothermic range. For rainbow trout, normothermic is between 5 and 25 °C and is also referred to as the proliferation zone (Bols et al., 1992). However, the boundaries are difficult to demonstrate precisely.

Any temperature below 5 °C can be considered as hypothermic for rainbow trout cell cultures. The temperature at which proliferation stops in cultures at the low end of the tolerance zone is difficult to define with certainty because this will be influenced by how long cultures are monitored and how well the incubator holds precisely to one temperature over a long incubation period plus culture factors, such as the initial plating density and serum concentration. For rainbow trout cells at 5 °C, cultures persist for months, mitotic figures are occasionally seen, and cell number can increase slightly (Bols et al., 1992; Plumb & Wolf, 1971). However, cell cultures at 0 to 4 °C survive for at least a week without any mitotic figures being apparent (Mosser et al., 1986) and so are considered to be in the endurance zone (Bols et al., 1992). To date, a lower lethal zone is yet to be defined because low temperature incubation periods that reproducibly lead to rainbow trout cell death have yet to be described.

Any temperature above 25 °C can be considered as hyperthermic for rainbow trout cell cultures. Proliferation has been observed to slow at 25 °C (Plumb & Wolf, 1971). In cultures at 26 °C, cell number remains largely unchanged over 6 days (Mosser et al., 1986). These cultures also consistently synthesise HSPs and so rainbow trout cell cultures at 26 °C and above are undergoing heat stress. At 28 °C, cultures do not accumulate cells over 6 days and begin to deteriorate with longer incubations (Mosser et al., 1986). Therefore 28 °C has been used to mark the upper limit of the endurance zone for rainbow trout cell cultures (Bols et al., 1992). Temperatures above 28 °C are in the upper lethal zone (Bols et al., 1992) because rainbow trout cells die within a few hours at 30 to 32 °C and in less than 1 h at 36 °C (Mosser et al., 1987).

Cellular thermotolerance is the acquisition, by cells through a prior heat exposure, of an enhanced capacity to recover functions after a potentially lethal heat stress. In mammalian cancer biology, the function often monitored is the continued ability of cells to reproduce or form colonies and HSPs have been implicated in the development of this thermotolerance (Landry et al., 1982). With the rainbow trout gonadal fibroblast cell line, RTG-2, which forms poor colonies (Bols et al., 1985), survival was measured as the capacity to remain adherent to the plastic culture surface. A 24 h exposure to 26 or 28 °C allowed RTG-2 to better survive subsequent exposures at 30 to 36 °C and HSPs appeared necessary for the development of this thermotolerance (Bols et al., 1992; Mosser et al., 1986, 1987; Mosser & Bols, 1988). Whether cell migration and wound healing can be become thermotolerant appears not to have been investigated in either mammals or fish.

Therefore, in this chapter the ability of rainbow trout epithelial cells, RTgutGC, to heal a wound was investigated at a hypo- (4 °C), normo- (18 °C) and hyperthermic (26 °C) temperature. Healing occurred over a similar time frame at 18 and 26 °C, but was slowed at 4 °C. When RTgutGC monolayers were incubated for 3 h in the upper lethal zone (32 °C) and then concurrently wounded and returned to 18 °C, the wound failed to be healed. However, the wound did heal when RTgutGC monolayers were first incubated for 24 h at 26 °C before being shifted to 32 °C, wounded after 3 h, and returned to 18 °C. Therefore, incubation at 26 °C induced thermotolerance in RTgutGC for cell migration.

5.2. MATERIALS AND METHODS

5.2.1. Cell culture and culture conditions

The cell line used was RTgutGC, a rainbow trout intestinal epithelial cell line (Kawano et al., 2011). Culturing media used was Leibovitz's L15 with 2.05 mM L-Glutamine (Thermo Fisher Scientific) supplemented with 10% fetal bovine serum (FBS, Sigma-Aldrich) and antibiotics (10,000 U/mL penicillin and 10,000 ug/mL streptomycin, P/S, Thermo Fisher Scientific) (L15/FBS). Subculturing with the use of trypsin (Thermo Fisher Scientific) occurred every week passaging the cells at a ratio of 1 to 2. Cells were maintained at 18 ^{o}C in BioLite 75 cm^2 cell culture treated flasks (Thermo Fisher Scientific).

5.2.2. Evaluating wound healing and restitution at 4, 18 and 26 °C

The ability of RTgutGC cells to migrate into a wound or gap was investigated at hypothermic (4 °C), normothermic (18 °C) and hyperthermic (26 °C) temperatures. The assay was done in 2-well culture inserts from Ibidi ect (as in previous chapters). These cultures were initiated in L15/FBS as described in Section 2.2.9. After 3 days at 18 °C, monolayers had developed and the inserts were removed to create the gaps, which were immediately photographed. Some cultures continued to be incubated at 18 °C whereas others were moved to either 4 °C or 26 °C. Photographs of the gaps were taken daily for up to 6 days afterwards. Photographs of the gaps were analyzed with ImageJ and the results expressed as % cell migration as described in Chapter 3 (section 3.2.8).

5.2.3. Evaluating wound healing and restitution after 3 h at 32 °C

The ability of RTgutGC cells to migrate into a wound or gap after experiencing a heat stress was investigated, using 2-well culture inserts from Ibidi. These insert cultures were set up at 18 °C and allowed to develop into monolayers as described in the previous section. Once monolayers had formed, some cultures were kept at 18 °C (controls), whereas others were shifted to 32 °C (Fig 5.1). After 3 h, the inserts were removed from both sets of cultures to create the gaps and the cultures that had been at 32 °C were returned to 18 °C. The gaps were immediately photographed and photographs were taken daily for up to 6 days afterwards. The photographs were analyzed as described above.

5.2.4. Evaluating thermotolerance for wound healing and restitution

The ability of RTgutGC cells at 18 °C to migrate into a wound or gap after recovering from a stress of 3 h at 32 °C was compared for cultures that first had 24 h at 26 °C before being shifted to 32 °C with cultures that were shifted directly from 18 °C to 32 °C (Fig 5.1). This was again done using 2-well culture inserts from Ibidi. Insert removal and gap creation occurred concurrently with the return of cultures from 32 °C to 18 °C. Photographs of the gaps were taken immediately and for up to 6 days afterwards and evaluated as described above.

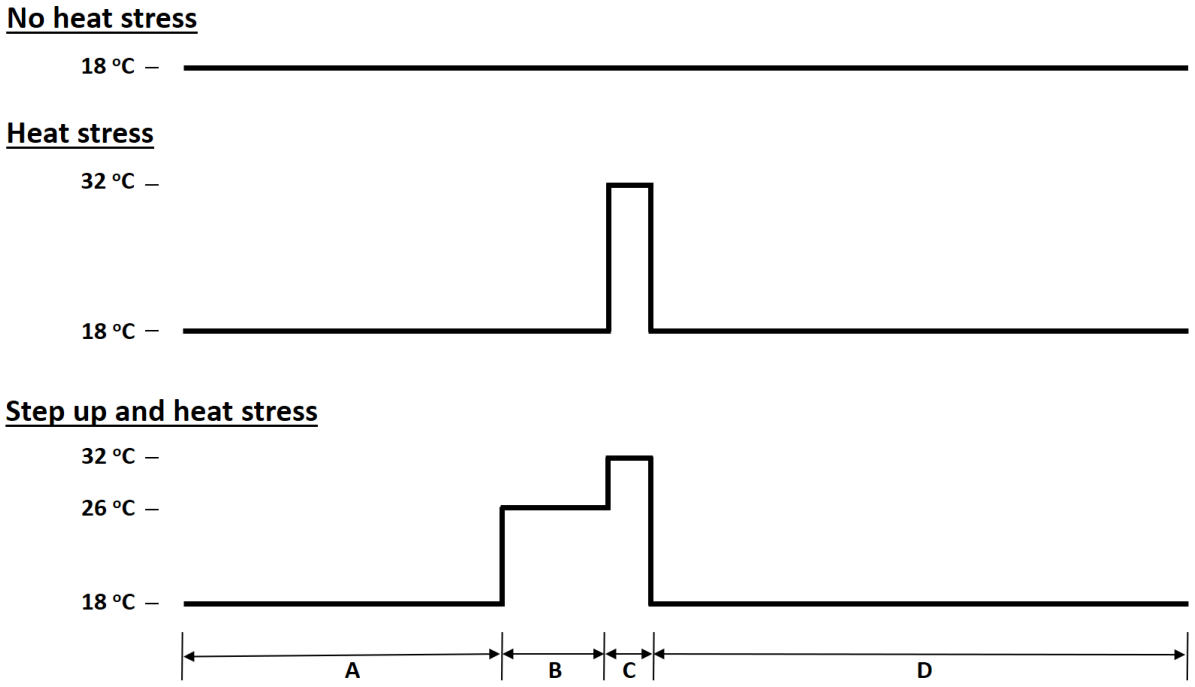

Figure 5.1. Step up heating protocol used to investigate thermotolerance for cell migration. Cell migration was monitored in a fence assay that utilized 2-well culture inserts. The 2-well cultures were set up within three separate plates at 18 °C. One plate with its 2-well cultures was placed continuously at 18 ° C (top, no heat stress). A second plate was incubated for 72 h at 18 ° C before being shifted to 32 ° C for 3 h before being returned to 18 °C (middle, heat stress). The third plate was incubated for 72 h at 18 °C before being shifted to 26 °C for 24 h and then to 32 °C for 3 h before being returned to 18 °C (bottom, step up and heat stress). The time line is summarized in the bottom arrows. A) 72 h establishment period at 18 °C. (B) 24 hour step up heating at 26 °C. (C) 3 hour heat stress period at 32 °C. (D) 6 day wound healing period at 18 °C. At 99 h (end of point C), the insert fence was lifted to create the gap and to allow cell migration to begin.

5.3. RESULTS

5.3.1. Wound healing and restitution at 4 °C, 18 °C and 26 °C

Wound healing by RTgutGC occurred at all temperatures but was slower at the hypothermic temperature of 4 °C than at the normothermic, 18 °C and the hyperthermic, 26 °C. Over 6 days, the filling in of a gap or wound with RTgutGC cells was very similar at 18 ^{o}C and 26 ^{o}C, albeit slightly faster at 26 ^{o}C (Fig 5.1 and 5.2). Near full closure of the gap was reached on day 3 for cells at 18 ^{o}C and 26 ^{o}C, where the percent migration was 98 ± 2% and 99 ± 1% respectively. Wound healing was observed to be slower but not inhibited for cells incubated at 4 ^{o}C. On day 6, cells at 18 ^{o}C and 26 ^{o}C reached 100% migration (completely closed the gap), whereas cell at 4 ^{o}C closed 77 ± 9% of the gap.

5.3.2. Wound healing and restitution after 3 h at 32 °C

A hyperthermic heat stress of 3 h at 32 °C profoundly influenced wound healing. RTgutGC cells maintained at 18 ^{o}C without being exposed to thermotolerant or heat shock conditions closed the cell free gap within 4 days (Fig 5.3 and 5.5). Cells exposed to a 3h 32 ^{o}C heat stress condition almost completely lost their wound healing abilities, where the percent migration remained below 10% eventually dropping negatively on day 6 as the cells began to die and peel off from a loss of adherence. An observation to note is that non-heat stressed cells migrated together into the gap as a sheet, eventually closing the gap, whereas the heat stress cells, for the most part, would individually migrate into the gap (Fig 5.4).

5.3.3. Demonstrating thermotolerance for wound healing and restitution

A prior heat treatment of 24 h at 26 °C allowed RTgutGC cells to recovery their ability to heal a wound after a heat stress of 3 h at 32 °C. After this thermal regimen, the cells at 18 °C eventually filled in the gap on day 6, a slower pace than seen with the non-heat stressed cells (Fig 5.3 and 5.5). However, without the prior exposure to 26 °C, the gap was open after 6 days. Therefore, the cells had acquired at 26 °C a thermotolerant capacity for wound healing and/or restitution.

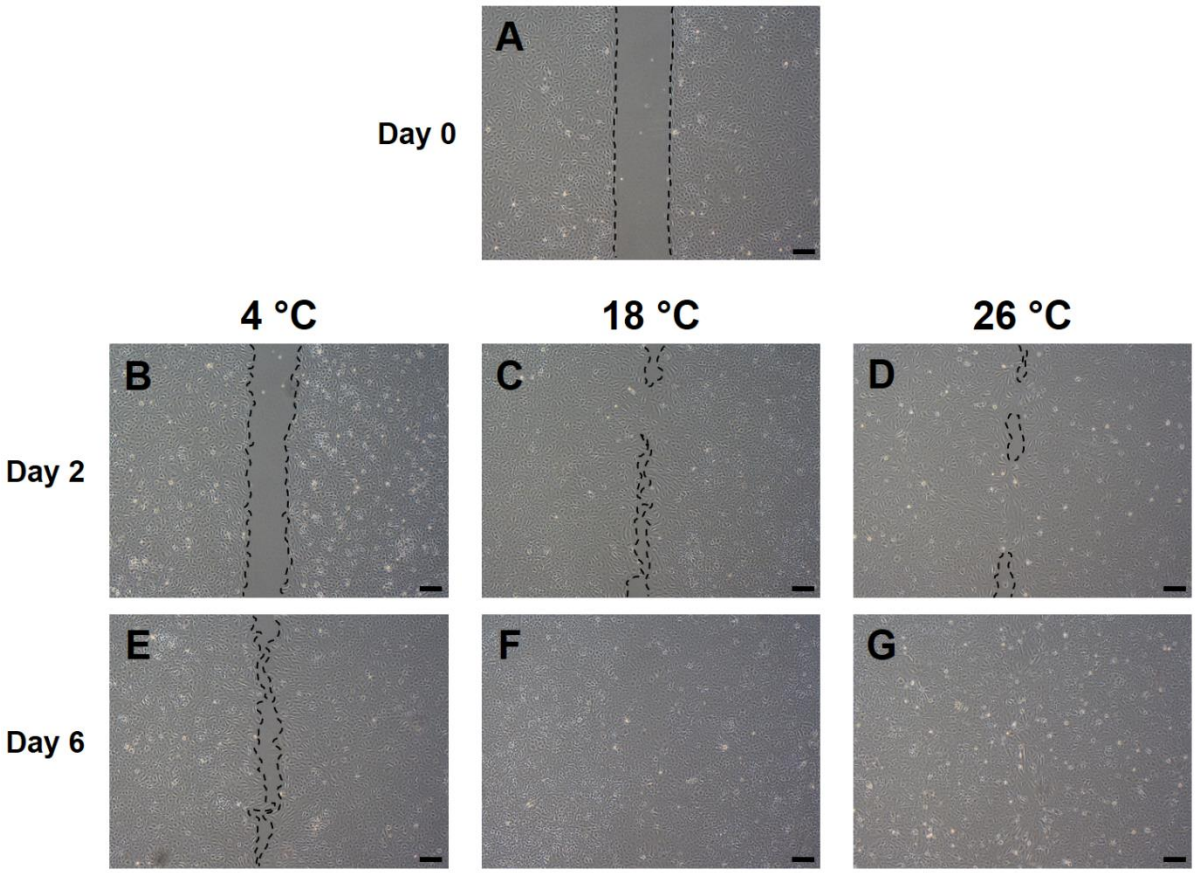

Figure 5.2. RTgutGC cells' ability to migrate into a cell free gap at either 4 ºC, 18 ºC, or 26 ºC. (A) Day 0 migration after a 3 day monolayer and gap establishment period. (B, C, D) Day 2 of wound healing at either 4 ºC, 18 ºC, or 26 ºC respectively. (E, F, G) Day 6 of wound healing at either 4 ºC, 18 ºC, or 26 ºC respectively. In each temperature condition, cells were in L15/FBS medium over the course of the experiment. Pictures were taken at a 40x magnification. Cell monolayer borders are traced in black to better visualize wound healing. Scale bar = 200 μm.

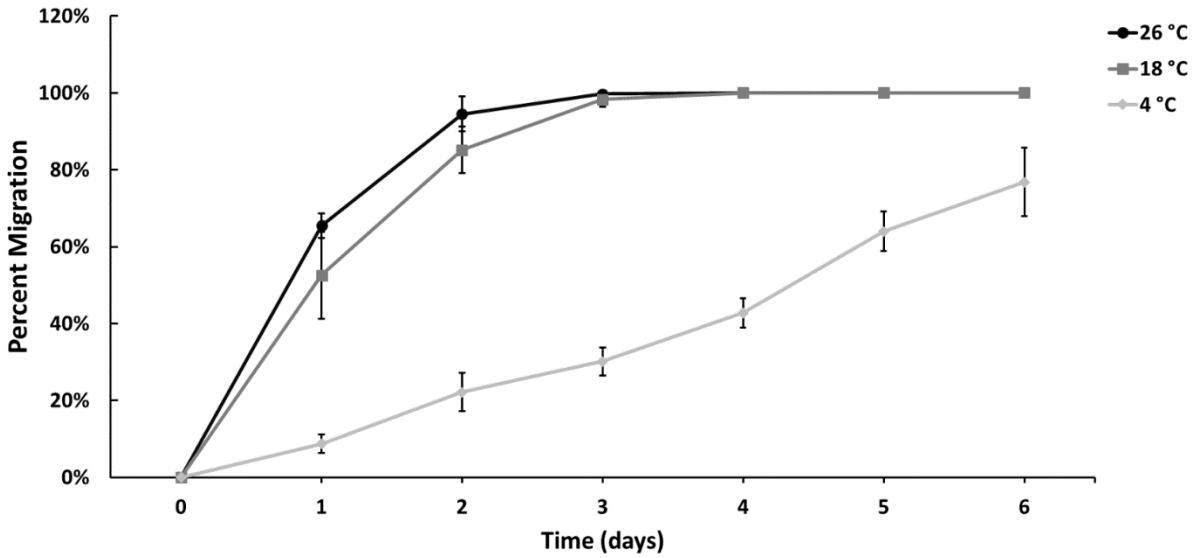

Figure 5.3. Percent migration of RTgutGC cells over time at either 4 ºC, 18 ºC, or 26 ºC. Three different temperatures (4 ºC, 18 ºC, or 26 ºC) were used to incubate the plates up to 6 days, periodically monitoring cellular migration into a cell free gap. 18 ºC is the common temperate to culture RTgutGC. In each temperature cells were in L15/FBS medium. Pictures were taken every day till day 6 with data expressed as percent migration from day 0. Data are expressed as the mean ± standard deviation.

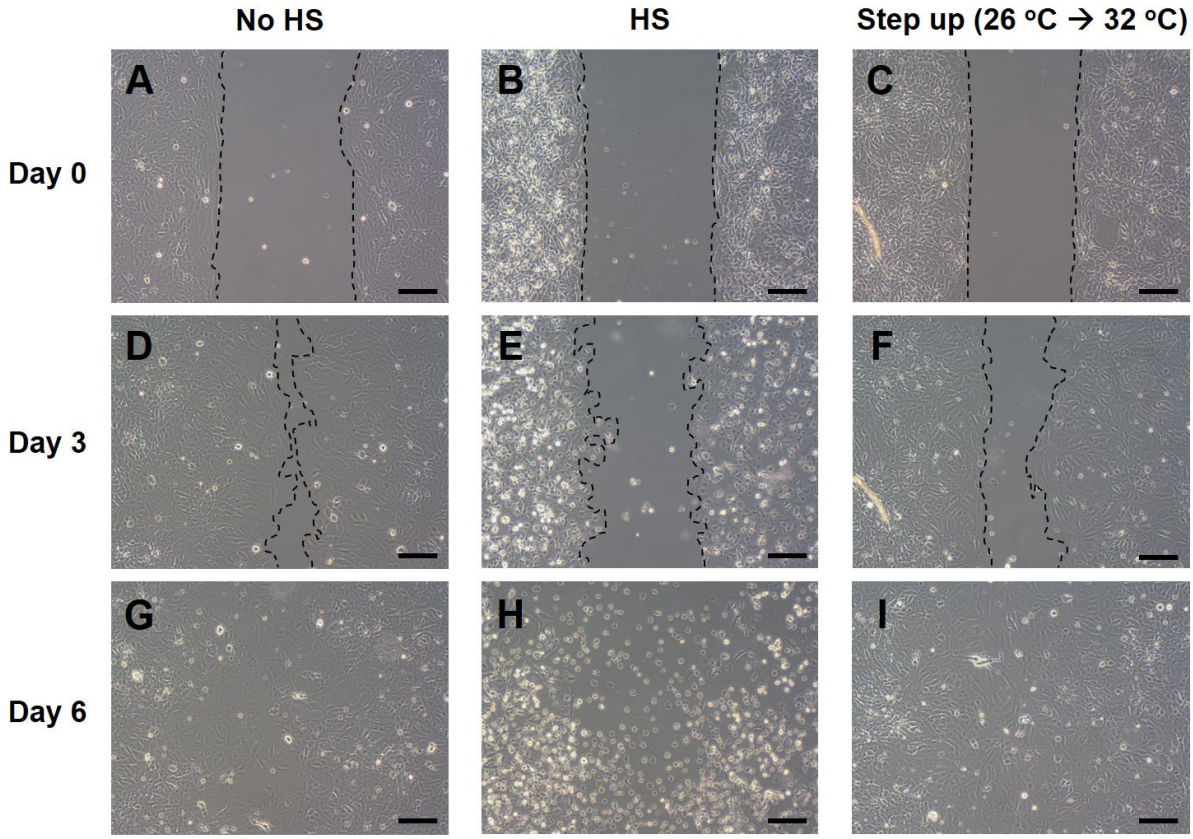

Figure 5.4. RTgutGC cells' ability to migrate into a cell free gap after being exposed to heat stress (3 h 32 ºC) or a step up protocol (24 h 26 ºC) before heat stress. After a 3 day establishment period, cells were either left at 18 ºC for the course of the experiment (No HS), exposed to 32 ºC heat stress for 3 h then returned to 18 ºC for six days (HS), or exposed to 26 ºC step up protocol for 24 h before a 3 h 32 ºC heat stress period (Step up). In each temperature condition, cells were in L15/FBS medium over the course of the experiment. See Fig. 5.1 for more detail. (A) Day 0 wound healing of cells not exposed to any HS or the step up protocol, (B) day 0 of cells exposed to HS, or (C) day 0 of cells exposed to step up. (D) Day 3 wound healing of cells not exposed to HS or step up, (E) day 3 of cells exposed to HS, or (F) day 3 of cells exposed to step up. (G) Day 6 wound healing of cells not exposed to HS or step up, (H) day 6 of cells exposed to HS, or (I) day 6 of cells exposed to step up. Pictures were taken at a 100x magnification. Cell monolayer borders are traced in black to better visualize wound healing. Scale bar = 100 μm.

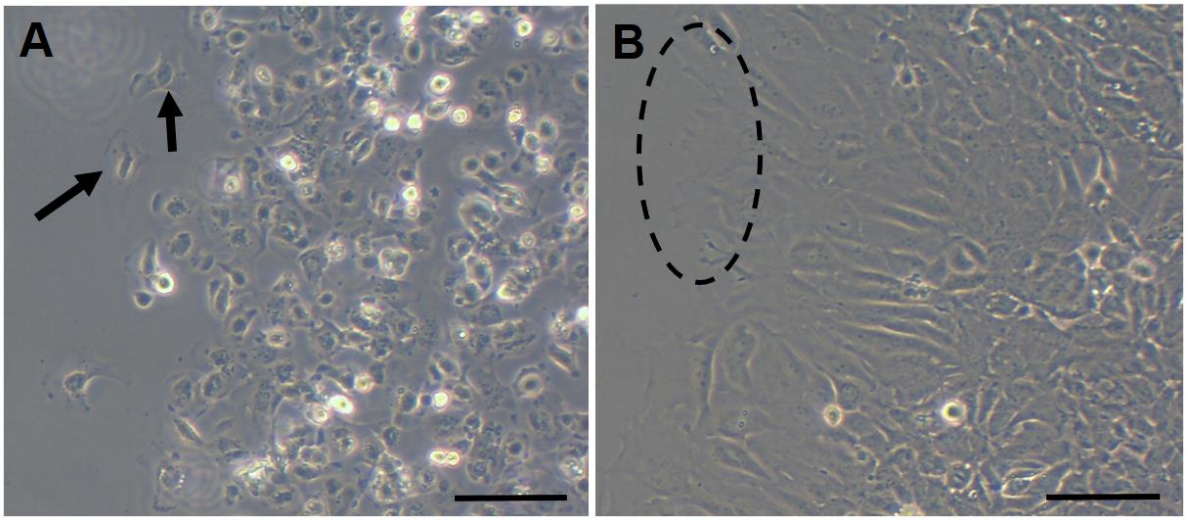

Figure 5.5. Differences in cellular migration of cells exposed to a 3h 32 ºC heat stress period compared to control cells. (A) Day 3 wound healing of cells exposed to a 3h 32 ºC heat stress. Arrows indicate individual cells migrating into the gap. (B) Day 3 wound healing of cells that were not exposed to any heat stress. Dashed oval demonstrates the cells migrating together into the gap as a sheet. Pictures were taken at a 100x magnification, however, these pictures were further enlarged. Scale bar = 100 μm.

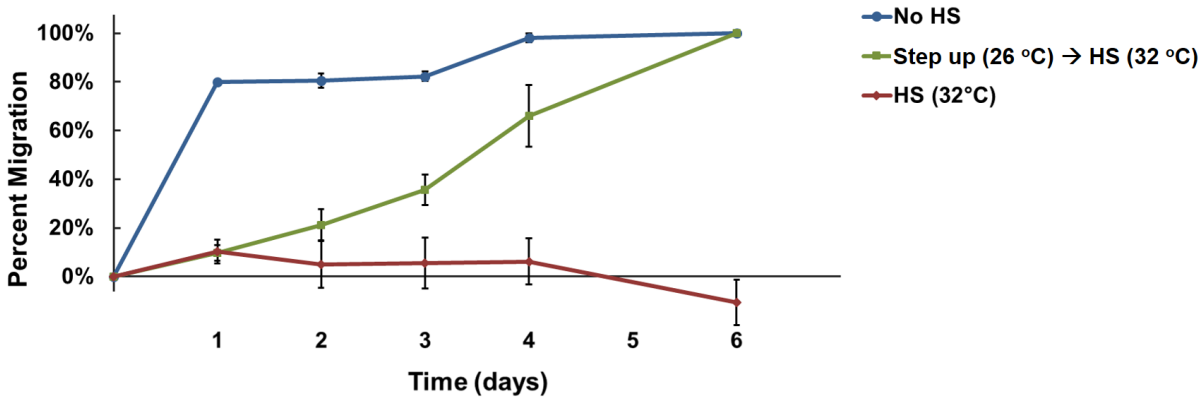

Figure 5.6. Percent migration of RTgutGC cells over time after being exposed to a heat stress period (3h 32 ºC) with or without a prior step up period (24h 26 ºC). Once a monolayer was established after 3 days, cells were either left at 18 ºC for the course of the experiment (No HS), exposed to 32 ºC heat stress for 3h then returned to 18 ºC for six days (HS), or exposed to 26 ºC for 24h before a 3h 32 ºC heat stress period (Step up → HS). After temperature treatment, the wound healing abilities of the cells were assessed. See Fig. 5.1. Cells were in L15/FBS medium over the course of the experiment. Pictures were taken every day until day 6 with data expressed as percent migration from day 0. Data are expressed as the mean ± standard deviation.

5.4. DISCUSSION

5.4.1. Wound healing and restitution at 4 °C, 18 °C and 26 °C

Wound healing by rainbow trout intestinal epithelial cells occurred at all temperatures but was slowest at the hypothermic temperature of 4 °C, and relative to the normothermic 18 °C, slightly faster at the hyperthermic temperature of 26 °C. The main cellular processes that contribute to wound healing *in vivo* are migration, proliferation, and differentiation (Iizuka & Kono, 2011), whereas for many *in vitro* assays, such as the one used in this study in which a gap becomes filled with cells, cellular migration (restitution) and proliferation are the main contributors. However, in the assay with RTgutGC at 4 and 26 °C, the wound was likely healed predominantly by cell migration because little or no proliferation occurs in rainbow trout cell cultures at these temperatures (Plumb & Wolf, 1971; Mosser et al., 1986; Bols et al., 1992). The slow migration at 4 °C and slightly faster migration at 26 °C might be due to the general phenomenon for ectothermic organisms of cellular metabolism and activities increasing as the temperature increases (Clarke & Johnston, 1999). However, some specific adaptations at 26 °C might be participating to the enhancement of wound healing. Putting rainbow trout cells at 26 °C induces HSPs synthesis (Mosser et al., 1986) and these HSPs might be aiding restitution as HSP70 and HSP90α have been implicated in human cell migration (Bhatia et al., 2016; Sims et al., 2011)

5.4.2. Wound healing and restitution after 3 h at 32 °C

During recovery at 18 °C from a 3 h heat stress (32 °C), RTgutGC cells were able to start healing a wound but could not continue the process. These results can be indicative of proper restitution being dependent of cells forming cell-to-cell contacts and migrating collectively. An interesting term recently "coined" and related to cellular sheet migration is plithotaxis, defined as the collective movement of cells in a monolayer towards the direction of maximal local stress (Gov, 2011). Under normal (non-wounded) conditions, cell monolayers are theoretically in balance as the forces the cells generate on each other are cancelled out on average. If a monolayer is broken and migration is initiated, the local stress field becomes polarized as the forces are no longer in balance (Gov, 2011). The leading migrating cells are the point of maximal stress pulling on neighbouring cells. This mechanical force on the neighbouring cells is hypothesized to polarize and guide their internal skeletal

motors to the direction of migration of the leading cells (Gov, 2011). Hence, all cells move in unison in a similar direction to close the wound. Heat stress has been shown to disorganize and/or disrupt cell-to-cell junctions in multiple cell lines, including the human intestinal epithelial cell line Caco-2 (Dokladny et al., 2006; Cai et al, 2011; Chen et al., 2008). Additionally, heat stress has been shown to cause the disassembly and collapse of cytoskeletal elements such as actin, tubulin, and intermediate filaments important in cellular migration (Richter et al., 2010; Toivola et al., 2010; Welch and Suhan, 1985; Welch and Suhan, 1986). Thus it is possible that heat stress condition is causing changes in cell-to-cell junctional complexes and to the cytoskeleton, compromising the cell monolayer and the function of plithotaxis leading to a severe reduction in cellular migration.

5.4.3. Thermotolerance for wound healing and restitution

Cells that had been subjected to a heating regimen of 26 °C for 24 h before being shifted up to 32 °C for 3 h and then returned to the normothermic 18 °C were able to recover enough functions to heal a wound but cells that did not have the 24 h at 26 °C prior to the heat stress could not heal a wound. Therefore, RTgutGC monolayers appeared to have become thermotolerant for wound healing. Wound healing involves both proliferation and cell migration (Iizuka & Kono, 2011), but other studies suggest that, in the current experiments, mainly cell migration contributed to the healing. For example, the rainbow trout fibroblast cell line, RTG-2, was found not to proliferate for at least 6 days after being returned to 22 °C from incubations at 32 °C (Mosser et al., 1986). Therefore, a more restrictive conclusion might be that RTgutGC monolayers had become thermotolerant for the coordinated cellular movement necessary for restitution.

The acquisition at 26 °C of thermotolerance for cell migration likely involved HSPs. Shifting RTG-2 cultures from room temperature to 26 -28 °C induced the rapid synthesis of the major HSPs, HSP70 and HSP90 (87 kDa) (Mosser et al., 1986). Concurrent with the HSP synthesis, RTG-2 acquired at 28 °C the ability to survive a heat stress (3 h at 32 °C) (Mosser et al., 1987), and blocking the HSP synthesis blocked the development of thermotolerance (Mosser & Bols, 1988). Survival was defined as the ability of cells to retain their shape and attachment to the plastic culture surface. Thus the cytoskeleton had become thermotolerant and likely contributed to cell migration becoming thermotolerant in the current experiments.

However, cell migration in restitution would require additional cellular structures and processes to become thermotolerant. These would include cell-to-cell contacts and the coordinated movement of cell sheets. Interestingly in other cell systems, HSPs have been shown to stabilize cytoskeletal elements (Mounier & Arrigo, 2002) and regulate tight junction protein expression (Dokladny et al., 2008). Thus the contribution of HSPs in the development of cell migration thermotolerance will be interesting to explore further in the future.

5.4.4. Summary and concluding thoughts

For the first time in any system, cells have been shown to acquire thermotolerance for cell migration into a wound. Future work should involve the possible role of HSPs in regulating cell-to-cell junctions and cytoskeletal elements in RTgutGC during heat stress. Furthermore, the role of HSP70 and HSP90α in RTgutGC or rainbow trout intestinal restitution is unknown and warrants future research.

CHAPTER 6

Effect of naringenin on the ability of rainbow trout intestinal epithelial cells to maintain their actin cytoskeleton and substrate adherence during recovery from heat stress

6.1. INTRODUCTION

Global warming is posing serious threats to the future of aquaculture (Brander, 2007), which is a farming practice that contributes to a large amount of worldwide animal protein consumption (Anyanwu et al., 2014). Rising temperatures could potentially impact aquaculture in numerous ways and one is through the impairment of fish gastrointestinal (GI) health. In humans and farm animals, heat stress has been found to target the intestinal epithelium (Dokladny et al., 2016; Pearce et al., 2013). An intact intestinal epithelium is essential for the GI tract to perform food digestion and nutrient absorption, ion secretion, barrier functions, and immunological protection. Any impairment in GI tract homeostasis could lead to decreased growth and increased infections.

A critical component of an animal GI tract is the layer of intestinal epithelial cells that forms a barrier between the internal milieu and the GI tract lumen, which is external. These cells sit on a thin basement membrane (BM) in close contact with one another, forming a continuous sheet. Yet intestinal epithelial cells can retract from their neighbours, lift off from the BM, and enter the GI tract lumen. One process by which this occurs is termed epithelial cellular extrusion (Andrade & Rosenblatt, 2011). The extruded cells usually die by apoptosis mediated by activation of caspase-3 or by a cell death mechanism mediated through caspase-1 (Liu et al., 2013). This process turns over the intestinal epithelium while maintaining the continuity of the epithelial sheet and gut health (Miguel et al., 2017). However, in a process termed pathological intestinal epithelial cell shedding (Miguel et al., 2017), breaks or gaps in the epithelial continuity occur, with detrimental health outcomes (Mayhew et al., 1999; Liu et al., 2011; 2013). The gaps have been seen in response to inflammation (Liu et al., 2011) and heat stress (Yu et al., 2010).

Several cellular structures and processes likely contribute to the epithelial cells adhering to each other and to the BM, allowing intact cellular sheet to persist in face of pathological insults, like heat stress. One of these is the actin cytoskeleton. Yet the actin cytoskeleton is vulnerable to disruption by heat (Dalle-Donne et al. 2001). When the heat stress is not too severe, the cytoskeleton and cells can recover. Presumably if intestinal epithelial cells recover from heat stress, the GI tract would recover as well. For mammals, dietary additions have been explored to aid the recovery of cells from heat stress (Varasteh et al., 2015). These include nutrients such as glutamine and threonine, increasing heat shock protein

levels (Baird et al., 2013), but phytochemicals such as naringenin are also worthy of investigation.

Therefore, in this chapter, attempts have been made to establish protocols with RTgutGC for evaluating how rainbow trout intestinal epithelial cells recover from a heat stress to keep monolayers adherent to a substrate and how naringenin might aid recovery.

6.2. MATERIALS AND METHODS

6.2.1. Cell cultures and culture conditions

RTgutGC, a rainbow trout epithelial cell line was used throughout the experiment. This cell line was developed in Niels C. Bols' laboratory at the University of Waterloo (Kawano et al., 2011). Medium used to culture the cells was Leibovitz's L15 with 2.05 mM L-Glutamine (Thermo Fisher Scientific) supplemented with 10% fetal bovine serum (FBS, Sigma-Aldrich) and antibiotics (10,000 U/mL penicillin and 10,000 μg/mL streptomycin, P/S, Thermo Fisher Scientific) (L15/FBS). Cells were subcultured or passaged using trypsin (Thermo Fisher Scientific) every week at a ratio of 1 to 2 and maintained at 18 ^{o}C. The cell culture vessels used were BioLite 75 cm^2 cell culture treated flasks (Thermo Fisher Scientific).

6.2.2. Heat stress timeline

All experiments involved with heat stressing the cells followed the timeline depicted below (Fig 6.1). Cells were first allowed to establish a monolayer in L15/FBS at 18 ^{o}C for 3-4 days. Afterwards, the medium was removed, the cells were washed with Dulbecco's phosphate-buffered saline solution (DPBS, Thermo Fisher Scientific) and varying concentrations of naringenin (Sigma-Aldrich) either in L15/FBS, L15, or in a salt solution of L15 (L15/salts) were added. The naringenin concentration used were 10, 30, 50, 75, and 100 μM from 200x stock solutions of the reagent dissolved in DMSO. Final DMSO concentration in control and media/naringenin solutions was 0.5% (v/v). The related naringenin concentration range is based on concentrations used on fish and mammalian cells in the literature (Menanteau-Ledouble et al., 2015; Noda et al., 2013). The cells were left to incubate in a naringenin containing solution for 30 minutes at 18 ^{o}C. Heat stress conditions then followed by exposing the cells to a temperature of 32 ^{o}C in an incubator for 1 ½ or 3 h depending on the assay. Cells were then left to recover back at 18 ^{o}C for 24 h to 96 h depending on the assay.

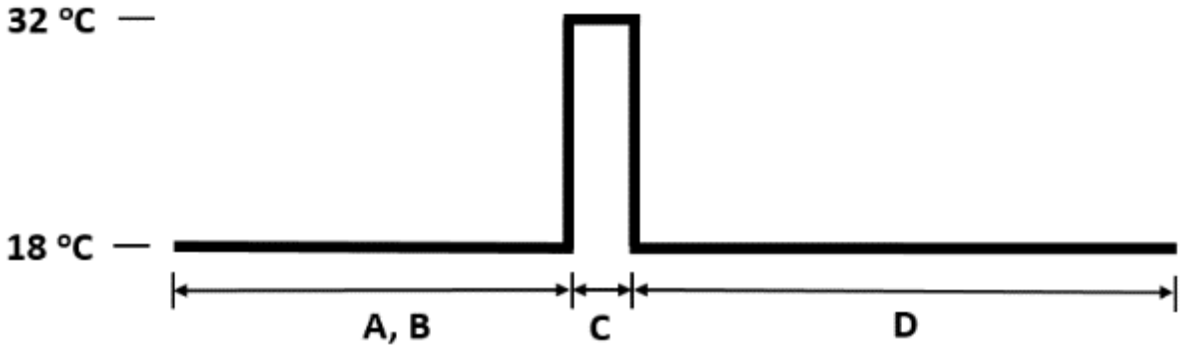

Figure 6.1. Experimental timeline with heat stress incubation. A: Establishment period of 3-4 days. B: Addition of naringenin and 30 minute incubation before heat stress. C: 1 ½ or 3 hour heat stress period. D: 24-96 hour recovery period. This is a visual representation of incubation temperatures and lengths; this is not an accurate representation of media temperatures changes during the timeline.

6.2.3. Cellular viability

Cellular viability was monitored by changes in cell morphology through phase contrast microscopy and with viability indicator dyes, Alamar Blue® (AB, ThermoFisher Scientific) and 5'-carboxyfluorescein diacetate acetoxymethyl ester (CFDA-AM, Sigma-Aldrich). AB provides a measure of metabolic activity while CFDA-AM provides a measure of plasma membrane integrity (Dayeh et al., 2013). The protocol used for the AB and CFDA-AM dyes follows closely Dayeh et al. (2013) methods. RTgutGC cells in L15/FBS were added to a 24-well plate at a plating density of 125,000 cells per well in replicates of 4. Plates followed an incubation timeline as seen in Fig 6.1 where the heat stress length was either 1 ½ or 3 hours followed by a recovery period of 24 hours. Temperature control plates remained at 18 ^{o}C throughout the timeline. The medium was then removed, the cells were washed with DPBS, and a solution containing 5% (v/v) AB and 4 μM CFDA-AM in DPBS was added to the cells. Plates were then incubated at room temperature for 1 hour in the dark. Using a series 4000 CytoFluor fluorescent plate reader (PerSeptive Biosystems - ThermoFisher Scientific), results were recorded as relative fluorescent units (RFUs). The mean RFUs for the experimental wells were expressed as a percentage of the mean RFUs for control wells.

6.2.4. Fluorescence microscopy of RTgutGC F-actin

F-actin was visualized using fluorescein isothiocyanate labeled phalloidin (FITC-phalloidin, Sigma-Aldrich) and confocal microscopy. The fluorescent conjugate of phalloidin,

FITC, is used to label F-actin and can be visualized by fluorescence or laser microscopy. A 5 mg/mL stock solution of FITC-phalloidin was prepared in DMSO. RTgutGC cells in L15/FBS were plated in a 4 chamber tissue culture treated glass Falcon CultureSlide® (Corning) at a density of 150,000 cells per chamber. Slides followed an incubation timeline as seen in Fig 6.1 where the heat stress length was 1 ½ hours followed by a recovery period of 24 hours. Temperature control slides remained at 18 ^{o}C throughout the timeline. Cells were washed with DPBS and fixed with 3% paraformaldehyde (Sigma-Aldrich) for 20 minutes at 4 ^{o}C. Following fixation, the cells were then permeabilized with 0.1% Triton X-100 (Sigma-Aldrich) for 10 minutes at room temperature. Afterwards, 5 μg/mL of FITC-phalloidin was added to the cells and allowed to incubate for 45 min at room temperature in the dark. Cells were then washed three times with DPBS and the slides were allowed to dry. Once dry, plastic chambers were removed from the slides and three drops of a mounting medium, Fluoroshield (Sigma-Aldrich), containing DAPI was added to the slides with a coverslip to help preserve the slide and counter stain for DNA. Confocal images were obtained with the Zeiss LSM 510 laser scanning microscope and were acquired and analyzed using a ZEN lite 2011 software.

6.2.5. Caspase-3 induction

Caspase-3 induction was detected using a Caspase-3/CPP32 colorimetric assay kit (BioVision). The assay detects caspase-3 activity by cleavage of the chromophore *p*-nitroaniline (*p*NA) from DEVD-*p*NA labelled substrate that the caspase recognizes. *p*NA can then be measured by spectrophotometric detection with a plater reader set to 400-405 nm. Cells were plated in 6-well plates with L15/FBS at a density of 1,500,000 cells per well. Cells then followed a timeline similar to Fig 6.1. 100 μM naringenin in L15 medium was administered 30 min before the heat stress period. The heat stress period was 3 hours. Immediately after heat stress, cells were washed with DPBS and removed from the wells with trypsin for cell counting. After pelleting by centrifugation, 50 μL of provided lysis buffer was used to resuspend the cells and the cell suspension was incubated on ice for 10 minutes followed by centrifuging for 1 minute at 10,000 x g. The protein concentration in the supernatant was then assayed using a Pierce BCA protein assay kit (ThermoFisher Scientific). Following the protocol for the Caspase-3/CPP32 colorimetric assay kit, proteins were diluted to 100 μg in 50 μL of the kit's lysis buffer into a 96-well plate. A reaction buffer containing 10 mM DTT was

then added followed by an addition of 4 mM DEVD-*p*NA substrate. The samples were then left to incubate at 37 ºC for 2 hours. Using a VICTOR^{3}V colorimetric plate reader (Perkin Elmer), sample absorbance was read at 400-405 nm. The data were then expressed as fold induction compared to the non-heat stressed control.

6.2.6. HSP70 detection

HSP70 was visualized by Western blotting. RTgutGC cells were plated in 6-well plates with L15/FBS at a density of 1,000,000 cells per well. Cells then followed a timeline similar to Fig 6.1. The heat stress period was 1 ½ hours with a recovery period of 3 days. After recovery, the cells were lysed by adding 200 µL of RIPA lysis buffer containing a protease inhibitor cocktail (Qiagen) directly to the plates. The cells were scraped off, transferred to microcentrifuge tubes, and allowed to sit on ice for 30 minutes. Tubes were then centrifuged at 10,000 x g for 1 minute and proteins in the supernatant were collected. Protein concentrations were determined using a Pierce BCA protein assay kit (ThermoFisher Scientific). SDS-PAGE was performed using a Mini-PROTEAN tetra system (Bio-Rad) with premade 1 mm thick handcast gels. Loaded gels were run at 120 volts for 1 ½ hours. The transfer step onto a nitrocellulose membrane was done in a Mini-Trans Blot Cell system (Bio-Rad) running at 150 milliamps for 1 hour. Equal protein loading was visualized by a 0.1 % Ponceau S stain in 5% (w/v) acetic acid. Before probing the membrane with rabbit anti-salmon HSP70 (Fish) polyclonal antibodies (SPC-314B, StressMarq), a 1 hour blocking step using 5% skim milk (w/v) in 1x TBS-T was performed. All antibodies were diluted in 5% skim milk (w/v) in 1x TBS-T. Rabbit anti-Salmon HSP70 (Fish) polyclonal antibodies were diluted 1:1000. To detect a reference protein, rabbit anti-actin antibodies (Sigma Aldrich) were used and diluted 1:600. The secondary antibody used was goat anti-rabbit IgG conjugated to alkaline phosphatase (Sigma Aldrich) diluted 1:5000. Protein bands were detected by NBT/BCIP. Membranes were scanned and bands quantified by densitometry using a Bio-Rad ChemiDoc MP imaging system without chemiluminescense option. The data were then normalized to the actin bands and expressed as a percentage of the control.

6.2.7. Statistical analyses

Variables were expressed as the mean ± standard deviation or standard error of the mean. Statistical analysis was done by a one-way ANOVA and Dunnet post hoc test. Statistical significance was defined as $p < 0.05$.

6.3. RESULTS

6.3.1. Recovery of RTgutGC monolayers from heat stress as judged by phase contrast microscopy

RTgutGC monolayers either in L15/FBS, L15 or L15/salts were subjected to different heat treatments and monitored afterwards by phase contrast microscopy during their 24 h of recovery at 18 °C either in L15/FBS (Fig 6.2 and 6.3), L15/salts (Fig 6.2 and 6.3) or L15 (Fig 6.4). The heat stress was 32 °C for 1.5 h (Fig 6.2) or 3 h (Fig 6.3 and 6.4). The appearance of stressed cultures was compared to cultures kept continuously at 18 °C. When cells in L15/FBS or L15/salts were stressed at 32 °C for 1.5 h, very few morphological differences were observed after 24 h of recovery (Fig 6.2). However, when cultures were stressed for 3 h, round floating cells were seen along with attached and spread cells that often had irregular phase dense outlines, giving a shrivelled appearance (Fig 6.3 and 6.4).

6.3.2. Effect of naringenin on the recovery of RTgutGC monolayers from heat stress as judged by phase contrast microscopy

Naringenin appeared to have slight or no effect on RTgutGC monolayers maintained 18 °C but did influence the morphology of cells recovering from heat stress. For cultures recovering from 1.5 h at 32 °C, 100 μM naringenin appeared to cause the periphery of cells in L15/salts to be more phase dark (Fig 6.2). Increasing concentrations of naringenin in cultures during the heat stress at 32 °C for 3 h and upon their return to 18 °C allowed cultures to recover better in L15/FBS, L15 or L15/salts (Fig 6.3 and 6.4). Fewer floating cells were seen and the attached cells appeared less shrivelled (Fig 6.4).

6.3.3. Metabolic activity and plasma membrane integrity

A 3 h heat stress period caused a decrease in both metabolic activity and plasma membrane integrity of cells in L15/FBS (Fig 6.5). The metabolic activity of cells in L15/FBS was more affected by a 3 h heat stress than the plasma membrane dropping relatively by 54%. Naringenin appeared to have little effect on the metabolic activity of non-heat stressed and heat stressed cells in L15/FBS (A, Fig 6.5). However, increasing concentrations of naringenin slightly decreased plasma membrane integrity in both non-heat stressed and heat stressed cells (B, Fig 6.5). Similar to the cells in L15/FBS, a 3 h heat stress of cells in L15/salts caused a

more significant drop (59%) in metabolic activity compared to plasma membrane integrity (Fig 6.6). However, the effects of naringenin on metabolic activity and plasma membrane integrity were more intensely seen when the cell were in L15/salts medium. In the non-heat stressed cells, increasing concentrations of naringenin caused a dose response drop in metabolic activity (A, Fig 6.6). In the heat-stressed cells, a drop in metabolic activity was seen only with 100 μM naringenin (A, Fig 6.6). Increasing concentrations of naringenin had no negative effects on the plasma membrane integrity of non-heat stressed cells in L15/salts where even a slight increase (15%) was observed with 10 μM naringenin (B, Fig 6.6). However, with the heat stressed cells, a dose response drop in plasma membrane activity was observed with increasing concentrations of naringenin, where at 100 μM naringenin it dropped by 58%.

6.3.4. Effect of naringenin and heat stress on F-actin staining

In response to naringenin and heat, RTgutGC cells in L15/salts showed considerable changes in staining for F-actin with fluorescently labelled phalloidin, but cells in L15/FBS showed fewer changes. For cultures at 18 °C in either L15/FBS or L15/salts, naringenin caused changes in the staining pattern for F-actin. As naringenin increased up to 100 μM, fewer stress fibers were seen and more circumferential actin was detected, especially for cells in L15/salts (A-D, Fig 6.7 and 6.8). Cultures in either L15/FBS or L15/salts were subjected to a heat stress of 32 °C for 1.5 h and allowed to recover for 24 h at 18 °C and compared for F-actin staining with cultures (controls) continuously incubated at 18 °C in either L15/FBS or L15/salts. For cells in L15/FBS, little difference was seen in actin staining between heat stressed and control cultures (Fig 6.7). However, cells recovering from heat stress in L15/salts had longer stress fibers and blebs of intense actin staining (Fig 6.8).

In cells recovering from heat stress either in L15/FBS or L15/salts, naringenin caused changes in F-actin staining in a dose-dependent manner (E-H, Fig 6.7 and 6.8). The staining of cytoplasmic stress fibers was diminished and circumferential actin was enhanced as naringenin concentration increased. These changes were most pronounced for cells in L15/salts (Fig 6.8).

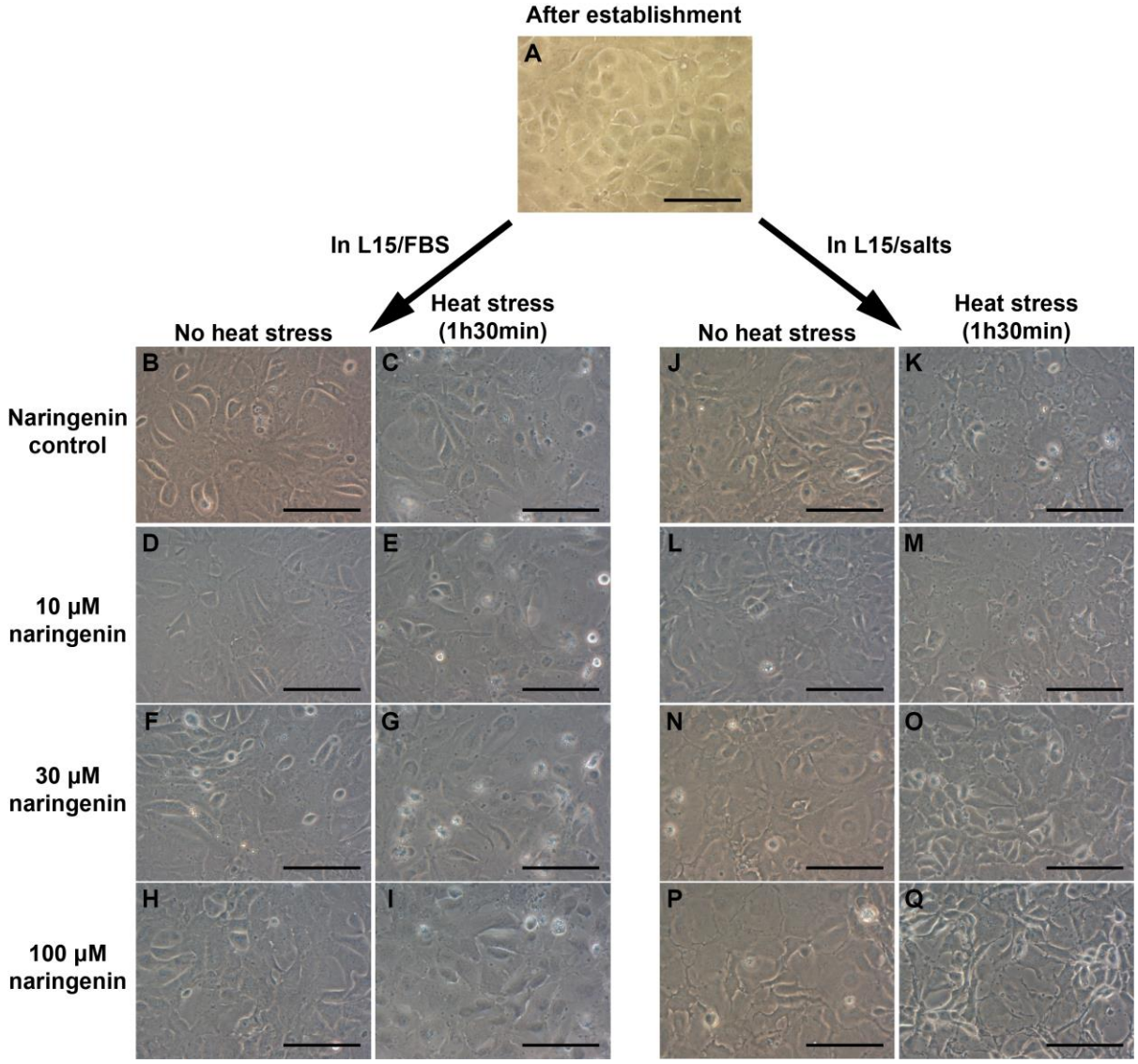

Figure 6.2. Phase-contrast observations of RTgutGC with 1 h 30 min heat stress and naringenin. Cells were incubated with different concentrations of naringenin (10, 30, and 100 µM) in either L15/FBS or L15/salts medium and subjected to a 1 h 30 min heat stress (32 ºC) period. Cells subjected to heat stress were allowed to recover at 18 ºC for 24 h before pictures were taken. Pictures represent magnification of 400x with a scale bar of 100 µm.

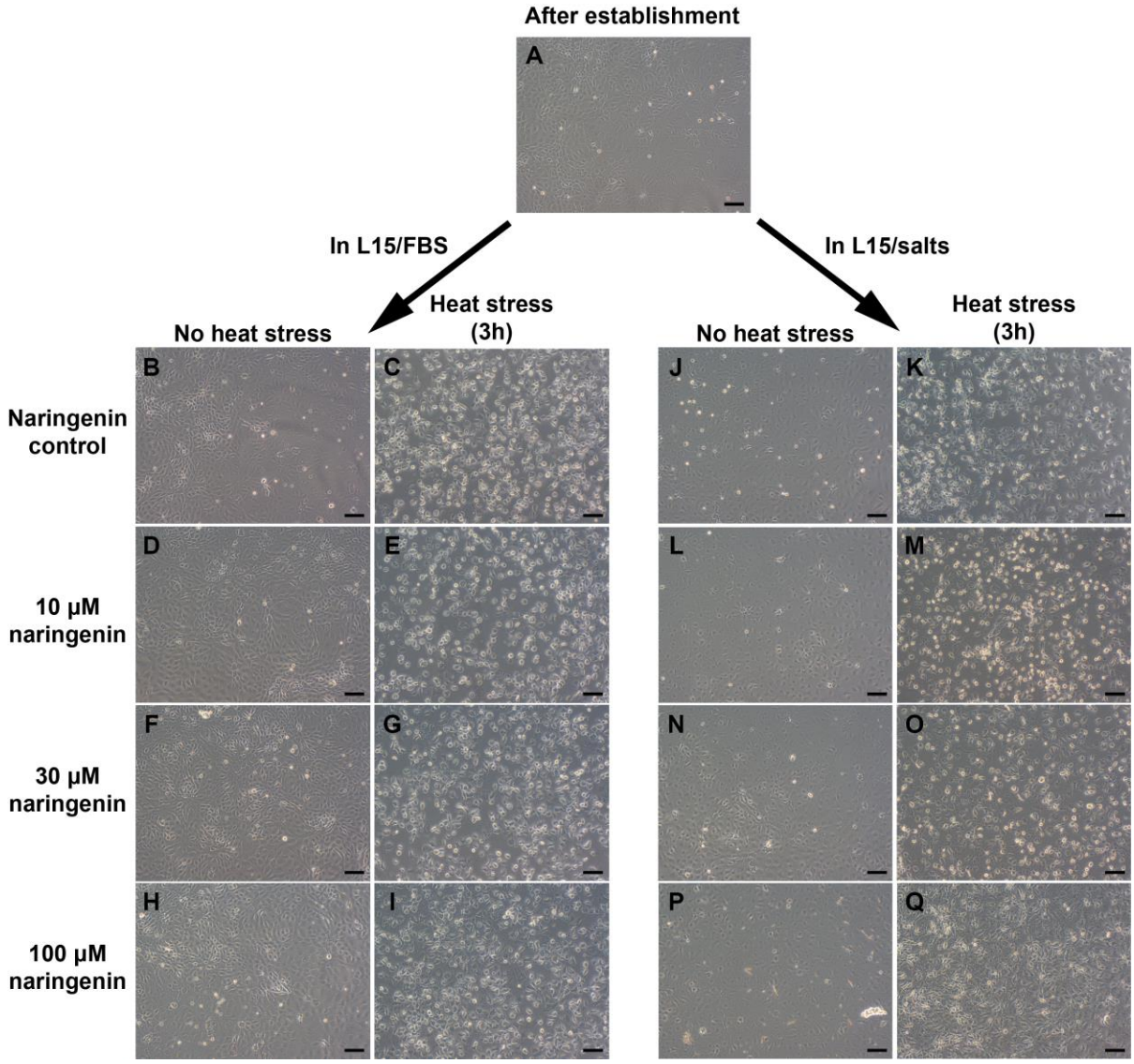

Figure 6.3. Phase-contrast observations of RTgutGC with 3 h heat stress and naringenin. Cells were incubated with different concentrations of naringenin (10, 30, and 100 µM) in either L15/FBS or L15/salts medium and subjected to a 3 h heat stress (32 ºC) period. Cells subjected to heat stress were allowed to recover at 18 ºC for 24 h before pictures were taken. Pictures represent a magnification of 100x with a scale bar of 100 µm.

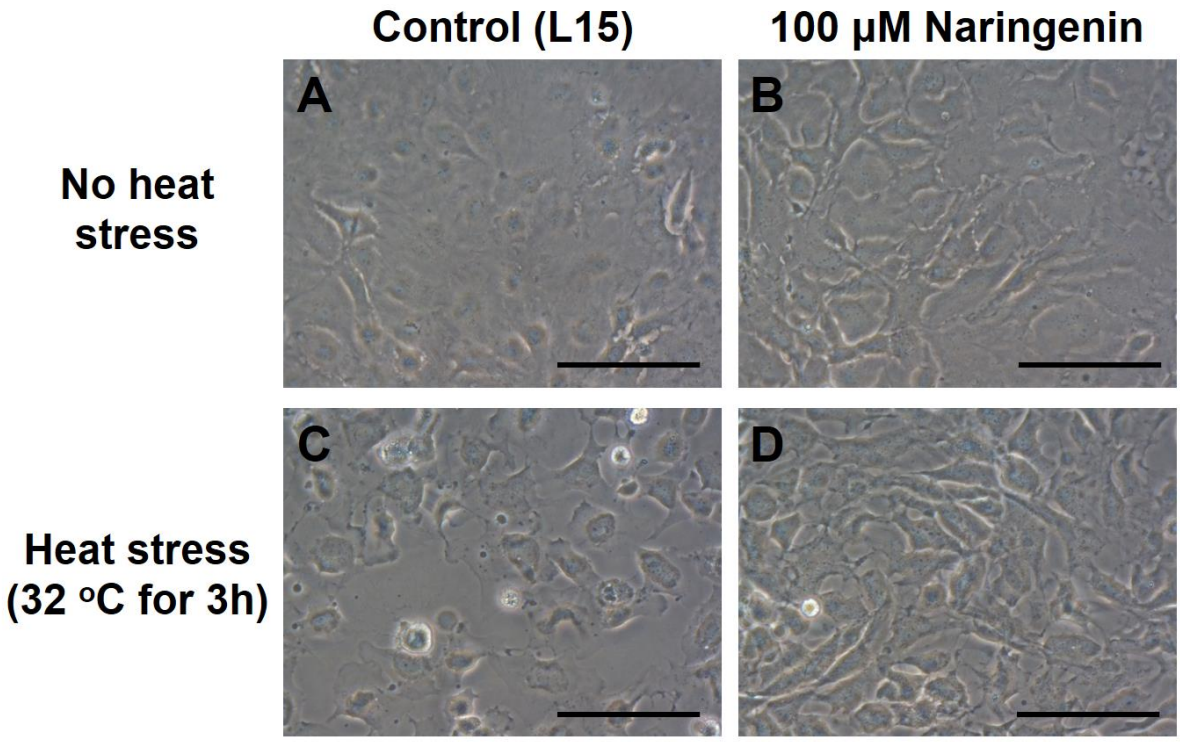

Figure 6.4. Phase-contrast observations of RTgutGC under heat stress with naringenin in L15 medium. (A) Cells in L15 medium without heat stress. (B) Cells incubated in L15 medium containing 100 µM naringenin without heat stress. (C) Cells in L15 medium with 3 h 32 °C heat stress. (D) Cells incubated in L15 medium containing 100 µM naringenin with 3 h 32 °C heat stress. Cells subjected to heat stress were allowed to recover at 18 °C for 24 h before pictures were taken. Pictures represent 400x field with a scale bar of 100 µm.

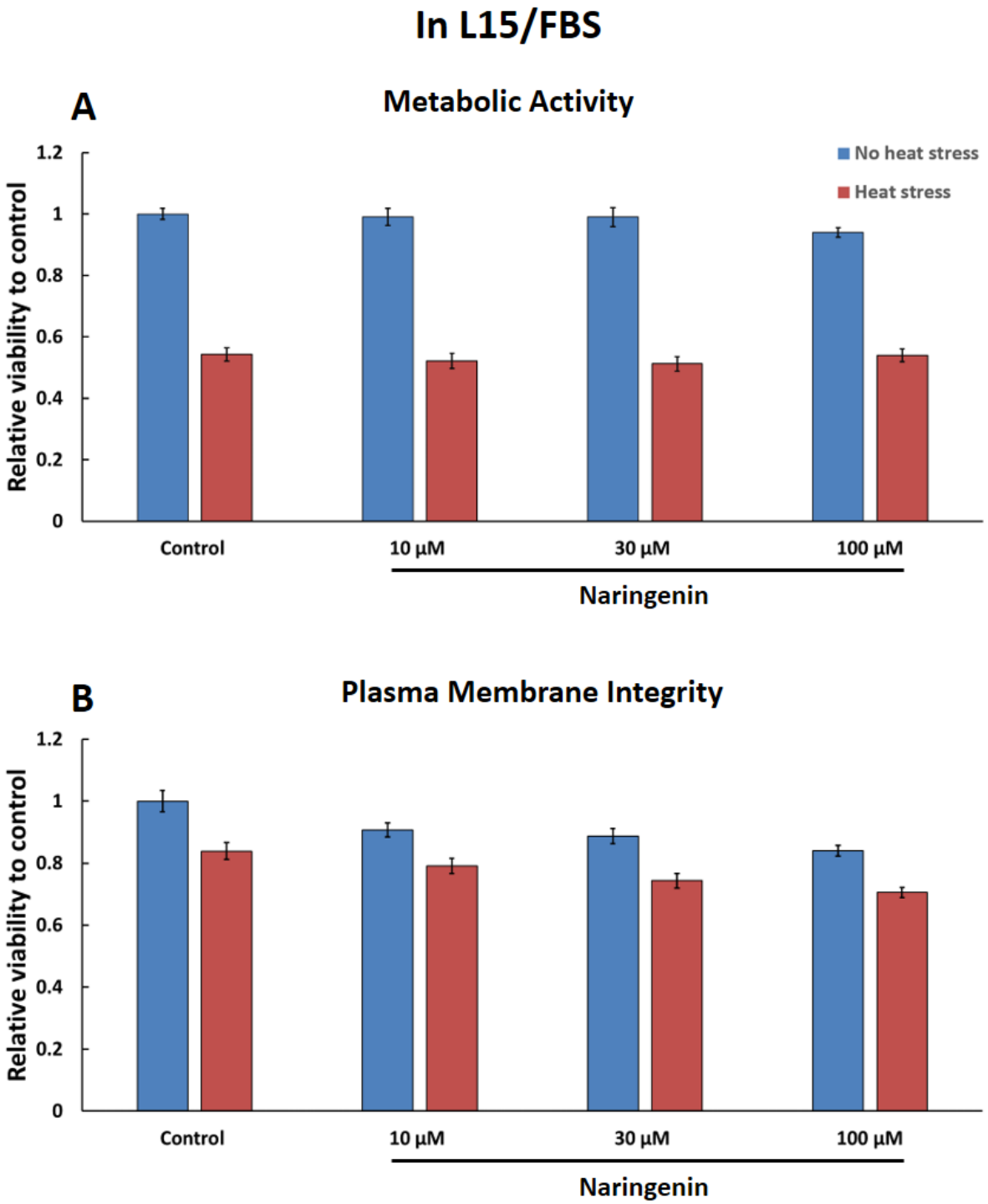

Figure 6.5. Cellular viability of RTgutGC with naringenin in L15/FBS. (A) Relative metabolic activity measured by alamarBlue reduction by non heat stressed and heat stressed (3h 32 ^{o}C) cells. (B) Relative plasma membrane integrity measured CFDA-AM conversion to CF and its retainement in non heat stressed and heat stressed (3h 32 ^{o}C) cells. Both indicators of cellular viability were measured after a 24h 18 ^{o}C recovery period. Values are means ± standard deviation. All data in (A) and (B) are significant ($p < 0.01$) compared to the 18^{o}C control. The no heat stress data was previously shown in Fig 3.4.

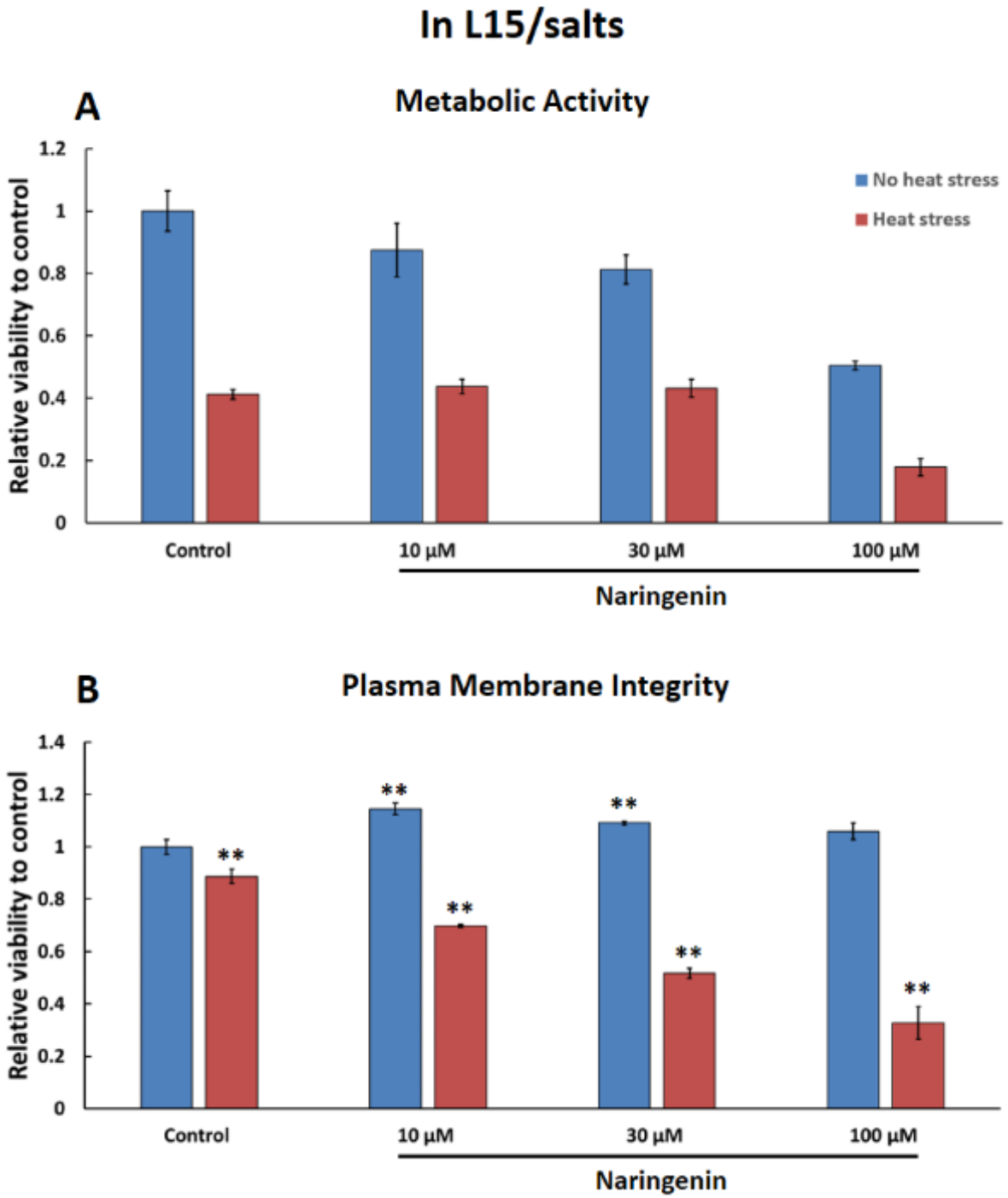

Figure 6.6. Cellular viability of RTgutGC with naringenin in L15/salts. (A) Relative metabolic activity measured by alamarBlue reduction by non heat stressed and heat stressed (3h 32 ^{o}C) cells. (B) Relative plasma membrane integrity measured by CFDA-AM conversion to CF and its retainement in non heat stressed and heat stressed (3h 32 ^{o}C) cells. Both indicators of cellular viability were measured after a 24h 18 ^{o}C recovery period. Values are means ± standard deviation. All data in (A) are significant ($p < 0.01$) compared to the 18^{o}C control. In (B), asterisks indicate significant differences when compared to the control: ** $p < 0.01$. The no heat stress data was previously shown in Fig 3.6.

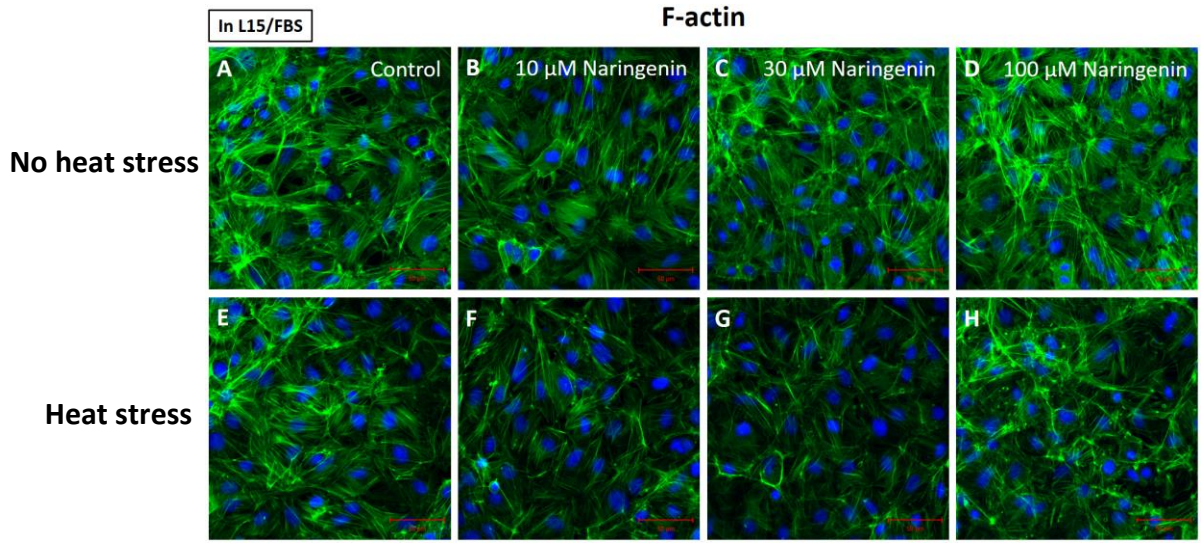

Figure 6.7. F-actin arrangement under the influence of naringenin and heat stress in L15/FBS medium. F-actin was visualized by FITC-phalloidin. Cells were exposed to a heat stress period of 1 h 30 min at 32 ºC. Staining occurred immediately after a 24 h 18 ºC recovery period. Scale bar = 50 µm.

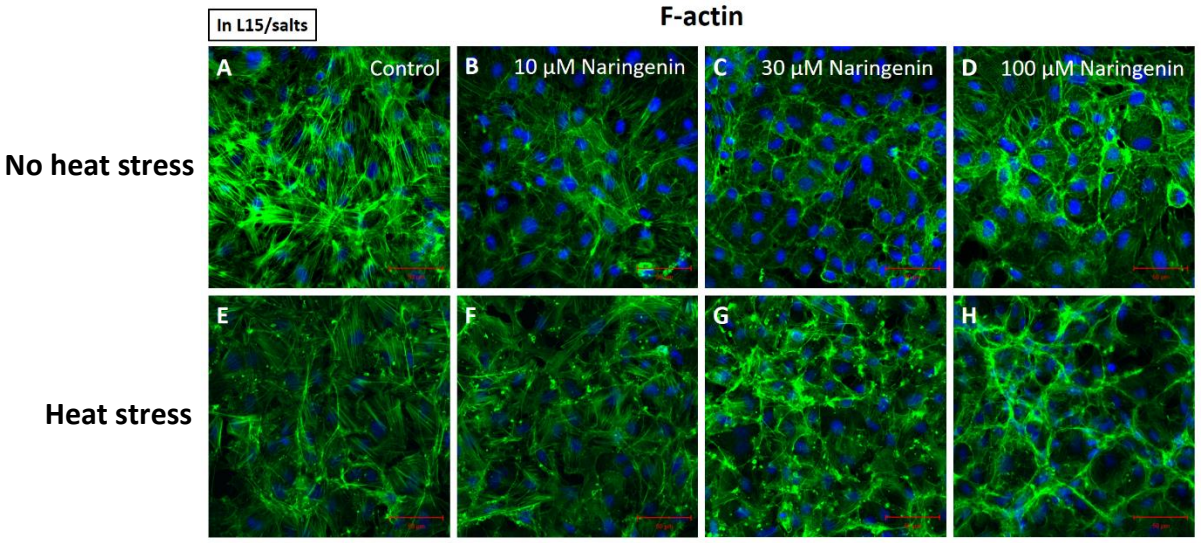

Figure 6.8. F-actin arrangement under the influence of naringenin and heat stress in L15/salts medium. F-actin was visualized by FITC-phalloidin. Cells were exposed to a heat stress period of 1 h 30 min at 32 ºC. Staining occurred immediately after 24 h 18 ºC recovery period. Scale bar = 50 µm.

6.3.5. Caspase-3 activation in RTgutGC by heat stress

Heat stress activated caspase-3 activity in RTgutGC cells that were stressed as monolayers in L15 (Fig 6.9). Immediately after RTgutGC monolayers had been held for 3 h at 32 °C, Caspase-3 activity was approximately 2.3-fold higher than before the heat stress. This stimulation of activity occurred even when 100 μM naringenin was present during the heat stress. Exposure of RTgutGC monolayers to naringenin for 3 h at 18 °C also activated caspase-3 but this neither enhanced nor impaired the activation by heat stress.

6.3.6. Effect of naringenin on HSP70 accumulation during recovery from heat stress in either L15/FBS or L15/salts

Naringenin appeared to have little effect on HSP70 accumulation in RTgutGC cells during their recovery at 18 °C from a heat stress of 1.5 h at 32 °C, although recovery in L15/salts might have been slightly impaired by naringenin (B, Figure 6.10 and 6.11). Western blotting revealed that cells either in L15/FBS (B, Fig 6.10, lane 1 top panel) or L15/salts (B, Fig 6.10, lane 1 top panel) had constitutive HSP70 levels. These HSP70 levels were unchanged by naringenin at up to 100 μM in either L15/FBS or L15/salts (Fig 6.10 and 6.11). After 3 days of recovering from the heat stress in L15/FBS, cells had accumulated noticeably higher HSP70 levels relative to unstressed cultures in L15/FBS (A, Fig 6.10 and 6.11). This was unchanged by the presence of naringenin at up to 100 μM during recovery (A, Fig 6.10 and 6.11). For cells heat stressed and allowed to recover in L15/salts, there were hints of at least two possible differences. Firstly, less HSP70 had accumulated after 3 days of recovery in L15/salts (B, Figure 6.10 and 6.11). Secondly when the flavanone was present during recovery, HSP levels appeared slightly lower at 100 μM naringenin (B, Figure 6.10 and 6.11).

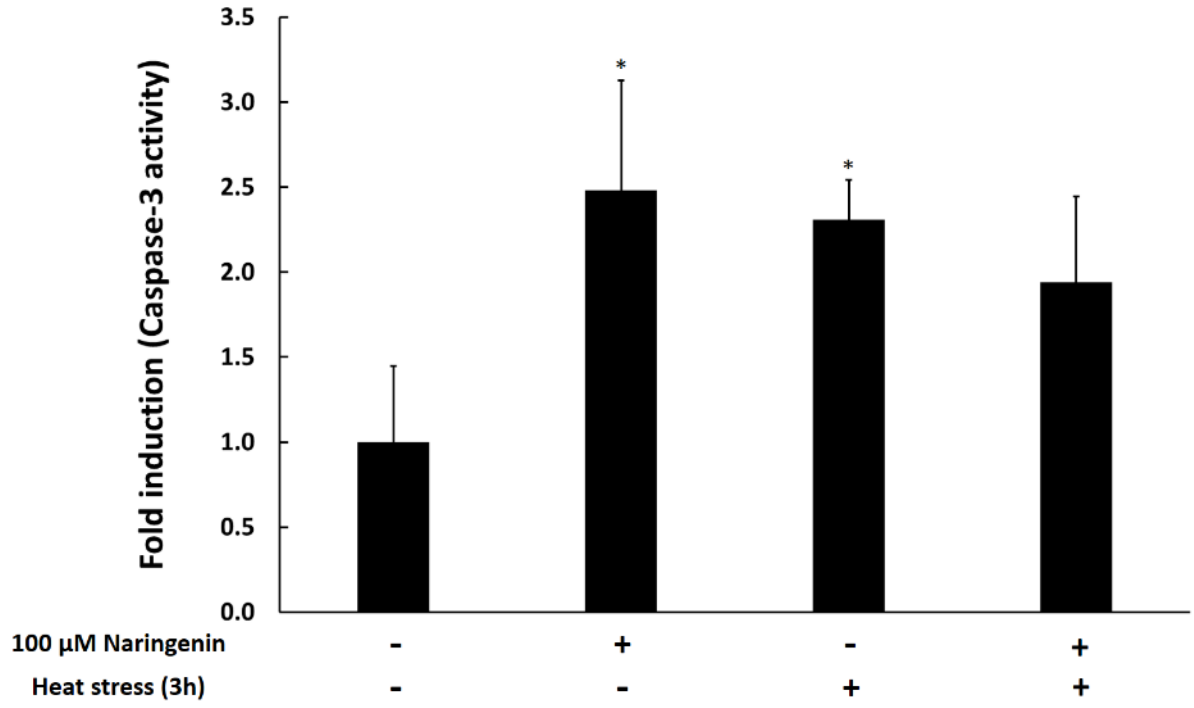

Figure 6.9. Caspase-3 activity under the presence of heat stress and naringenin. 100 µM naringenin in L15 medium was administered to the cells 30 min before heat stress. Heat stress period was 3 h at 32 ºC. Cells were processed immediately post-heat stress for caspase-3 activity. Values are means ± standard deviation. Asterisks indicate significant differences when compared to the control: * $p < 0.05$

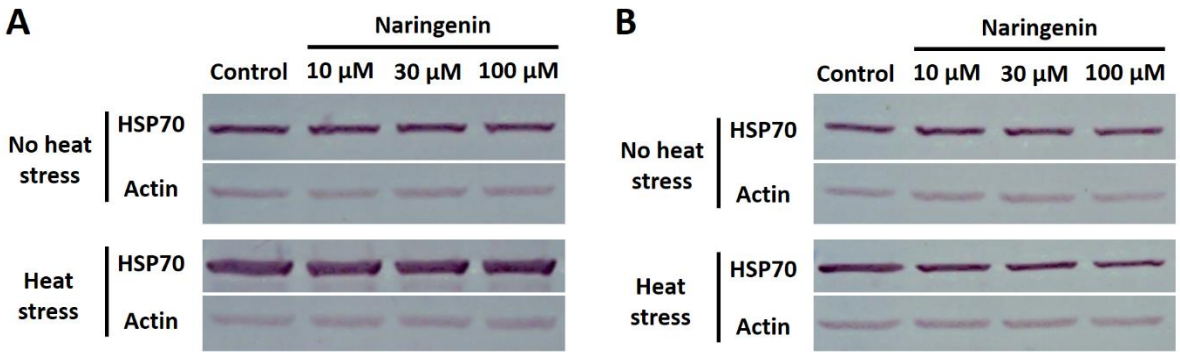

Figure 6.10. HSP70 protein levels visualized by Western blotting. Visualization of HSP70 expression and actin control in either (A) L15/FBS medium or (B) L15/salts medium with and without heat stress (1 h 30 min at 32 ºC) under 10, 30, and 100 µM of naringenin. Post-heat stress, cells were allowed to recover at 18 ºC for 3 days before being processed. (A) and (B) respectively represent separate Western blots. The no heat stress data was previously shown in Fig 3.12.

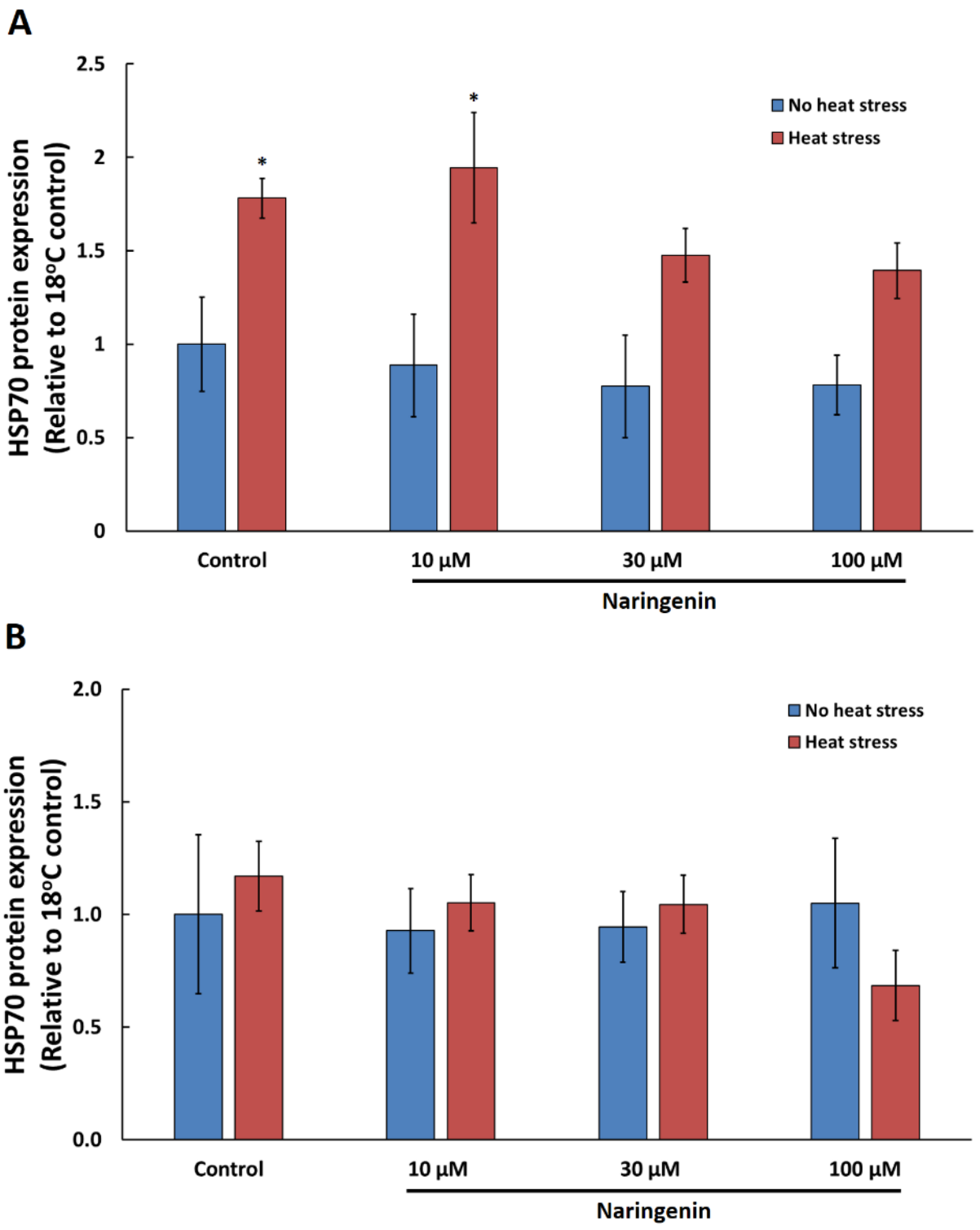

Figure 6.11. Relative HSP70 protein levels by densitometric analysis of Western blots. HSP70 protein expression in either (A) L15/FBS medium or (B) L15/salts medium under 10, 30, and 100 µM of naringenin with or without a 1 h 30 min 32 °C heat stress period. Values are means ± standard error of the mean. Asterisks indicate significant differences when compared to the 18 °C control: * $p < 0.05$. The no heat stress data was previously shown in Fig 3.12.

6.4. DISCUSSION

6.4.1. Naringenin prevented heat stress induced cell detachment but did not improve viability after heat stress

100 μM of naringenin helped retain adherence and morphology of RTgutGC cells exposed to a 3h heat stress period in L15/FBS, L15, and L15/salts. However, this was matched with a decrease in metabolic activity and plasma membrane activity of heat stressed cells in L15/salts with 100 μM of naringenin. This decrease was less prominent in L15/FBS. Nonetheless, naringenin showed no trend in the improvement of cellular viability with or without heat stress. Interestingly, L15/FBS diminished the effects of heat stress on plasma membrane integrity compared to L15/salts. L15/FBS contains lipids and many nutritional compounds helping synthesis and maintenance of the plasma membrane (Gimenez et al., 2011). Additionally, fatty acid composition of membrane phospholipids can be highly influenced by exogenous factors (Gimenez et al., 2011).

6.4.2. Naringenin increased caspase-3 activity but did not alter the heat activation of caspase-3

Naringenin is a compound of interest in cancer research due to its abilitiy to induce apoptosis in human cancer cells (Ahamad et al., 2014; Arul & Subramanian, 2013). Effective concentrations of naringenin in apoptosis activation are seen above 100 μM in human cancer cells (Ahamad et al., 2014; Arul & Subramanian, 2013). Naringenin can activate the mitochondrial-mediated apoptosis pathway, with increases in Bax/Bcl-2 ratio, release of cytochrome C, and sequential activation of caspase-3 (Arul & Subramanian, 2013). In this study we observed increased caspase-3 activity with 100 μM naringenin. Additionally, naringenin has been observed to induce apoptosis via reactive oxygen species generation (Ahamad et al., 2011). This study additionally demonstrated that naringenin had no positive or negative effect on the heat activation of caspase-3.

6.4.3. Naringenin failed to modulate HSP70 levels in HS or non-HS conditions

Studies of naringenin on a human intestinal cell line, Caco-2, revealed HSP70 modulating abilities of naringenin. Naringenin was able to increase HSP70 levels (Noda et al., 2013). Additionally, increases in claudin 4 proteins levels were associated with the activation

of the transcription factor Sp1, known to bind to the human HSP70 promoter site, by naringenin (Morgan, 1989; Noda et al., 2013). Hence, HSP70 might play a role in the maintance during heat stress of cell-to-cell contacts such as tight junctions. However, the current study revealed that naringenin has no effect on HSP70 levels in RTgutGC either recovering from heat stress or not. Hence, naringenin's protective effects to adherence and cell shape was most likely not due to increased levels of HSP70.

6.4.4. Naringenin induces changes in the actin cytoskeleton under heat stress

Improved recovery and adherence of RTgutGC cells after heat stress by naringenin might be from re-organizations in F-actin. Naringenin promoted circumferential actin bundles while decreasing stress fibers under heat stress. This reorganization in actin has been observed in the literature and is a sign of actin strongly associating cell adhesion proteins and ZO-1 tight junction proteins, generating stronger cell-to-cell contacts, whereas the loss of circumferential actin is sometimes indicative of a more permeable monolayer with weaker cell-to-cell contacts (Noda et al., 2010; Yukiura et al., 2015). Cells undergoing heat stress with naringenin were able to maintain stronger cell contacts and thus remain adhered to the culture vessel surface.

6.4.5. Summary and concluding thoughts

Increases in naringenin exerted protective effects from heat stress on cell adherence, shape, and monolayer integrity possibly due to changes in F-actin organization from fewer stress fibers to more circumferentially located bundles. Circumferential actin bundles are highly associated with stronger cell-to-cell contacts. However, naringenin did not improve cell viability after heat stress. Additionally, naringenin did not alter heat induced caspase-3 activation and on its own, caused an increase in caspase-3 activity. It was concluded that HSP70 plays no role in mediating the improvement by naringenin in the recovery of cell shape from heat stress. Future studies could look into other HSPs, effects of naringenin on barrier functions under heat stress, and understanding the mechanism of naringenin's caspase-3 activation.

CHAPTER 7

General summary and future directions

7.1. GENERAL SUMMARY AND FUTURE DIRECTIONS

A rainbow trout intestinal epithelial cell line, RTgutGC, has been investigated in this thesis as a possible tool for studying the effects of various types of stresses relevant to aquaculture and to screen for feed additives. This *in vitro* approach has been guided by the example of the successes in human health research with human intestinal cell lines, such as Caco-2. The guidance has included culture systems, such as permeable supports dividing two culture chambers, and experimental endpoints. Among the endpoints were cell viability, cytoskeletal organization, and epithelial barrier function. Cell viability was monitored with the indicator dyes alamar Blue (AB) and 5'-carboxyfluoresscein diacetate acetoxymethyl ester (CFDA-AM). Cytoskeletal organization was visualized by immunocytochemical (ICC) staining and confocal microscopy. Epithelial barrier function was evaluated with trans epithelial electrical resistance (TEER) and Lucifer Yellow (LY) permeability measurments. These and other assays were used in four lines of investigation with RTgutGC. A general discovery from each line of research is highlighted below along with suggestions on how the discovery might be expanded further in the future.

1. RTgutGC cells can survive a 7 day nutritional deprivation but this generated major cellular changes that impacted restitution and barrier functions

The effects of nutritional deprivation at the cellular level generating functional changes to intestinal systems are not well known. The use of RTgutGC as a fish intestinal model in response to nutritional deprivation uncovered various negative effects. The cell line's barrier functions and restitution capabilities were almost completely lost under serum deprivation and further amino acid, vitamin, and sugar deprivation for 7 days. Cellular health was also severely impacted from nutritional deprivation conditions. Changes in cytoskeletal arrangement were also observed with increasing intensities of nutritional deprivations. Additionally, reductions in migratory abilities of the cells were observed. Nothethless, in the end most cells were able to survive a 7 day nutritional deprivation period.

Future studies can involve the role of energy metabolism during nutritional deprivation and cytoskeletal arrangement as an anaerobic metabolic state may favour the reduced expression cytoskeleton-related proteins (Modrego et al., 2012). Additionally, the cell cycle progression during nutritional deprivation is a favourable path of study. It is likely that

RTgutGC undergoes cell cycle arrest during starvation; however, the appearance of a large microtubule organizing centres (MTOCs) under starvation raises questions. Studies have shown that differentiated cells contain nc-MTOCs (Sanchez & Feldman, 2010). If cell cycle arrest occurs, it is possible that RTgutGC produces nc-MTOCs. Currently speculations, future studies focusing on cell cycle arrest and MTOCs could help understand the function of microtubules under nutritional deprivation.

2. Assays with RTgutGC showed that the phytochemical, naringenin, could be potentially be beneficial to fish intestinal health

The search for beneficial feed additives is a focus for many in the feed industry. Intestinal health is extremely important to consider when choosing new additives as the intestine is the first organ systems to come in contact with ingested food and has major roles in nutrient absorption. The use of RTgutGC monolayers as an *in vitro* intestinal model provided useful information on the flavanone naringenin, its effects on fish intestinal cell health *in vitro*, and its use as a potential feed additive. Naringenin was found to enhance barrier integrity of RTgutGC without any compromise in cellular health and migration rate at a concentration of 30 μM. Naringenin also caused changes in cytoskeletal arrangement. Ultimately naringenin could be introduced into feed and tested in fish to see if it is indeed beneficial.

How naringenin is exerting its effects on RTgutGC monolayers is poorly understood. Thus, future molecular studies on the cAMP and PKA pathway could be useful as studies suggest that naringenin exerts some effects on those pathways (Yang et al., 2008). Additionally, studying naringenin's antioxidant capabilities would further help promote naringenin as a beneficial fish feed additive.

3. RTgutGC restitution assays revealed how anti-nutritional factors (ANFs) could act to impair the intestine at the cellular level

The effects of ANFs on rainbow trout intestinal function are poorly understood but are important to know because of the shift to plant meals in fish feed. Wheat germ agglutinin (WGA) from wheat germ meal and the Bowman Birk inhibitor (BBI) from soybean meal were found for the first time to impede restitution. RTgutGC could serve as a preliminary screen of

plant meals and feed additives to eliminate some before *in vivo* testing, saving money, time, and fish.

4. Changes in nutrition and temperature impacted the cytoskeletal arrangement and migration of RTgutGC but inducing a thermotolerant state helped the cells recover from heat stress

The capacity of RTgutGC cells in L15/FBS to heal a wound whether through a combination of cell migration and proliferation or just cell migration (restitution) was heavily influenced by temperature. For the first time in any system, cells have been shown to acquire thermolerance for cell migration into a wound. Heat conditioning RTgutGC to a thermotolerant state prevented the inhibition of restitution by heat stress, whereas, a heat stress of 32 ^{o}C for 3 hours without any heat conditioning completely inhibited migration, and increased cell death.

Further work on the role of heat shock protein (HSPs) and thermotolerance in RTgutGC is needed. An interesting path for future studies would be to see if HSP90α plays any role in RTgutGC restitution. HSP90α is a key player in mammalian restitution, initiating cell sheet migration (Bhatia et al., 2016). Also, as restitution was a focus of this study, the effects of heat stress and thermotolerance on RTgutGC barrier functions, measured by TEER, LY permeability, and tight junction protein levels, are interesting future paths of study.

5. Naringenin exerts protective effects from heat stress on cell adherence, shape, and monolayer integrity but not cell viability or regulation of HSP70

Whether naringegin could exert any protective actions on the recovery of RTgutGC cells from a heat stress was investigated. Naringenin helped cells morphologically withstand from heat stress. Cells retained adherence and shape after a 1 ½ to 3 h heat stress period.

However, no trend of improvement was observed in cell viability as measured with AB or CFDA-AM. Additionally, naringenin did not alter the heat activation of caspase-3. Yet increasing naringenin did alter the organization of F-actin in during recovery. Fewer stress fibers were observed, whereas circumferential actin became more pronounced with increasing naringenin. Thus the reorganization F-actin to the cell periphery might have helped improved the recovery of cell shape after a heat stress. Naringenin failed to modulate HSP70 levels whether cells were recovering from a heat stress or not. Therefore, HSP70 was unlikely to be

mediating the improvement by naringenin in the recovery of cell shape from heat stress. An interesting path of study would be to look into the role of HSPs, other than HSP70, in naringenin's protective morphological actions. Cell-to-cell and cell-to-substrate connections play an important role in maintaining proper cell morphology and adherence; thus, studying TJ proteins such as claudins, occludin, and ZOs, AJ proteins such as cadherins, and cell adhesion proteins such as integrin under naringenin and heat stress might be an interesting future path. Additionally, studying barrier functions through TEER and LY assay could completment those studies. Lastly, understanding the role of circumferential actin and possible involvements in aiding recovery from heat stress is another promising research path.

LETTER OF COPYRIGHT PERMISSION

ELSEVIER LICENSE
TERMS AND CONDITIONS

Jul 05, 2017

This Agreement between Patrick Pumputis ("You") and Elsevier ("Elsevier") consists of your license details and the terms and conditions provided by Elsevier and Copyright Clearance Center.

License Number	4142590826250
License date	Jul 05, 2017
Licensed Content Publisher	Elsevier
Licensed Content Publication	Respiratory Physiology & Neurobiology
Licensed Content Title	Tight junctions, tight junction proteins and paracellular permeability across the gill epithelium of fishes: A review
Licensed Content Author	Helen Chasiotis,Dennis Kolosov,Phuong Bui,Scott P. Kelly
Licensed Content Date	Dec 1, 2012
Licensed Content Volume	184
Licensed Content Issue	3
Licensed Content Pages	13
Start Page	269
End Page	281
Type of Use	reuse in a thesis/dissertation
Portion	figures/tables/illustrations
Number of figures/tables/illustrations	2
Format	both print and electronic
Are you the author of this Elsevier article?	No
Will you be translating?	No
Order reference number	
Original figure numbers	Figure 2 and 3
Title of your thesis/dissertation	The use of a rainbow trout intestinal cell line, RTgutGC, to evaluate feed additives and environmental stressors (will possibly change)
Expected completion date	Jul 2017
Estimated size (number of pages)	150
Elsevier VAT number	GB 494 6272 12
Requestor Location	Patrick Pumputis 163 Victoria St S Kitchener, ON N2G 2B7 Canada Attn: Patrick Pumputis
Total	0.00 CAD

ELSEVIER LICENSE
TERMS AND CONDITIONS

Jul 05, 2017

This Agreement between Patrick Pumputis ("You") and Elsevier ("Elsevier") consists of your license details and the terms and conditions provided by Elsevier and Copyright Clearance Center.

License Number	4142600129664
License date	Jul 05, 2017
Licensed Content Publisher	Elsevier
Licensed Content Publication	Mechanisms of Development
Licensed Content Title	Intestinal growth and differentiation in zebrafish
Licensed Content Author	Kenneth N. Wallace,Shafinaz Akhter,Erin M. Smith,Kristin Lorent,Michael Pack
Licensed Content Date	Feb 1, 2005
Licensed Content Volume	122
Licensed Content Issue	2
Licensed Content Pages	17
Start Page	157
End Page	173
Type of Use	reuse in a thesis/dissertation
Intended publisher of new work	other
Portion	figures/tables/illustrations
Number of figures/tables/illustrations	1
Format	both print and electronic
Are you the author of this Elsevier article?	No
Will you be translating?	No
Order reference number	
Original figure numbers	Figure 2
Title of your thesis/dissertation	The use of a rainbow trout intestinal cell line, RTgutGC, to evaluate feed additives and environmental stressors (will possibly change)
Expected completion date	Jul 2017
Estimated size (number of pages)	150
Elsevier VAT number	GB 494 6272 12
Requestor Location	Patrick Pumputis 163 Victoria St S Kitchener, ON N2G 2B7 Canada Attn: Patrick Pumputis

Terms and Conditions

INTRODUCTION

1. The publisher for this copyrighted material is Elsevier. By clicking "accept" in connection with completing this licensing transaction, you agree that the following terms and conditions apply to this transaction (along with the Billing and Payment terms and conditions established by Copyright Clearance Center, Inc. ("CCC"), at the time that you opened your Rightslink account and that are available at any time at http://myaccount.copyright.com).

GENERAL TERMS

2. Elsevier hereby grants you permission to reproduce the aforementioned material subject to the terms and conditions indicated.
3. Acknowledgement: If any part of the material to be used (for example, figures) has appeared in our publication with credit or acknowledgement to another source, permission must also be sought from that source. If such permission is not obtained then that material may not be included in your publication/copies. Suitable acknowledgement to the source must be made, either as a footnote or in a reference list at the end of your publication, as follows:
"Reprinted from Publication title, Vol /edition number, Author(s), Title of article / title of chapter, Pages No., Copyright (Year), with permission from Elsevier [OR APPLICABLE SOCIETY COPYRIGHT OWNER]." Also Lancet special credit - "Reprinted from The Lancet, Vol. number, Author(s), Title of article, Pages No., Copyright (Year), with permission from Elsevier."
4. Reproduction of this material is confined to the purpose and/or media for which permission is hereby given.
5. Altering/Modifying Material: Not Permitted. However figures and illustrations may be altered/adapted minimally to serve your work. Any other abbreviations, additions, deletions and/or any other alterations shall be made only with prior written authorization of Elsevier Ltd. (Please contact Elsevier at permissions@elsevier.com). No modifications can be made to any Lancet figures/tables and they must be reproduced in full.
6. If the permission fee for the requested use of our material is waived in this instance, please be advised that your future requests for Elsevier materials may attract a fee.
7. Reservation of Rights: Publisher reserves all rights not specifically granted in the combination of (i) the license details provided by you and accepted in the course of this licensing transaction, (ii) these terms and conditions and (iii) CCC's Billing and Payment terms and conditions.
8. License Contingent Upon Payment: While you may exercise the rights licensed immediately upon issuance of the license at the end of the licensing process for the transaction, provided that you have disclosed complete and accurate details of your proposed use, no license is finally effective unless and until full payment is received from you (either by publisher or by CCC) as provided in CCC's Billing and Payment terms and conditions. If full payment is not received on a timely basis, then any license preliminarily granted shall be deemed automatically revoked and shall be void as if never granted. Further, in the event that you breach any of these terms and conditions or any of CCC's Billing and Payment terms and conditions, the license is automatically revoked and shall be void as if never granted. Use of materials as described in a revoked license, as well as any use of the materials beyond the scope of an unrevoked license, may constitute copyright infringement and publisher reserves the right to take any and all action to protect its copyright in the materials.
9. Warranties: Publisher makes no representations or warranties with respect to the licensed material.
10. Indemnity: You hereby indemnify and agree to hold harmless publisher and CCC, and their respective officers, directors, employees and agents, from and against any and all claims arising out of your use of the licensed material other than as specifically authorized pursuant to this license.

11. No Transfer of License: This license is personal to you and may not be sublicensed, assigned, or transferred by you to any other person without publisher's written permission.
12. No Amendment Except in Writing: This license may not be amended except in a writing signed by both parties (or, in the case of publisher, by CCC on publisher's behalf).
13. Objection to Contrary Terms: Publisher hereby objects to any terms contained in any purchase order, acknowledgment, check endorsement or other writing prepared by you, which terms are inconsistent with these terms and conditions or CCC's Billing and Payment terms and conditions. These terms and conditions, together with CCC's Billing and Payment terms and conditions (which are incorporated herein), comprise the entire agreement between you and publisher (and CCC) concerning this licensing transaction. In the event of any conflict between your obligations established by these terms and conditions and those established by CCC's Billing and Payment terms and conditions, these terms and conditions shall control.
14. Revocation: Elsevier or Copyright Clearance Center may deny the permissions described in this License at their sole discretion, for any reason or no reason, with a full refund payable to you. Notice of such denial will be made using the contact information provided by you. Failure to receive such notice will not alter or invalidate the denial. In no event will Elsevier or Copyright Clearance Center be responsible or liable for any costs, expenses or damage incurred by you as a result of a denial of your permission request, other than a refund of the amount(s) paid by you to Elsevier and/or Copyright Clearance Center for denied permissions.

LIMITED LICENSE

The following terms and conditions apply only to specific license types:
15. **Translation**: This permission is granted for non-exclusive world **English** rights only unless your license was granted for translation rights. If you licensed translation rights you may only translate this content into the languages you requested. A professional translator must perform all translations and reproduce the content word for word preserving the integrity of the article.
16. **Posting licensed content on any Website**: The following terms and conditions apply as follows: Licensing material from an Elsevier journal: All content posted to the web site must maintain the copyright information line on the bottom of each image; A hyper-text must be included to the Homepage of the journal from which you are licensing at http://www.sciencedirect.com/science/journal/xxxxx or the Elsevier homepage for books at http://www.elsevier.com; Central Storage: This license does not include permission for a scanned version of the material to be stored in a central repository such as that provided by Heron/XanEdu.
Licensing material from an Elsevier book: A hyper-text link must be included to the Elsevier homepage at http://www.elsevier.com . All content posted to the web site must maintain the copyright information line on the bottom of each image.

Posting licensed content on Electronic reserve: In addition to the above the following clauses are applicable: The web site must be password-protected and made available only to bona fide students registered on a relevant course. This permission is granted for 1 year only. You may obtain a new license for future website posting.
17. **For journal authors:** the following clauses are applicable in addition to the above:
Preprints:
A preprint is an author's own write-up of research results and analysis, it has not been peer-reviewed, nor has it had any other value added to it by a publisher (such as formatting, copyright, technical enhancement etc.).
Authors can share their preprints anywhere at any time. Preprints should not be added to or enhanced in any way in order to appear more like, or to substitute for, the final versions of articles however authors can update their preprints on arXiv or RePEc with their Accepted Author Manuscript (see below).

If accepted for publication, we encourage authors to link from the preprint to their formal publication via its DOI. Millions of researchers have access to the formal publications on ScienceDirect, and so links will help users to find, access, cite and use the best available version. Please note that Cell Press, The Lancet and some society-owned have different preprint policies. Information on these policies is available on the journal homepage.
Accepted Author Manuscripts: An accepted author manuscript is the manuscript of an article that has been accepted for publication and which typically includes author-incorporated changes suggested during submission, peer review and editor-author communications.
Authors can share their accepted author manuscript:

- immediately
  - via their non-commercial person homepage or blog
  - by updating a preprint in arXiv or RePEc with the accepted manuscript
  - via their research institute or institutional repository for internal institutional uses or as part of an invitation-only research collaboration work-group
  - directly by providing copies to their students or to research collaborators for their personal use
  - for private scholarly sharing as part of an invitation-only work group on commercial sites with which Elsevier has an agreement
- After the embargo period
  - via non-commercial hosting platforms such as their institutional repository
  - via commercial sites with which Elsevier has an agreement

In all cases accepted manuscripts should:

- link to the formal publication via its DOI
- bear a CC-BY-NC-ND license - this is easy to do
- if aggregated with other manuscripts, for example in a repository or other site, be shared in alignment with our hosting policy not be added to or enhanced in any way to appear more like, or to substitute for, the published journal article.

Published journal article (JPA): A published journal article (PJA) is the definitive final record of published research that appears or will appear in the journal and embodies all value-adding publishing activities including peer review co-ordination, copy-editing, formatting, (if relevant) pagination and online enrichment.
Policies for sharing publishing journal articles differ for subscription and gold open access articles:
Subscription Articles: If you are an author, please share a link to your article rather than the full-text. Millions of researchers have access to the formal publications on ScienceDirect, and so links will help your users to find, access, cite, and use the best available version.
Theses and dissertations which contain embedded PJAs as part of the formal submission can be posted publicly by the awarding institution with DOI links back to the formal publications on ScienceDirect.
If you are affiliated with a library that subscribes to ScienceDirect you have additional private sharing rights for others' research accessed under that agreement. This includes use for classroom teaching and internal training at the institution (including use in course packs and courseware programs), and inclusion of the article for grant funding purposes.
Gold Open Access Articles: May be shared according to the author-selected end-user license and should contain a CrossMark logo, the end user license, and a DOI link to the formal publication on ScienceDirect.
Please refer to Elsevier's posting policy for further information.
18. **For book authors** the following clauses are applicable in addition to the above:
Authors are permitted to place a brief summary of their work online only. You are not

allowed to download and post the published electronic version of your chapter, nor may you scan the printed edition to create an electronic version. **Posting to a repository:** Authors are permitted to post a summary of their chapter only in their institution's repository.
19. **Thesis/Dissertation**: If your license is for use in a thesis/dissertation your thesis may be submitted to your institution in either print or electronic form. Should your thesis be published commercially, please reapply for permission. These requirements include permission for the Library and Archives of Canada to supply single copies, on demand, of the complete thesis and include permission for Proquest/UMI to supply single copies, on demand, of the complete thesis. Should your thesis be published commercially, please reapply for permission. Theses and dissertations which contain embedded PJAs as part of the formal submission can be posted publicly by the awarding institution with DOI links back to the formal publications on ScienceDirect.

Elsevier Open Access Terms and Conditions
You can publish open access with Elsevier in hundreds of open access journals or in nearly 2000 established subscription journals that support open access publishing. Permitted third party re-use of these open access articles is defined by the author's choice of Creative Commons user license. See our open access license policy for more information.
Terms & Conditions applicable to all Open Access articles published with Elsevier:
Any reuse of the article must not represent the author as endorsing the adaptation of the article nor should the article be modified in such a way as to damage the author's honour or reputation. If any changes have been made, such changes must be clearly indicated.
The author(s) must be appropriately credited and we ask that you include the end user license and a DOI link to the formal publication on ScienceDirect.
If any part of the material to be used (for example, figures) has appeared in our publication with credit or acknowledgement to another source it is the responsibility of the user to ensure their reuse complies with the terms and conditions determined by the rights holder.
Additional Terms & Conditions applicable to each Creative Commons user license:
CC BY: The CC-BY license allows users to copy, to create extracts, abstracts and new works from the Article, to alter and revise the Article and to make commercial use of the Article (including reuse and/or resale of the Article by commercial entities), provided the user gives appropriate credit (with a link to the formal publication through the relevant DOI), provides a link to the license, indicates if changes were made and the licensor is not represented as endorsing the use made of the work. The full details of the license are available at http://creativecommons.org/licenses/by/4.0.
CC BY NC SA: The CC BY-NC-SA license allows users to copy, to create extracts, abstracts and new works from the Article, to alter and revise the Article, provided this is not done for commercial purposes, and that the user gives appropriate credit (with a link to the formal publication through the relevant DOI), provides a link to the license, indicates if changes were made and the licensor is not represented as endorsing the use made of the work. Further, any new works must be made available on the same conditions. The full details of the license are available at http://creativecommons.org/licenses/by-nc-sa/4.0.
CC BY NC ND: The CC BY-NC-ND license allows users to copy and distribute the Article, provided this is not done for commercial purposes and further does not permit distribution of the Article if it is changed or edited in any way, and provided the user gives appropriate credit (with a link to the formal publication through the relevant DOI), provides a link to the license, and that the licensor is not represented as endorsing the use made of the work. The full details of the license are available at http://creativecommons.org/licenses/by-nc-nd/4.0.
Any commercial reuse of Open Access articles published with a CC BY NC SA or CC BY NC ND license requires permission from Elsevier and will be subject to a fee.
Commercial reuse includes:

- Associating advertising with the full text of the Article
- Charging fees for document delivery or access

- Article aggregation
- Systematic distribution via e-mail lists or share buttons

Posting or linking by commercial companies for use by customers of those companies.

20. **Other Conditions**:

v1.9

Questions? customercare@copyright.com or +1-855-239-3415 (toll free in the US) or +1-978-646-2777.

REFERENCES

Chapter 1 References

Agle, K.A., Vongsa, R.A. & Dwinell, M.B. (2010) Calcium mobilization triggered by the chemokine CXCl12 regulates migration in wounded intestinal monolayers. *Journal of Biological Chemistry*, **285**, 16066-16075.

Akhmanova, A. & Steinmetz, M.O. (2015) Control of microtubule organization and dynamics: two ends in the limelight. *Nature Reviews*, **16**, 711-726.

Albrecht-Buehler, G. (1976) Filopodia of spreading 3T3 cells: Do they have a substrate exploring function? *Journal of Cell Biology*, **69**, 275-286.

Albrecht-Buehler, G., Lancaster, R.M. (1976) A quantitative description of the extension and retraction of surface protrusions in spreading 3T3 mouse fibroblasts. *Journal of Cell Biology*, **711**, 370-382.

Alvarez, A., Garcia Garcia, B., Garrido, M.D. & Hernandez, M.D. (2008) The influence of starvation time prior to slaughter on the quality of commercial-sized gilthead seabream (*Sparaus aurata*) during ice storage. *Aquaculture*, **284**, 106-114.

Amasheh, M., Andres, S., Amasheh, S., Fromm, M. & Schulzke, J.D. (2009) Barrier effects of nutritional factors. *Annals of the New York Academy of Science*, **1165**, 267-273.

Amasheh, M., Schlichter, S., Amasheh, S., Mankertz, J., Zeitz, M., Fromm, M. & Schulzke, J.D. (2008) Quercetin enhances epithelial barrier function and increases claudin-4 expression in Caco-2 cells. *Journal of Nutrition*, **138**, 1067-1073.

Arima, Y. & Iwata, H. (2015) Preferential adsorption of cell adhesive proteins from complex media on self-assembled monolayers and its effect on subsequent cell adhesion. *Acta Biomaterialia*, **26**, 72-81.

Arnal, M.E. & Lalles, J.P. (2016) Gut epithelial heat-shock proteins and their modulation by diet and the microbiota. *Nutrition Reviews*, **74**, 181-197.

Ashley, P.J. (2007) Fish welfare: current issues in aquaculture. *Applied Animal Behaviour Science*, **104**, 195-235.

Baird, C.H., Niederlechner, S., Beck, R., Kallweit, A.R. & Wischmeyer, P.E. (2013) L-Threonine induces heat shock protein expression and decreases apoptosis in heat-stressed intestinal epithelial cells. *Nutrition*, **29**, 1404-1411.

Basson, M.D., Turowski, G. & Emenaker, N.J. (1996) Regulation of human (Caco-2) intestinal epithelial cell differentiation by extracellular matrix proteins. *Experimental Cell Research*, **225**, 301-315.

Beaverfjord, G. & Krogdahl, A. (1996) Development and regression of soybean meal induced enteritis in Atlantic salmon, *Salmo salar* L, distal intestine: a comparison with the intestines of fasted fish. *Journal of Fish Diseases*, **19**, 375-387.

Bermejo-Poza, R., De La Fuente, J., Perez, C., de Chavarri, E.G., Diaz, M.T., Torrent, F. & Villarroel, M. (2017) Determination of optimal degree days of fasting before slaughter in rainbow trout (*Oncorhynchus mykiss*). *Aquaculture*, **473**, 272-277.

Bhatia, A., O'Brien, K., Chan, M., Woodley, D.T. & Li, W. (2016) Keratinocyte-secreted heat shock protein-90alpha: Leading wound reepithelialisation and closure. *Advances in Wound Care*, **5**, 176-184.

Blanchoin, L., Boujemaa-Paterski, R., Sykes, C. & Plastino, J. (2014) Actin dynamics, architecture, and mechanics in cell motility. *Physiological Reviews*, **94**, 235-263.

Bols, N.C., Dayeh, V.R., Lee, L.E.J. & Schirmer, K. (2005) Use of fish cell lines in toxicology of fish. In: Biochemistry and Molecular Biology of Fishes-Environmental Toxicology. Vol. 6. Edited by T.W. Moon and T. P. Mommsen. Amsterdam: Elsevier Science. pp. 43-84.

Brander, K.M. (2007) Global fish production and climate change. *Proceedings of the National Academy of Science U.S.A.*, **104**, 19709-19714.

Bryson, S.P., Joyce, E.M., Martell, D.J., Lee, L.E.J., Holt, S.E., Kales, S.C., Fujiki, K., Dixon B. & Bols, N.C. (2006) Development of a cell line, HEW, from embryos of haddock (*Melanogrammus aeglefinius*) and defining its capacity to tolerate environmental extremes. *Marine Biotechnology*, **8**, 641-653.

Bu, X.D., Li, N., Tian, X.Q., & Huang, P.L. (2011) Caco-2 and LS174T cell lines provide different models for studying mucin expression in colon cancer. *Tissue Cell*, **43**, 201-206.

Burrells, C., Williams, P.D., Southgate, P.J. & Crampton, V.O. (1999) Immunological, physiological and pathological responses of rainbow trout (*Oncorhynchus mykiss*) to increasing dietary concentrations of soybean proteins. *Veterinary Immunology and Immunopathology*, **72**, 277-288.

Buttle, L.G., Burrells, A.C., Good, J.E., Williams, P.D., Southgate, P.J. & Burrells, C. (2001) The binding of soybean agglutinin (SBA) to the intestinal epithelium of Atlantic salmon *Salmo salar* and Rainbow trout, *Oncorhynchus mykiss*, fed high levels of soybean meal. *Veterinary Immunology and Immunopathology*, **80**, 237-244.

Canani, R.B., Costanzo, M.D., Leone, L., Pedata, M., Meli, R. & Calignano, A. (2011) Potential beneficial effects of butyrate in intestinal and extraintestinal diseases. *World Journal of Gastroenterology*, **17**, 1519-1528.

Chasiotis, H., Kolosov, D., Bui, P. & Kelly, S.P. (2012) Tight junctions, tight junction proteins and paracellular permeability across the gill epithelium of fishes: A review. *Respiratory Physiology & Neurobiology*, **184**, 269-281.

Chen, B., Ji, B. & Gao, H. (2015) Modeling active mechanosensing in cell-matrix interactions. *Annual Review of Biophysics*, **44**, 1-32.

Chow, A. & Zhang, R. (1998) Glutamine reduces heat shock-induced cell death in rat intestinal epithelial cells. *Journal of Nutrition*, **128**, 1296-1301.

Clelland, E.S., Bui, P., Bagherie-Lachidan, M. & Kelly, S.P. (2010) Spatial and salinity-induced alterations in claudin-3 isoform mRNA along the gastrointestinal tract of the pufferfish *Tetraodon nigroviridis*. *Comparative Biochemistry and Physiology Part A: Molecular & Integrative Physiology*, **155**, 154-163.

Coss, R.A. & Linnemans, W.A.M. (1996) The effects of hyperthermia on the cytoskeleton: a review. *International Journal of Hyperthermia*, **12**, 173-196.

Dokladny, K., Zuhl, M.N. & Moseley, P.L. (2016) Intestinal epithelial barrier function and tight junction proteins with heat and exercise. *Journal of Applied Physiology*, 120, 692-701.

Eelen, G., Cruys, B., Welti, J., De Bock, K. & Carmeliet, P. (2013) Control of vessel sprouting by genetic and metabolic determinants. *Trends in Endocrinology Metabolism*, **24**, 589-596.

Esumi, H., Izuishi, K., Kato, K., Hashimoto, K., Kurashima, Y., Kishimoto, A., Ogura, T. & Ozawa, T. (2002) Hypoxia and nitric oxide treatment confer tolerance to glucose starvation in a 5'-AMP-activated protein kinase-dependent manner. *Journal of Biological Chemistry*, **277**, 32791-32798.

Evans, M.E., Jones, D.P. & Ziegler, T.R. (2005) Glutamine inhibits cytokine-induced apoptosis in human colonic epithelial cells via the pyrimidine pathway. *American Journal of Physiology – Gastrointestinal and Liver Physiology*, **289**, G388-G396.

Exton, M.S. (1997) Infection-induced anorexia: active host defence strategy. *Appetite*, **29**, 369-383.

FAO, 2016. The state of world fisheries and aquaculture 2016. Contributing to food security and nutrition for all. Rome, 200 pp.

Ferraris, R.P. & Carey, H.V. (2000) Intestinal transport during fasting and malnutrition. *Annual Reviews of Nutrition*, **20**, 195-219.

FOC, 2012. Aquaculture in Canada 2012. A report on aquaculture sustainability. 34 pp.

Francis, G., Makkar, H.P.S. & Becker, K. (2001) Antinutritional factors present in plant-derived alternate fish feed ingredients and their effects in fish. *Aquaculture*, **199**, 197-227.

Geppert, M., Sigg, L. & Schirmer, K. (2016) A novel two-compartment barrier model for investigating nanoparticle transport in fish intestinal epithelial cells. *Environmental Science: Nano*, **3**, 388-395.

Glencross, B. & Rutherford, N. (2010) Dietary strategies to improve the growth and feed utilization of barramundi, *Lates calcarifer* under high water temperature conditions. *Aquaculture Nutrition*, **16**, 343-350.

González-Mariscal, L., Betanzos, A., Nava, P. & Jaramillo, B.E. (2003) Tight junction proteins. *Progress in Biophysics & Molecular Biology*, **81**, 1-44.

Green, M., Niewold, T.A. (2011) Optimizing culture conditions of a porcine epithelial cell line IPEC-J2 through a histological and physiological characterization. *Cytotech*, **63**, 415-423.

Hamiel, C.R., Pinto, S., Hau, H. & Wischmeyer, P.E. (2009) Glutamine enhances heat shock protein 70 expression via increased hexosamine biosynthetic pathway activity. *American Journal of Physiology - Cell Physiology*, **297**, C1509-C1519.

Hansen, R.K., Oesterreich, S., Lemieux, P., Sarge, K.D. & Fuqua, S.A. (1997) Quercetin inhibits heat shock protein induction but not heat shock factor DNA-binding in human breast carcinoma cells. *Biochemical and Biophysical Research Communications*, **239**, 851-856.

Hartsock, A. & Nelson, W.J. (2008) Adherens and tight junctions: Structure, function and connections to the actin cytoskeleton. *Biochimica et Biophysica Acta*, **1778**, 660-669.

Heath, J.P. & Dunn, G.A. (1978) Cell to substratum contacts of chick fibroblasts and their relation to the microfilament system. A correlated interference-reflexion and high-voltage electron-microscope study. *Journal of Cell Science*, **29**, 197-212.

Hermansen, O. & Heen, K. (2012) Norwegian salmonid farming and global warming: socioeconomic impacts. *Aquaculture Economics & Management*, **16**, 202-221.

Hess, J.R. & Greenberg, N.A. (2012) The role of nucleotides in the immune and gastrointestinal systems: Potential clinical applications. *Nutrition in Clinical Practice*, **27**, 281-294.

Hilgers, A.R., Conradi, R.A. & Burton, P.S. (1990) Caco-2 cell monolayers as a model for drug transport across the intestinal mucosa. *Pharmaceutical Research*, **7**, 902-910.

Hotulainen, P. & Lappalainen, P. (2006) Stress fibers are generated by two distinct actin assembly mechanisms in motile cells. *Journal of Cell Biology*, **173**, 383-394.

Iizuka, M. & Konno, S. (2011) Wound healing of the intestinal epithelial cells. *World Journal of Gastroenterology*, **17**, 2161-2171.

Izuishi, K., Kato, K., Ogura, T., Kinoshita, T. & Esumi, H. (2000) Remarkable tolerance of tumor cells to nutrient deprivation: possible new biochemical target for cancer therapy. *Cancer Research*, **60**, 6201-6207.

Jobling, M. (2015) Fish nutrition research: past, present and future. *Aquaculture International*, **24**, 767-786.

Jolly, C. & Morimoto, R.I. (2000) Role of the heat shock response and molecular chaperones in oncogenesis and cell death. *Journal of the National Cancer Institute*, **92**, 1564-1572.

Kawano, A., Haiduk, C., Schirmer, K., Hanner, R., Lee, L.E.J, Dixon, B. & Bols, N.C. (2011) Development of a rainbow trout intestinal epithelial cell line and its response to lipopolysaccharide. *Aquaculture Nutrition*, **17**, e241-e252.

Khurana, S., Tomar, A., George, S.P., Wang, Y., Siddiqui, M.R., Guo, H., Tiyi, G. & Mathew, S. (2008) Autoaxin and lysophosphatidic acid stimulate intestinal epithelial cell motility by redistribution of the actin modifying protein villin to the developing lamellipodia. *Experimental Cell Research*, **314**, 530-542.

Kim, S.E., Park, H.J., Jeong, H.K., Kim, M.J., Kim, M., Bae, O.N. & Baek, S.H. (2015) Autophagy sustains the survival of human pancreatic cancer PANC-1 cells under extreme nutrient deprivation conditions. *Biochemical and Biophysical Research Communication*, **463**, 205-210.

Kolosov, D., Bui, P., Chasiotis, H. & Kelly, S.P. (2013) Claudins in teleost fishes. *Tissue Barriers*, **1**, e25391.

Krause, M. & Gautreau, A. (2014) Steering cell migration: lamellipodium dynamics and the regulation of directional persistence. *Nature Reviews: Molecular Cell Biology*, **15**, 577-590.

Krogdahl, A. & Blake-McKellep, A.M. (2005) Fasting and refeeding cause rapid changes in intestinal tissue mass and digestive enzyme capacities of Atlantic salmon (*Salmo salar* L.). *Comparative Biochemistry and Physiology - Part A: Molecular & Integrative Physiology*, **141**, 450-460.

Lange, K. (2010) Fundamental role of microvilli in the main functions of differentiated cells: outline of an universal regulating and signaling system at the cell periphery. *Journal of Cellular Physiology*, **226**, 896-927.

Larson, S.D., Li, J., Chung, D.H. & Evers, B.M. (2007) Molecular mechanisms contributing to glutamine-mediated intestinal cell survival. *American Journal of Physiology – Gastrointestinal and Liver Physiology*, **293**, G1262-G1271.

Lei, N.Y., Jabaji, Z., Wang, J., Joshi, V.S., Brinkley, G.J., Khalil, H., Wang, F., Jaroszewicz, A., Pellegrini, M., Li, L., Lewis, M., Stelzner, M., Dunn, J.C.Y. & Martín, M.G. (2014). Intestinal subepithelial myofibroblasts support the growth of intestinal epithelial stem cells. *PLoS ONE*, **9**, e84651.

Leibovitz, A. (1963) The growth and maintenance of tissue-cell cultures in free gas exchange with the atmosphere. *American Journal of Hygiene*, **78**, 173–180.

Li, N., Lewis, P., Samuelson, D., Liboni, K. & Neu, J. (2004) Glutamine regulates Caco-2 cell tight junction proteins. *American Journal of Physiology – Gastrointestinal and Liver Physiology*, **287**, G726-G733.

Lignot, J.H. & LeMaho, Y. (2012) A history of modern research into fasting, starvation, and inanition. Chapter 2. Comparative Physiology of Fasting, Starvation, and Food Limitation (ed MD McCue).

Lindquist, S. & Craig, E.A. (1988) The heat shock proteins. *Annual Review of Genetics*, **22**, 631-677.

Lines, J.A. & Spence, J. (2012) Safeguarding the welfare of fish at harvest. *Fish Physiology and Biochemistry*, **38**, 153-162.

Liu, H., Dicksved, J., Lundh, T. & Lindberg, E. (2014) Heat shock proteins: Intestinal gatekeepers that are influenced by dietary components and the gut microbiota. *Pathogens*, **3**, 187-210.

Liu, J., Mai, K., Xu, W., Zhang, Y., Zhou, H. & Ai, Q. (2015) Effects of dietary glutamine on survival, growth performance, activities of digestive enzyme, antioxidant status and hypoxia stress resistance of half-smooth tongue sole (*Cynoglossus semilaevis* Gunther) post larvae. *Aquaculture*, **446**, 48-56.

Lopez-Luna, J., Torrent, F. & Villarroel, M. (2014) Fasting up to 34 °C days in rainbow trout, *Oncorhynchus mykiss*, has little effect on flesh quality. *Aquaculture*, **420-421**, 63-70.

Lopez-Luna, J., Vasquez, L., Torrent, F. & Villarroel, M. (2013) Short-term fasting and welfare prior to slaughter in rainbow trout, *Oncorhynchus mykiss*. *Aquaculture*, **400-401**, 142-147.

Mattila, P.K. & Lappalainen, P. (2008) Filopodia: molecular architecture and cellular functions. *Nature*, **9**, 446-454.

Maninova, M., Caslasvsky, J. & Vomastek, T. (2017) The assembly and function of perinuclear actin cap in migrating cells. *Protoplasma*, **254**, 1207-1218.

Mayer, M.P. & Bukau, B. (2005) Hsp70 chaperones: cellular functions and molecular mechanism. *Cell and Molecular Life Sciences*, **62**, 670-684.

Mazumder, S.K., De, M., Mazlan, A.G., Zaidi, C., Rahim, S.M. & Simon, K.D. (2015) Impact of global climate change on fish growth, digestion and physiological status: developing a hypothesis for cause and effect relationships. *Journal of Water and Climate Change*, doi: 10.2166/wcc.2014.146.

McCue, M.D. (2010) Starvation physiology: reviewing the different strategies animals use to survive a common challenge. *Comparative Biochemistry and Physiology - Part A: Molecular and Integrative Physiology*, **156**, 1-18.

Metcalfe, N.B. & Thorpe, J.E. (1992) Anorexia and defended energy levels in over-wintering juvenile salmon. *Journal of Animal Ecology*, **61**, 175-181.

Miller, T.A., Smith, G.S., Banan, A. & Kokoska, E.R. (2000) Cytoskeleton as a target for injury in damaged intestinal epithelium. *Microscopy Research and Technique*, **51**, 149-155.

Minghetti, M., Drieschner, C., Bramaz, N., Schug, H. & Schirmer, K. (2017) A fish intestinal epithelial barrier model established from the rainbow trout (*Oncorhynchus mykiss*) cell line, RTgutGC. *Cell Biology and Toxicology*, doi: 10.1007/s10565-017-9385-x.

Mitchell, D.M. & Ball, J.M. (2004) Characterization of a spontaneously polarizing HT-29 cell line, HT-29/el.f8. *In Vitro Cellular & Developmental Biology*, **40**, 297-302.

Modis, K., Gero, D., Nagy, N., Szoleczky, P., Toth, Z.D. & Szabo, C. (2009) Cytoprotective effects of adenosine and inosine in an *in vitro* model of acute tubular necrosis. *British Journal of Pharmacology*, **158**, 1565-1578.

Noda, S., Tanabe, S. & Suzuki, T. (2013) Naringenin enhances intestinal barrier function through the expression and cytoskeletal association of tight junction proteins in Caco-2 cells. *Molecular Nutrition & Food Research*, **57**, 2019-2028.

Nordrum, S., Bakke-Mckellep, A.M., Krogdahl, A. & Buddington, R.K. (2000) Effects of soybean meal and salinity on the intestinal transport of nutrients in Atlantic salmon (*Salmo salar* L.) and rainbow trout (*Oncorhynchus mykiss*). *Comparative Biochemistry and Physiology - Part B: Biochemistry and Molecular Biology*, **125**, 317-335.

Palermo, F.A., Cardinaletti, G., Cocci, P., Tibaldi, E., Polzonetti-Magni, A. & Mosconi, G. (2013) Effects of dietary nucleotides on acute stress response and cannabinoid receptor 1 mRNAs in sole, *Solea solea*. *Comparative Biochemistry and Physiology*, **164**, 477-482.

Palmeri, G., Turchini, G.M., Marriott, P.J., Morrison, P. & De Silva, S.S. (2009) Biometric, nutritional and sensory characteristic modifications in farmed Murray cod (*Maccullochella peelii peelii*) during the purging process. *Aquaculture*, **287**, 354-360.

Pearce, S.C., Mani, V., Boddicker, R.L., Johnson, J.S., Weber, T.E., Ross, J.W., Rhoads, R.P., Baumarg, L.H. & Gabler, N.K. (2013) Heat stress reduces intestinal epithelial barrier integrity and favors intestinal glucose transport in growing pigs. *PLOS ONE*, **8**, e70215.

Pellegrin, S. & Mellor, H. (2007) Actin stress fibres. *Journal of Cell Science*, **120**, 3491-3499.

Peterson, L.W. & Artis, D. (2014) Intestinal epithelial cells: regulators of barrier function and immune homeostasis. *Nature Reviews Immunology*, **14**, 141-153.

Pirhonen, J., Schreck, C.B., Reno, P.W. & Ogut, H. (2003) Effect of fasting on feed intake, growth and mortality Chinook salmon, *Onchorhynchus tshawytscha*, during an induced *Aeromonas salmonicida* epizootic. *Aquaculture*, **216**, 31-38.

Pohlenz, C., Buentello, A., Bakke, A.M. & Gatlin III, D.M. (2012) Free dietary glutamine improves intestinal morphology and increases enterocyte migration rates, but has limited effects on plasma amino acid profile and growth performance of channel catfish *Ictalurus punctatus*. *Aquaculture*, **370-371**, 32-39.

Pottinger, T.G., Rand-Weaver, M. & Sumpter, J.P. (2003) Overwinter fasting and re-feeding in rainbow trout: plasma growth hormone and cortisol levels in relation to energy mobilization. *Comparative Biochemistry and Physiology - Part B: Biochemistry and Molecular Biology*, **136**, 403-417.

Powell, D.W., Mifflin, R.C., Valentich, J.D., Crowe, S.E., Saada, J.I. & West, A.B. (1999) Myofibroblast. II. Intestinal subepithelial myofibroblasts. *American Journal of Physiology*, **277**, C183-C201.

Raffaghello, L., Lee, C., Safdie, F.M., Wei, M., Madia, F., Bianchi, G. & Longo, V.D. (2008) Starvation-dependent differential stress resistance protects normal but not cancer cells against high-dose chemotherapy. *Proceedings of the National Academy of Sciences of the United States of America*, **105**, 8215-8220.

Rajasekaran, S.A., Beyenbach, K.W & Rajasekaran, A.K. (2008) Interactions of tight junctions with membrane channels and transporters. *Biochimica et Biophysica Acta*, **1778**, 757-769.

Ramsay, J.M., Feist, G.W., Schreck, C.B., Couture, R., O'Neil, J. & Noakes, D.L.G. (2009) The effect of food deprivation on the cortisol response to crowding in juvenile steelhead. *North American Journal of Aquaculture*, **71**, 130-133.

Rathbone, M.P., Christjanson, L., Deforge, S., Beluca, B., Gysbers, J.W., Hindley, S., Jovetich, M., Middlemiss, P. & Takhal, S. (1992) Extracellular purine nucleosides stimulate cell division and morphogenesis: pathological and physiological implications. *Medical Hypotheses*, **37**, 232-240.

Regost, C., Arzel, J., Cardinal, M., Laroche, M. & Kaushik, S.J. (2001) Fat deposition and flesh quality in seawater reared, triploid brown trout (*Salmo trutta*) as affected by dietary fat levels and starvation. *Aquaculture*, **193**, 325-345.

Ren, H., Musch, M.W., Kojima, K., Boone, D., Ma, A. & Chang, E.B. (2001) Short-chain fatty acids induce intestinal epithelial heat shock protein 25 expression in rats and in IEC 18 cells. *Gastroenterology*, **121**, 631-639.

Richter, K., Haslbeck, M. & Buchner, J. (2010) The heat shock response: Life on the verge of death. *Molecular Cell*, **40**, 253-266.

Roche, H.M., Terres, A.M., Black, I.B., Gibney, M.J. & Kelleher, D. (2001) Fatty acids and epithelial permeability: effect of conjugated linoleic acid in Caco-2 cells. *Gut*, **48**, 797-802.

Rodriguez-Serrano, F., Marchal, J.A., Rios, A., Martinez-Amat, A., Boulaiz, H., Prados, J., Peran, M., Caba, O., Carrillo, E., Hita, F. & Aranega, A. (2007) Exogenous nucleosides modulate proliferation of rat intestine epithelial IEC-6 cells. *Journal of Nutrition*, **137**, 879-884.

Rosella, O., Sinclair, A. & Gibson, P.R. (2000) Polyunsaturated fatty acids reduce non-receptor-mediated transcellular permeation of protein across a model of intestinal epithelium in vitro. *Journal of Gastroenterology and Hepatology*, **15**, 626-631.

Ross, J.A. & Kasum, C.M. (2002) Dietary flavonoids: bioavailability, metabolic effects, and safety. *Annual Review of Nutrition*, **22**, 19-34.

Rozza, A.L., Hiruma-Lima, C.A., Tanimoto, A. & Pellizon, C.H. (2012) Morphological and pharmacological investigations in the epicatechin gastroprotective effect. *Evidence-Based Complementary and Alternative Medicine*, **2012**, 708156.

Sanchez, A.D. & Feldman, J.L. (2016) Microtubule-organizing centers: from the centrosome to non-centrosomal sites. *Current Opinion in Cell Biology*, **44,** 93-101.

Sato, K., Tsuchichara, K., Fuji, S., Sugiyama, M., Goya, T., Atomi, Y., Ueno, T., Ochiai, A. & Esumi, H. (2007) Autophagy is activated in colorectal cancer cells and contributes to the tolerance to nutrient deprivation. *Cancer Research,* **67**, 9677-9684.

Sato, N., Nakano, T., Kawakami, H. & Idota, T. (1999) In vitro and in vivo effects of exogenous nucleotides on the proliferation and maturation of intestinal epithelial cells. *Journal of Nutritional Science and Vitaminology,* **45**, 107-118.

Schirmer, K., Chan, A.G.J., Greenberg, B.M., Dixon, D.G. & Bols, N.C. (1997) Methodology for demonstrating and measuring the photocytotoxicity of fluoranthene to fish cells in culture. *Toxicology In Vitro*, **11**, 107-119.

Schneider, G. & Burridge, K. (1994) Formation of focal adhesions by osteoblasts adhering to different substrata. *Experimental Cell Research*, **214**, 264-269.

Shimohara, S., Murakami, T., Morikawa, M., Matsuo, J., Nagayama, S., Shuto, T., Suico, M.A., Okiyoneda, T., Yamatsu, I., Mizushima, T., Shimasaki, T. & Kai, H. (2005) Vitamins K1 and K2 potentiate hyperthermia by down-regulating Hsp72 expression in vitro and in vivo. *International Journal of Oncology*, **27**, 1527-1533.

Small, J.V. & Rottner, K. (2010) Elementary cellular processes driven by actin assembly: lamellipodia and filopodia. In Actin-based motility (ed MF Carlier) Chapter 1 pp 3-33.

Sokolova, A.V., Kreplak, L., Wedig, T., Mucke, N., Svergun, D.I., Herrmann, H., Aebi, U. & Strelkov, S.V. (2006) Monitoring intermediate filament assembly by small-angle x-ray scattering reveals the molecular architecture of assembly intermediates. *Proceedings of the National Academy of Sciences of the United States of America*, **31**, 16206-16211.

St-Pierre, N.R., Cobanov, B. & Schnitkey, G. (2003) Economic losses from heat stress by US livestock industries. *Journal of Dairy Science*, **86**, E52-E77.

Sturm, A., & Dignass, A.U. (2008) Epithelial restitution and wound healing in inflammatory bowel disease. *World Journal of Gastroenterology*, **14**, 348–353.

Surco-Laos, F., Duenas, M., Gonzalez-Manzano, S., Cabello, J., Santos-Buelga, C. & Gonzalez-Paramas, A.M. (2012) Influence of catechins and their methylated metabolites on lifespan and resistance to oxidative and thermal stress of *Caenorhabditis elegans* and epicatechin uptake. *Food Research International*, **46**, 514-521.

Szekeres, P., Eliason, E.J., Lapointe, D., Donaldson, M.R., Brownscombe, J.W. & Cooke, S.J. (2016) On the neglected cold side of climate change and what it means to fish. *Climate Research*, **69**, 239-245.

Tahmasebi-Kohyani, A., Keyvanshokooh, S., Nematollahi, A., Mahmoudi, N. & Pasha-Zanoosi, H. (2012) Effects of dietary nucleotides supplementation on rainbow trout (*Oncorhynchus mykiss*) performance and acute stress response. *Fish Physiology and Biochemistry*, **38**, 431-440.

Tojander, S., Gateva, G. & Lappalainen, P. (2012) Actin stress fibers-assembly, dynamics and biological roles. *Journal of Cell Science*, **125**, 1855-1864.

Torres, M.I., Fernandez, M.I., Gil, A., Rios, A. (1997) Dietary nucleotides have cytoprotective properties in rat liver damaged by thioacetamide. *Life Sciences*, **62**, 13-22.

Umar, S. (2010) Intestinal stem cells. *Current Gastroenterology Reports*, **12**, 340-348.

Uran, P.A., Schrama, J.W., Rombout, J.H.W.M., Obach, A., Jensen, L., Koppe, W. & Verreth, J.A.J. (2008) Soybean meal-induced enteritis in Atlantic salmon (*Salmo salar* L.) at different temperatures. *Aquaculture Nutrition*, **14**, 324-330.

Van den Ingh, T.S.G.A.M., Krogdahl, A., Olli, J.J., Hendriks, H.G.C.J.M. & Koninks, J.G.J.F. (1991) Effect of soybean-containing diets on the proximal and distal intestine in Atlantic salmon (*Salmo salar*): a morphological study. *Aquaculture*, **94**, 297-305.

Vllasaliu, D., Falcone, F.H., Stolnik, S. & Garnett, M. (2014) Basement membrane influences intestinal epithelial cell growth and presents a barrier to the movement of macromolecules. *Experiment Cell Research*, **323**, 218-231.

Wallace, K.N., Akhter, S., Smith, E.M., Lorent, K. & Pack, M. (2005) Intestinal growth and differentiation in zebrafish. *Mechanisms of Development*, **122**, 157-173.

Wang, T., Hung, C.C.Y. & Randall, D.J. (2006) The comparative physiology of food deprivation: from feast to famine. *Annual Review of Physiology*, **68**, 223-251.

Welker, T.L., Lim, C., Yildirim-Aksoy, M. & Klesius, P.H. (2011) Effects of dietary supplementation of a purified nucleotide mixture on immune function and disease and stress resistance in channel catfish, *Ictalurus punctatus*. *Aquaculture Research*, **42**, 1878-1889.

Willemsen, L.E., Koetsier, M.A., Balvers, M., Beermann, C., Stahl, B. & van Tol, E.A. (2008) Polyunsaturated fatty acids support epithelial barrier integrity and reduces IL-4 mediated permeability in vitro. *European Journal of Nutrition*, **47**, 183-191.

Wischmeyer, P.E., Mush, M.W., Madonna, M. B., Thisted, R. & Chang, E.B. (1997) Glutamine protects intestinal epithelial cells: role of inducible HSP70. *American Journal of Physiology*, **272**, G879-G884.

Zhang, L., Jie, G., Zhang, J. & Zhao, B. (2009) Significant longevity-extending effects of EGCG on *Caenorhabditis elegans* under stress. *Free Radical Biology and Medicine*, **46**, 414-421.

Chapter 2 References

Antonopoulou E., Kentepozidou E., Feidantsis K., Roufidou C., Despoti S., & Chatzifotis S. (2013) Starvation and re-feeding affect Hsp expression, MAPK activation and antioxidant enzymes activity of European Sea Bass (*Dicentrarchus labrax*). *Comparative Biochemistry & Physiology – Part A: Molecular & Integrative Physiology*, **165**, 79–88.

Ashley, P.J. (2007) Fish welfare: current issues in aquaculture. *Applied Animal Behaviour Science*, **104**, 195-235.

Azodi, M., Ebrahimi, E., Farhadian, O., Mahboobi-Soofiani, N. & Morshedi, V. (2015) Compensary growth response of rainbow trout *Oncorhynchus mykiss* Walbaum following short starvation periods. *Chinese Journal of Oceanology and Limnology*, **33,** 928-933.

Balda, M.S. & Matter, K. (2000) The tight junction protein ZO-1 and an interacting transcription factor regulate ErbB-2 expression. *The EMBO Journal*, **19**, 2024-2033.

Beamish, F.W.A. (1978) Swimming capacity of fish. *Fish Physiology*, **7**, 101-187.

Bian, C., Xu, G., Wang, J., Ma, J., Xiang, M. & Chen, P. (2009) Hypercholesterolaemic serum increases the permeability of endothelial cells through zonula occludens-1 with phosphatidylinositol 3-kinase signaling pathway. *Journal of Biomedicine and Biotechnology*, **2009**, 814979.

Bloch, S.R., Kim, J.J., Pham, P.H., Hodson, P.V., Lee, L.E.J. & Bols, N.C. (2017) Responses of an American eel brain endothelial-like cell line to selenium deprivation and to selenite, selenate and selenomethionine additions in different exposure media. *In Vitro Cellular & Developmental Biology – Animal* (in press).

Boraldi, F., Annovi, G., Paolinelli-Devincenzi, C., Tiozzo, R. & Quaglino, D. (2008) The effect of serum withdrawal on the protein profile of quiescent human dermal fibroblasts in primary cell culture. *Proteomics*, **8**, 66-82.

Boutilier, R.G. (2001) Mechanisms of cell survival in hypoxia and hypothermia. *Journal of Experimental Biology*, **204**, 3171-3181.

Bryson, S.P., Joyce, E.M., Martell, D. J., Lee, L.E.J., Holt, S.E., Kales, S.C., Fujiki, K., Dixon, B. & Bols, N.C. (2006) A cell line (HEW) from embryos of haddock (*Melanogrammus aeglefinius*) and its capacity to tolerate environmental extremes. *Marine Biotechnology*, **8**, 641-653.

Cara, J.B., Aluru, N., Moyano, F.J. & Vijayan, M.M. (2005) Food deprivation induces HSP 70 and HSP 90 protein expression in larval and gilthead sea bream and rainbow trout. *Comparative Biochemistry & Physiology - Part B: Biochemistry & Molecular Biology*, **142**, 426-431.

Chang, C., Wang, X. & Caldwell, R.B. (1997) Serum opens up tight junctions and reduces ZO-1 protein in retinal epithelial cells. *Journal of Neurochemistry*, **69**, 859-867.

Chasiotis, H., Kolosov, D., Bui, P. & Kelly, S.P. (2012) Tight junctions, tight junction proteins and paracellular permeability across the gill epithelium of fishes: A review. *Respiratory Physiology & Neurobiology*, **184**, 269-281.

Colgan, O.C., Collins, N.T., Ferguson, G., Murphy, R.P., Birney, Y.A., Cahill, P.A. & Cummins, P.M. (2008) Influence of basolateral condition on the regulation of brain microvascular endothelial tight junction properties and barrier function. *Brain Research*, **1193**, 84-92.

Dayeh, V.R., Bols, N.C., Tanneberger, K., Schirmer, K., Lee, L.E.J. (2013) The use of fish derived cell lines for investigation of environmental contaminants: an update following OECD's fish toxicity testing Framework No. 171. *Current Protocols in Toxicology*, 1.5.1-1.5.20.

Eslamloo, K., Morshedi, V., Azodi, M., & Akhavan, S.R. (2017) Effect of starvation on some immunological and biochemical parameters in tinfoil barb (*Barbonymus schwanenfeldii*). *Journal of Applied Animal Research*, **45**, 173-178.

Fanarraga, M.L., Villegas, J.C., Carranza, G., Castano, R. & Zabala, J.C. (2009) Tubulin cofactor B regulates microtubule densities during microglia transition to the reactive states. *Experimental Cell Research*, **315**, 535–541.

Gronquist, D. & Berges, J.A. (2013) Effects of aquarium-related stressors on the zebrafish: a comparison of behavioral, physiological, and biochemical indicators. *Journal of Aquatic Animal Health*, **25**, 53-65.

Jobling, M. (1983) Towards an explanation of specific dynamic action (SDA). *Journal of Fish Biology*, **23**, 549-555.

Jolly, C. & Morimoto, R.I. (2000) Role of the heat shock response and molecular chaperones in oncogenesis and cell death. *Journal of the National Cancer Institute*, **92**, 1564-1572.

Ham, R.G. (1981) Cell growth requirements –the challenge we face. In: Waymouth C.., Ham R.G. and Chapple P.J. (eds.) The growth requirements of vertebrate cells in vitro. Cambridge University Press, Cambridge. pp 1-15

Hashimoto, K., Takeda, K., Nakayama, T. & Shimizu, M. (1995) Stabilization of the tight junction of the intestinal Caco-2 cell monolayer by milk whey proteins. *Bioscience, Biotechnology, and Biochemistry*, **59**, 1951-1952.

Iizuka, M. & Konno, S. (2011) Wound healing of intestinal epithelial cells. *World Journal of Gastroenterology*, **17**, 2161-2171.

Kawano, A., Haiduk, C., Schirmer, K., Hanner, R., Lee, L.E.J, Dixon, B. & Bols, N.C. (2011) Development of a rainbow trout intestinal epithelial cell line and its response to lipopolysaccharide. *Aquaculture Nutrition*, **17**, e241-e252.

Lines, J.A. & Spence, J. (2012) Safeguarding the welfare of fish at harvest. *Fish Physiology and Biochemistry*, **38**, 153-162.

Martin, S.A., Douglas, A., Houlihan, D.F. & Secombes, C.J. (2010) Starvation alters the liver transcriptome of the innate immune response in atlantic salmon (*Salmo salar*). *BMC Genomics*, **11**, 418.

Maninova, M., Caslasvsky, J. & Vomastek T. (2017) The assembly and function of perinuclear actin cap in migrating cells. *Protoplasma*, **254**, 1207-1218.

Nakamura, T., Murata, T., Hori, M. & Ozaki, H. (2013) UDP induces intestinal epithelial migration via the P2Y (6) receptor. *British Journal of Pharmacology*, **170**, 883-892.

Niehoff, B. (2000) Effect of starvation on the reproductive potential of *Calanus finmarchicus*. *Journal of Marine Science*, **57**, 1764-1772.

Paddenberg, R., Loos, S., Schöneberger, H-J., Wulf, S., Müller, A., Iwig, M. & Mannherz, H.G. (2001) Serum withdrawal induces a redistribution of intracellular gelsolin towards F-actin in NIH 3T3 fibroblasts preceding apoptotic cell death. *European Journal of Cell Biology*, **80**, 366–378.

Ramsay, J.M., Feist, G.W., Schreck, C.B., Couture, R., O'Neil, J. & Noakes, D.L.G. (2009) The effect of food deprivation on the cortisol response to crowding in juvenile steelhead. *North American Journal of Aquaculture*, **71**, 130-133.

Rastogi, H., Pinjari, J., Honrao, P., Praband, S. & Somani, R. (2013) The impact of permeability enhancers on assessment for monolayer of colon adenocarcinoma cell line (CACO-2) used in in vitro permeability assay. *Journal of Drug Delivery and Therapeutics*, **3**, 20-29.

Ridley, A.J. & Hall, A. (1992) The small GTP-binding protein rho regulates the assembly of focal adhesions and actin stress fibers in response to growth factors. *Cell*, **70**, 389-399.

Sanchez, A.D. & Feldman, J.L. (2016) Microtubule-organizing centers: from the centrosome to non-centrosomal sites. *Current Opinion in Cell Biology*, **44,** 93-101.

Schirmer, K., Chan, A.G.J., Greenberg, B.M., Dixon, D.G. & Bols, N.C. (1997) Methodology for demonstrating and measuring the photocytoxicity of fluoranthene to fish cells in culture. *Toxicology in Vitro*, **11**, 107-113.

Schmitz, H-D. & Bereiter-Hahn, J. (2002) Glyceraldehyde-3-phosphate dehydrogenase associates with actin filaments in serum deprived 3T3 cells only. *Cell Biology International*, **26**, 155-164.

Srinivasan, B., Kolli, A. R., Esch, M. B., Abaci, H. E., Shuler, M. L. & Hickman, J. J. (2015) TEER measurement techniques for in vitro barrier model systems. *Journal of Laboratory Automation*, **20**, 107-126.

Szymanski, D. (2002) Tubulin folding cofactors: half a dozen for a dimer. *Current Biology*, **12**, R767–R769.

Tavares, S., Vieira, A.F., Taubenberger, A.V., Araújo, M., Martins, N.P., Brás-Pereira, C., Polónia, A., Herbig, M., Barreto, C., Otto, O., Cardoso, J., Pereira-Leal, J.B., Guck, J., Paredes, J. & Janody, F. (2017) Actin stress fiber organization promotes cell stiffening and proliferation of pre-invasive breast cancer cells. *Nature Communications*, **8**, 15237.

Weber, T.E. & Bosworth, B.G. (2005) Effect of 28 day exposure to cold temperature or feed restriction on growth, body composition, and expression of genes related to muscle growth and metabolism in channel catfish. *Aquaculture*, **246**, 483-492.

Chapter 3 References

Chasiotis, H., Kolosov, D., Bui, P. & Kelly, S.P. (2012) Tight junctions, tight junction proteins and paracellular permeability across the gill epithelium of fishes: A review. *Respiratory Physiology & Neurobiology*, **184**, 269-281.

Clelland, E.S., Bui, P., Bagherie-Lachidan, M. & Kelly, S.P. (2010) Spatial and salinity-induced alterations in claudin-3 isoform mRNA along the gastrointestinal tract of the pufferfish *Tetraodon nigroviridis*. *Comparative Biochemistry and Physiology Part A: Molecular & Integrative Physiology*, **155**, 154-163.

Dayeh, V.R., Bols, N.C., Tanneberger, K., Schirmer, K., Lee, L.E.J. (2013) The use of fish derived cell lines for investigation of environmental contaminants: an update following OECD's fish toxicity testing Framework No. 171. *Current Protocols in Toxicology*, 1.5.1-1.5.20.

Dourdin, N., Bhatt, A.K., Dutt, P., Greer, P.A., Arthur, J.S.C., Elce, J.S. & Huttenlocher, A. (2001) Reduced cell migration and disruption of the actin cytoskeleton in calpain-deficient embryonic fibroblasts. *The Journal of Biological Chemistry*, **276**, 48382-48388.

Evans, M.E., Jones, D.P. & Ziegler, T.R. (2005) Glutamine inhibits cytokine-induced apoptosis in human colonic epithelial cells via the pyrimidine pathway. *American Journal of Physiology - Gastrointesinal and Liver Physiology*, **289**, G388–G396.

Frabasile, S., Koishi, A.C., Kuczera, D., Silveira, G.F., Verri, W.A., dos Santos, C.N.D. & Bordignon, J. (2017) The citrus flavanone naringenin impairs dengue virus replication in human cells. *Nature Scientific Reports*, **7**, 41864.

Fukada, H., Furutani, T., Shimizu, R. & Masumoto, T. (2014) Effects of yuzu (*Citrus junos*) peel from waste as an aquaculture feed supplement on growth, environmental load, and dark muscle discoloration in yellowtail *Seriola quinqueradiata*. *Journal of Aquatic Food Product Technology*, **23**, 511-521.

Fukuhara, S., Sakurai, A., Sano, H., Yamagishi, A., Somekawa, S., Takahura, N., Saito, Y., Kangawa, K. & Mochizuki, N. (2005) Cyclic AMP potentiates vascular endothelial cadherin-mediated cell-cell contact to enhance endothelial barrier function through an Epac-Rap1 signaling pathway. *Molecular and Cell Biology*, **25**, 136-146.

Gerits, N., Mikalsen, T., Kostenko, S., Shiryaev, A., Johannessen, M. & Moens, U. (2007) Modulation of f-actin rearrangement by the cyclic AMP/cAMP-dependent protein kinase (PKA) pathway is mediated by MAPK-activated protein kinase 5 and requires PKA-induced nuclear export of MK5. *The Journal of Biological Chemistry*, **282**, 37232-37243.

Glen, H.L. & Jacobson, B.S. (2003) Cyclooxygenase and cAMP-dependent protein kinase reorganize the actin cytoskeleton for motility in HeLa cells. *Cell Motility and the Cytoskeleton*, **55**, 265-277.

Howe, A.K. (2004) Regulation of actin-based migration by cAMP/PKA. *Biochimica et Biophysica Acta*, **1692**, 159-174.

Kawano, A., Haiduk, C., Schirmer, K., Hanner, R., Lee, L.E.J, Dixon, B. & Bols, N.C. (2011) Development of a rainbow trout intestinal epithelial cell line and its response to lipopolysaccharide. *Aquaculture Nutrition*, **17**, e241-e252.

Khan, M.K., Zill-E-Huma & Dangles, O. (2014) A comprehensive review on flavanones, the major citrus polyphenols. *Journal of Food Composition and Analysis*, **33**, 85-104.

Kim, S., Harris, M. & Varner, J.A. (2000) Regulation of integrin alpha vbeta 3-mediated endothelial cell migration and angiogenesis by integrin alpha5beta1 and protein kinase A. *Journal of Biological Chemistry*, **275**, 33920-33928.

Kolosov, D., Bui, P., Chasiotis, H. & Kelly, S.P. (2013) Claudins in teleost fishes. *Tissue Barriers*, **1**, e25391.

Kuma, A. & Mizushima, N. (2010) Physiological role of autophagy as an intracellular recycling system: With and emphasis on nutrient metabolism. *Seminars in Cell & Developmental Biology*, **21**, 683-690.

Leonardi, T., Vanamala, J., Taddeo, S.S., Davidson, L.A., Murphy, M.E., Patil, B.S., Wang, N., Carroll, R.J., Lupton, J.R. & Turner, N.D. (2010) Apigenin and naringenin suppress colon carcinogenesis through the aberrant crypt stage in azoxymethane-treated rats. *Experimental Biology and Medicine (Maywood)*, **235**, 710-717.

Li, A.Q., Zhao, L., Zho, T.F., Zhang, M.Q. & Qin, X.M. (2015) Exendin-4 promotes endothelial barrier enhancement via PKA- and Epac1-dependent Rac1 activation. *The American Journal of Physiology – Cell Physiology*, **15**, C164-C175.

Li, N., Lewis, P., Samuelson, D., Liboni, K. & Neu, J. (2004) Glutamine regulates Caco-2 cell tight junction proteins. *The American Journal of Physiology – Gastrointestinal and Liver Physiology*, **287**, G726-G733.

Menanteau-Ledouble, S., Krauss, I., Santos, G., Fibi, S., Weber, B. & El-Matbouli, M. (2015) Effect of a phytogenic feed additive on the susceptibility of *Onchorhynchus mykiss* to *Aeromonas salmonicida*. *Diseases of Aquatic Organisms*, **115**, 57-66.

Morgan, W.D. (1989) Transcription factor Sp1 binds to and activates a human hsp70 gene promoter. *Molecular and Cell Biology*, **9**, 4099-4104.

Mulvihill, E.E., Allister, E.M., Sutherland, B.G., Telford, D.E., Sawyez, C.G., Edwards, J.Y., Markle, J.M., Hegele, R.A. & Huff, M.W. (2009) Naringenin prevents dyslipidemia, apolipoprotein B overproduction, and hyperinsulinemia in LDL receptor-null mice with diet-induced insulin resistance. *Diabetes*, **58**, 2198-2210.

Nadella, K.S., Saji, M., Jacob, N.K., Pavel, E., Ringel, M.D. & Kirschner, L.S. (2009) Regulation of actin function by protein kinase A-mediated phosphorylation of Limk1. *EMBO Reports*, **10**, 599-605.

Noda, K., Zhang, J., Fukuhara, S., Kunimoto, S., Yoshimura, M. & Mochizuki, N. (2010) Vascular endothelial-cadherin stabilizes at cell-cell junctions by anchoring to circumferential actin bundles through α- and β-catenins in cyclic AMP-Epac-Rap1 signal-activated endothelial cells. *Molecular Biology of the Cell*, **21**, 584-596.

Noda, S., Tanabe, S. & Suzuki, T. (2013) Naringenin enhances intestinal barrier function through the expression and cytoskeletal association of tight junction proteins in Caco-2 cells. *Molecular Nutrition & Food Research*, **57**, 2019-2028.

Park, H.Y., Kim, G.Y. & Choi, Y.H. (2012) Naringenin attenuates the release of pro-inflammatory mediators from lipopolysaccharide-stimulated BV2 microglia by inactivating nuclear factor-kB and inhibiting mitogen-activated protein kinases. *International Journal of Molecular Medicine*, **30**, 204-210.

Plopper, G.E., Huff, J.L., Rust, W.L., Schwartz, M.A. & Quaranta, V. (2000) Antibody-induced activation of beta1 integrin receptors stimulates cAMP-dependent migration of breast cells on laminin-5. *Molecular Cell Biology Research Communications*, **4**, 129-135.

Roth, E. (2008) Nutritive effects of glutamine. *Journal of Nutrition*, **138**, 2025S– 2031S.

Shinyoshi, S., Kamada, Y., Matsusaki, K., Chigwechokha P.K., Tepparin, S., Araki, K., Komatsu, M. & Shiozaki, K. Naringenin suppresses *Edwardsiella tarda* infection in GAKS cells by NanA sialidase inhibition. *Fish & Shellfish Immunology*, **61**, 86-92.

Søberg, K., Jahnsen, T., Rognes, T., Skålhegg, B.S. & Laerdahl, J.K. (2013) Evolutionary paths of the cAMP-dependant protein kinase (PKA) catalytic subunits. *PLoS ONE*, **8**, e60935.

Spurzem, J.R., Gupta, J., Veys, T., Kneifl, K.R., Rennard, S.I. & Wyatt, T.A. (2002) Activation of protein kinase A accelerates bovine bronchial epithelial cell migration. *American Journal of Physiology – Lung Cellular and Molecular Physiology*, **282**, L1108-L1116.

Stelzner, T.J., Weil, J.V. & O'Brien, R.F. (1989) Role of cyclic adenosine monophosphate in the induction of endothelial barrier properties. *Journal of Cellular Physiology*, **139**, 157-166.

Testai, L., Da Pozzo, E., Piano, I., Pistelli, L., Gargini, C., Breschi, M.C., Braca, A., Martini, C., Martelli, A. & Calderone, V. (2017) The citrus flavanone naringenin produces cardioprotective effects in hearts from 1 year old rats, through activation of mitoBK channels. *Frontiers in Pharmacology*, **8**, 10.3389/fphar.2017.00071,

Vallenius, T. (2013) Actin stress fiber subtypes in mesenchymal-migrating cells. *Open Biology*, **3**, 130001.

Varasteh, S., Braber, S., Akbari, P., Garssen, J. & Fink-Gremmels, J. (2015) Differences in susceptibility to heat stress along the chicken intestine and the protective effects of galacto-oligosaccharides. *PLoS ONE*, **10**, e0138975.

Wang, J., Yang, Z., Zhao, Z., Lui, Z. & Lui, X. (2012) Protective effects of naringenin against lead-induced oxidative stress in rats. *Biological Trace Element Research*, **146**, 354-359.

Whelan, M.C. & Senger, D.R. (2003) Collagen I initiates endothelial cell morphogenesis by inducing actin polymerization through suppression of cyclic AMP and protein kinase A. *Journal of Biological Chemistry*, **278**, 327-334.

Willemsen, L.E., Koetsier, M.A., Balvers, M., Beermann, C., Stahl, B. & van Tol, E.A. (2008) Polyunsaturated fatty acids support epithelial barrier integrity and reduces IL-4 mediated permeability in vitro. *European Journal of Nutrition*, **47**, 183-191.

Yamagishi, N., Yamamoto, Y., Noda, C. & Hatayama, T. (2012) Naringenin inhibits the aggregation of expanded polyglutamine tract-containing protein through the induction of endoplasmic reticulum chaperone GRP78. *Biological and Pharmaceutical Bulletin*, **35**, 1836-1840.

Yang, Z.H., Yu, H.J., Pan, A., Du, J.Y., Ruan, Y.C., Ko, W.H., Chan, H.C. & Zhou, W.L. (2008) Cellular mechanisms underlying the laxative effect of flavonol naringenin on rat constipation model. *PLoS ONE*, **3**, e3348.

Yukiura, H., Kano, K., Kise, R., Inoue, A. & Aoki, J. (2015) LPP3 localizes LPA_6 signalling to non-contact sites in endothelial cells. *Journal of Cell Science*, **128**, 3871-3877.

Zimmerman, N.P., Kumar, S.N., Turner, J.R. & Dwinell, M.B. (2012) Cyclic AMP dysregulates intestinal epithelial cell restitution through PKA and RhoA. *Inflammatory Bowel Diseases*, **18**, 1081-1091.

Chapter 4 References

Bakker, A.M., Chiktwati, E.M., Venold, F.F., Sahlmann, C., Holm, H., Penn, M.H., Oropeza-Moe, M. & Krogdahl, Å. (2014) Bile enhances glucose uptake, reduces permeability, and modulates effects of lectins, trypsin inhibitors and saponins on intestinal tissue. *Comparative Biochemistry and Physiology, Part A*, **168**, 96-109.

Beck, B. H., & Peatman, E. (2015). Mucosal Health in Aquaculture. Academic Press.

Daehn, I.S., Varelias, A. & Rayner, T.E. (2006). Sodium butyrate induced keratinocyte apoptosis. *Apoptosis: An International Journal on Programmed Cell Death*, **11**, 1379–1390.

de Punder, K., & Pruimboom, L. (2013). The dietary intake of wheat and other cereal grains and their role in inflammation. *Nutrients*, *5*, (3), 771–787.

Dourdin, N., Bhatt, A.K., Dutt, P., Greer, P.A., Arthur, J.S.C., Elce, J.S. & Huttenlocher, A. (2001) Reduced cell migration and disruption of the actin cytoskeleton in calpain-defecient embryonic fibroblasts. *The Journal of Biological Chemistry*, **276**, 48382-48388.

Draaijer, M., Koninkx, J., Hendriks, H., Kik, M., van Dijk, J. & Mouwen, J. (1989) Actin cytoskeletal lesions in differentiated human colon carcinoma Caco-2 cells after exposure to soybean agglutinin. *Biology of the Cell*, **65**, 29-35.

FAO, 1997. Review of the state of world aquaculture, 1997. FAO Fisheries Circular. No. 886, Rev. 1. FAO, Rome, 163 pp.

FAO, 2016. The state of world fisheries and aquaculture 2016. Contributing to food security and nutrition for all. Rome, 200 pp.

Francis, G., Makkar, H.P.S. & Becker, K. (2001) Antinutritional factors present in plant-derived alternate fish feed ingredients and their effects on fish. *Aquaculture*, **199**, 197-227.

Fung, K. Y. C., Brierley, G. V., Henderson, S., Hoffmann, P., McColl, S. R., Lockett, T., Head, R. & Cosgrove, L. (2011). Butyrate-induced apoptosis in HCT116 colorectal cancer cells includes induction of a cell stress response. *Journal of Proteome Research*, **10**, 1860–1869.

Gordon, S. R., & Wood, M. (2009). Soybean agglutinin binding to corneal endothelial cell surfaces disrupts in situ monolayer integrity and actin organization and interferes with wound repair. *Cell and Tissue Research*, **335**, 551–563.

Hart, S.D., Bharadwa, A.S. & Brown, P.B. (2010) Soybean lectins and trypsin inhibitors, but not oligosaccharides or the interactions of factors, impact weight gain of rainbow trout (*Oncorhynchus mykiss*). *Aquaculture*, **306**, 310–314.

Kawano, A., Haiduk, C., Schirmer, K., Hanner, R., Lee, L.E.J, Dixon, B. & Bols, N.C. (2011) Development of a rainbow trout intestinal epithelial cell line and its response to lipopolysaccharide. *Aquaculture Nutrition*, **17**, e241-e252.

Kobayashi, H., Suzuki, M., Kanayama, N. & Terao, T. (2004) A soybean kunitz trypsin inhibitor suppresses ovarian cancer cell invasion by blocking urokinase upregulation. *Clinical & Experimental Metastasis*, **21**, 159-166.

Losso, J.N. (2008) The biochemical and functional food properties of the Bowman-Birk inhibitor. *Critical Reviews in Food Science and Nutrition*, **48**, 94-118.

Lotz, M.M., Rabinovitz, I. & Mercurio, A.M. (2000) Intestinal restitution: progression of actin cytoskeleton rearrangements and integrin function in a model of epithelial wound healing. *The American Journal of Pathology*, **156**, 985–996.

Naylor, R.L., Goldburg, R.J., Primavera, J.H., Kautsky, N., Beveridge, M.C.M., Clay, J., Folke, C., Lubchenco, J., Mooney, H., Troell, M., 2000. Effect of aquaculture on world fish supplies. *Nature*, **405**, 1017–1024.

Peng, L., He, Z., Chen, W., Holzman, I.R. & Lin, J. (2007) Effects of butyrate on intestinal barrier function in a Caco-2 cell monolayer model of intestinal barrier. *Pediatric Research*, **61**, 37-41.

Ruemmele, F. M., Schwartz, S., Seidman, E. G., Dionne, S., Levy, E. & Lentze, M. J. (2003) Butyrate induced Caco-2 cell apoptosis is mediated via the mitochondrial pathway. *Gut*, **52**, 94–100.

Sargent, J.R. & Tacon, A.G.J. (1999) Development of farmed fish: a nutritionally necessary alternative to meat. *Proceedings of the Nutrition Society*, **58**, 377–383.

Sjolander, A. & Magnusson, K.E. (1988) Effects of wheat germ agglutinin on the cellular content of filamentous actin in intestine 407 cells. *European Journal of Cell Biology*, **47**, 32-35.

Sturm, A., & Dignass, A.U. (2008) Epithelial restitution and wound healing in inflammatory bowel disease. *World Journal of Gastroenterology*, **14**, 348–353.

Teves, J.F.C. & Ragaza, J.A. (2016) The quest for indigenous aquafeed ingredients: a review. *Reviews in Aquaculture*, **8**, 154-171.

Tsai, J.C. & Hwang P.P. (1998) Effects of wheat germ agglutinin and cochicine on microtubules of the mitochondria-rich cells and Ca^{2+} uptake in Tilapia (*Oreochromis mossambicus*) larvae. *Journal of Experimental Biology*, **210**, 2263-2271.

Vallenius, T. (2013) Actin stress fiber subtypes in mesenchymal-migrating cells. *Open Biology*, **3**, 130001.

Chapter 5 References

Bols, N.C., Mosser, D.D. & Steels, G.B. (1992) Temperature studies and recent advances with fish cells *in vitro*. *Comparative Biochemistry Physiology*, **103A**, 1-14.

Bols, N.C., Boliska, S.A., Dixon, D.G., Hodson, P.V. & Kaiser, K.L.E. (1985) The use of fish cell cultures as an indication of contaminant toxicity to fish. *Aquatic Toxicology*, **6**, 147-155.

Bhatia, A., O'Brien, K., Chan, M., Woodley, D.T. & Li, W. (2016) Keratinocyte-secreted heat shock protein-90alpha: Leading wound reepithelialisation and closure. *Advances in Wound Care*, **5**, 176-184.

Cai, H., Ren, Y., Li, X.X., Yang, J.L., Zhang, C.P., Chen, M., Fan, C.H., Hu, X.Q., Hu, Z.Y., Gao, F. & Liu, Y.X. (2011) Scrotal heat stress causes a transient alteration in tight junctions and induction of TGF-β expression. *International Journal of Andrology*, **34**, 352-362.

Chen, M., Cai, H., Yang, J.Q., Lu, C.L., Liu, T., Yang, W., Guo, J., Hu, X.Q., Fan, C.H., Hu, Z.Y., Gao, F. & Liu, Y.X. (2008) Effect of heat stress on expression of junction-associated molecules and upstream factors androgen receptor and Wilms' tumor 1 in monkey sertoli cells. *Endocrinology*, **149**, 4871-4882.

Cheng, C-.F., Fan, J., Fedesco, M., Guan, S., Li, Y., Bandyopadhyay, B., Bright, A.M., Yerushalmi, D., Liang, M., Chen, M., Han, Y-.P., Woodley, D.T. & Li, W. (2008) Transforming growth factor α (TGFα)-stimulated secretion of HSP90α: Using the receptor LRP-1/CD91 to promote human skin cell migration against a TGFβ-rich environment during wound healing. *Molecular and Cellular Biology*, **28**, 3344-3358.

Chow, A. & Zhang, R. (1998) Glutamine reduces heat shock-induced cell death in rat intestinal epithelial cells. *Journal of Nutrition*, **128**, 1296-1301.

Clarke, A. & Johnston, N.M. (1999) Scaling of metabolic rate with body mass and temperature in teleost fish. *Journal of Animal Ecology*, **68**, 893-905.

Dokladny, K., Ye, D., Kennedy, J.C., Moseley, P.L. & Ma, T.Y. (2008) Cellular and molecular mechanism of heat stress-induced up-regulation of occluding protein expression. *The American Journal of Pathology*, **172**, 659-670.

Dokladny, K., Moseley, P.L. & Ma, T.Y. (2006) Physiological relevant increase in temperature causes an increase in intestinal epithelial tight junction permeability. *American Journal of Physiology – Gastrointestinal and Liver Physiology*, **290**, G204-G212.

Gov, N. (2011) Cell mechanics: Moving under peer pressure. *Nature Materials*, **10**, 412-414.

Ham, R.G. (1981) Cell growth requirements-the challenge we face. In: Waymouth, C., Ham, R.G. & Chapple, P.J. (eds) The growth requirements of vertebrate cells in vitro. Cambridge University Press, Cambridge. pp 1-15.

Iizuka, M. & Konno, S. (2011) Wound healing of the intestinal epithelial cells. *World Journal of Gastroenterology*, **17**, 2161-2171.

Kawano, A., Haiduk, C., Schirmer, K., Hanner, R., Lee, L.E.J, Dixon, B. & Bols, N.C. (2011) Development of a rainbow trout intestinal epithelial cell line and its response to lipopolysaccharide. *Aquaculture Nutrition*, **17**, e241-e252.

Landry, J., Bernier, D., Chretien, P., Nicole, L.M., Tanguay, R.M. & Marceau, N. (1982) Synthesis and degradation of heat shock proteins during development and decay of thermotolerance. *Cancer Research*, **42**, 2457-2461.

Meir, M., Flemming, S., Burkard, N., Wagner, J., Germer, C.T., Schlegel, N. (2016) The glial cell-line derived neutrophic factor: a novel regulator of intestinal barrier function in health and disease. *American Journal of Physiology - Gastrointestinal and Liver Physiology*, **310**, G1118-G1123.

Mosser, D. & Bols, N.C. (1988) Relationship between heat-shock protein synthesis and thermotolerance in rainbow trout fibroblasts. *Journal of Comparative Physiology B: Biochemical, Systems, and Environmental Physiology*, **158**, 457-467.

Mosser, D.D., Heikkila, J.J. & Bols, N.C. (1986) Temperature ranges over which rainbow trout fibroblasts survive and synthesize heat-shock proteins. *Journal of Cell Physiology*, **128**, 432-440.

Mosser, D.D., van Oostrom, J. & Bols, N.C. (1987). Induction and decay of thermotolerance in rainbow trout fibroblasts. *Journal of Cellular Physiology*, **132**, 155-160.

Mounier, N. & Arrigo, A.P. (2002) Actin cytoskeleton and small heat shock proteins: how do they interact? *Cell Stress Chaperones*, **7**, 167-176.

Osada, T., Iijima, K., Tanaka, H., Hirose, M., Yamamoto, J. & Watanabe, S. (1999) Effect of temperature and mechanical strain on gastric epithelial cell line GSM06 wound restoration *in vitro*. *Journal of Gastroenterology and Hepatology*, **14**, 489-494.

Plumb, J.A. & Wolf, K. (1971) Fish cell growth rates. *In Vitro*, **7**, 42-25.

Richter, K., Haslbeck, M. & Buchner, J. (2010) The heat shock response: Life on the verge of death. *Molecular Cell*, **40**, 253-266.

Simard, J.P., Reynolds, D.N., Kraguljac, A.P., Smith, G.S.T. & Mosser, D.D. (2011) Overexpression of HSP70 inhibits cofilin phosphorylation and promotes lymphocyte migration in heat-stressed cells. *Journal of Cell Science*, **124**, 2367-2374.

Sims, J.D., McCready, J. & Jay, D.G. (2011) Extracellular heat shock protein (Hsp)70 and Hsp90α assist in matrix metalloproteinase-2 activation and breast cancer cell migration and invasion. *PLoS ONE*, **6**, e18848.

Subjeck, J.R. & Shyy, T-T. (1986) Stress protein systems of mammalian cells. *American Journal of Physiology*, **250**, C1-C17.

Toivola, D.M., Strnad, P., Habtezion, A., & Omary, M.B. (2010) Intermediate filaments take the heat as stress proteins. *Trends in Cell Biology*, **20**, 79–91.

Uran, P.A., Schrama, J.W., Rombout, J.H.W.M., Obach, A., Jensen, L., Koppe, W. & Verreth, J.A.J. (2008) Soybean meal-induced enteritis in Atlantic salmon (*Salmo salar* L.) at different temperatures. *Aquaculture Nutrition*, **14**, 324-330.

Welch, W.J., & Suhan, J.P. (1985) Morphological study of the mammalian stress response: characterization of changes in cytoplasmic organelles, cytoskeleton, and nucleoli, and appearance of intranuclear actin filaments in rat fibroblasts after heat-shock treatment. *Journal of Cell Biology*, **101**, 1198–1211.

Welch, W.J., & Suhan, J.P. (1986) Cellular and biochemical events in mammalian cells during and after recovery from physiological stress. *Journal of Cell Biol*ogy, **103**, 2035–2052.

Chapter 6 References

Ahamad, S., Siddiqui, S., Jafri, A., Ahmad, S., Afzal, M. & Arshad. (2014) Inductions of apoptosis and antiproliferative activity of naringenin in human epidermoid carcinoma cell through ROS generation and cell cycle arrest. *PLOS ONE*, **9**, e110003.

Andrade, D. & Rosenblatt, J. (2011) Apoptotic regulation of epithelial cellular extrusion. *Apoptosis*, **16**, 491-501.

Anyanwu, C.N., Osuigwe, D.I. & Adaka, G.S. (2014) Climate change: Impacts and threats on freshwater aquaculture. *Journal of Fisheries and Aquatic Science*, **9**, 419-424.

Arul, D. & Subramanian, P. (2013) Naringenin (citrus flavonone) induces growth inhibition, cell cycle arrest and apoptosis in human hepatocellular carcinoma cells. *Pathology & Oncology Research*, **19**, 763-770.

Brander, K.M. (2007) Global fish production and climate change. *Proceedings of the National Academy of Science U.S.A.*, **104**, 19709-19714.

Dalle-Donne, I., Rossi, R., Milzani, A., Simplicio, P.D. & Colombo, R. (2001) The actin cytoskeleton response to oxidants: from small heat shock protein phosphorylation to changes in the redox of state of actin itself. *Free Radical Biology & Medicine*, **31**, 1624-1632.

Dayeh, V.R., Bols, N.C., Tanneberger, K., Schirmer, K. & Lee, L.E.J. (2013) The use of fish derived cell lines for investigation of environmental contaminants: an update following OECD's fish toxicity testing Framework No. 171. *Current Protocols in Toxicology*, 1.5.1-1.5.20.

Dokladny, K., Zuhl, M.N. & Moseley, P.L. (2016) Intestinal epithelial barrier function and tight junction proteins with heat and exercise. *Journal of Applied Physiology*, 120, 692-701.

Gimenez, M.S., Oliveros, L.B. & Gomez, N.N. (2011) Nutritional deficiencies and phospholipid metabolism. *International Journal of Molecular Sciences*, **12**, 2408-2433.

Kawano, A., Haiduk, C., Schirmer, K., Hanner, R., Lee, L.E.J, Dixon, B. & Bols, N.C. (2011) Development of a rainbow trout intestinal epithelial cell line and its response to lipopolysaccharide. *Aquaculture Nutrition*, **17**, e241-e252.

Liu, J.J., Davis, E.M., Wine, E., Lou, Y.F., Rudzinski, J.K., Alipour, M., Boulanger, P., Thiesen, A.L., Sergi, C., Fedorak, R.N., Muruve, D., Madsen, K.L. & Irvin, R.T. (2013) Epithelial cell extrusion leads to breaches in the intestinal epithelium. *Gastrointestinal Endoscopy*, **77**, 624-630.

Liu, J.J., Wong, K., Thiesen, A.L., Mah, S.J., Dieleman, L.A., Clagget, B., Saltzman, J.R. & Fedorak, R.N. (2011) Increased epithelial gaps in the small intestines of patients with inflammatory bowel disease: density matters. *Gastrointestinal Endoscopy*, **73**, 1174-1180.

Mayhew, T.M., Myklebust, R., Whybrow, A. & Jenkins, R. (1999) Epithelial integrity, cell death and cell loss in mammalian small intestine. *Histology and Histopathology*, **14**, 257-267.

Miguel, J.C., Maxwell, A.A., Hsieh, J.J., Harnisch, L.C., Al Alam, D., Polk, D.B., Lien, C.L., Watson, A.J.M. & Frey, M.R. (2017) Epidermal growth factor suppresses intestinal epithelial cell shedding through a MAPK-dependent pathway. *Journal of Cell Science*, **130**, 90-96.

Morgan, W.D. (1989) Transcription factor Sp1 binds to and activates a human hsp70 gene promoter. *Molecular and Cell Biology*, **9**, 4099-4104.

Noda, K., Zhang, J., Fukuhara, S., Kunimoto, S., Yoshimura, M. & Mochizuki, N. (2010) Vascular endothelial-cadherin stabilizes at cell-cell junctions by anchoring to circumferential actin bundles through α- and β-catenins in cyclic AMP-Epac-Rap1 signal-activated endothelial cells. *Molecular Biology of the Cell*, **21**, 584-596.

Noda, S., Tanabe, S. & Suzuki, T. (2013) Naringenin enhances intestinal barrier function through the expression and cytoskeletal association of tight junction proteins in Caco-2 cells. *Molecular Nutrition & Food Research*, **57**, 2019-2028.

Pearce, S.C., Mani, V., Boddicker, R.L., Johnson, J.S., Weber, T.E., Ross, J.W., Rhoads, R.P., Baumarg, L.H. & Gabler, N.K. (2013) Heat stress reduces intestinal epithelial barrier integrity and favors intestinal glucose transport in growing pigs. *PLOS ONE*, **8**, e70215.

Yu, J., Yin, P., Liu, F., Cheng, G., Guo, K., Lu, A., Zhu, X., Luan, W. & Xu, J. (2010) Effect of heat stress on the porcine small intestine: a morphological and gene expression study. *Comparative Biochemistry and Physiology - Part A: Molecular & Integrative Physiology*, **156**, 119-128.

Yukiura, H., Kano, K., Kise, R., Inoue, A. & Aoki, J. (2015) LPP3 localizes LPA_6 signalling to non-contact sites in endothelial cells. *Journal of Cell Science*, **128**, 3871-3877.

Varasteh, S., Braber, S., Garssen, J. & Fink-Gremmels, J. (2015) Galacto-oligosaccharides exert a protective effect against heat stress in a Caco-2 cell model. *Journal of Functional Foods*, **16**, 265-277.

Chapter 7 References

Bhatia, A., O'Brien, K., Chan, M., Woodley, D.T. & Li, W. (2016) Keratinocyte-secreted heat shock protein-90alpha: Leading wound reepithelialisation and closure. *Advances in Wound Care*, **5**, 176-184.

Modrego, J., Lopez-Farré, A.J., Martinez-Lopez, I., Muela, M., Macaya, C., Serrano, J. & Monux, G. (2012) Expression of cytoskeleton and energetic metabolism-related proteins at human abdominal aortic aneurysm sites. *Journal of Vascular Surgery*, **55**, 1124-1133.

Sanchez, A.D. & Feldman, J.L. (2016) Microtubule-organizing centers: from the centrosome to non-centrosomal sites. *Current Opinion in Cell Biology,* **44,** 93-101.

Yang, Z.H., Yu, H.J., Pan, A., Du, J.Y., Ruan, Y.C., Ko, W.H., Chan, H.C. & Zhou, W.L. (2008) Cellular mechanisms underlying the laxative effect of flavonol naringenin on rat constipation model. *PLoS ONE*, **3**, e3348.